

PhD Expo

2017

25 maggio – 5 giugno
2017
Campus Rizzi
via delle Scienze 206
Udine

L'evento, organizzato dall'Università di Udine in collaborazione con l'Acceleratore digitale 'Friuli Innovazione', presenta la vetrina delle attività di ricerca condotte dai dottorandi iscritti al terzo anno dei corsi di dottorato.

Gli obiettivi:

- **comunicare** i risultati di ricerche e progetti
- **condividere** le idee e le proposte
- **confrontare** le esperienze e le competenze
- **contaminare** i diversi saperi



HR EXCELLENCE IN RESEARCH



**UNIVERSITÀ
DEGLI STUDI
DI UDINE**
hic sunt futura



Centro di Ricerca e di Trasferimento Tecnologico



FONDAZIONE
FRIULI

Tutti i poster e tutti gli autori 30° ciclo corsi di dottorato



HR EXCELLENCE IN RESEARCH

SCIENZE SOCIALI E UMANISTICHE SOCIAL SCIENCES AND HUMANITIES

CORSO DOTTORATO SCIENZE GIURIDICHE

BUSET GIACOMO
La concessione in godimento a scopo traslativo

CIMAROSTI ALIDA
Ripensare al part time, ripensare il part time? Il lavoro a tempo parziale tra sfide demografiche e crisi economica

DELLA TORRE JACOPO
La giustizia negoziata in Europa

MAGGIO IDA CARLA
La connessione impropria e la tutela dei diritti individuali omogenei

MARINO DENISE
I confini del diritto

URBAN FEDERICA
Il potere discrezionale del giudice penale nella definizione della pena e gli automatismi sanzionatori

CORSO DOTTORATO SCIENZE MANAGERIALI E ATTUARIALI

BELFANTI NICOLE
Lean Management come cambiamento organizzativo: le persone contano

CARZEDDA MATTEO
Agrifood systems and sustainability: The role of Alternative Food Networks

DAN NELU
Sentence-based Topic Models Aspect Discovery and Latent Aspect Regression Rating

SLONIMSKAYA ANASTASIYA
Public-private partnership (PPP) in CIS countries – (hard) work in progress

CORSO DOTTORATO STUDI LINGUISTICI E LETTERARI

GESIOT JACOPO
Lelio Manfredi traduttore: la ricezione delle letterature iberiche nell'Italia del primo '500

GIRO ALESSANDRA
I personaggi migranti e la narrazione in prima persona nella letteratura italiana 2001-2014

SIANO PAOLA
Il carteggio Michele Barbi - Ernesto Giacomo Parodi (1895-1922). Personalità, studi e problemi verso la «Nuova Filologia»

CORSO DOTTORATO STUDI STORICO ARTISTICI E AUDIOVISIVI

BONANOMI MATTEO MIRKO
La decorazione pubblica in Italia tra Unità e Prima guerra mondiale

DOTTO SIMONE
Un moderno sentire. Culture dei media sonori nell'Italia tra le due guerre.

PASCALE GUIDOTTI MAGNANI CATERINA
I Guidotti tra arte e società a Bologna (XVI-XVIII secolo)

PERIN CHIARA
Realismo in Italia, 1944-1954

SIARDI MASSIMO
Nuove prospettive per il Digital Heritage italiano tra il 2010 e il 2015

SCIENZE DELLA VITA LIFE SCIENCES

CORSO DOTTORATO SCIENZE E BIOTECNOLOGIE AGRARIE

CAPPELLETTI MARTINA
Development and assessment of plant protein hydrolysates as biopesticides against zucchini powdery mildew

COLUSSI ALICE
Salivary cortisol: a marker of the adaptive response of the dog to different environmental stimuli

DE MORI GLORIA
Fine physical mapping of a resistance region to Sharka (Plum Pox Virus) in apricot

NARDIN TIZIANA
Study of alpine herb alkaloid profiles and research of milk traceability markers by high resolution mass spectrometry

NIKULINA ANNA
Rumen utilization of urea-based feeds by in vitro studies

POLANO CESARE
Next-Generation-Sequencing Metagenomic Analysis of Phytopathogenic Prokaryotes

RUOCCO SILVIA
Improvement of chemical quality index of wines from interspecific hybrids

TACOLI FEDERICO
Grapevine pest management through natural compounds and agronomic practices

Lotta contro i fitofagi della vite con sostanze di origine naturale e pratiche agronomiche

ZULIANI ANNA
Il benessere della bovina da latte: un'opportunità per produttori e consumatori

CORSO DOTTORATO SCIENZE BIOMEDICHE E BIOTECNOLOGICHE

BIASUTTI LEA
Oxidative metabolism during wheelchair propulsion tests in patients with spinal cord injury: effects of lesion level

CANTARUTTI CRISTINA
Citrate-stabilized gold nanoparticles hinder fibrillogenesis of a pathological variant of β 2-microglobulin

CUTANO VALENTINA
Investigating the role of HDAC7 in the control of mammary gland morphogenesis and transformation

DE ZUANI MARCO
Mast cells during *Candida albicans* infections: new insights for an old player in fungal clearance

DONGMO FOUUMTHUIM CEDRIX JURGAL
Molecular dynamics simulations of β 2-microglobulin interaction with hydrophobic surfaces

MALFATTI MATILDE CLARISSA
Repair of modified ribonucleotides embedded in DNA

MIGLIETTA GIULIA
Development of anti-cancer therapies targeting RAS oncogene through non-canonical RNA structures.

TECNICO SCIENTIFICA PHYSICAL SCIENCES AND ENGINEERING

CORSO DOTTORATO INFORMATICA E SCIENZE MATEMATICHE E FISICHE

ANTICOLI LINDA
Entangle: from Quantum Programming to Quantum Model Checking

BASALDELLA MARCO
Extracting (key)technical terms from scientific documents

LISSI DAVIDE
Pseudospectral methods for the stability of linear periodic delay models

PERESANO MICHELE
Very high zenith angle observations of the Crab Nebula with MAGIC telescopes

SILVETTI SIMONE
Verification and Validation of Complex Systems

SOVRANO ELISA
Multiplicity of positive solutions for indefinite Neumann problems

CORSO DOTTORATO INGEGNERIA INDUSTRIALE E DELL'INFORMAZIONE

ARRIGONI FEDERICA
Synchronization of Multiple Views

BADAMI OVES
Numerical Modeling of Multigate nano-FETs

BANDIZIOL ANDREA
Design of an interface for high-speed serial links in automotive micro-controller

CITOSI MARCO
Biomass Characterization for Solar Pyrolysis

GANIS ALEXANDER RUDOLF
Architectures and Algorithms for the Signal Processing of Advanced MIMO RADAR Systems

KAPIDANI BERNARD
Explicit Time-Domain Full Maxwell Solvers over Tetrahedral Grids

KRAS ALEKSANDER
Flywheel Inertial Transducer For Energy Harvesting And Vibration Control

PESSOT ELENA
La Valutazione della Complessità nei Progetti e l'Influenza sull'Apprendimento

TURCO EMANUELE
Noise and vibration control of cylindrical structures with tuneable vibration absorbers

VACI LUBOS
Context-Based Goal-Driven Reasoning for Improved Target Tracking

YAKUSHEVA NADEZDA
An ADAS Design Based on IoT V2X Communications

ZIENTEK MICHAL WLADISLAW
Metamaterial panel with piezoelectric patches connected to multi-resonant electrical shunts

CORSO DOTTORATO SCIENZE DELL'INGEGNERIA ENERGETICA E AMBIENTALE

AHMADI SOMAYEH
Wall transform mechanism in a viscosity stratified turbulent flow

GAGLIARDI ANDREA
Structured Approach to the Failure Analysis

MASSOLINO GIULIA
Methodological proposal for the preliminary dynamic assessment of soil-structure interaction on energy production and distribution facilities through ambient vibration tests

PAGNACCO FABIO
Analisi delle prestazioni termiche in sistemi di raffreddamento avanzati di palette di turbine a gas

ROCCON ALESSIO
Coalescence & breakage of drops in turbulence

SUZZI NICOLA
Numerical Simulation of Thin Film Breakup on Non-wettable surfaces

TOSO ALESSANDRA
Pd/CeO₂ based catalysts: resistant materials for methane emissions abatement from NGVs

VECLANI DANIELE
Nano Strutture per Macro Problemi: Nano-Tubi di Carbonio per la Rimozione di Antibiotici



UNIVERSITÀ
DEGLI STUDI
DI UDINE
hic sunt futura



Centro di Ricerca e di Trasferimento Tecnologico



FONDAZIONE
FRIULI

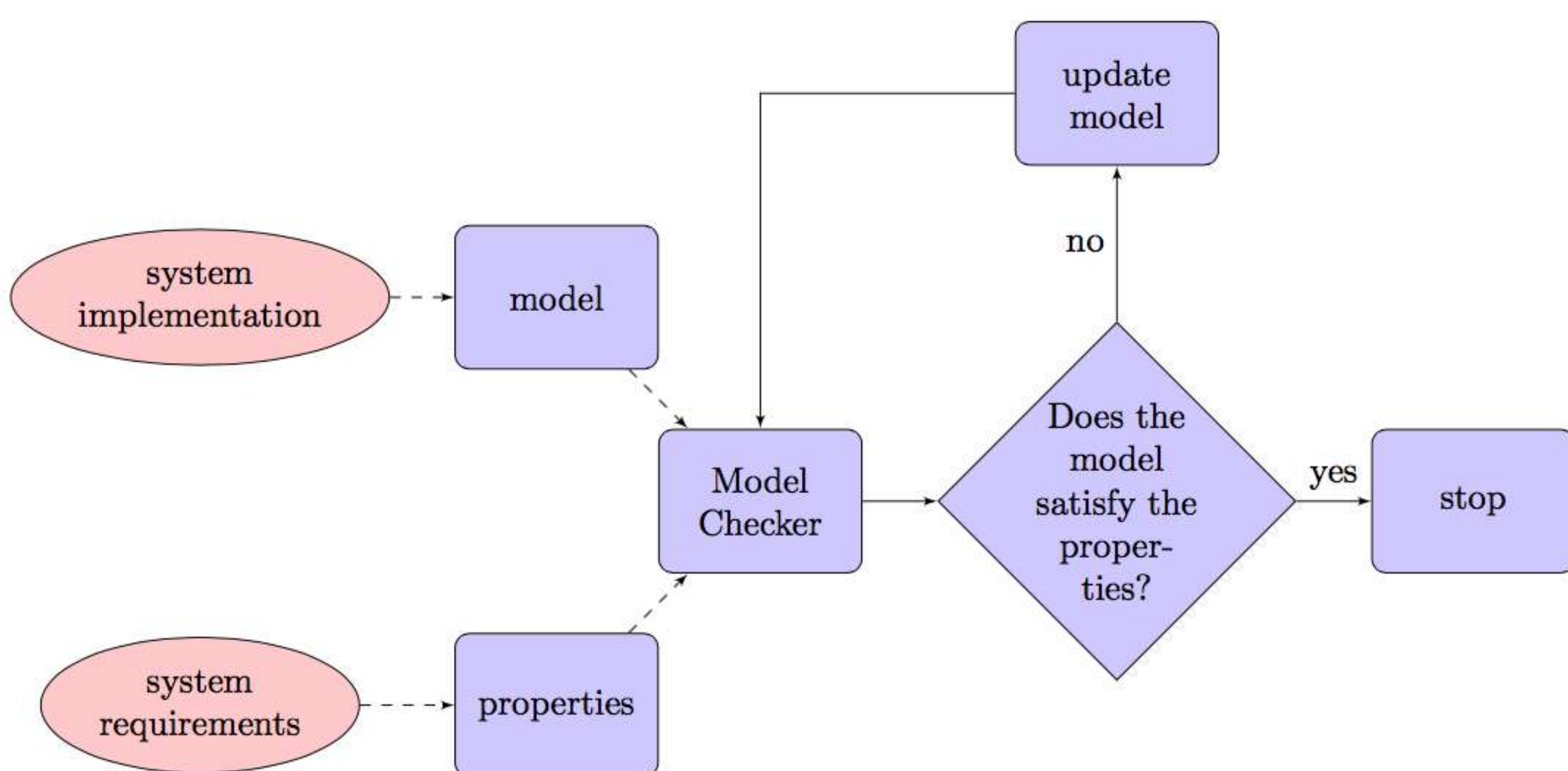
Entangle: from Quantum Programming to Quantum Model Checking

Model Checking

Model checking is an automatic technique for verifying correctness properties of a system. In order to perform such a verification we need:

- Modelling languages to describe the system;
- Specification languages to formulate the properties;
- Algorithms for the verification process.

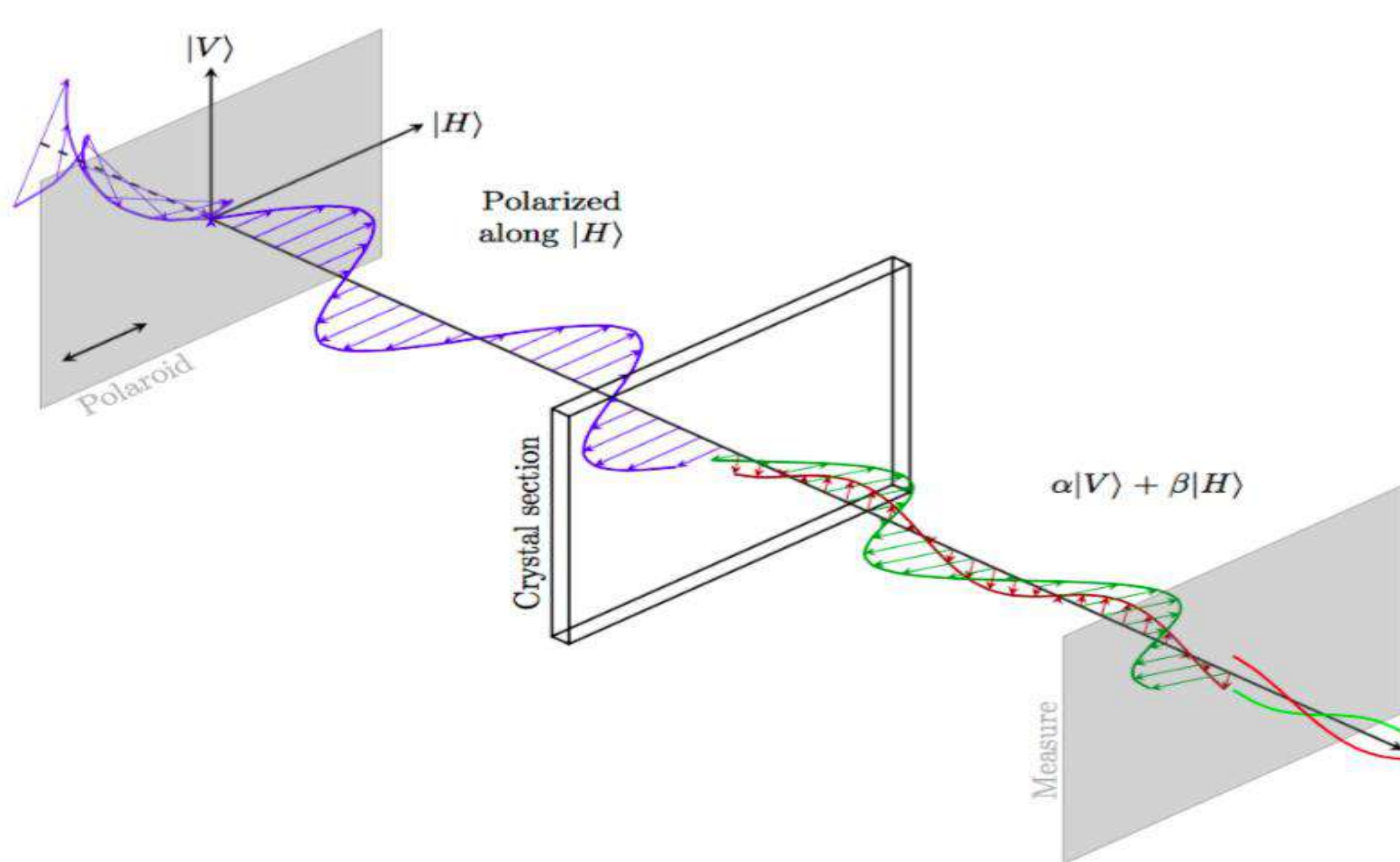
The whole process can be summarized as follows:



Quantum Computation

Quantum computing is a theoretical, inherently probabilistic model of computation based on *the rules of quantum physics*. The basic unit of computation is the *qubit*, which can take value 1, 0 as a classical bit, or both values at the same time:

$$|\psi\rangle = \alpha|0\rangle + \beta|1\rangle$$



Dott. Linda Anticoli
Prof. Carla Piazza
Prof. Paolo Zuliani

Info:

Indirizzo mail:
 anticoli.linda@spes.uniud.it

Indirizzo mail:
 carla.piazza@uniud.it

Riferimenti bibliografici

Towards Quantum Programs
 Verification: From Quipper Circuits
 to QPMC- L. Anticoli · C. Piazza · L.
 Taglialegna · P. Zuliani

Riconoscimenti

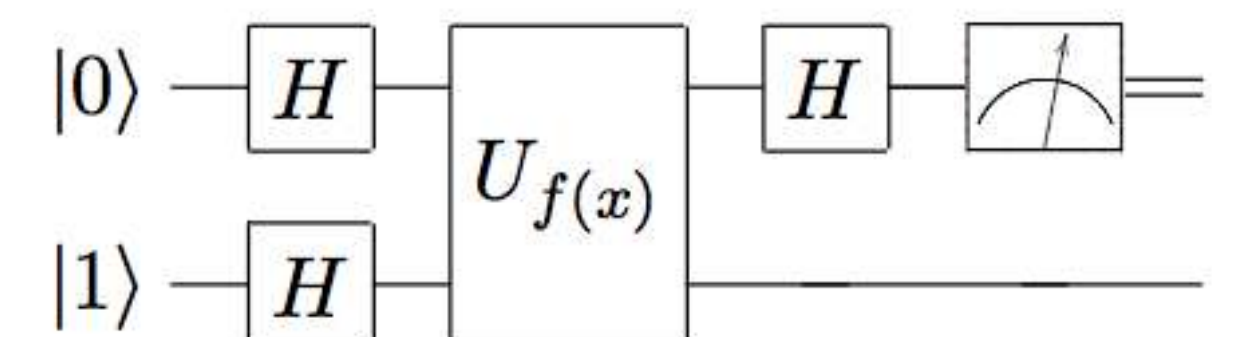
This work has been partially
 supported by the GNCS group of
 INdAM.

Wavelike effects such as *superposition*, *interference* and *entanglement* allow us an important speedup for difficult computational problems plus a more reliable cryptography.

Quantum Algorithms Programming and Verification

Quantum algorithms are represented as quantum circuits. Recently these can be encoded using quantum programming languages, such as *Quipper*.

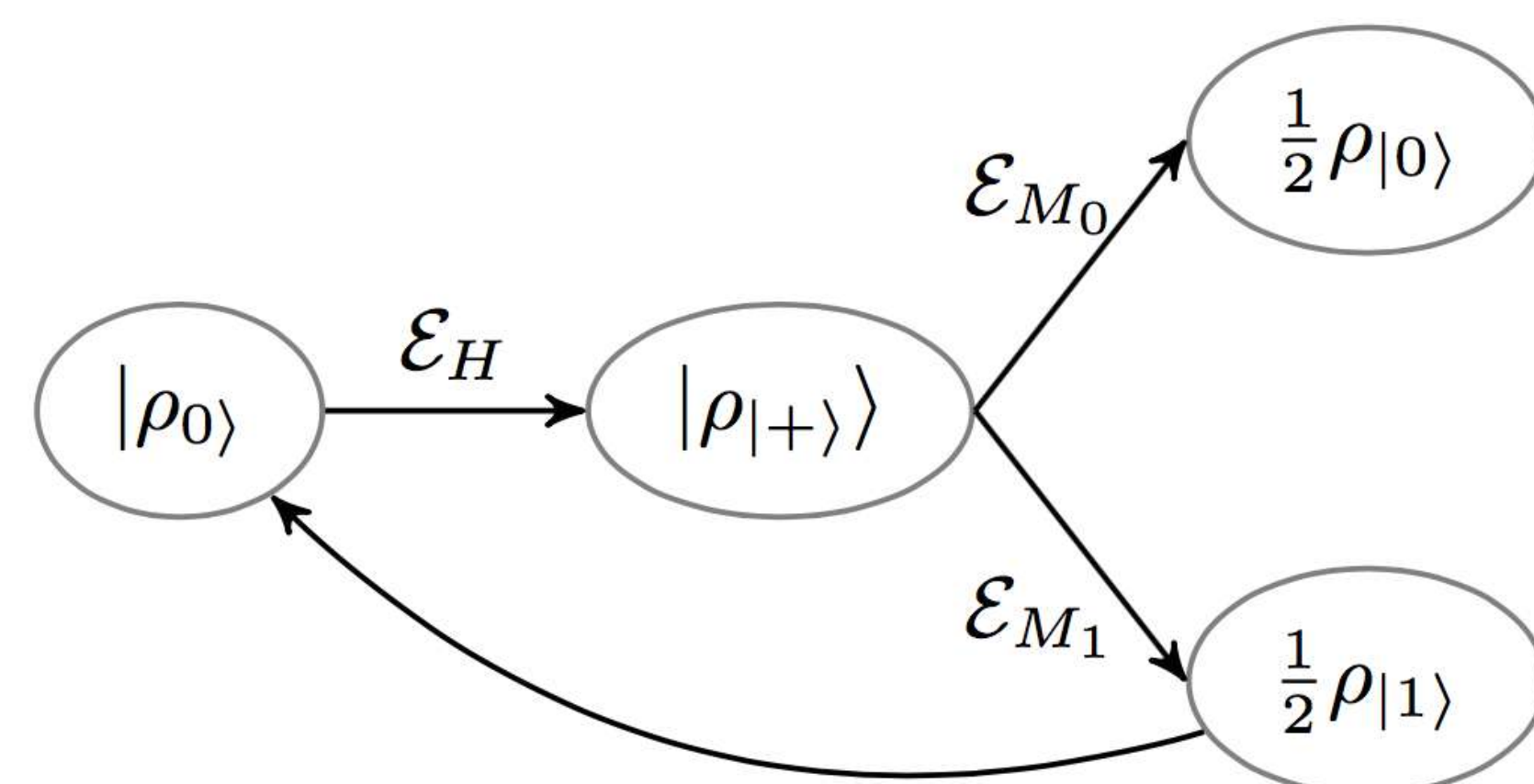
```
deutsch :: (Qubit, Qubit) -> Circ
  Bit
deutsch (q1, q2) = do
  hadamard q1
  hadamard q2
  Gate(U) (q2, q1)
  hadamard q1
  measure q1
```



We developed a framework, Entangle, that allows us to translate the Quipper code into a formal verification language, QPMC, that performs model checking on quantum algorithms, represented as Superoperator weighted Quantum Markov Chains.

The tool is available at <https://github.com/miniBill/entangle>.

Lately, we provided an extended version allowing also the translation of (tail) recursive quantum programs, i.e., programs in which there are loops, with the conditional branches depending on the measurements outcomes.



We are investigating on interesting properties to be verified on this representation of quantum programs.

Extracting (key|technical) terms from scientific documents

Introduction

The number of academic papers published each year is growing at a fast pace, posing a serious issue to scholars looking for relevant information for their research.

For example, as of 2015, we have [1]:

- 28,100 English language and 6,450 non-English language journals;
- 2,5 million articles published in journals each year (i.e. excluding conference papers) in the Scientific, Technical, and Medical fields
- An annual growth rate of journals and articles published in journals between 3% and 3.5%.

In our laboratory, we worked with two different approaches for extracting relevant information from this huge body of data: keyphrase extraction and technical term extraction.

Keyphrase Extraction

Automatic Keyphrase Extraction (AKE) is the task of finding phrases of one or more words that capture the main topics of a document [2]. For example, if our document is:

“Marco is a researcher in the field of artificial intelligence. His latest research was conducted in the Artificial Intelligence Lab at the University of Udine.”

The possible keyphrases may be **Marco, researcher, Artificial Intelligence**.

Biomedical Term Extraction

On the other hand, we can choose to extract only the terms that belong to a specific field, using a technique called Technical Term Extraction (TTE). For example, in the biomedical domain, an example document may be:

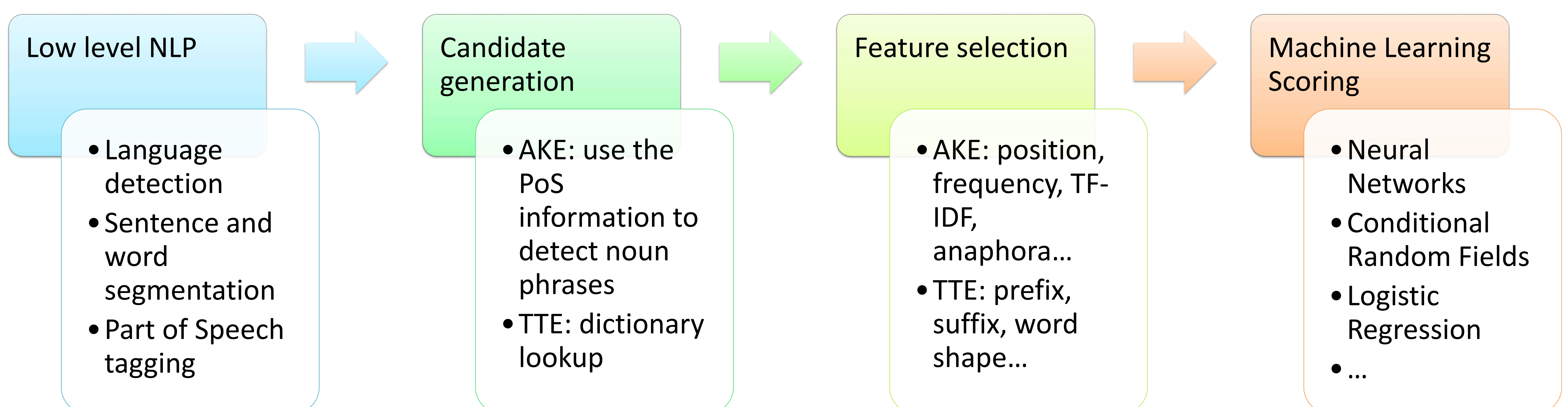
“Glaucoma is a leading cause of blindness but its molecular etiology is poorly understood. Glaucoma involves retinal ganglion cell death and optic nerve damage that is often associated with elevated intraocular pressure (IOP).”

The technical terms are **glaucoma, blindness, retinal ganglion cell, and optic nerve**.

The extraction pipeline

Keyphrases and technical terms are extracted using the pipeline described in figure. In both approaches, the possible key and technical terms (the *candidates*) and their features are handed to a machine learning (ML) classifier that, after being trained on a specific corpus, selects the correct (key|technical) terms only. The main differences are:

- AKE: the candidate terms are all the noun phrases, and the features used in the ML step are tailored to reflect their importance in the document: frequency, position, number of terms that reference them... [3]
- TTE: we choose the candidate terms from domain ontologies, and the ML features reflect their importance in the domain: prefixes, affixes, number of capital letters, of symbols... [4]



Dott. Marco Basaldella
Prof. Carlo Tasso

Info:

Tel. +39 0432 558446
marco.basaldella@uniud.it
carlo.tasso@uniud.it

Riferimenti bibliografici

- [1]: Mark Ware, Michael Mabe. "The STM Report, 4° edition". International Association of Scientific, Technical, and Medical Publishers, 2015.
- [2]: P. D. Turney, "Learning algorithms for keyphrase extraction", Information Retrieval, vol. 2, no. 4, pp. 303-336, 2000.
- [3]: Marco Basaldella, Giorgia Chiaradia, and Carlo Tasso. "Evaluating Anaphora and Coreference Resolution to improve Automatic Keyphrase Extraction". Proceedings of the 26th International Conference on Computational Linguistic (COLING 2016), Osaka (Japan).
- [4]: Marco Basaldella, Lenz Furrer, et al. (2016). "Using a Hybrid Approach for Entity Recognition in the Biomedical Domain". Proceedings of the 7th International Symposium on Semantic Mining in Biomedicine, Potsdam (Germany)

Pseudospectral methods for the stability of linear periodic delay models

Motivation

A delay equation determines the future evolution of a quantity based not only on its present value, but also on its past values. Delay equations are used in various fields of science, including biology, engineering, physics and climatology. In many applications the interest is in the long time behavior of the system, which naturally leads to studying the stability of certain solutions of the equations. Periodic solutions are of fundamental importance in many applications; see [4] for an example in population dynamics.

Delay equations give rise to infinite-dimensional dynamical systems, hence the need to discretize them (in the present work with pseudospectral techniques) in order to obtain a finite-dimensional problem.

Pseudospectral methods

Pseudospectral methods rest on a simple key idea: when computing something about a function, use an interpolating polynomial instead. Their main advantage is the phenomenon of spectral accuracy: if the function is smooth, then the error vanishes faster than any polynomial in the number of nodes.

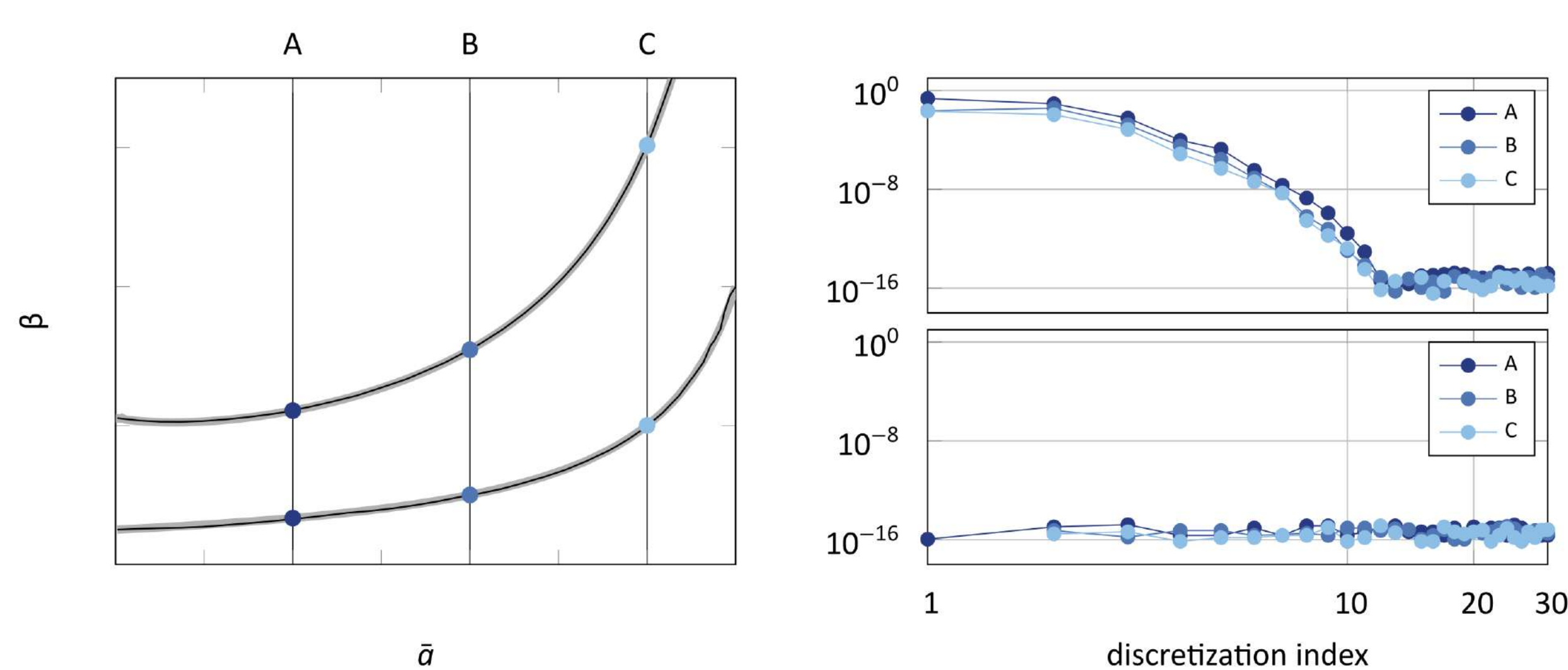
Pseudospectral methods for studying the stability of equilibria and periodic solutions of Delay Differential Equations (DDE) [3] and of equilibria of Renewal Equations (RE) and coupled RE/DDE have been recently developed [2]. The present work extends the method for the stability of periodic solutions of DDE to RE and coupled RE/DDE, i.e., equations of the type

$$\begin{cases} x(t) = F(x_t, y_t), \\ y'(t) = G(x_t, y_t), \end{cases}$$

where x_t and y_t are the past-to-current histories of x and y .

Theory

Linearizing a nonlinear coupled RE/DDE around a periodic solution yields a linear equation with time-periodic coefficients. Floquet theory for DDE proves that the stability of the solution depends on the eigenvalues of the monodromy operator, i.e., the operator that advances the solution forward one period.



Dott. Davide Liessi
Prof. Dimitri Breda

Info:

Tel. +39 0432 558401
liessi.davide@spes.uniud.it

An analogous Floquet theory for RE and coupled RE/DDE is still missing; its development is work in progress with O. Diekmann and S. M. Verduyn Lunel (U. Utrecht).

Numerics

Applying a pseudospectral discretization to the infinite-dimensional monodromy operator after a convenient reformulation provides a finite-dimensional approximation, i.e., a matrix, whose eigenvalues can be computed using standard methods. As a fundamental result, we rigorously proved that the eigenvalues of the monodromy operator are approximated by the eigenvalues of its discretization with spectral accuracy.

Application 1: logistic *Daphnia* (coupled RE/DDE) [2]

First figure: stability chart for the nontrivial equilibrium of

$$\begin{cases} b(t) = \beta S(t) \int_{\bar{a}}^4 b(t - \theta) d\theta, \\ S'(t) = S(t)(1 - S(t)) - S(t) \int_{\bar{a}}^4 b(t - \theta) d\theta. \end{cases}$$

The curves approximate the boundaries of the positivity (lower curves) and stability (upper curves) regions. The gray curves are obtained analytically (lower) and numerically with [2] (upper), the black ones with the present method.

Second figure: errors on the 0 real part of the leading eigenvalue along the upper (top) and lower (bottom) curves.

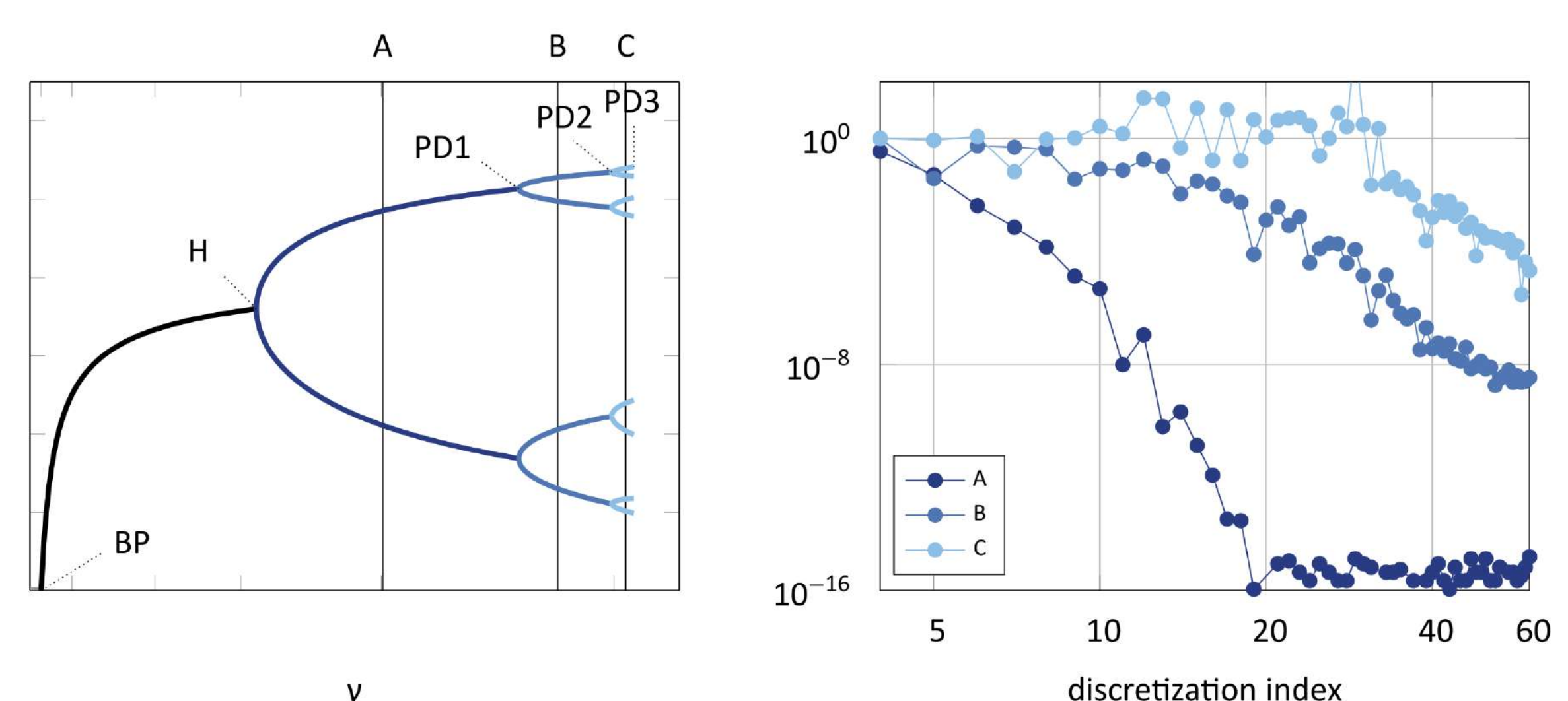
Application 2: RE with quadratic nonlinearity [1]

Third figure: bifurcation diagram of

$$x(t) = \frac{\gamma}{2} \int_1^3 x(t - \theta)(1 - x(t - \theta)) d\theta.$$

The stable equilibria and the local extrema of stable periodic solutions are plotted. The stability is studied with [2] for equilibria and with the present method for periodic solutions.

Fourth figure: errors on the known eigenvalue 1 of the monodromy operator.



References

- [1] Breda, Diekmann, Liessi, and Scarabel, *Numerical bifurcation analysis of a class of nonlinear renewal equations*, Electron. J. Qual. Theory Differ. Equ., 65 (2016), pp. 1–24.
- [2] Breda, Diekmann, Maset, and Vermiglio, *A numerical approach for investigating the stability of equilibria for structured population models*, J. Biol. Dyn., 7 (2013), pp. 4–20.
- [3] Breda, Maset, and Vermiglio, *Stability of linear delay differential equations. A numerical approach with MATLAB*, Springer Briefs in Control, Automation and Robotics, Springer, New York, 2015.
- [4] McCauley, Nelson, and Nisbet, *Small-amplitude cycles emerge from stage-structured interactions in *Daphnia*-algal systems*, Nature, 455 (2008), pp. 1240–1243.



UNIVERSITÀ
DEGLI STUDI
DI UDINE
hic sunt futura

PHYSICAL SCIENCES AND ENGINEERING

30° ciclo

Corso di dottorato in Informatica e Scienze
Matematiche e Fisiche

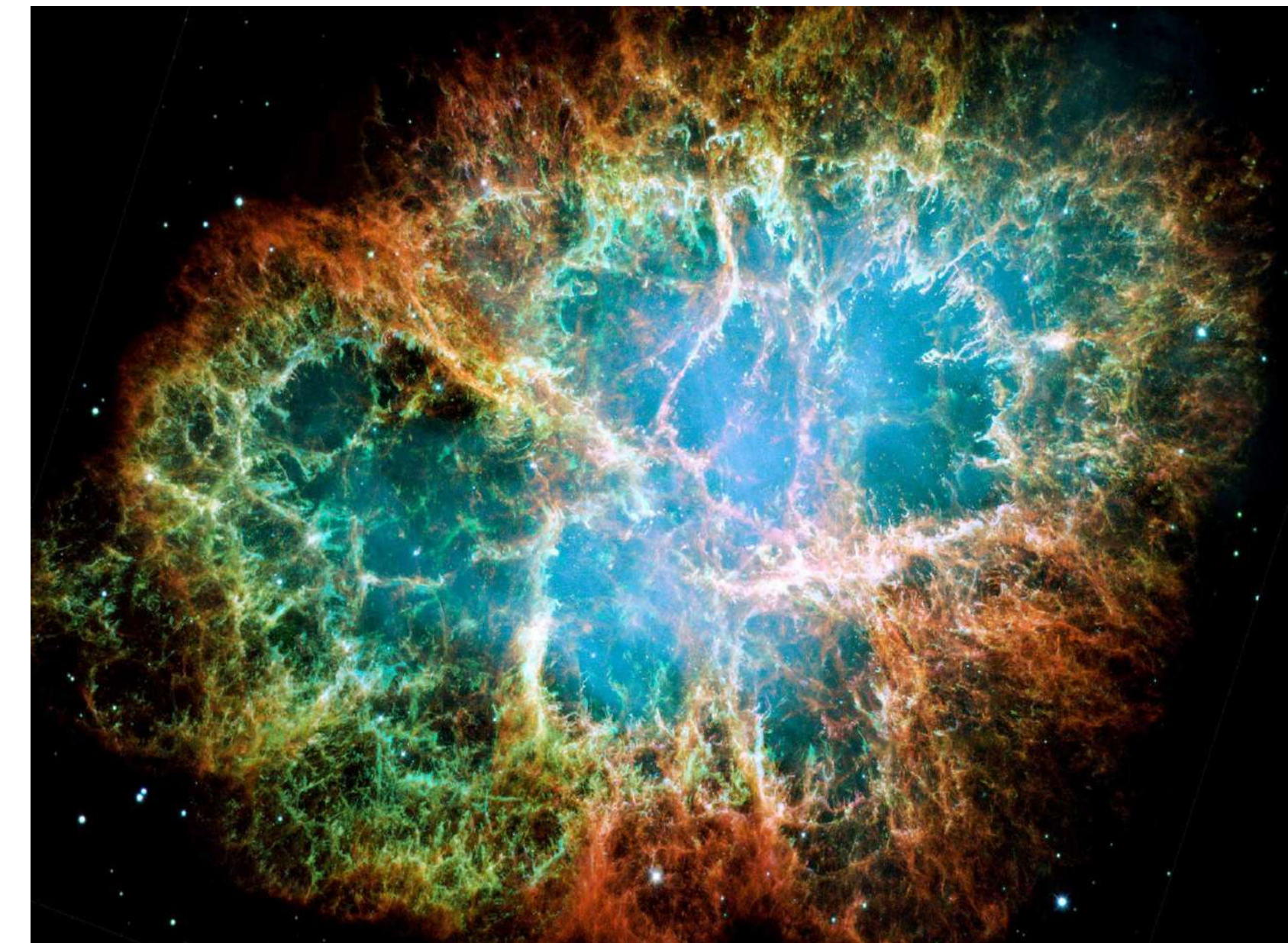
Very high zenith angle observations of the Crab Nebula with the MAGIC telescopes

The MAGIC telescopes exploit the cosmic gamma ray light impacting our atmosphere to monitor the night sky at very high energies (VHE, with 10^{12} eV = 1 TeV). VHE photons and particles, collectively known as cosmic rays, by impacting the atmosphere, generate showers of particles that develop downwards. While propagating, these particles cause the emission of a specific (Cherenkov) radiation, that is finally measured by the telescopes. Shower properties change when shifting from the Zenith to the horizon. Exploiting such changes we aim to measure the highest energy particles. Our current research focuses on the largest zenith-angle-observations ever ($>70^\circ$), and the technical challenges to be met in order to optimize the data analysis. This will allow us to understand relevant systematics of our instruments in such conditions, and in perspective, to enhance the sensitivity of MAGIC and to improve science results.



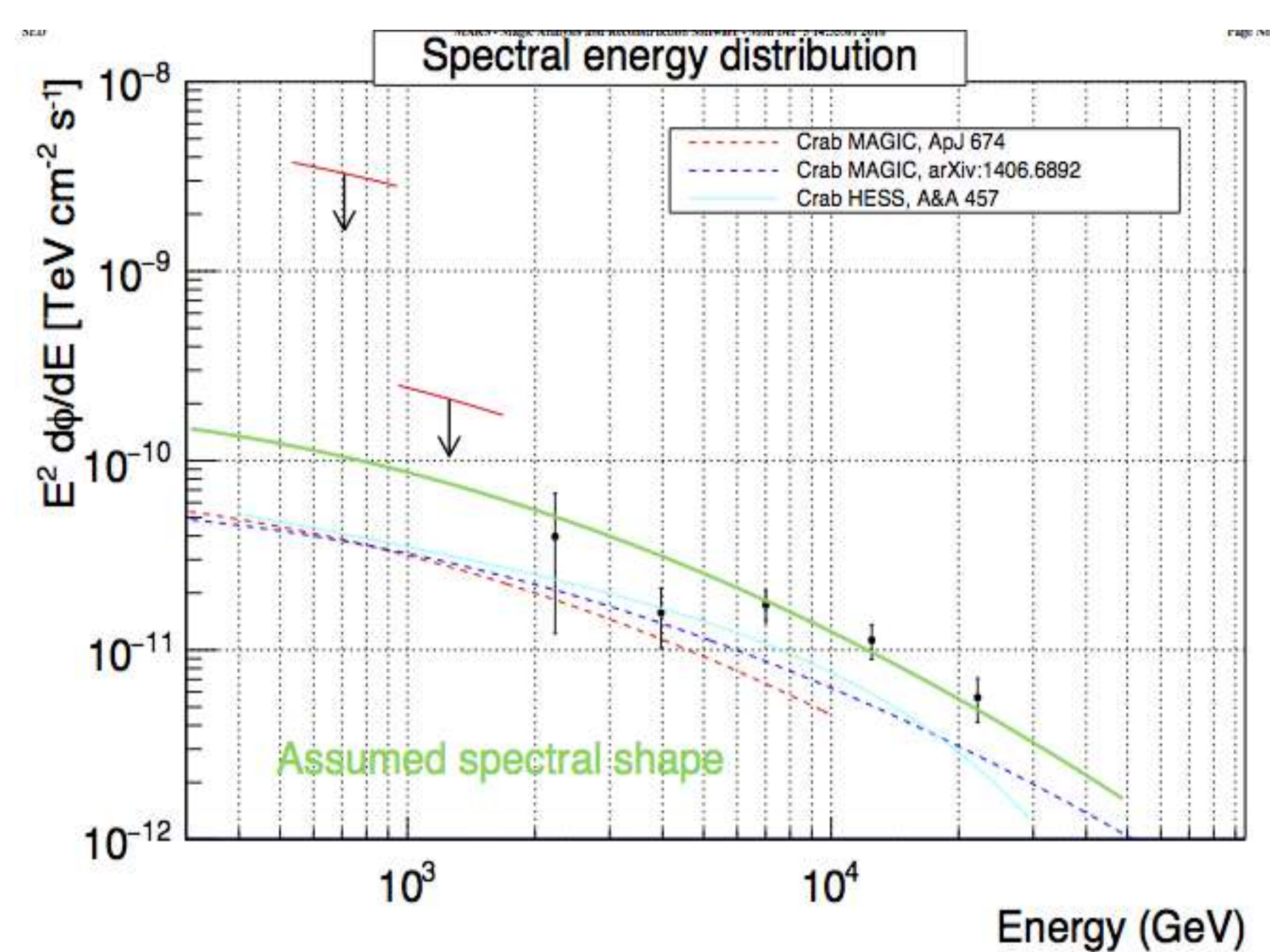
The MAGIC telescopes

They work in pair on the Canary island of La Palma, making stereoscopic images of the showers¹. Light is projected by mirrors into a camera, where it is converted in electrical signals. Information about the cosmic particles is reconstructed by analyzing the projected images of the showers.



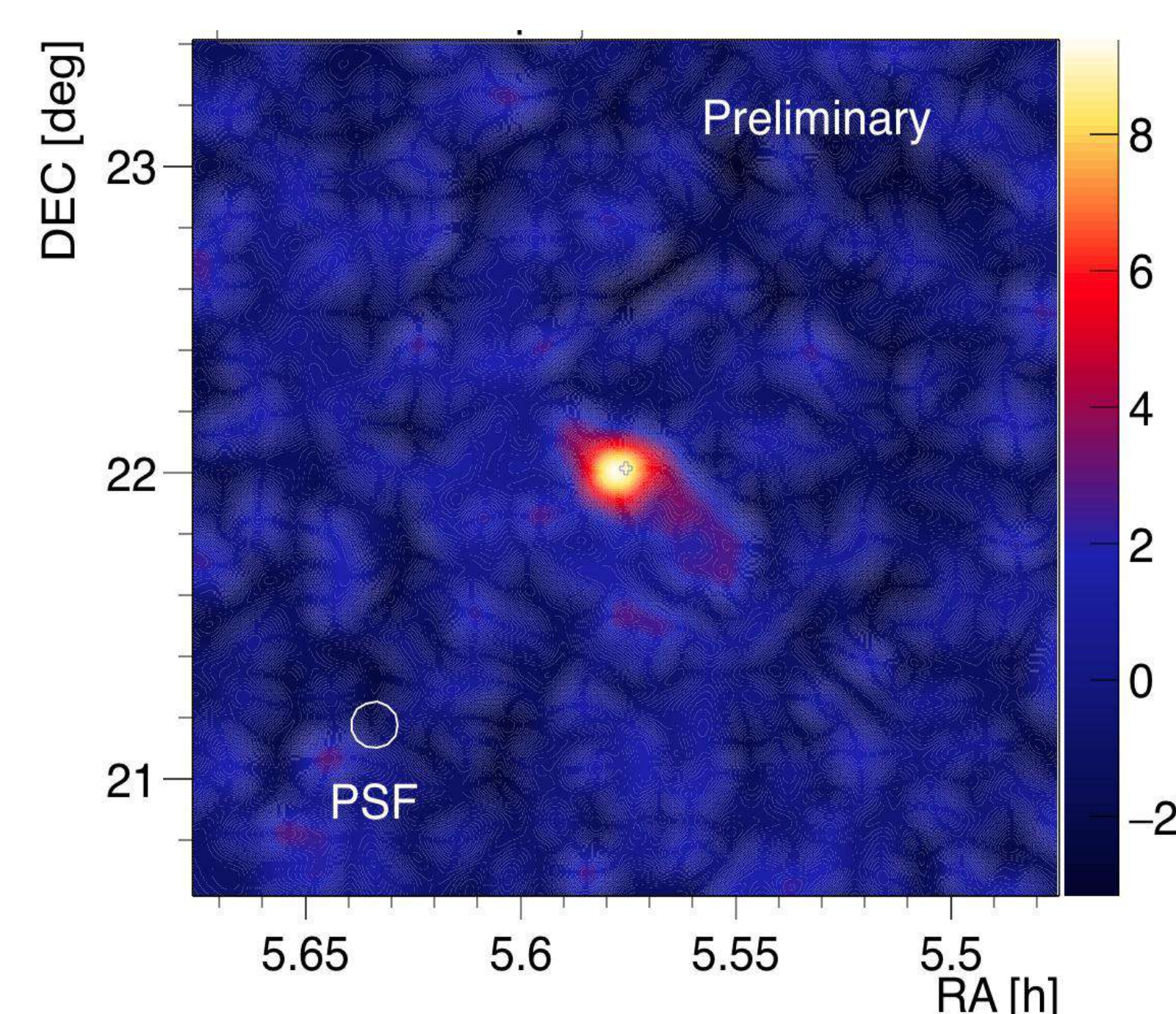
The Crab Nebula

A supernova remnant $\sim 6,500$ light years away², it is a powerful source of gamma rays. Here it is shown as seen by the Hubble Space Telescope in the optical. At its center lies a rotating neutron star, emitting radiation from radio to gamma-rays. The surrounding material gets heated, and particles are accelerated to high energies. Gamma-ray astrophysics studies the underlying acceleration mechanism.



Our preliminary observations

Left: Energy flux per energy interval, compared with radiation models of the source; scarce signal values are given as upper limits. We improve previous observations by a factor 2³, reaching energies > 20 TeV. The reason is twofold. Observing at higher zenith angles allows us to increase the area on which photons can be detected. Furthermore the latter are on average more energetic, because showers cross more atmosphere to reach us. Thanks to this, the source's astrophysics may be tested beyond energies currently probed. *Right:* Signal in gamma-rays; note how images of the same object at different wavelengths change (see upper right image), reflecting different physics. A signal level of at least 5 standard deviations is required for detection, while minor values are compatible with background fluctuations.



Riferimenti bibliografici

1. Aleksić, J. et al. The major upgrade of the MAGIC telescopes, Part I: The hardware improvements and the commissioning of the system. *Astropart. Phys.* 72, 61–75 (2016).
2. Hester, J. J. The Crab Nebula: An Astrophysical Chimera. *Annu. Rev. Astron. Astrophys.* 46, 127–155 (2008).
3. Aleksić, J. et al. The major upgrade of the MAGIC telescopes, Part II: A performance study using observations of the Crab Nebula. *Astropart. Phys.* 72, 76–94 (2015).

Dott. Michele Peresano*
Prof. Barbara De Lotto*

* also INFN Trieste – gruppo collegato di Udine

Info:

Tel. +39 0432 558209

peresano.michele@spes.uniud.it

barbara.delotto@uniud.it



**UNIVERSITÀ
DEGLI STUDI
DI UDINE**
hic sunt futura

PHYSICAL SCIENCES AND ENGINEERING

30° ciclo

**Corso di dottorato in Informatica e Scienze
Matematiche e Fisiche**

Verification and Validation of Complex Systems

Introduction

The verification and validation of complex system has a crucial role in the design of Cyber-Physical Systems (CPS). The model based development technique is widely used to build a «in silicio» model of a real products and the modelchecking techniques with the purpose of quality assurance are currently used. Unfortunately the complexity of the model increased so much that the standard verification techniques are no more efficient. For this reason the falsification approach is considered a viable approach to quality assurance as described in [1]

The Falsification Approach

Considering a system M with its input domain D and a specification ϕ (described by means of Signal Temporal Logic). We can define two problems:

- **Falsification:** find a counterexample i.e an input values x in D such that the corresponding output $M(x)$ violates the specification ϕ
- **Coverage:** find a subset of counterexamples which is homogeneously distributed in the falsification area and which represents all the possibile falsification path existing in the CPS.

Considering that in the industrial world the simulation of a CPS could be extremely expensive, the main challenge is to define an algorithm which is able to solve the *Falsification* and *Coverage* problem with few simulations. A standard approach consists in setting up and optimization process with the aim of minimizing the robustness semantics associated to the specification ϕ . An output which has a negative robustness entails that the specification is violated, for this reason the standard approach consists in solving:

$$\rho' = \min(\rho(\phi, M(x), 0))$$

With the purpose of verifying if

$$\rho' < 0.$$

Active Learning & Machine Learning

The use of active learning approach has been partially explored in [2], but an exhaustive study has not been performed yet. We have decided to follow a slightly different approach.

Instead of iteratively approximate the robustness with the purpose of function minimization (i.e. estimating ρ'), we use the Gaussian Processes regression to approximate the probability that a new input will generate an output with negative robustness, i.e. the probability $P(x \in S)$ where

$$S = \{x \in D \mid \rho(\phi, M(x), 0) < 0\}$$

Considering a train set formed by the couple input - robustness evaluation $K = \{(x_i, \rho(\phi, M(x_i), 0))\}_{i \leq n}$ (representing the partial knowledge we have collected after n iterations) and a Gaussian process which has been trained on K :

$$f_K = GP(m_K(x), \sigma_K(x, x'))$$

We can easily estimate:

$$P(x \in S) = \Phi(-m_K(x)/\sigma_K(x, x))$$

Which has to be intended as a description of our uncertainty in the Gaussian Processes reconstruction that the function assumes a negative value than a property of the function itself, which is usually deterministic. Φ is the cumulative distribution of the standard normal distribution.

Finally this probability estimation is used to iteratively sample homogeneously distributed points in the predicted falsification area. Clearly with the increase of the iterations the algorithm converges to the real falsification area.

This sampling approach entails that the absolute values of the robustness does not affect the procedure i.e. two inputs both falsifying the specification are considered without preferring the one with lower robustness value.

The last implication is extremely important if we are interested in finding multiple counterexamples.

Dott. Simone Silveti
Prof. Alberto Policriti
Prof. Luca Bortolussi

Info:

silveti.simone@spes.uniud.it
silveti@esteco.com

Bibliography

- [1] Annpureddy, Yashwanth, et al. "S-talro: A tool for temporal logic falsification for hybrid systems." *International Conference on Tools and Algorithms for the Construction and Analysis of Systems*. Springer Berlin Heidelberg, 2011.
- [2] Akazaki, Takumi. "Falsification of Conditional Safety Properties for Cyber-Physical Systems with Gaussian Process Regression." *International Conference on Runtime Verification*. Springer International Publishing, 2016.

Acknowledgements

Thanks to Esteco Spa for funding my PhD



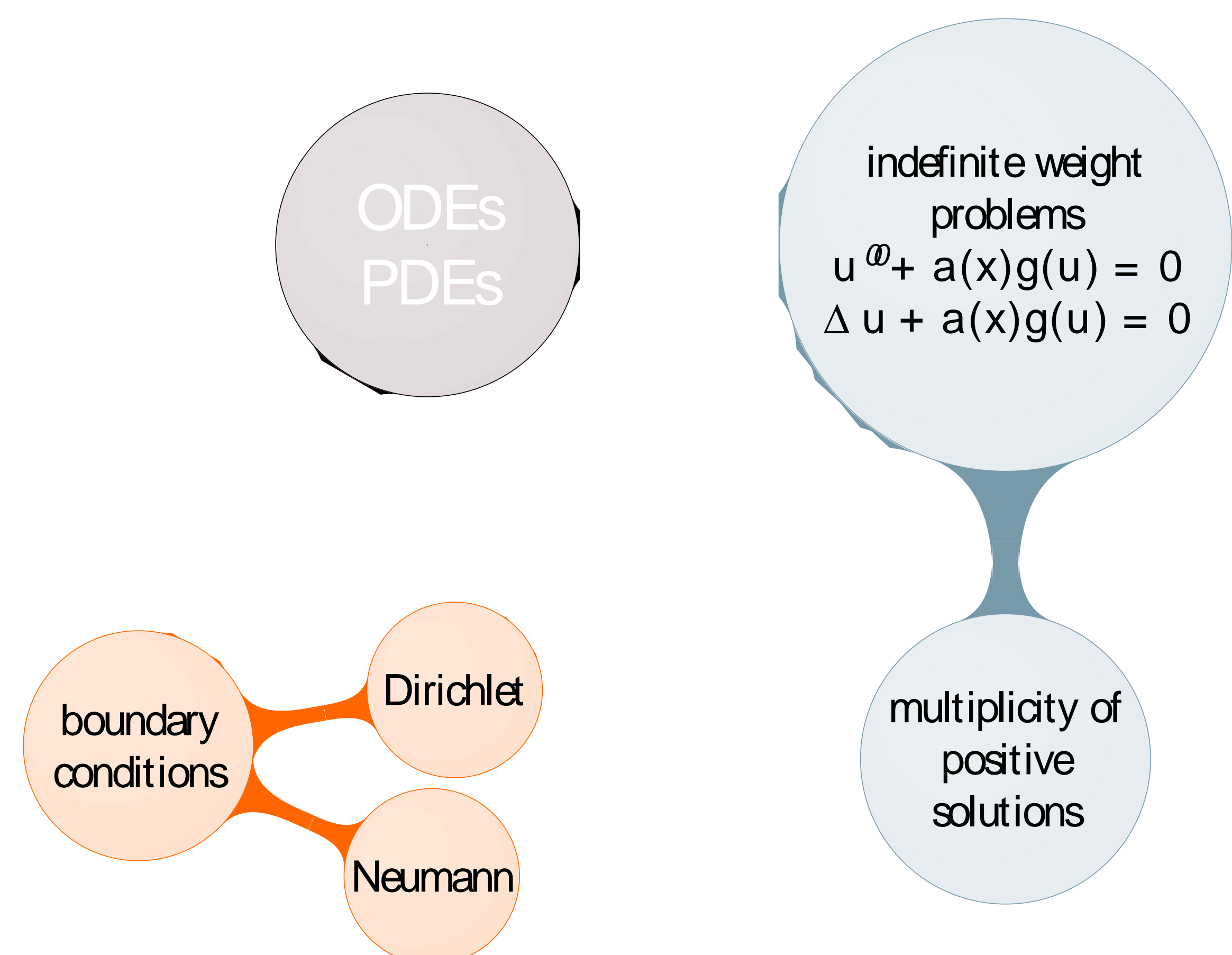
**UNIVERSITÀ
DEGLI STUDI
DI UDINE**
hic sunt futura

PHYSICAL SCIENCES AND ENGINEERING

30° ciclo

**Corso di dottorato in Informatica e Scienze
Matematiche e Fisiche**

Multiplicity of positive solutions for indefinite Neumann problems



Introduction

The study of Neumann problems *with an indefinite weight* is a relevant topic in nonlinear analysis. Natural applications arise in various fields of applied mathematics as biomathematics, population dynamics and reaction-diffusion processes. The interest on these problems can be traced back to 1948 with the paper of Haldane on the field of population genetics. The feature "with an indefinite weight" indicates the presence of a factor in the nonlinear term of the differential equation that changes its sign. Usually such kind of boundary value problems read as:

$$(\mathcal{N}) \quad \begin{cases} \Delta u + a(x)g(u) = 0 & \text{in } \Omega \\ \frac{\partial u}{\partial n} = 0 & \text{on } \partial\Omega \end{cases}$$

where $\Omega \subseteq \mathbb{R}^N$ with $N \geq 1$, $a(x)$ is the weight and $g(u)$ is the nonlinearity characterizing the problem. Depending on the assumptions made on $g(u)$ two open problems are solved in the present work.

Objectives

Looking for *positive solutions* of indefinite Neumann boundary value problems associated with nonlinear ODEs and PDEs. Our main purpose is about *multiplicity results* for the problem (\mathcal{N}) in the two cases that the nonlinearity:

- satisfies the hypotheses of the conjecture of Lou and Nagylaki (2002),
- or
- has an oscillatory potential.

Method

The framework involves a weight $a(x)$ such that it has exactly one "positive hump" and one "negative hump". The proofs are based on a topological argument called shooting method (see Fig. 1). This approach works with ODEs and relies on the study of the deformation of a planar curve under the action of the vector field associated to the second order scalar differential equation of the boundary value problem.

Conclusions

We have found new multiplicity results of positive solutions for two different indefinite Neumann problems. The results potentially will lead to further developments e.g., the stability/instability of steady states of reaction diffusion equations and what will be the minimal assumptions on the nonlinearity so that the uniqueness result holds.

Dott. Elisa Sovrano
Prof. Fabio Zanolin

Info:

Tel. +39 0432 558401
sovrano.elisa@spes.uniud.it

Results

- A negative answer to the conjecture of Lou and Nagylaki that guesses uniqueness of a positive solution is given in [1], taking into account the achievements obtained in [2]. In particular, numerical evidence of multiple positive solutions is obtained in the case of the example below.
- Multiplicity of positive radially symmetric solutions under the only assumption that the primitive of the nonlinearity $G(u)$ presents some oscillations at infinity, expressed by the condition $\liminf G(u)/u^2 = 0 < \limsup G(u)/u^2$ (cf. [3]).

Example

The Neumann problem

$$\begin{cases} u'' + \lambda a(x)g(u) = 0 \\ u'(-0.21) = 0 = u'(0.20) \end{cases}$$

with the weight given by $a(x) = -\chi_{[-0.21,0[} + \chi_{[0,0.20]}$ and the nonlinearity defined as $g(u) = u(1-u)(1-3s+3u^2)$ has *at least 3 positive solutions* for $\lambda = 45$ (see Fig. 2). In Fig. 1, solutions are identified by means of the intersection points between the black curve and the gray segment.

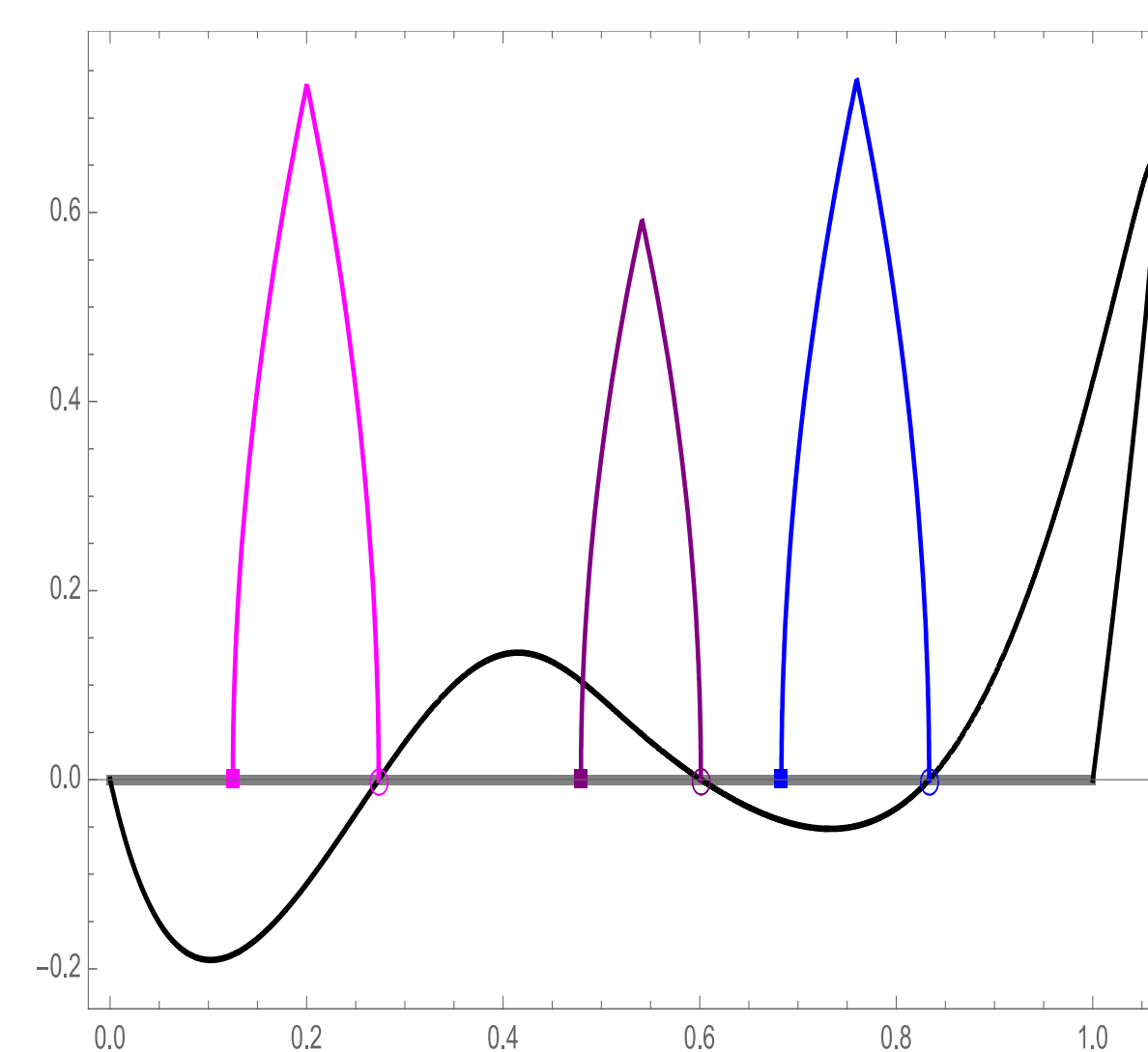


Figure 1. Application of the shooting method to the example.

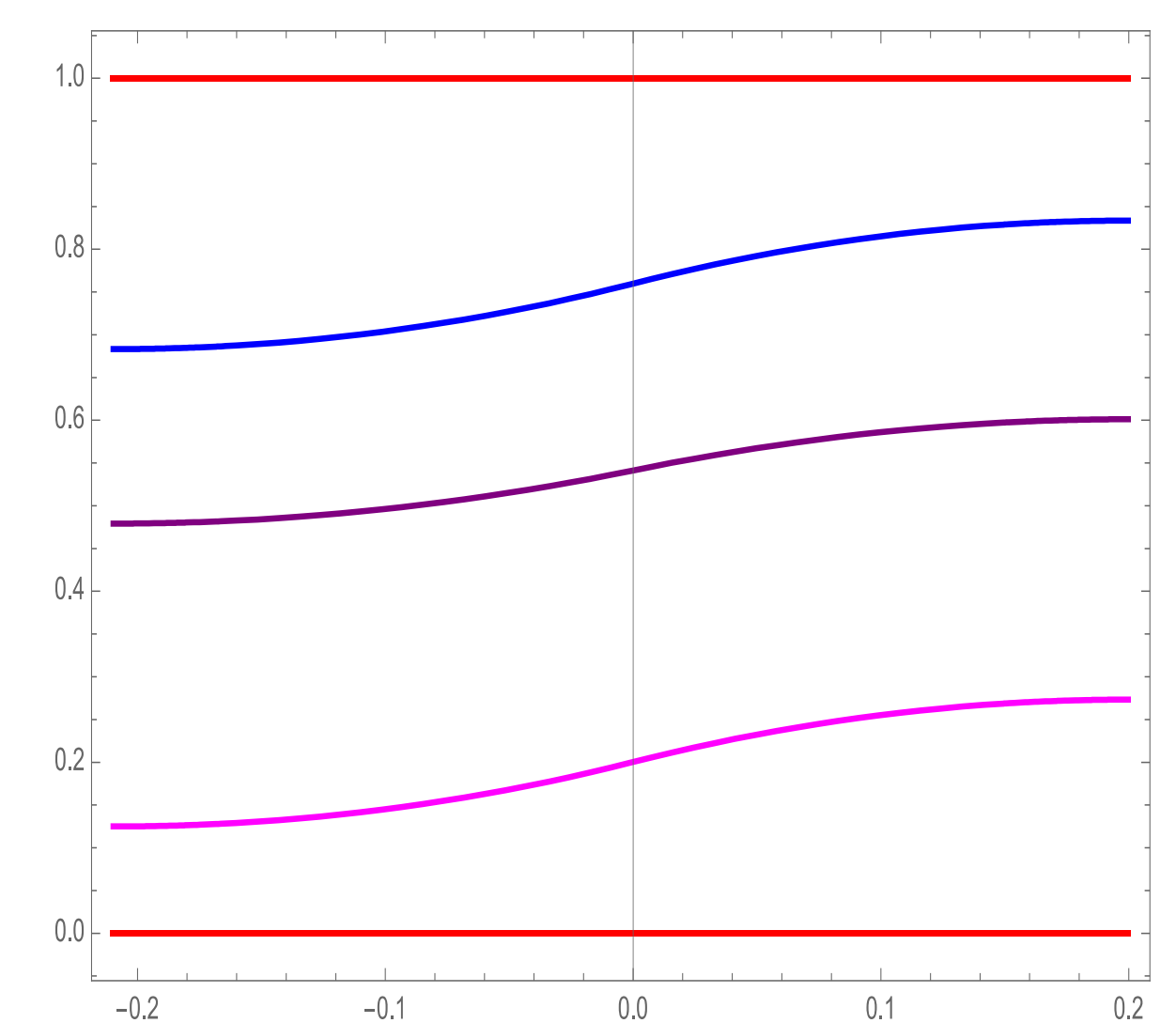


Figure 2. Three positive solutions of the Neumann problem in the example.

References

- [1] E. Sovrano. A negative answer to a conjecture arising in the study of selection-migration models in population genetics. *Journal of Mathematical Biology*, Accepted for publication, 2017.
- [2] E. Sovrano and F. Zanolin. Remarks on Dirichlet problems with sublinear growth at infinity. *Rend. Istit. Mat. Univ. Trieste*, 47:267–305, 2015.
- [3] E. Sovrano and F. Zanolin. Indefinite weight nonlinear problems with Neumann boundary conditions. *J. Math. Anal. Appl.*, 452(1):126–147, 2017.



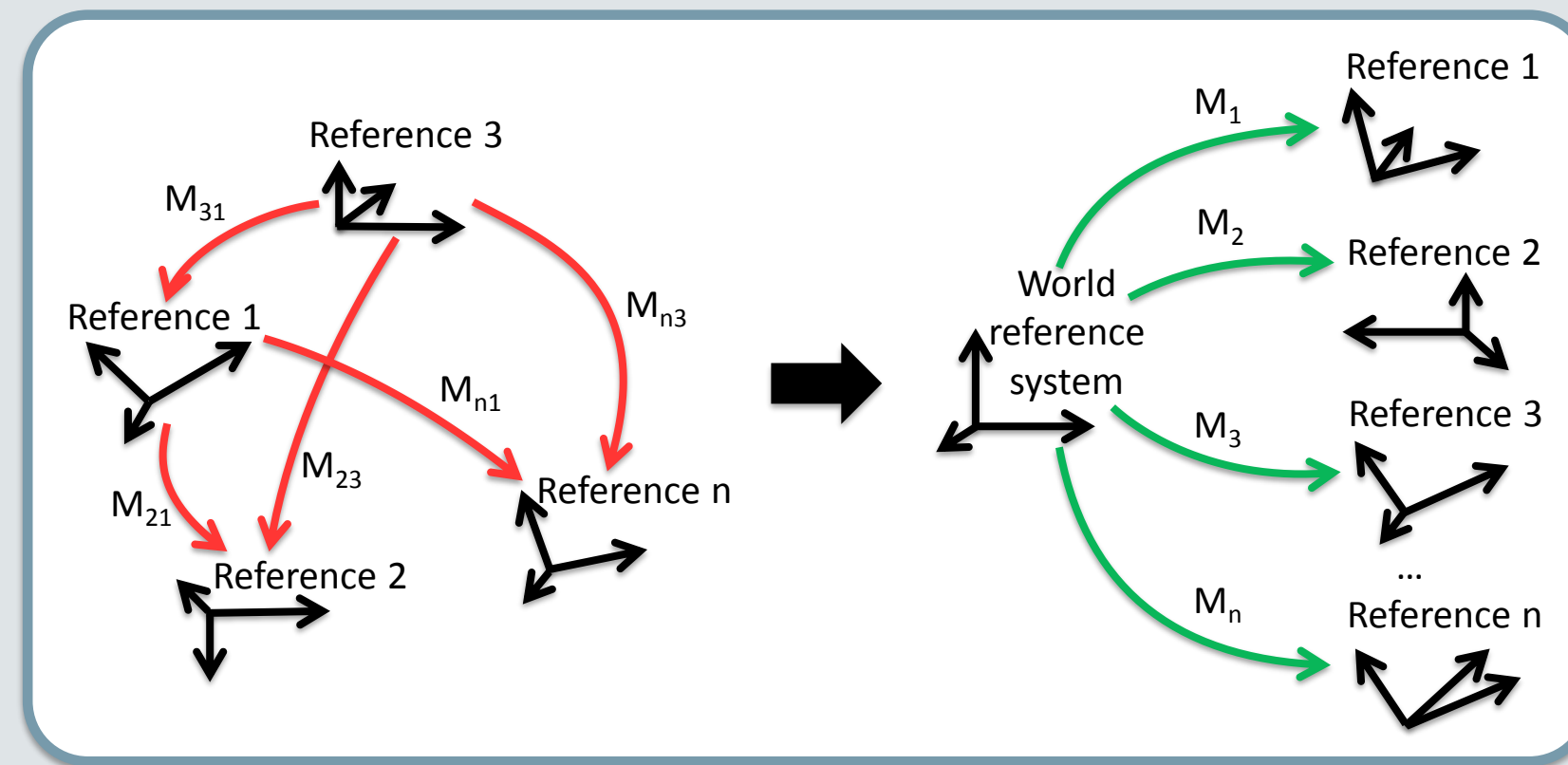
**UNIVERSITÀ
DEGLI STUDI
DI UDINE**
hic sunt futura

PHYSICAL SCIENCES AND ENGINEERING
30° cycle
**Ph.D. course in Computer Science, Mathematics
and Physics**

Synchronization of Multiple Views

The goal is to recover the **absolute orientation** (position and angular attitude) of a number of 3D reference frames, given a redundant set of **relative orientations**.

$$M_{ij} = M_i M_j^{-1} \iff \begin{cases} R_{ij} = R_i R_j^T \\ \mathbf{t}_{ij} = -R_i R_j^T \mathbf{t}_j + \mathbf{t}_i \end{cases}$$



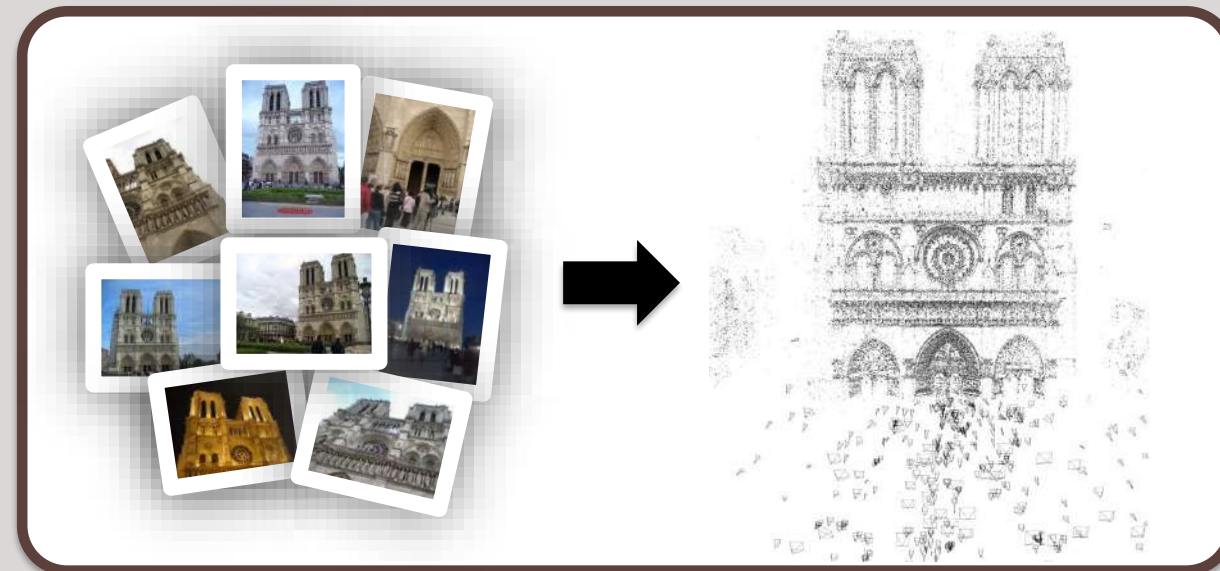
Absolute/relative orientations are elements of the **Special Euclidean Group**.

$$SE(3) = \left\{ M = \begin{pmatrix} R & \mathbf{t} \\ \mathbf{0}^T & 1 \end{pmatrix}, R \in SO(3), \mathbf{t} \in \mathbb{R}^3 \right\}$$

$$SO(3) = \{ R \in \mathbb{R}^{3 \times 3}, RR^T = I, \det(R) = 1 \}$$

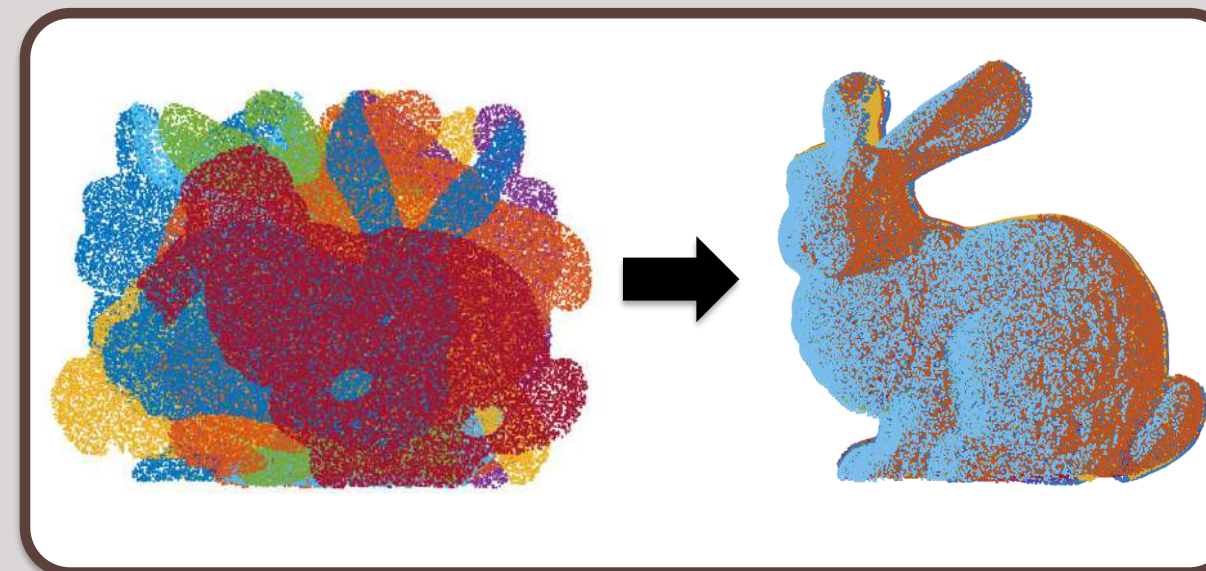
Structure from Motion

The goal is to recover both 3D coordinates of scene points and camera orientation, starting from a collection of images.



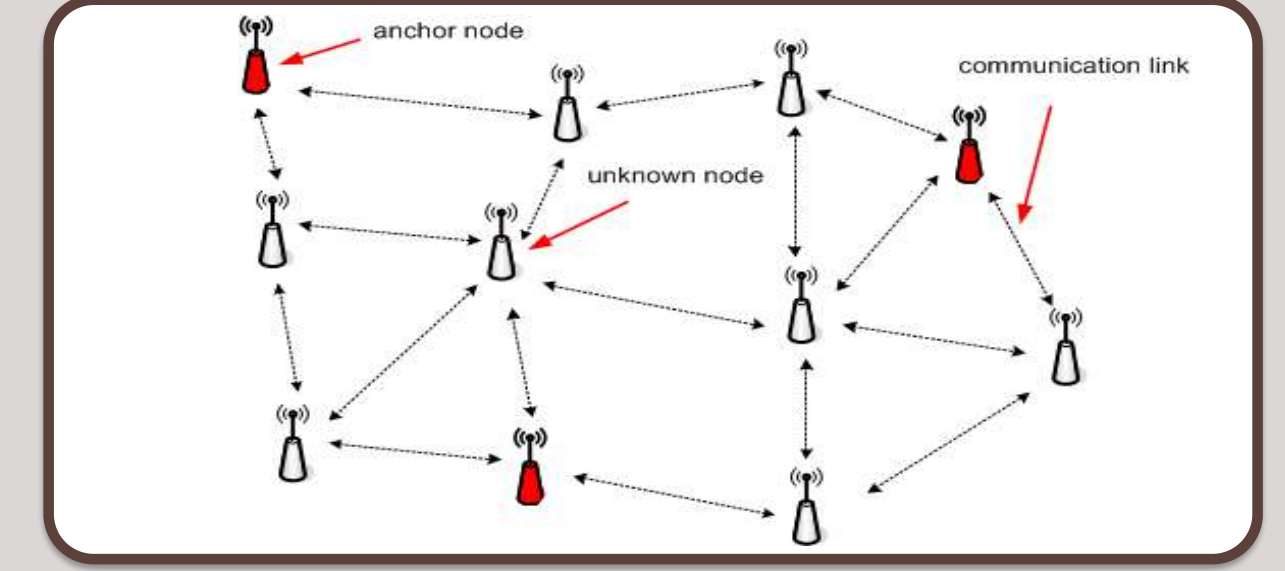
Multiple Point-set Registration

The goal is to find the rigid transformations that bring multiple 3D point sets into alignment.



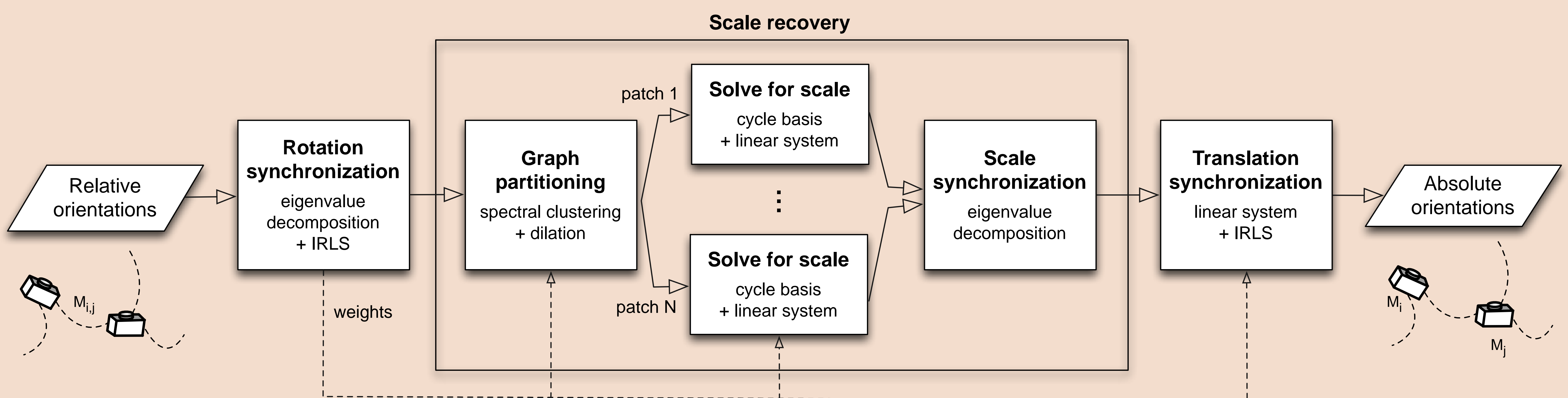
Sensor Network Localization

The goal is to express positions of sensors in an absolute reference frame, starting from local measures.



APPLICATIONS

PROPOSED SOLUTION

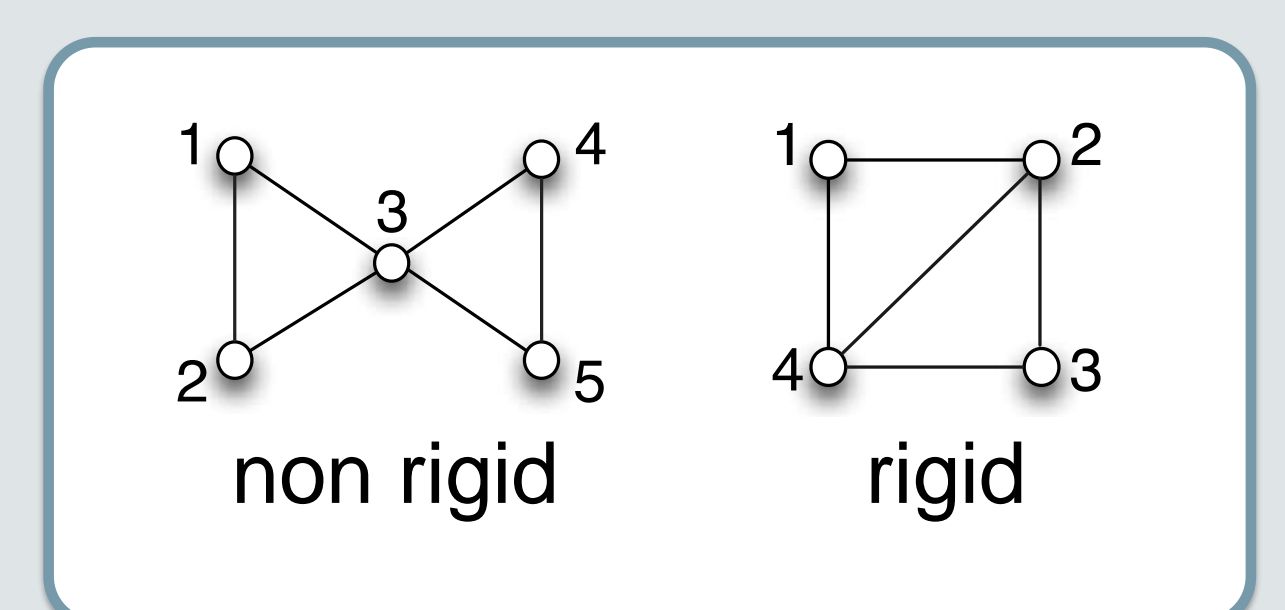


Median errors and execution times

Dataset	miss %	Our Pipeline				IDSfM			CLS			LUD			Cui et al.		
		n	rot.	tra.	time	n	tra.	time	n	tra.	time	n	tra.	time	n	tra.	time
Vienna Cathedral	74	684	1.0	2.8	69	836	6.6	302	836	8.8	578	836	5.4	787	578	3.5	242
Alamo	47	499	1.0	0.6	40	577	1.1	158	577	1.3	239	577	0.4	385	500	0.6	259
Notre Dame	32	530	0.6	1.5	27	553	10	154	553	0.8	512	553	0.3	707	539	0.3	366
Tower of London	80	408	2.5	1.6	10	572	11	78	572	16	55	572	4.7	88	393	4.4	100
Montreal Notre Dame	52	423	0.5	0.4	14	450	2.5	114	450	1.1	180	450	0.5	271	426	0.8	125
Yorkminster	72	386	1.6	1.4	10	437	3.4	122	437	6.2	62	437	2.7	103	341	3.7	45
Madrid Metropolis	65	268	2.7	7.5	7	341	9.9	43	341	6.4	46	341	1.6	67	-	-	-
NYC Library	68	295	1.5	1.1	8	332	2.5	76	332	5.0	52	332	2.0	102	288	1.4	42
Piazza del Popolo	58	297	0.8	1.0	14	328	3.1	58	328	3.5	62	328	1.5	88	294	2.6	51

Theoretical results

Camera positions can be uniquely recovered (up to translation and scale) if and only if the graph is **parallel rigid**.



Dott. Federica Arrigoni
Prof. Andrea Fusiello

Info:
arrigoni.federica@spes.uniud.it
andrea.fusiello@uniud.it

References

- 1) F. Arrigoni, B. Rossi and A. Fusiello. *Robust and efficient camera motion synchronization via matrix decomposition*. ICIAP, 2015.
- 2) F. Arrigoni, A. Fusiello and B. Rossi. *On computing the translations norm in the epipolar graph*. 3DV, 2015.
- 3) F. Arrigoni, B. Rossi and A. Fusiello. *Global registration of 3D point sets via LRS decomposition*. ECCV, 2016.
- 4) F. Arrigoni, A. Fusiello and B. Rossi. *Camera motion from group synchronization*. 3DV, 2016.
- 5) F. Arrigoni, B. Rossi and A. Fusiello. *Spectral synchronization of multiple views in SE(3)*. SIAM Journal on Imaging Sciences, 2016.
- 6) F. Arrigoni, A. Fusiello, B. Rossi and P. Fragneto. *Robust rotation synchronization via low-rank and sparse matrix decomposition*. International Journal of Computer Vision, submitted.
- 7) F. Arrigoni, E. Maset and A. Fusiello. *Synchronization in the symmetric inverse semigroup*. ICIAP, submitted.
- 8) E. Maset, F. Arrigoni and A. Fusiello. *Practical and efficient multi-view matching*. ICCV, submitted.
- 9) F. Arrigoni and A. Fusiello. *Bearing-based network localizability: a unifying view*. ICCV, submitted.

Numerical Modeling of Multigate nano-FETs

Motivation:

- Advancements in manufacturing technology has made it possible to fabricate devices with different cross-section shapes and 3D stacks of the NW [1].
- Fabrication cost for transistor has steadily increased with each node.
- Sophisticated models (for transport and electrostatics) are needed for accurate numerical modeling of the devices.
- We have developed a complete device simulator that can account for different geometries, architecture and biasing schemes.

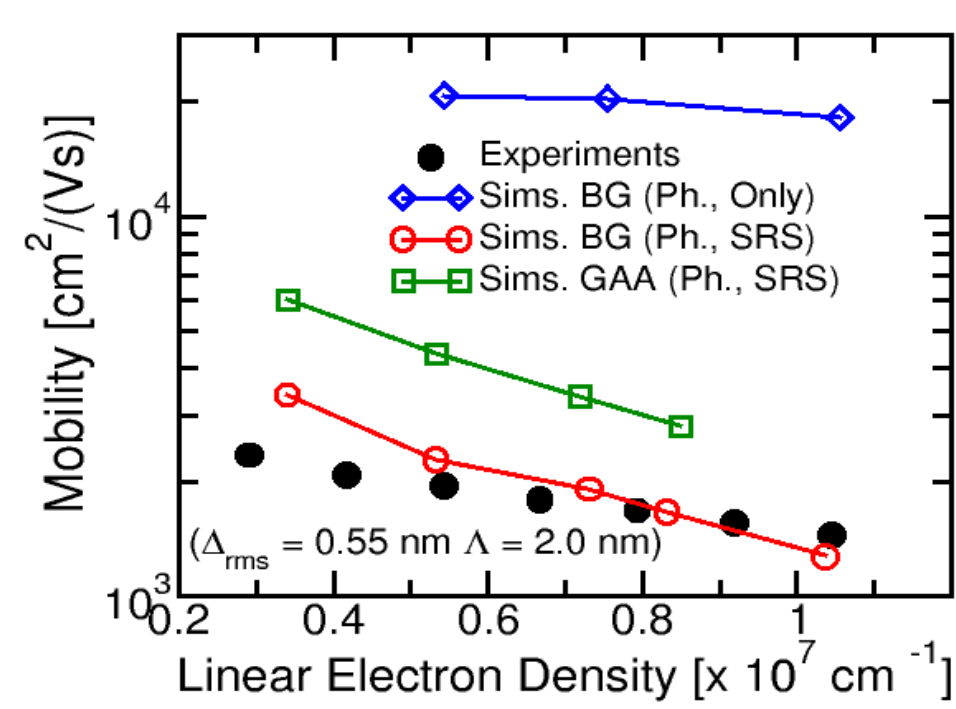
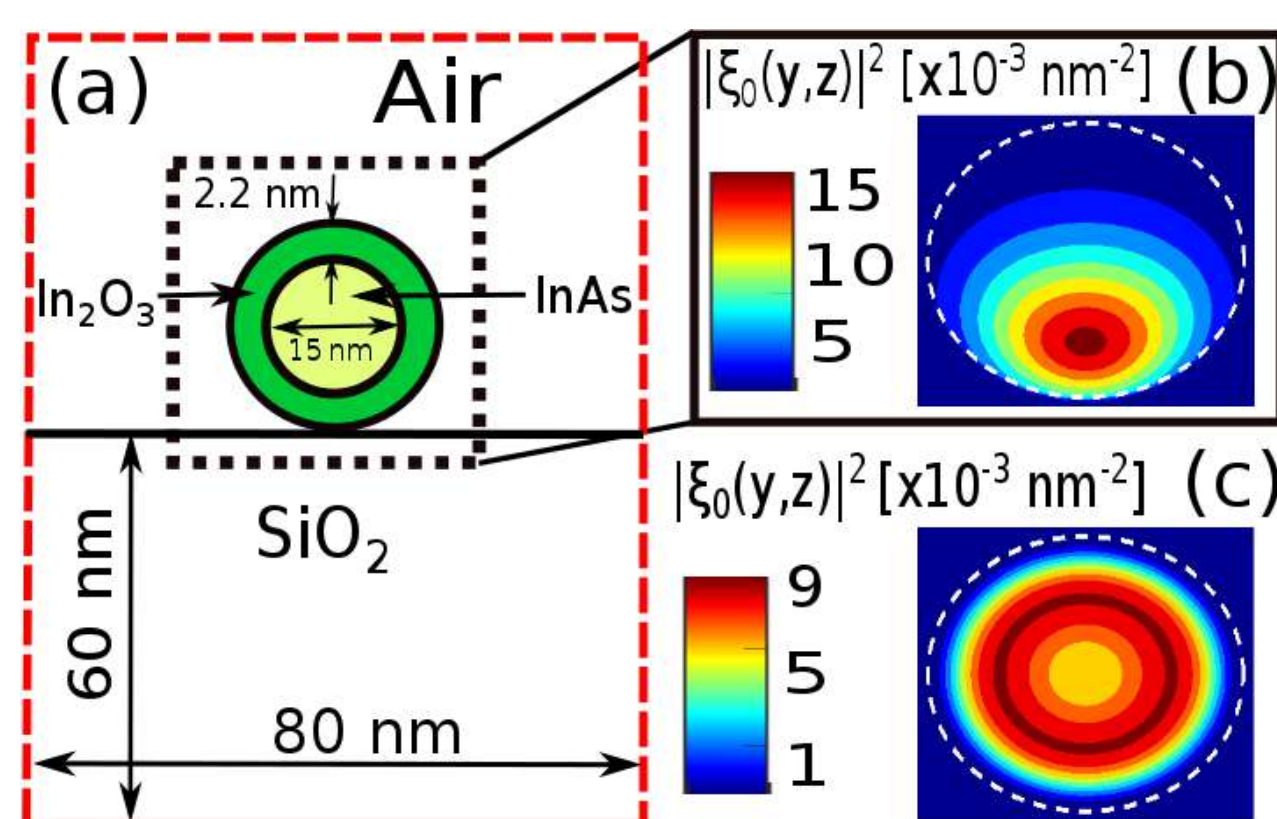
Device Simulator Modules:

- **Geometry:** Different cross-section and biasing schemes are taken into account. Meshing is done using gmsh for 3D structures (Reticula for 2D)
- **Electrostatics:** Schrödinger + Poisson.
- **Transport:** Deterministic Boltzmann Transport equation.
- **Mobility:** Boltzmann Transport equation with uniform field approximation [2,3].

Mobility Analysis:

- Mobility is one of the most important performance parameters as it is directly related to the on-state current.

Experimental Verification [4]



Exp.: A. Ford *et al.* Nanoletters, 2009

- Good match between the experimental mobilities are obtained with credible values of the SR parameters.
- Significantly different mobility values are obtained if GAA architecture is used instead of back-gated biasing.

Conclusion and Future Work:

- We have developed a full 3D device simulator with most relevant scattering mechanisms.
- Different cross-section shapes have similar values of mobility due to strong surface roughness scattering.
- Include self-heating in the device simulator[4].
- Perform a thorough analysis of the devices with different device cross-section shapes and architectures.

Dott. Oves Badami

Prof. David Esseni

Info:

Tel. +39 0432 558260

Fax. +39 0432 558251

david.esseni@uniud.it

badami.oves@spes.uniud.it

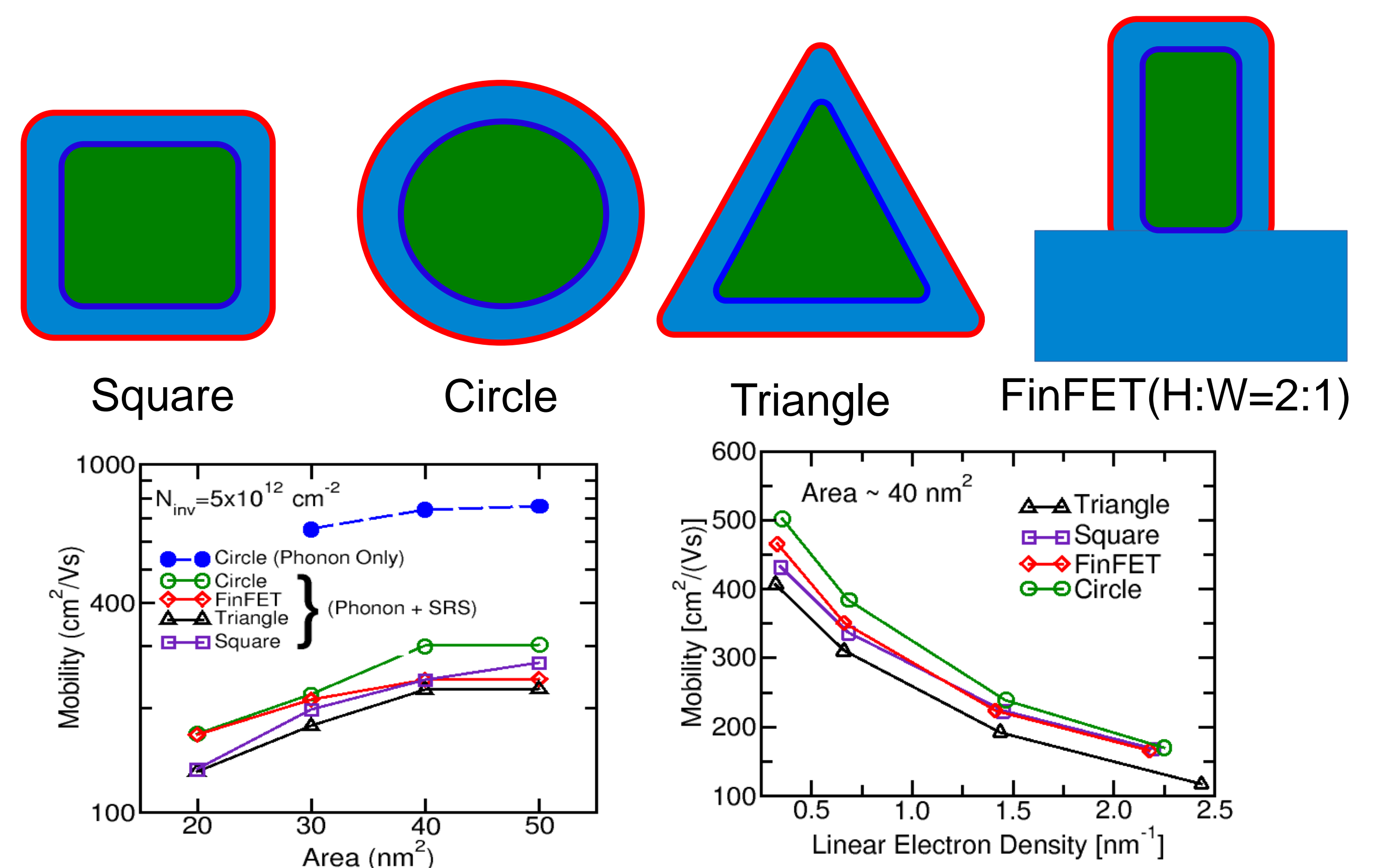
Bibliography

1. Dupre *et al.* IEDM 2009.
2. Badami *et al.* IEDM 2016.
3. Lizzit *et al.* JAP 2017 (submitted)
4. A. Ford *et al.* Nanoletters, 2009
5. Pala *et al.* JAP 2015

Acknowledgement

I would like to acknowledge Dr. Lizzit and prof. Specogna for many helpful discussions

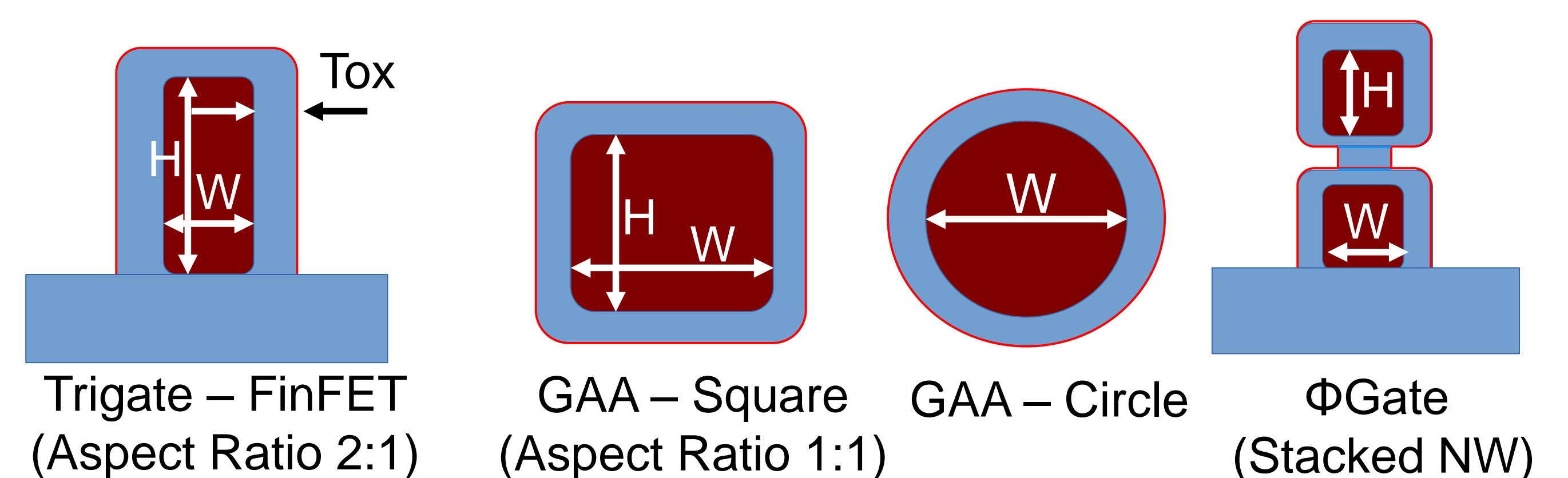
Mobility Analysis for different cross-section (Material: Si)



- Surface roughness is the dominant scattering mechanism.
- For silicon, changing cross-section shapes provides only marginal improvement (for considered shapes).

Performance benchmarking of architectures for 3D FETs:

- Here we perform full 3D-simulations.
- The cross-section shapes are shown below.



Device Parameters

Height = 5 nm (10 nm for FinFET)

Width = 5nm

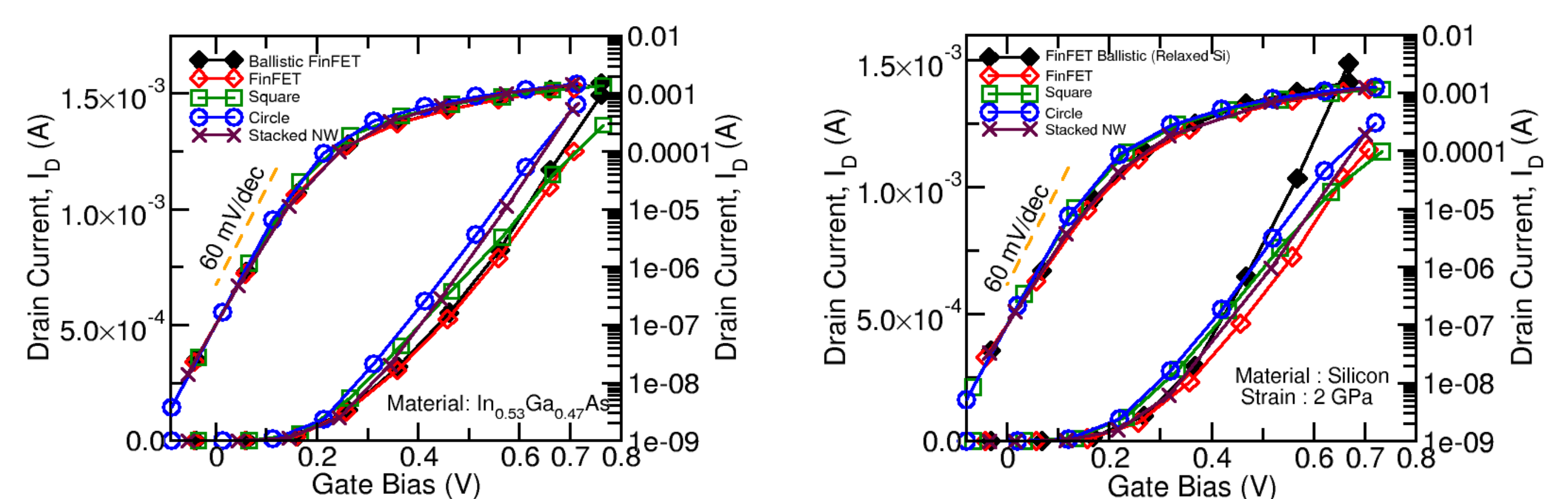
T_{ox} = 2.8 nm (EOT = 0.5 nm)

L_c = 14 nm (ITRS HP spec)

L_{sd} = 25 nm

V_{DD} = 0.7 V (ITRS spec)

R_{ext} = 202 $\Omega \cdot \mu m$ (ITRS spec)



- Different architectures have different on-current and subthreshold slope.
- On-current is directly related with the SS (exception stacked NW)



UNIVERSITÀ
DEGLI STUDI
DI UDINE
hic sunt futura

PHYSICAL SCIENCES AND ENGINEERING

30° ciclo

Corso di dottorato in Ingegneria Industriale e dell'Informazione

Design of an interface for high-speed serial links in automotive micro-controller

Introduction

The goal of the PhD is the design of a transceiver for High-Speed Serial Interfaces (fig.1) to be implemented in a microcontroller for automotive Electronic Control Unit (ECU), pushing the transmission speed up to 10 Gbps. At these frequencies, the channel loss corrupts the bits and thus there is need for equalization, both at TX and RX. Fig.2 shows the speed of serial links for consumer electronics applications, but automotive electronics lags behind it, so the goal is to reach a 10Gbps design robust over a broad range of operating temperatures, voltages and technological corners.

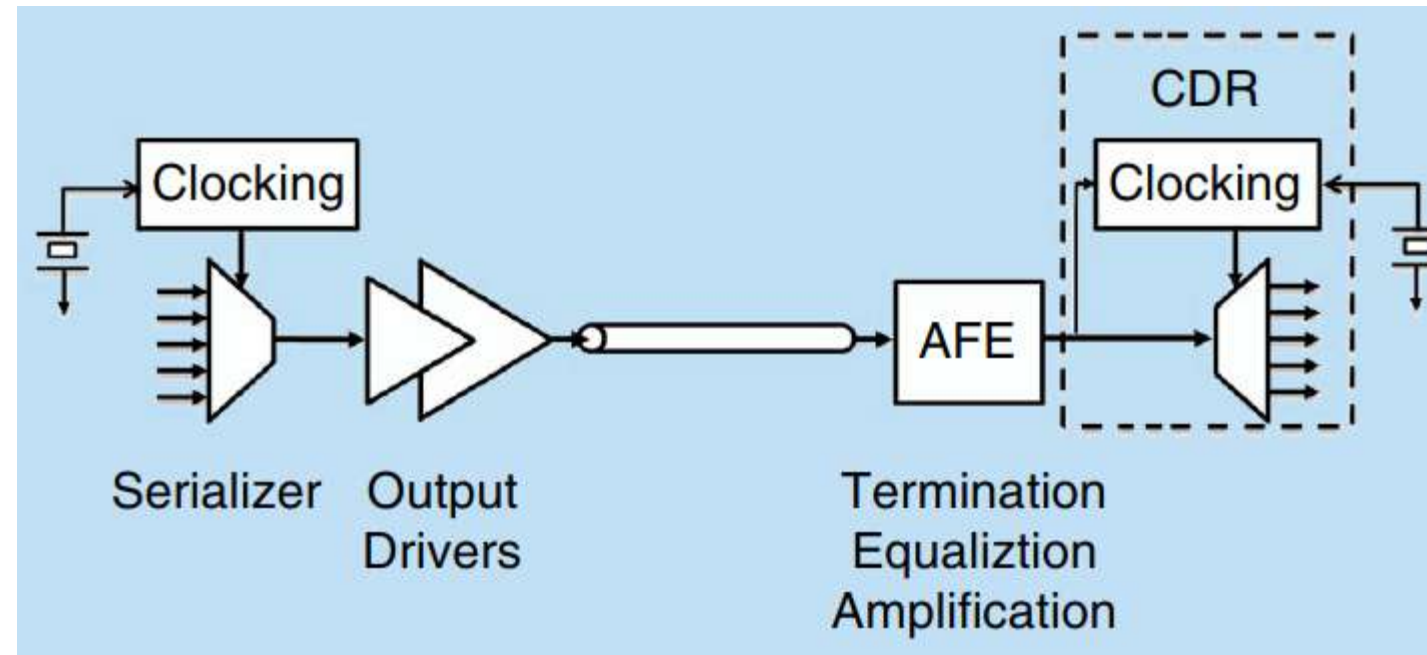


Fig. 1: Architecture of a generic serial interface. The clock is not transmitted with the data, but is reconstructed at the RX by the CDR from the data themselves.

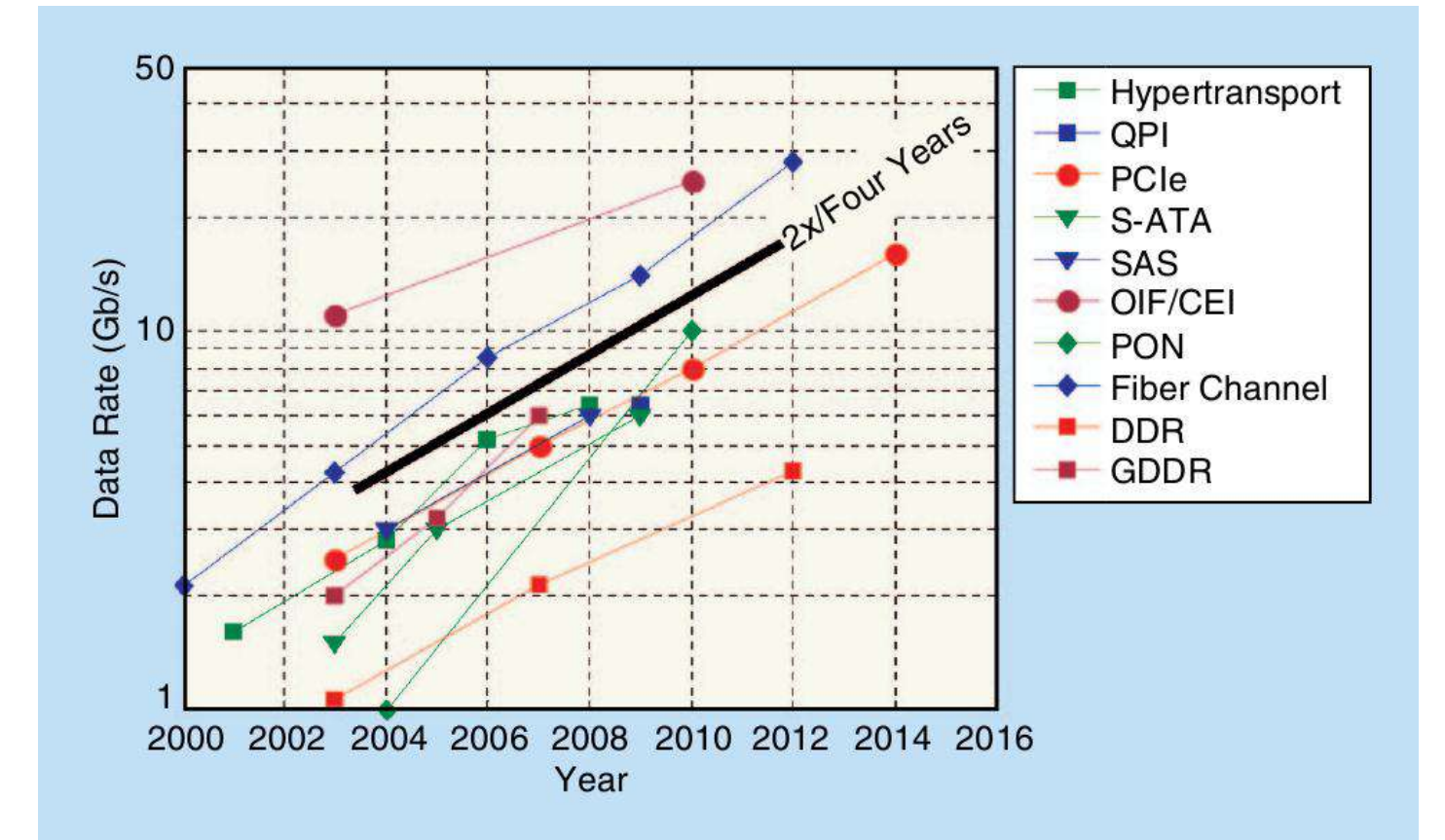


Fig. 2: Evolution of data rates for serial links along the years [1]

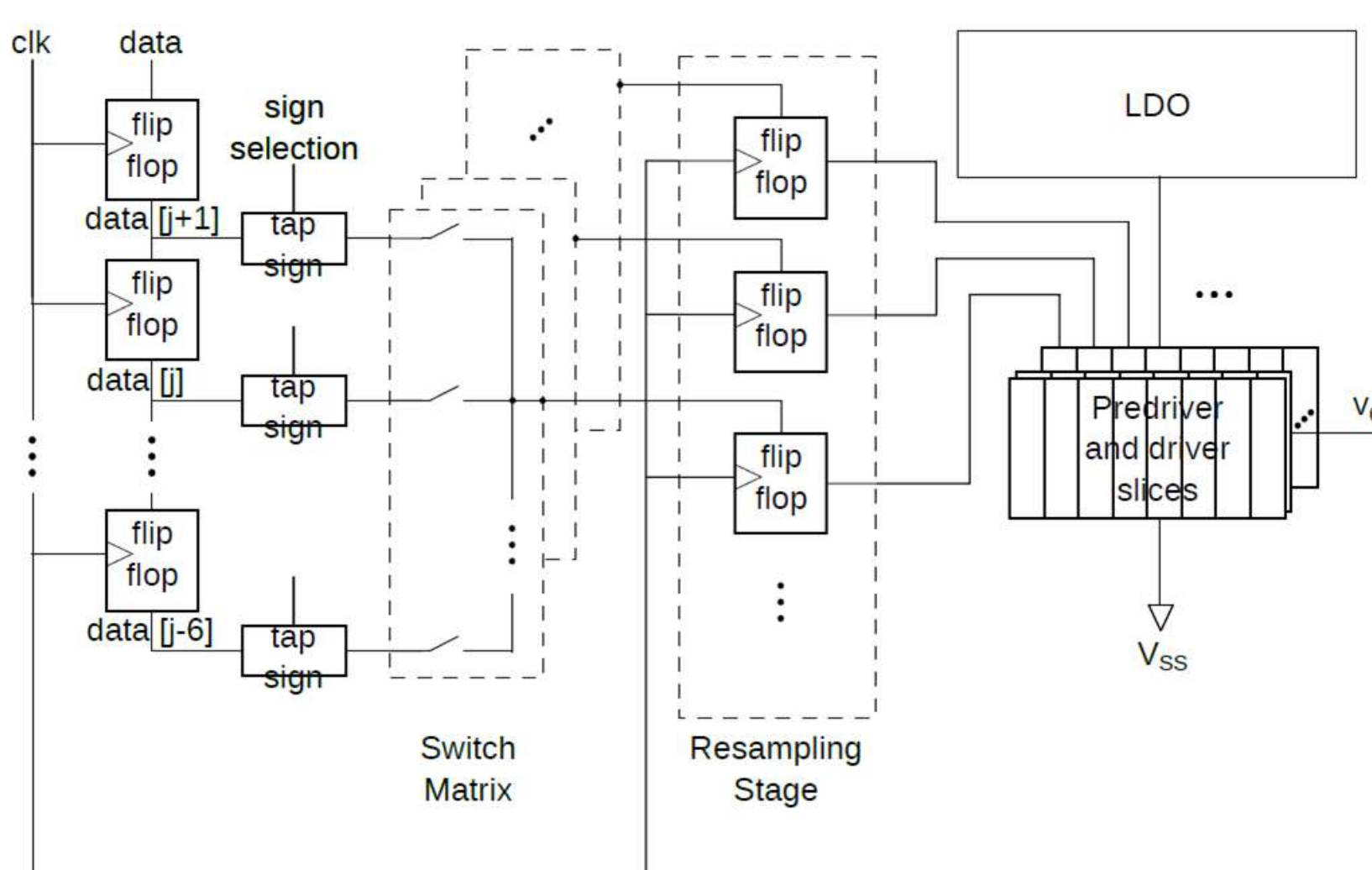


Fig. 3: Architecture of the TX, including the delay line with the input data stream (left) and the driver slices (right) that receive the supply from an LDO (top-right).

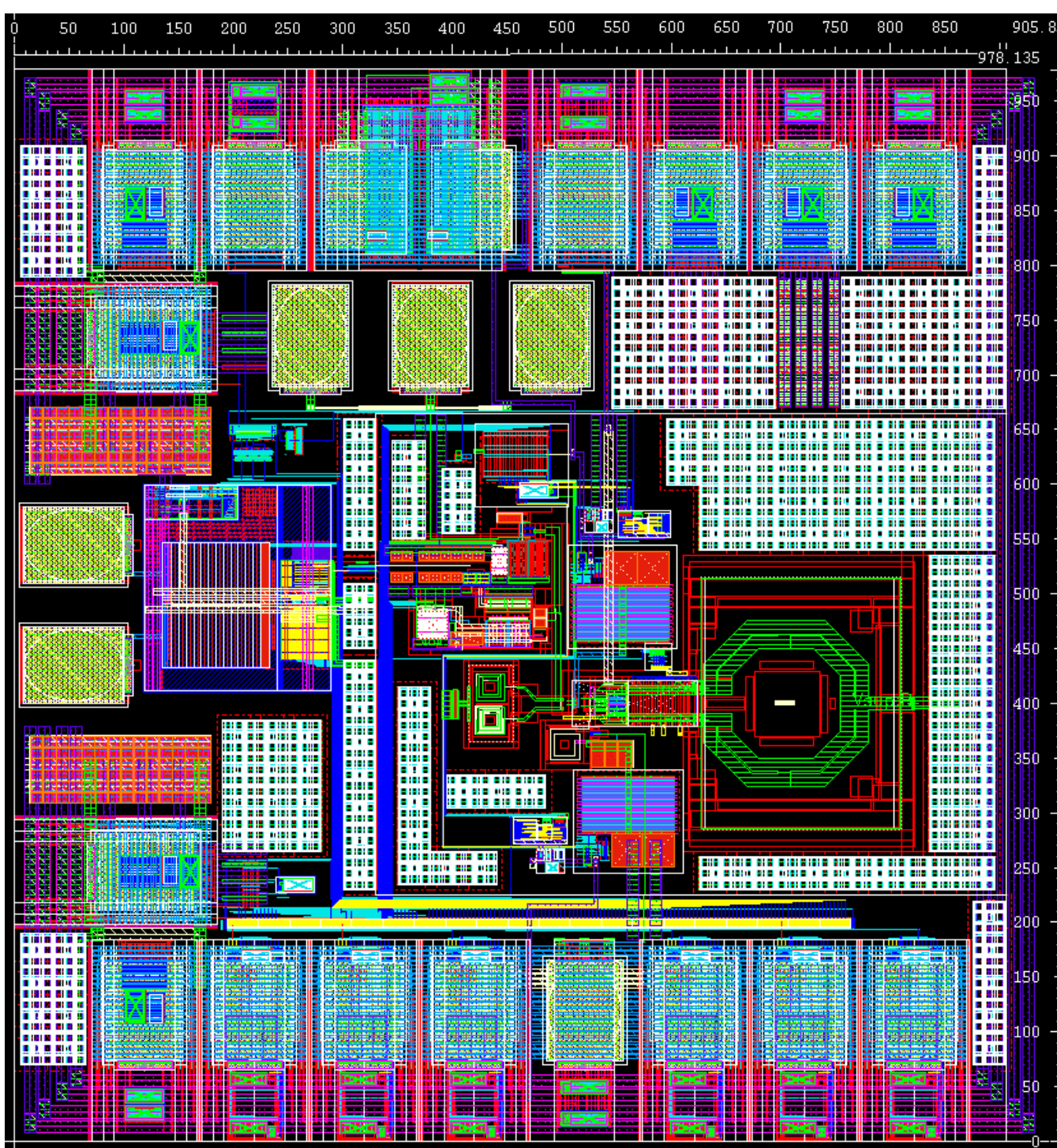


Fig. 5: Layout view of the test-chip with pads (top, bottom and left), TX (center-left) and VCO (right).

Transmitter Design

The first step in the TX design was at system level, from the equalization concept [2] to the driver topology and the supply distribution (fig.3). After this, the schematic level design followed, using a 28nm technology (fig.4). Having chosen to use a full-rate architecture [3] for area concerns, the design of some blocks has been particularly challenging, also due to the very low worst-case supply voltage (800mV). Once the circuit design has been finalized, the layout of the circuit kicked off: this phase consisted in a close collaboration with layouters and continue tuning of the schematics according to their needs. Finally, the transmitter block has been surrounded with all the supporting circuitry that needed to correctly operate and included in a test-chip (fig.5). The transmitter receives a 10GHz clock from a VCO, but supports also 5GHz and 2.5GHz clock modes, which scale the bit rate accordingly. Other settings, like the amount of equalization and the output eye opening, can be set via custom JTAG interface. The whole free space of the test-chip has been filled with decoupling capacitance, taking care not to generate unwanted oscillation frequencies in the whole chip. The final area of the chip is 0.96mm². The whole test-chip has then been simulated and an eye-diagram obtained (fig.6). Sample chips will be measured in June.

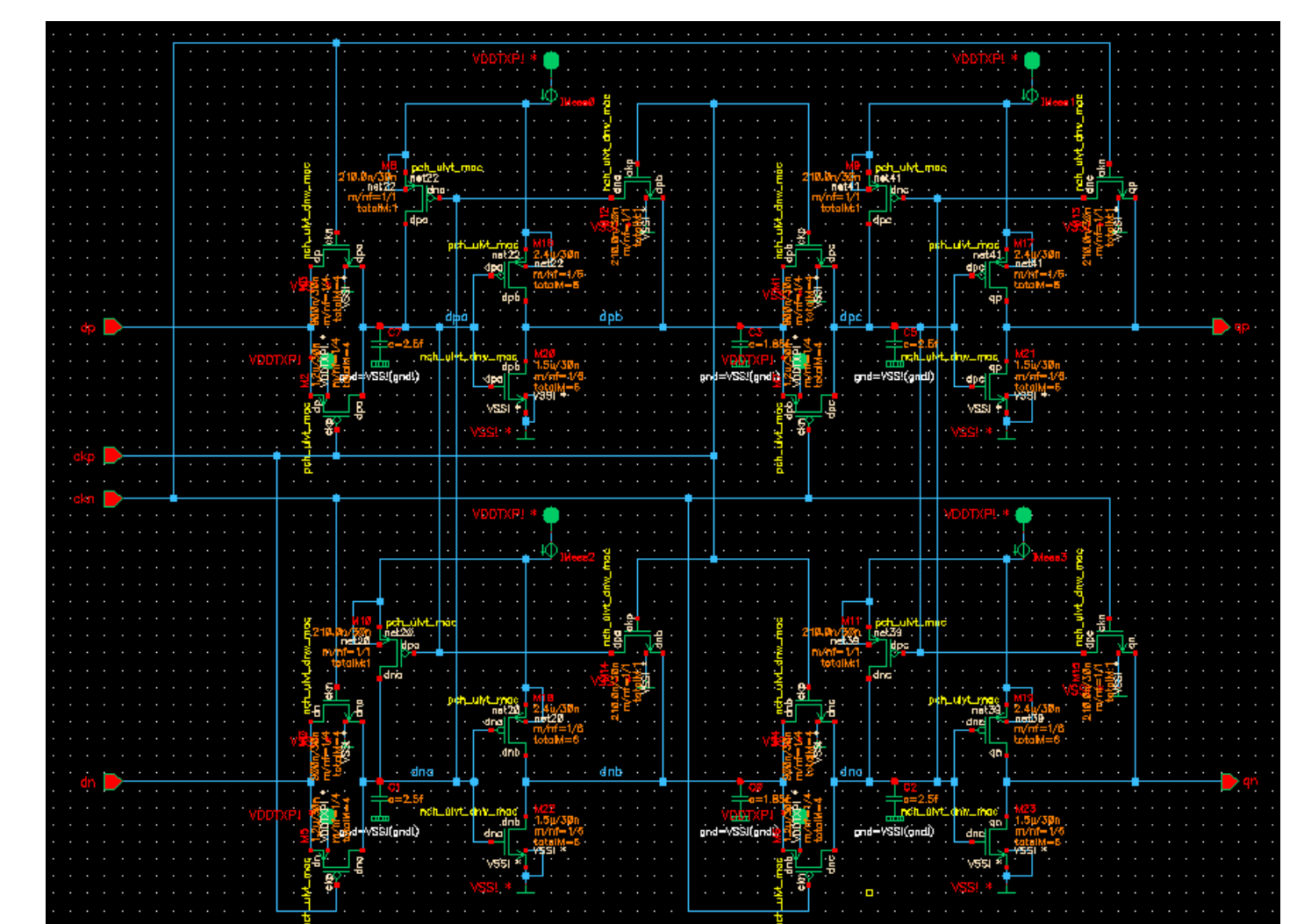


Fig. 4: Schematic of the pseudo-differential flip-flop used in the delay line and in the resampling stage.

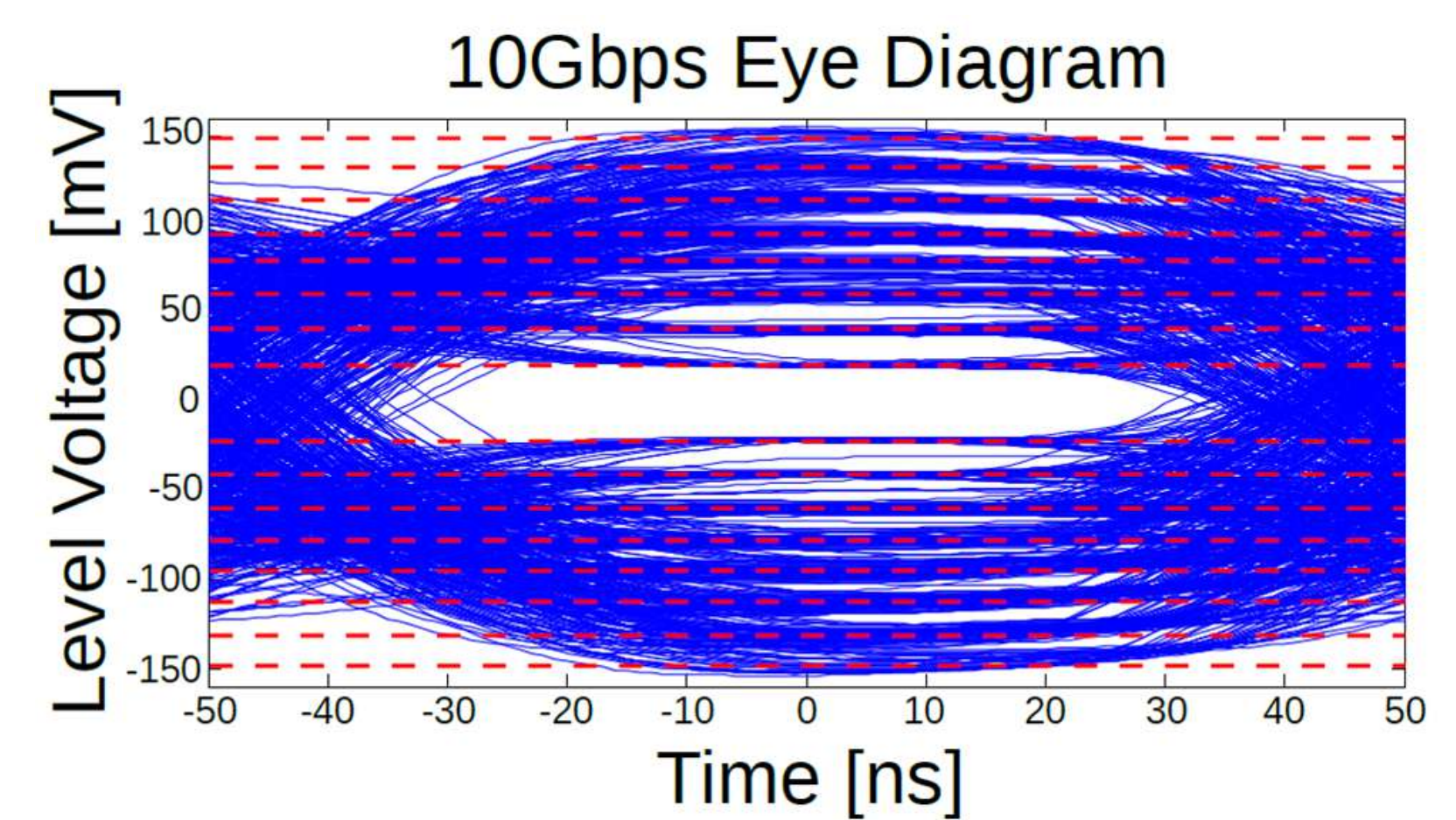


Fig. 6: Eye Diagram at the output of the transmitter when equalization is activated as obtained from top-level simulations [4].

Receiver Design

So far, only a system level analysis has been carried out for the receiver. Mixing concepts from literature (half-rate, DFE, loop unrolling, CDR) has not been an easy task (fig.7), but finally a Simulink model has been developed which demonstrates the correctness of the equalization, clock recovery and half-rate concept (fig.8). The schematic design is already ongoing and the goal is to have the full transceiver on test-chip by the end of July 2017.

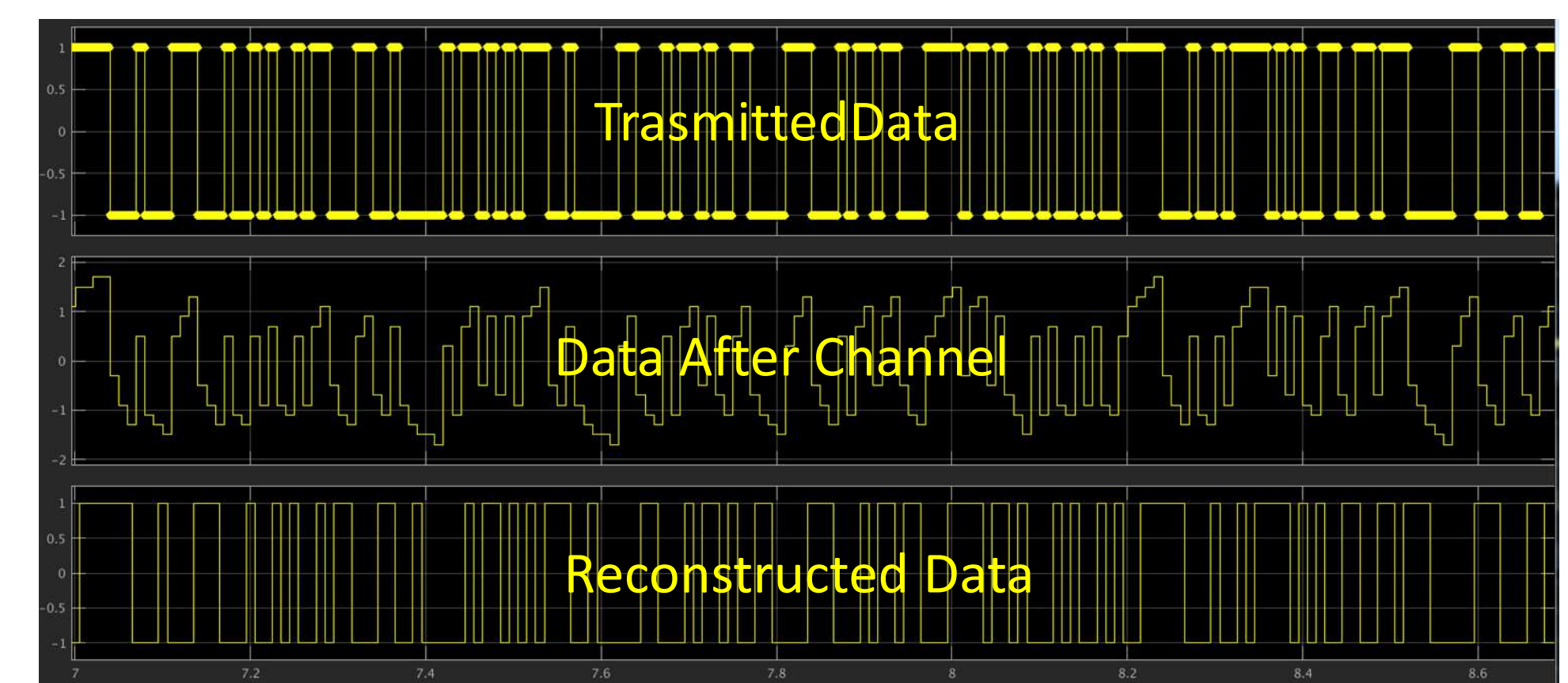
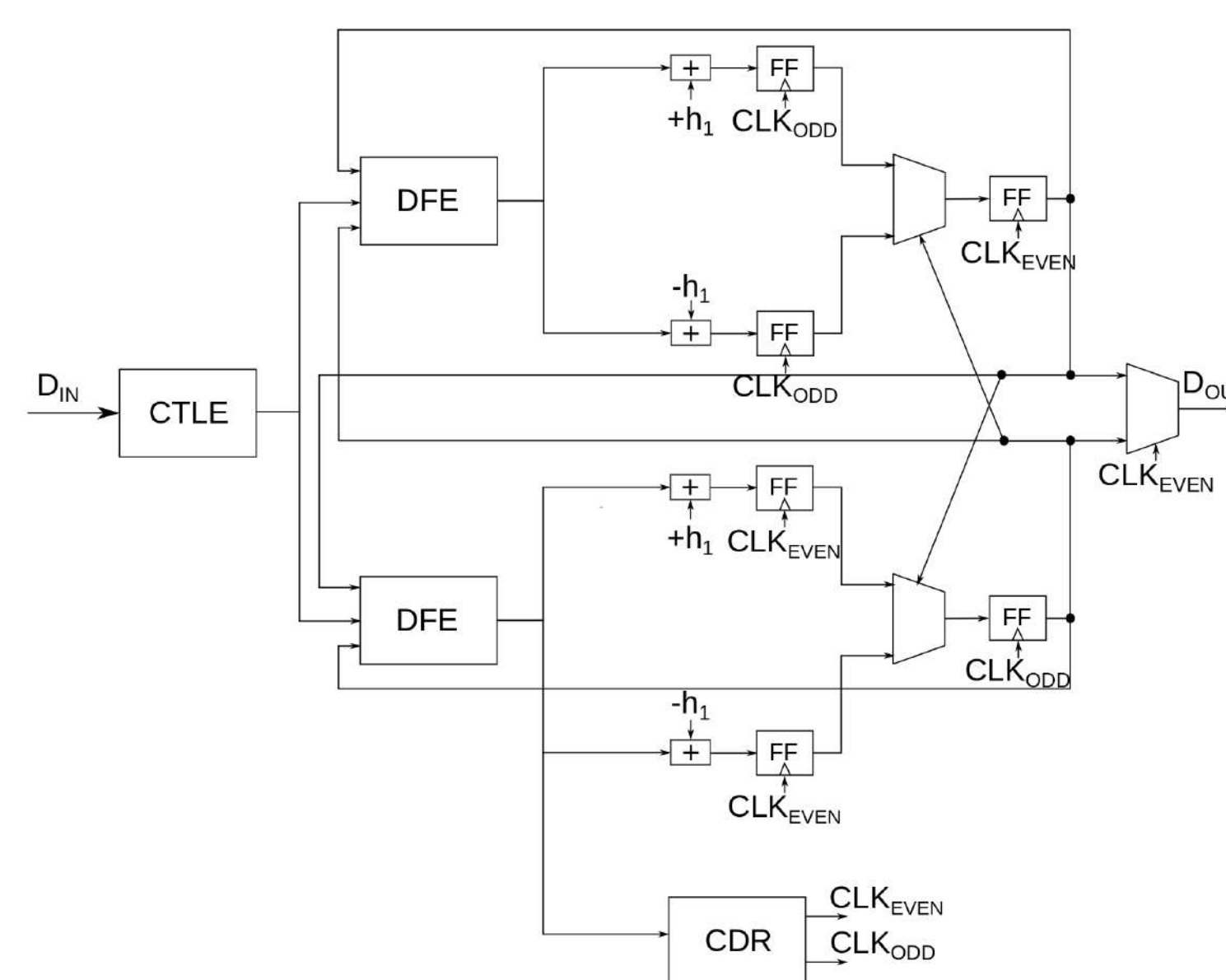


Fig. 7-8: On the left, block diagram of the half-rate RX, including linear and discrete equalization and CDR. On top, simulation results of the Simulink model showing correct reconstruction of data.

Dott. Andrea Bandiziol
Prof. Pierpaolo Palestri
Tel. +39
bandiziol.andrea@spes.uniud.it
pierpaolo.palestri@uniud.it

Bibliography

- [1] T.C.Carusone, «Introduction to Digital I/O», SSC Magazine, IEEE, vol.7, n.4, 2015, pp. 14-22
- [2] A. Bandiziol, «Design of a transmitter for high-speed interfaces», MiPro Proceedings, 2016
- [3] M. Kossel, «A T-Coil-enhanced 8.5Gb/s transmitter», SSC Journal, IEEE, vol. 42, n.12, 2008, pp. 2905-2920
- [4] A. Bandiziol, «Design of a 8-taps, 10Gbps transmitter for automotive micro-controllers», APCCAS 2016

Acknowledgments

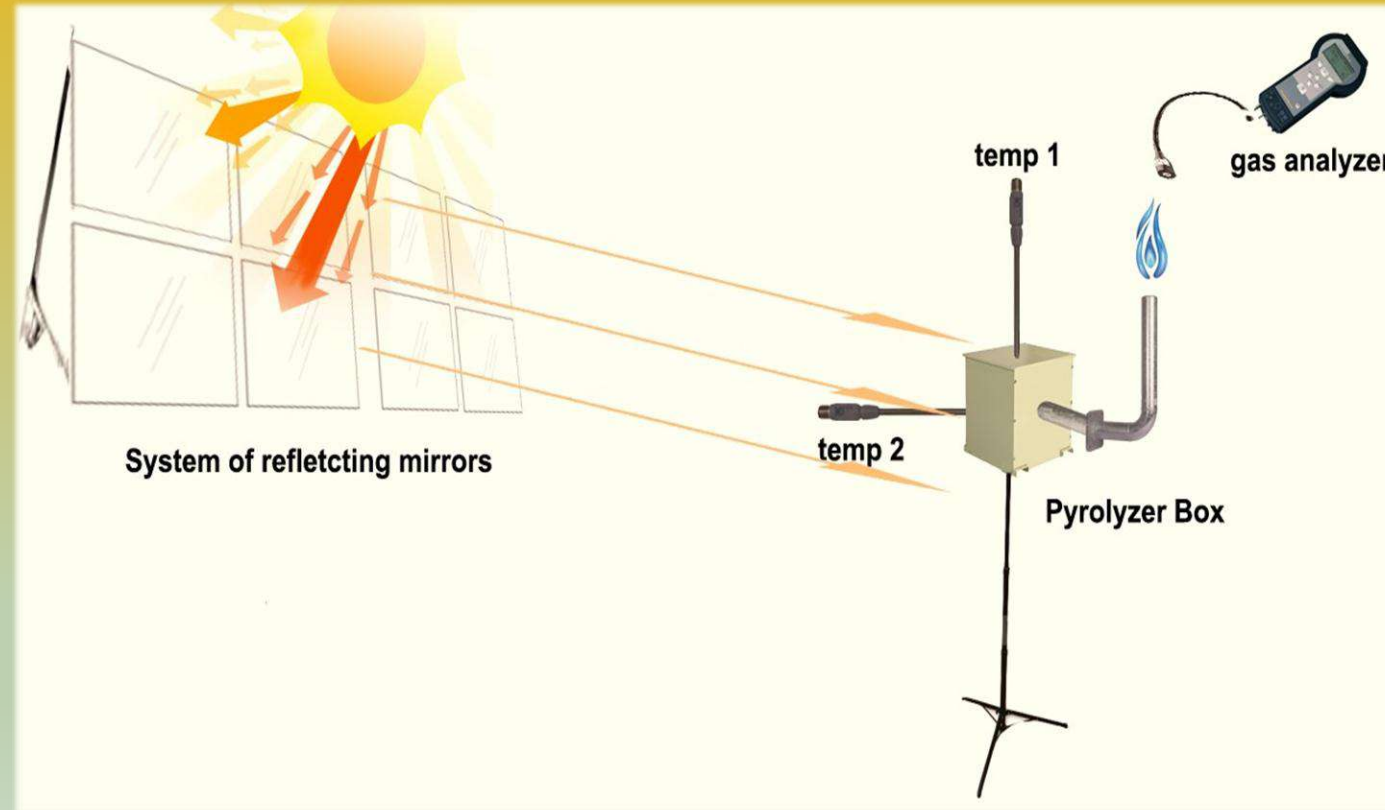
The PhD is partially funded and carried out in collaboration with Infineon Technologies, Villach (A).

Biomass Characterization for Solar Pyrolysis

1. Abstract

A simple and innovative prototype for biomass pyrolysis is presented, together with some experimental results. The setup uses only the thermal solar energy provided by a system of reflecting mirrors (Linear Mirror II*) to heat a selected local agro-waste biomass. A detailed study of the chemical and physics characteristics of several feedstocks to be used in solar pyrolysis, not yet existing in literature, is done.

2. Prototype device for solar pyrolysis



A system of sensors have been developed for monitoring temperature of biomass in the pyrolyzer.

3. Innovative Technical Aspects

In conventional pyrolysis, biomass is heated by burning fossil fuels, consuming part of the processed biomass or with the use of an electrical furnace. Several are the advantages of a solar driven thermal carbonization:

- ✓ it delivers a higher carbonized material output per unit of feedstock since no portion of the feedstock is combusted for process heat;
- ✓ the process is CO₂ neutral and discharge of pollutants in the environment is avoided;
- ✓ it offers an efficient way of chemically store the discontinuous solar energy in the form of a readily transportable fuel.

4. Chemical and Physical Characterization of different local feedstocks to be used in solar pyrolysis

Several samples of different local feedstocks have been heated at different temperatures in controlled conditions, using an oven for tests. The chemical and physical properties of the samples are summarized in the table below.

Parameters (wt%)	Wheat straw			Vine shoot			Corncob			Pellet		
	300°C	400°C	500°C	300°C	400°C	500°C	300°C	400°C	500°C	300°C	400°C	500°C
Carbon	59±1	70±1	74±1	69±1	73±1	80±1	61±1	68±1	74±1	68±1	75±1	85±1
Hydrogen	5.4±0.1	3.5±0.1	2.8±0.1	4.7±0.1	3.6±0.1	2.9±0.1	2.6±0.1	2.5±0.1	2.0±0.1	4.3±0.1	3.8±0.1	3.4±0.1
Nitrogen	0.7±0.1	0.9±0.1	0.8±0.1	1.0±0.1	0.8±0.1	0.8±0.1	0.9±0.1	0.8±0.1	0.8±0.1	0.2±0.1	0.1±0.1	0.1±0.1
Oxygen	29±1	15±1	10±1	19±1	15±1	7±1	32±1	25±1	17±1	25±1	19±1	8±1
Ash	5.9±0.1	10.1±0.1	12.0±0.1	4.9±0.1	6.4±0.1	7.0±0.1	3.5±0.1	3.6±0.1	6.6±0.1	2.2±0.1	2.1±0.1	3.2±0.1
HHV (MJ/kg)	22.6±0.1	27.5±0.1	28.5±0.1	24.9±0.1	26.3±0.1	27.9±0.1	23.8±0.1	26.9±0.1	29.2±0.1	24.5±0.1	27.0±0.1	29.4±0.1
Residual mass (%)	51±1	40±1	31±1	33±1	26±1	23±1	37±1	30±1	22±1	38±1	31±1	23±1

5. Chemical Comparison between Wheat Straw and Solar Carbon

When heating wheat straw in a standard oven, an increase in temperature corresponds to a decrease in the residual mass percentage as expected, and an increase in the higher heating value (HHV). These values can be compared to the corresponding values obtained for the solar carbon. HHV of a good quality carbon is about 28-32 MJ/kg.

Parameters (wt%)	Wheat straw	Wheat straw	Wheat straw
	no pyrolysed	400°C	pyrolysed with the Linear Mirror II (solar carbon)
Carbon	46±1	70±1	70±1
Hydrogen	6.0±0.1	3.5±0.1	3.5±0.1
Nitrogen	0.3±0.1	0.9±0.1	0.8±0.1
Oxygen	41±1	15±1	15±1
Ash	7.0±0.1	10.1±0.1	10.5±0.1
HHV (MJ/kg)	22.6±0.1	27.5±0.1	28.2±0.1
Residual mass (%)	---	40±1	31±1

6. Conclusions and Future Directions

Solar pyrolysis of cheap biomass offers an interesting combination of traditional solar thermal energy with biomass energy which can help to substitute fossil fuels. The goal of my research activities is to building and testing a new prototype for solar pyrolysis, making it also an industrial product, build a system to control the pyrolyser electronic sensors, analyze and compare local feedstocks to be used in solar pyrolysis.

Dott. Marco Citossi
Prof. Marina Cobal
Tel. +39 0432 558235
Email citossi.marco.1@spes.uniud.it
Email marina.cobal@cern.ch

References

[1] Grassmann, H., Boaro, M., Citossi, M., Cobal, M., Ersettis, E., Kapllaj, E. and Pizzariello, A. (2015) Solar Biomass Pyrolysis with the Linear Mirror II. *Smart Grid and Renewable Energy*, 6, 179-186.
doi:[10.4236/sgre.2015.67016](https://doi.org/10.4236/sgre.2015.67016).

Congresso SIF 2016

Caratterizzazione chimico-fisica di biomasse tipiche del nord-est per la pirolisi solare mediante il Linear Mirror II (<https://congresso.sif.it/talk/557>).

Acknowledgement

This work was in part sponsored by a grant from Camera di Commercio di Gorizia (Fondo Gorizia) and was supported by Area Science Park Trieste.

* Isomorph Production Srl

Architectures and Algorithms for the Signal Processing of Advanced MIMO RADAR Systems

Introduction

MIMO Imaging RADAR systems are a central topic of today's applications in the fields of advanced assistance systems in both automotive and aerospace scenarios. They allow the detection, tracking and classification of targets with the advantage of having all-weather capabilities, material penetration properties and usability at day and night.

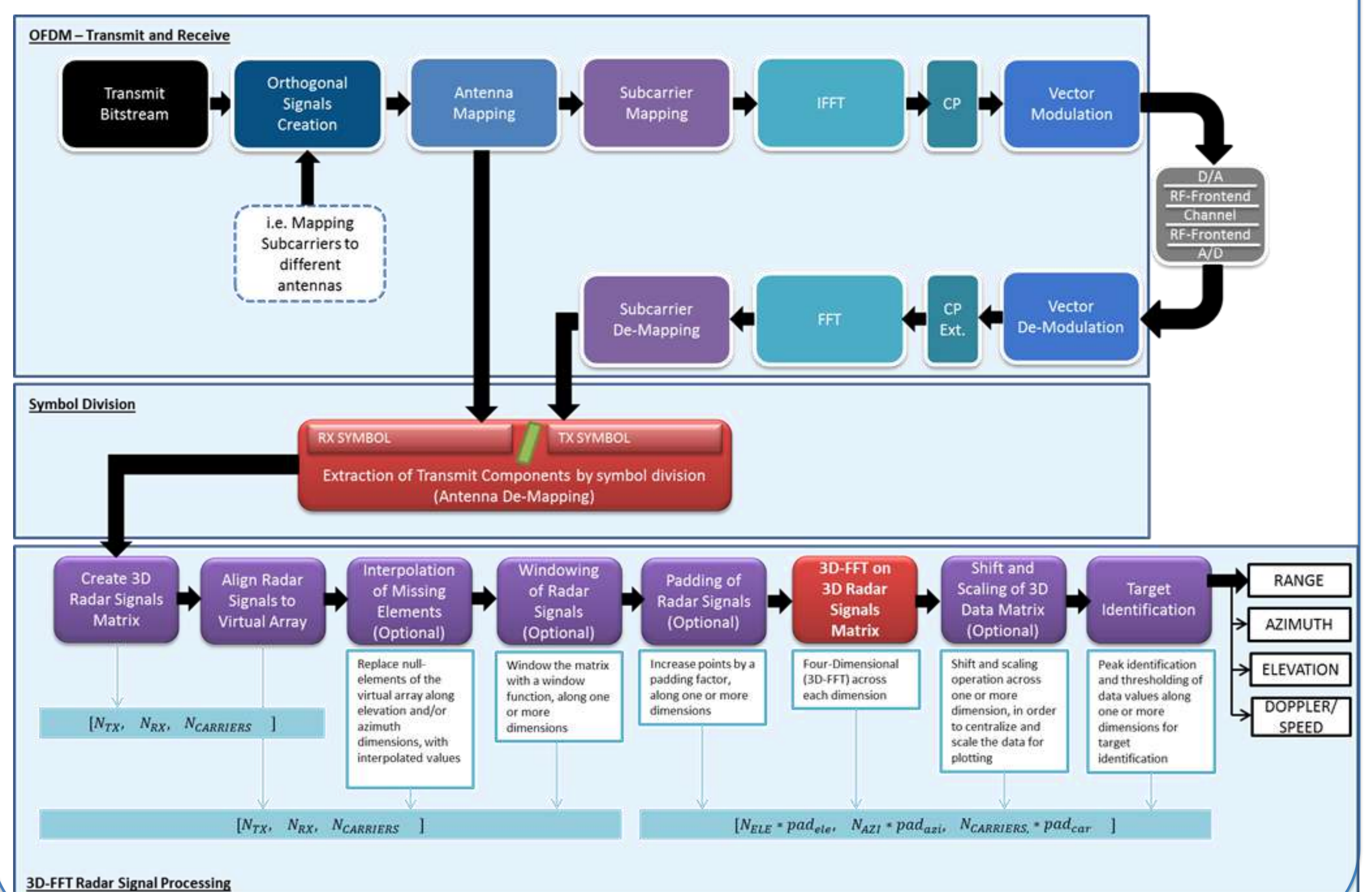
Scope of the Research

The scope of this research, conducted in the premises of the Airbus Group Innovations buildings in Munich (Germany), is to:

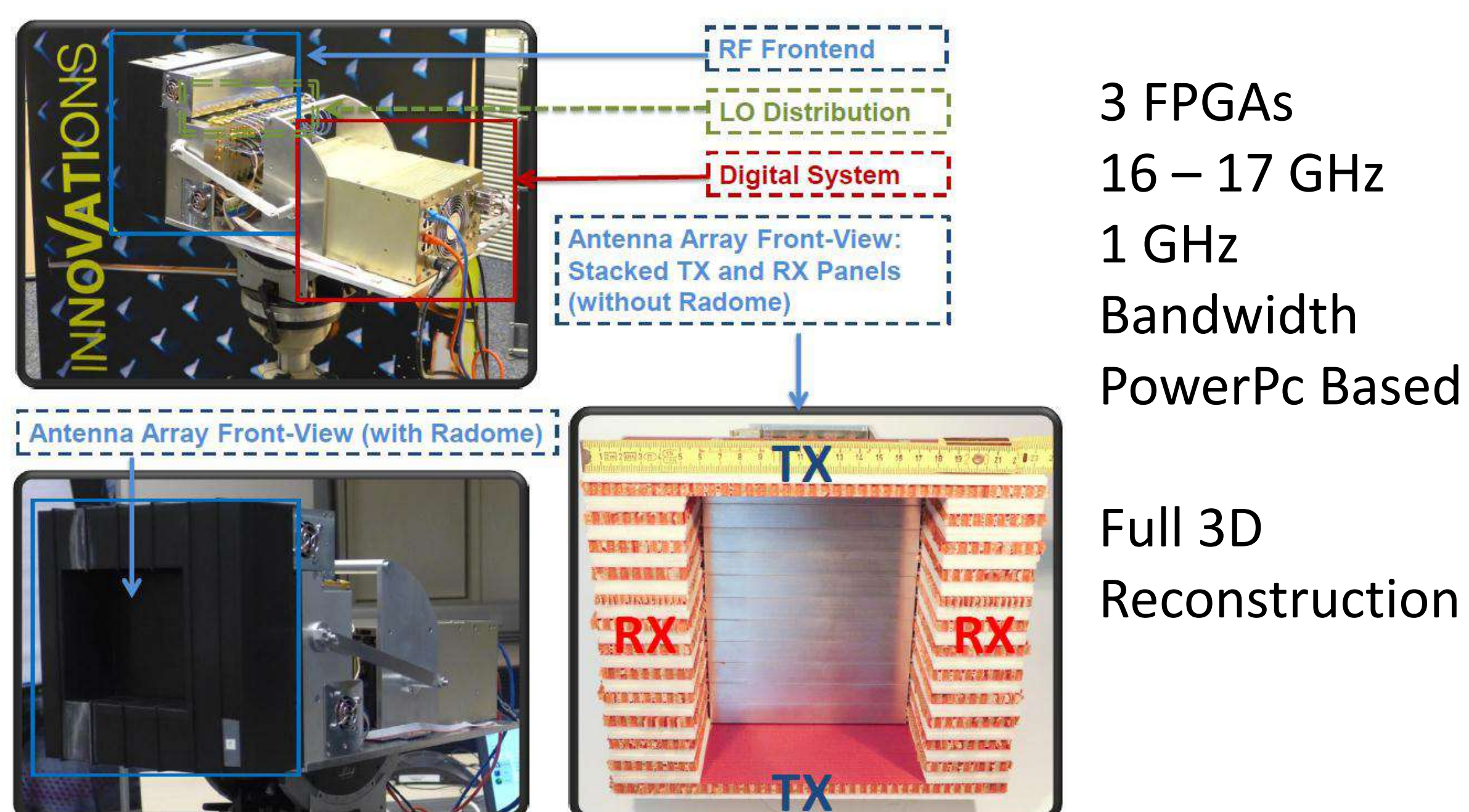
- Develop innovative digital architectures for MIMO RADAR systems, in both Time-Division-Multiplexing (TDM) and Frequency-Division-Multiplexing (FDM) modes;
- Develop state of the art, Real-Time beam-forming and Direction-Of-Arrival (DOA) algorithms for target detection;
- Create advanced system concepts and simulations for the Real-Time digital RADARs of the future (ex. OFDM based);
- Investigate new constant envelope orthogonal waveforms for Real-Time MIMO RADAR systems.

3D Real-Time OFDM MIMO RADAR Concept and Simulation [1]

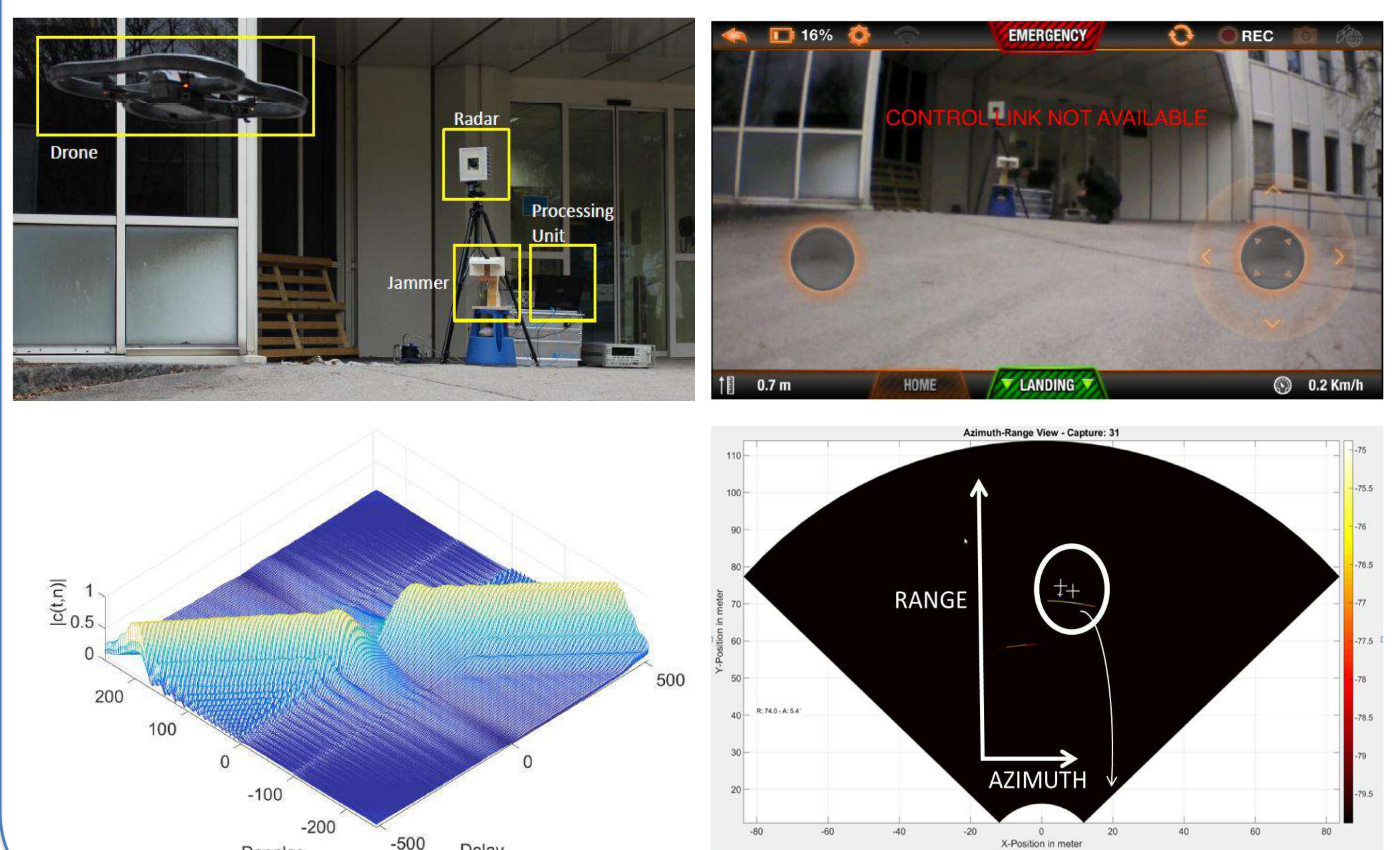
Complete model simulation implementation of a system concept for the radar of the future, OFDM based, with 3D-FFT based reconstruction and orthogonal and adaptive waveforms.



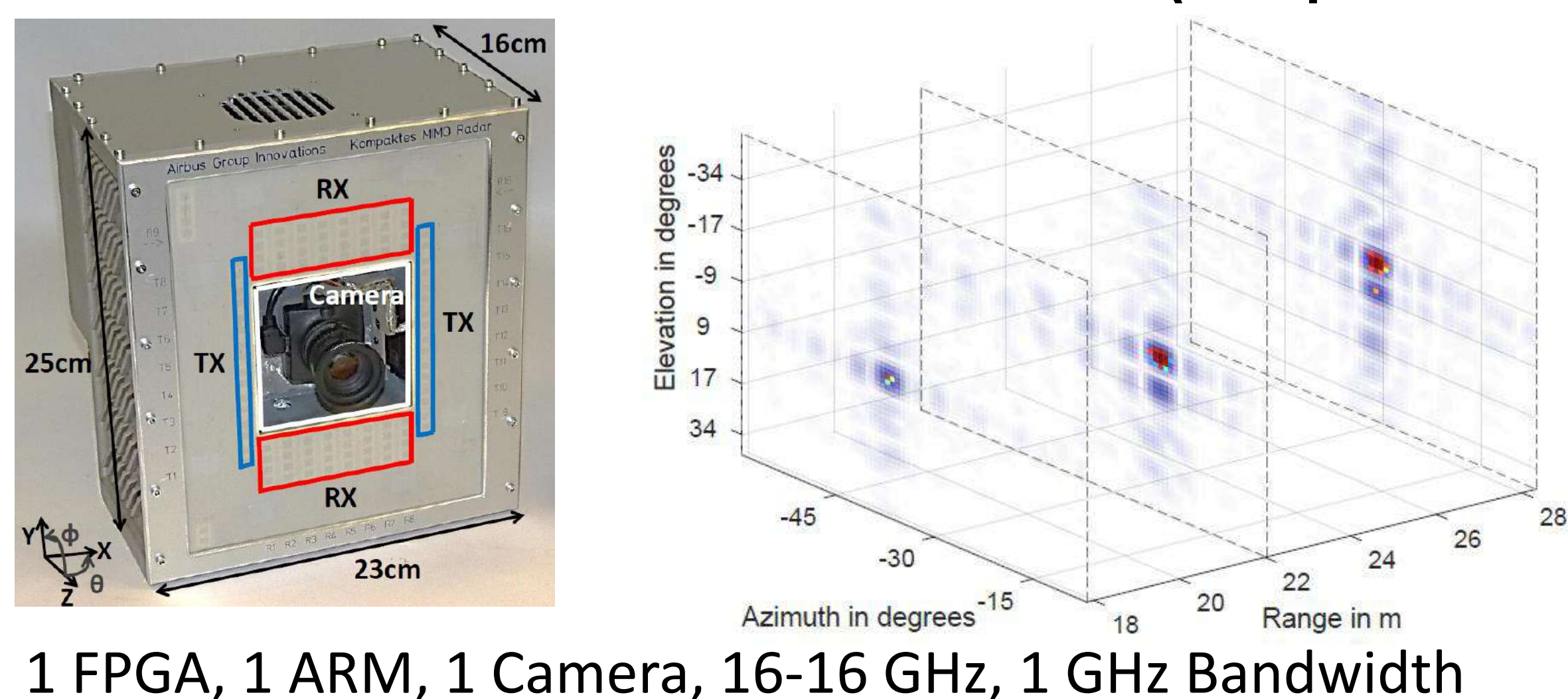
24 x 24 FMCW MIMO Radar Demonstrator (Static Images)



DOA Algorithms -> Tracking Algorithms -> Threat Prevention



16 x 16 FMCW MIMO Radar Demonstrator (Compact Version)



Applications

Possible applications are situation-awareness for rotorcraft flight operations and for critical landing operations, obstacle detection, terrain mapping, sensor systems for medium-sized unmanned aerial vehicles (UAV) and more generally, surveillance of wide-zones and infrastructures.

Dott. Alexander Rudolf Ganis
Prof. Mirko Loghi
Info:
 ganis.alexanderrudolf@spes.uniud.it

Patents and Publications
 3 Journals pending.
 5 Patents filed.

Bibliography
 [1] A. Ganis et al., "A system concept for a 3D real-time OFDM MIMO radar for flying platforms", in *2016 German Microwave Conference (GeMiC)*, Bochum, Germany, 2016, pp. 201-204.

Acknowledgments
 This PhD is supported and sponsored by Airbus Group Innovations, Airbus Defence and Space GmbH, with registered office in Ottobrunn, Munich (Germany).
www.airbus-group.com

Explicit Time-Domain Full Maxwell Solvers over Tetrahedral Grids

AIM

The tools currently available for the time-domain numerical solution of Maxwell's equations in 3D are either inaccurate in dealing with complex geometries, like the Finite Difference Time Domain method (FDTD) or its Finite Integration Technique (FIT) reformulation, or computationally expensive, like the Finite Element Method (FEM). We aim to develop tools that solve both issues.

APPROACH

We chose the method of [1], based on the Discrete Geometric Approach (DGA) :

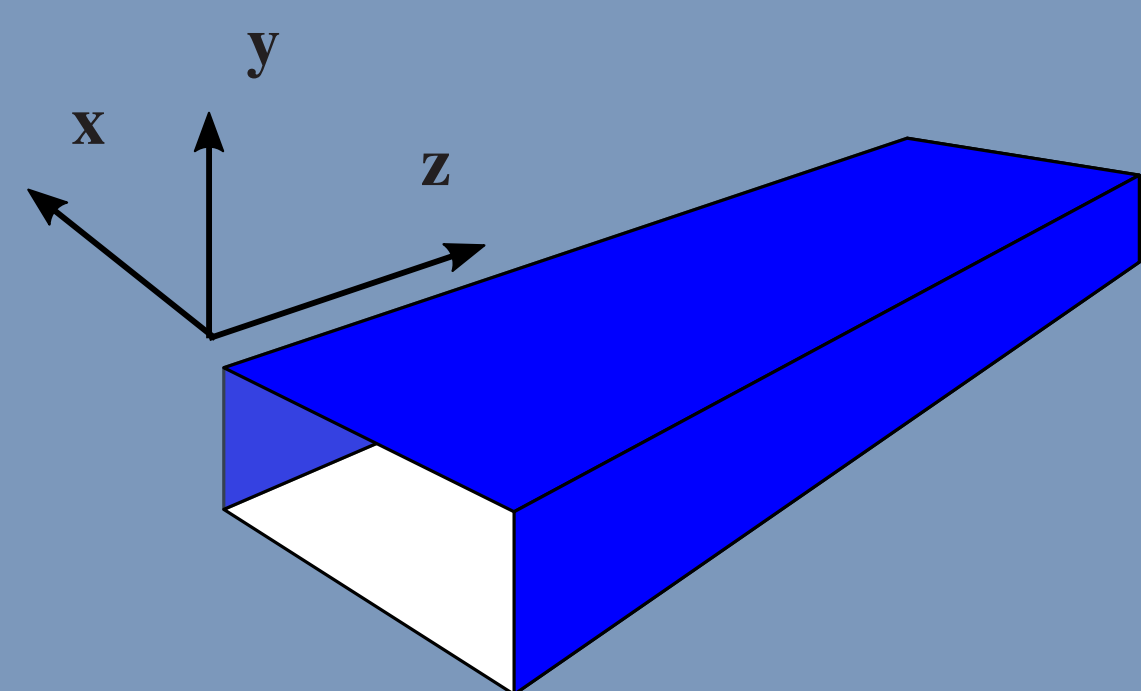
- Explicit \Rightarrow Computationally fast and parallelizable, contrary to FEM
- Consistent (the error in the approximation of constitutive equations vanishes as the spatial grain of the grid goes to zero)
- Second order accurate in time (dual interlocked time grids as original FDTD)
- Conditionally stable
- Works with tetrahedral grids \Rightarrow allows to represent complex geometries, contrary to FDTD

MILESTONES

- We wrote a C++14 code with user friendly script file input
- We showed that massive parallelism can be exploited by using GPUs [2]
- We derived an analytic form for a Courant–Friedrich–Lewy condition for the stability of the method of [1]
- We extended the algorithm to handle lossy, possibly anisotropic, materials

NUMERICAL RESULTS

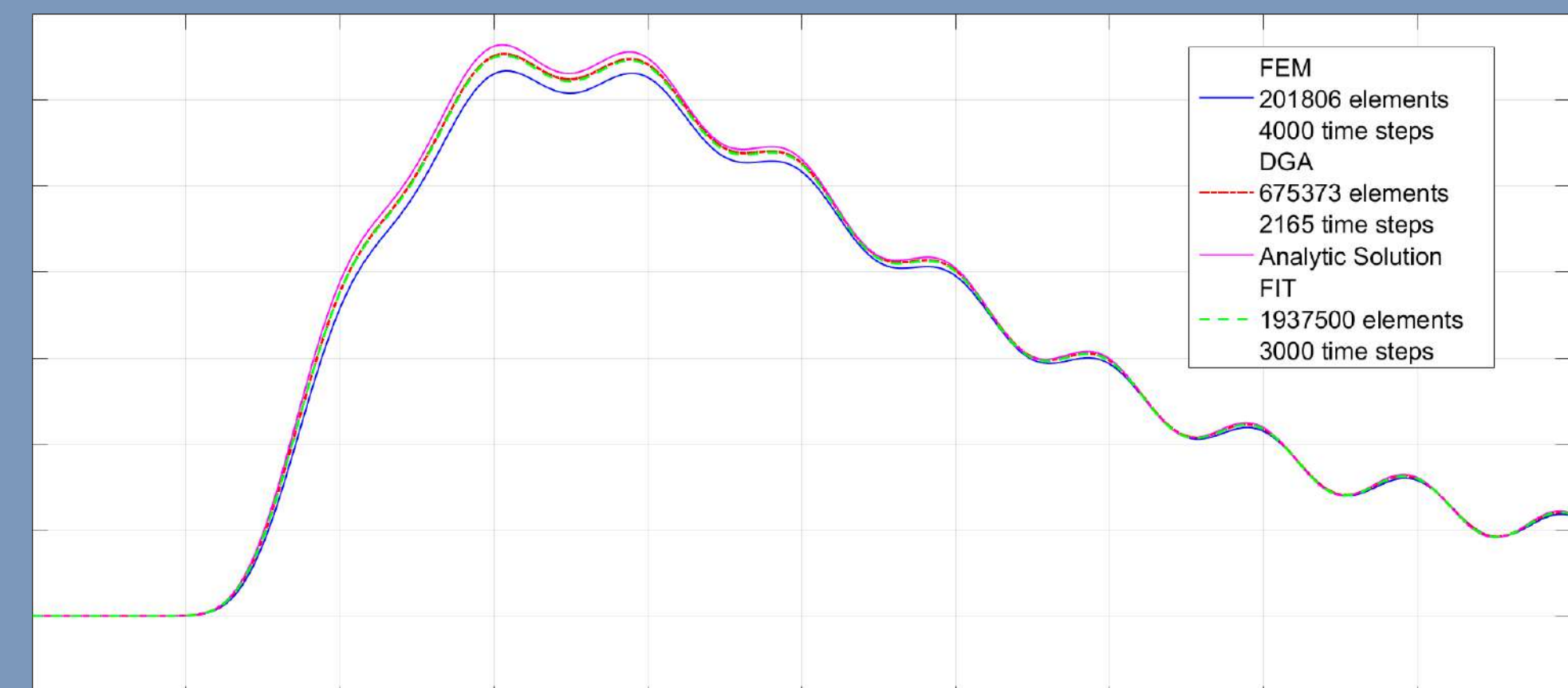
Our main test-bench concerns the simulation of a rectangular waveguide of size 5×2.5 cm and length 10 cm in the z direction. At $z = 0$, a TE_{10} electric field is applied while at the other end ($z = 10$ cm) a Perfect Electric Conductor (PEC) termination is applied.



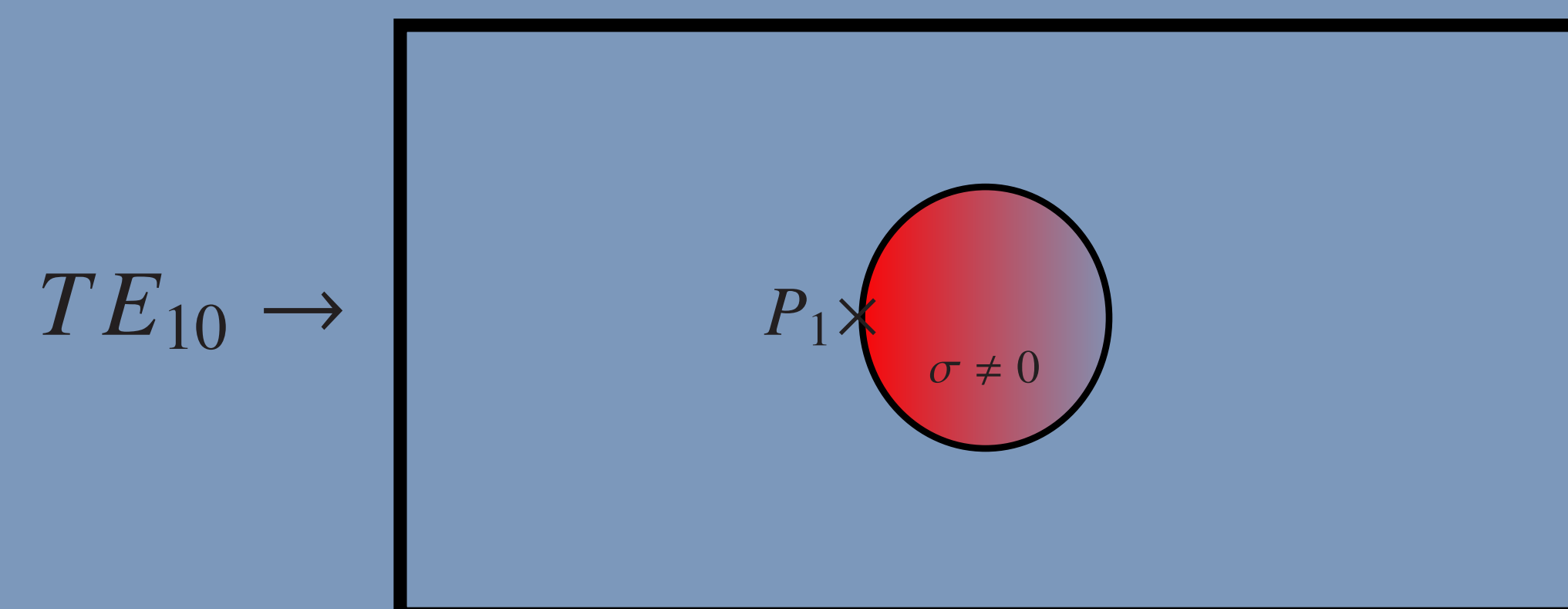
To show the promise of our method, we fill the waveguide with a medium with non negligible electric conductivity (see next box on the right).

NUMERICAL RESULTS

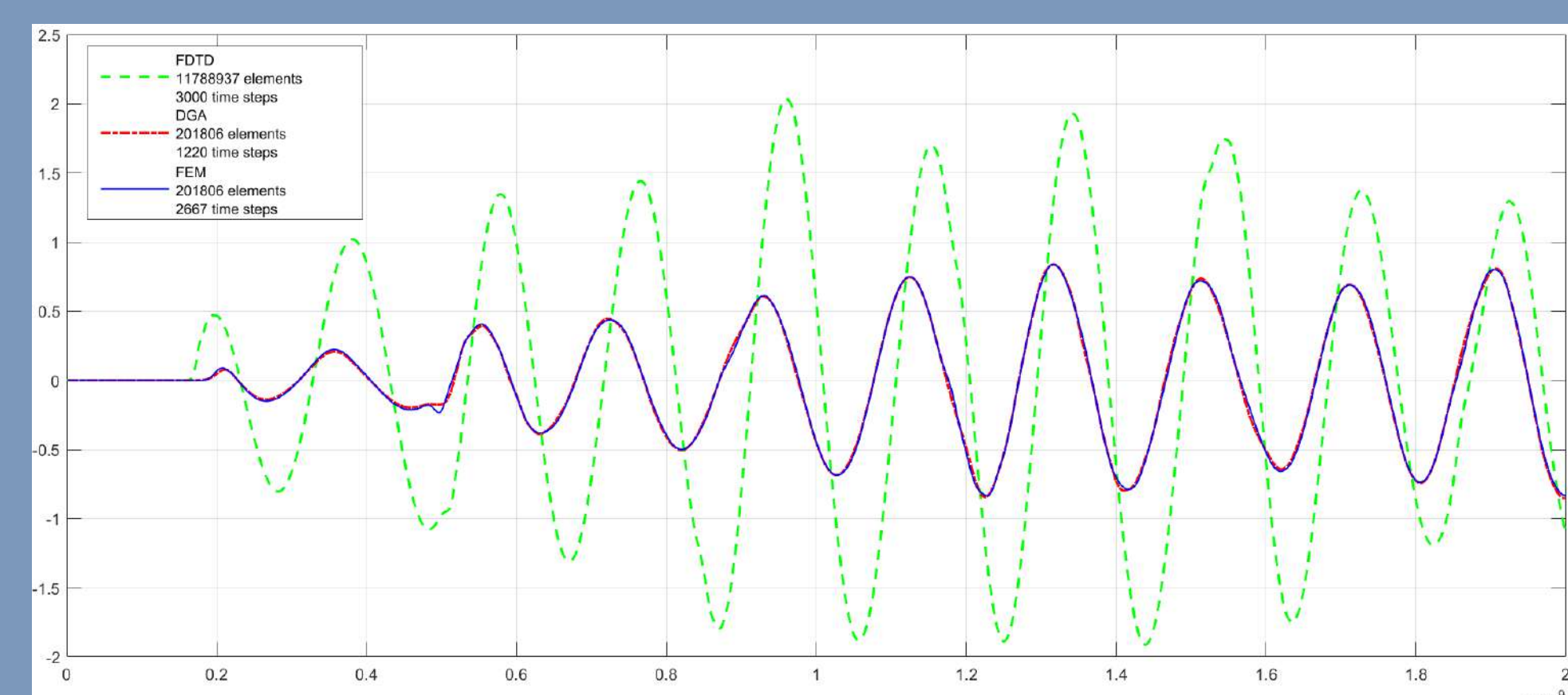
It was found that, in this rather simple case, a closed form for the solution of Maxwell's equations is still possible in the framework of the theory of waveguides. Thus, a comparison with an analytic solution can be shown.



In the above Figure $\sigma_{Ge} = 2.17$ (corresponding to undoped germanium). The x axis shows the simulation time from 0 to 2 nanoseconds, while the y axis shows the E_y transverse electric field at the center of the waveguide. As a further test, we wanted to test the accuracy of the method with material discontinuities with curved geometries, so we put a conductive ball in a dielectric homogenous waveguide.



We found that near the interface (point P_1), FDTD fails to represent the field at P_1 even with very fine grids (due to staircasing). Our method instead yields good agreement with FEM (which, even though accurate, is an order of magnitude slower).



where, again the x axis shows the simulation time from 0 to 2 nanoseconds, while the y axis shows the E_y transverse electric field at point P_1 .

APPLICATIONS

Time domain methods for the solution of Maxwell's equations are ubiquitous in commercial softwares and have a wide range of practical uses, from the validation of Electromagnetic Compatibility (EMC) tests to the modeling of waveguides, photonic crystals, etc.

REFERENCES

- [1] L. Codecasa, M. Politi, Explicit, Consistent and Conditionally Stable Extension of FDTD by FIT, *IEEE Transactions on Magnetics*, Vol. 44, Np. 6, pp. 1258-1261, 2008.
- [2] B. Kapidani, M. Cicuttin, L. Codecasa, R. Specogna, F. Trevisan, GPU accelerated time domain DGA method for wave propagation problems on tetrahedral grids, Accepted for oral presentation, *Compumag Conference 2017*, Daejeon, South Korea, 18-22 June 2017.
- [3] B. Kapidani, L. Codecasa, R. Specogna, F. Trevisan, A Consistent and Conditionally Stable Time-Domain Explicit Scheme on Tetrahedral Meshes for Wave Propagation Problems in Lossy Materials, *IEEE Transactions on Magnetics*, in preparation.

Dott. Bernard Kapidani
Prof. Ruben Specogna

Info:

Tel. +39 0432 558025
kapidani.bernard@spes.uniud.it



UNIVERSITÀ
DEGLI STUDI
DI UDINE

hic sunt futura

PHYSICAL SCIENCES AND ENGINEERING

30° ciclo

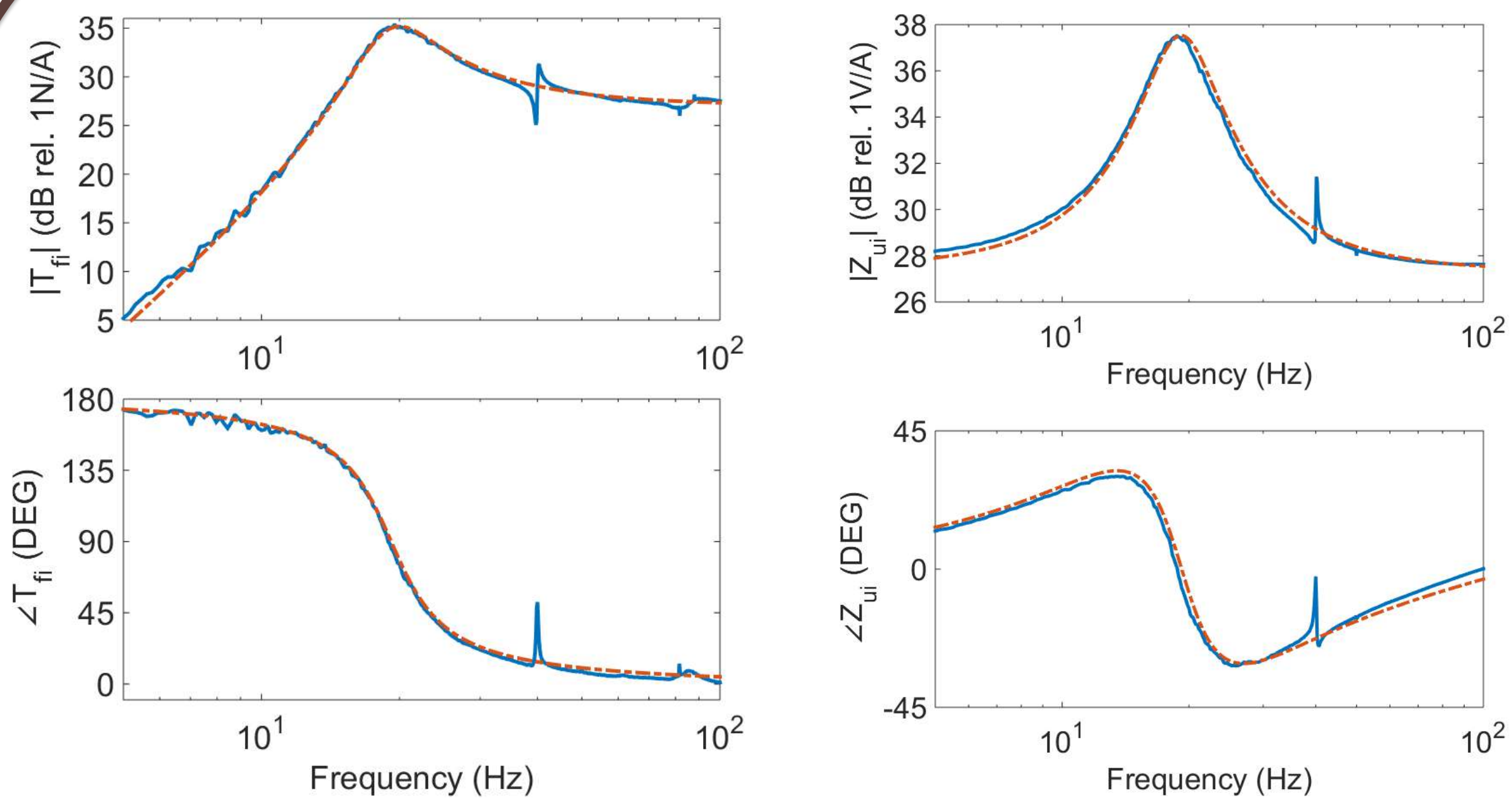
Corso di dottorato in Ingegneria Industriale e
dell'Informazione

Flywheel Inertial Transducer For Energy Harvesting And Vibration Control

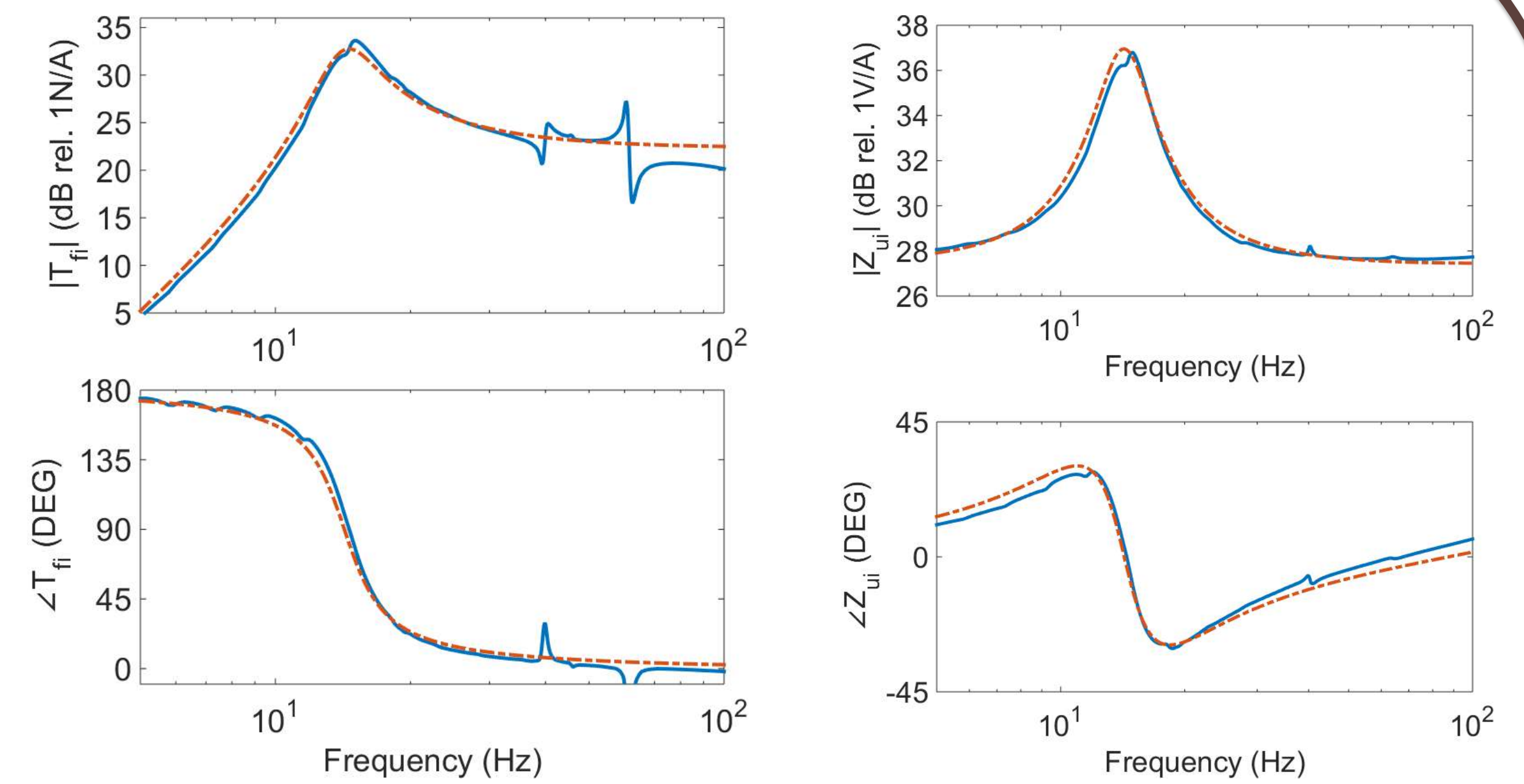
Introduction: Coil-magnet inertial transducers can be used for energy harvesting and vibration control, where:

Energy harvesting – requires lightly damped transducer to maximise the energy absorption,
Vibration control – requires highly damped transducer with low fundamental resonance frequency.
 This poster presents comparative studies on classical and flywheel inertial transducers.

CLASSICAL CONFIGURATION

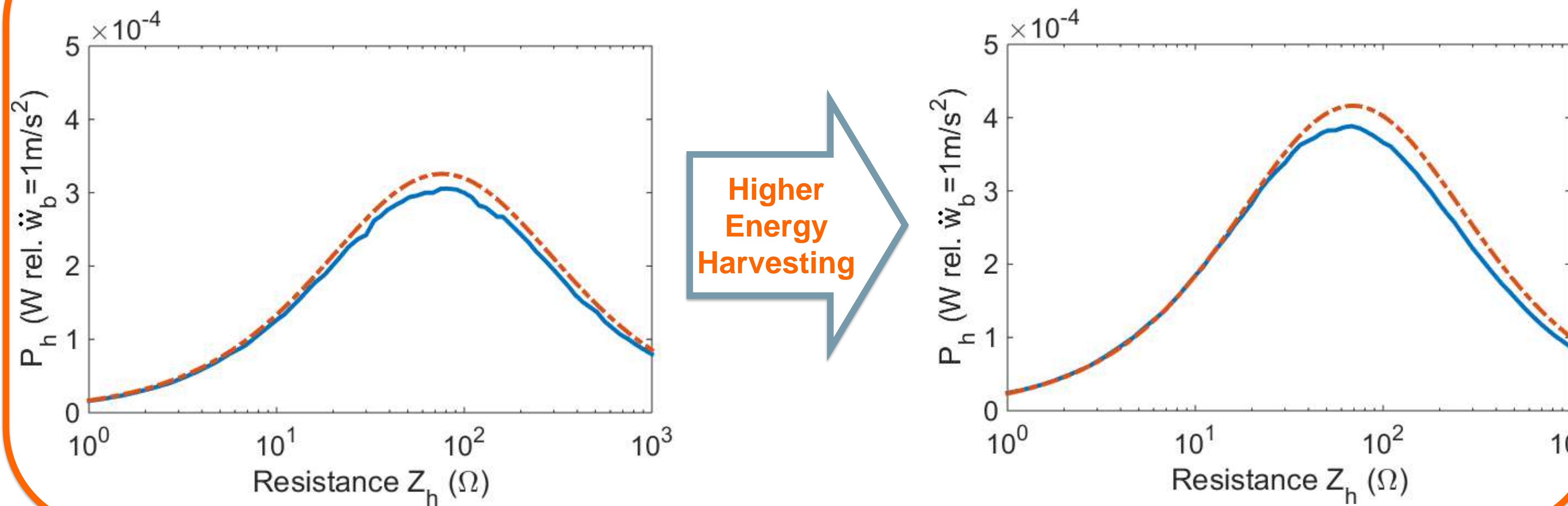


FLYWHEEL CONFIGURATION

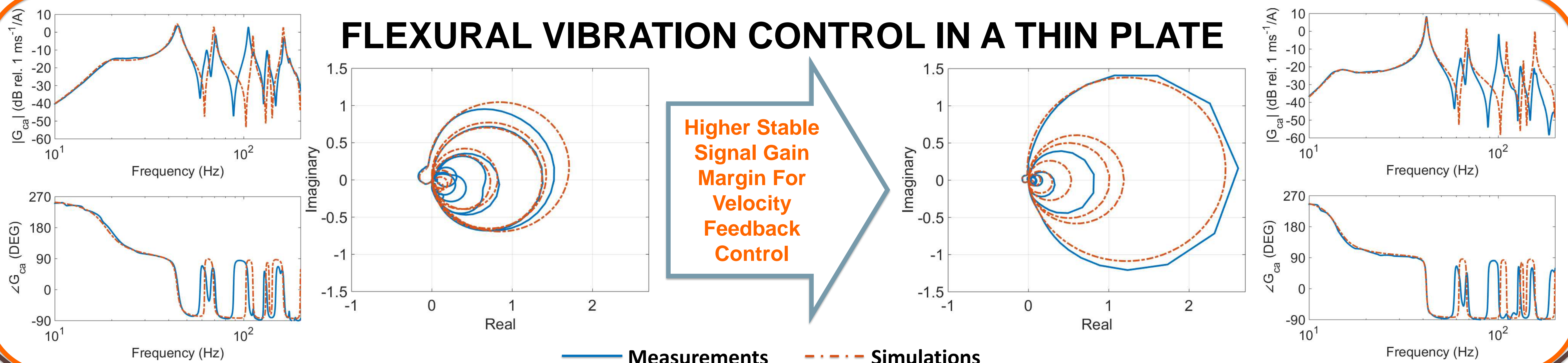


Lower
Fundamental
Resonance
Frequency
&
Lower
damping

ENERGY HARVESTING



FLEXURAL VIBRATION CONTROL IN A THIN PLATE



Conclusion: The flywheel inertial transducer improves performance in both applications and can be used in: industrial machinery, land, air, sea transportation vehicles, buildings, transportation infrastructures, etc.

Dott. Aleksander Kras
Prof. Paolo Gardonio

Info:
Tel. +39 0432 558035
Fax. +39 0432 558251
E-mail contacts:
aleksander.kras@uniud.it
paolo.gardonio@uniud.it

References

- [1] A. Kras, P. Gardonio, Velocity feedback control with a flywheel proof mass actuator, *Journal of sound and vibration* (2017)
- [2] A. Kras, P. Gardonio, Flywheel proof mass transducer for energy harvesting applications, *8th ECCOMAS conference SMART2017* (2017)
- [3] A. Kras, P. Gardonio, Experimental tests of a flywheel inertial actuator, *24th ICSV24 conference* (2017)

Acknowledgement

The authors gratefully acknowledge the European Commission for its support of the Marie Skłodowska Curie program through the ITN ANTARES project (GA 606817)

ANTARES



**UNIVERSITÀ
DEGLI STUDI
DI UDINE**
hic sunt futura

PHYSICAL SCIENCES AND ENGINEERING

30° ciclo

Corso di dottorato in Ingegneria Industriale e dell'Informazione

LA VALUTAZIONE DELLA COMPLESSITÀ NEI PROGETTI E L'INFLUENZA SULL'APPRENDIMENTO

OBIETTIVI E METODO DI RICERCA

Nei progetti di maggiori dimensioni e nelle organizzazioni che operano su commessa, la complessità è riconosciuta come una tra le caratteristiche con il maggiore impatto sulle performance chiave (tempo, costo, qualità) e sul conseguente successo del progetto.

Il lavoro di ricerca ha l'obiettivo di:

- definire e individuare le caratteristiche dei fattori di complessità nei progetti;
- valutare il livello di complessità di un progetto in relazione alle performance ottenute rispetto alla pianificazione;
- approfondire le modalità con cui diversi livelli di complessità di progetto impattano sulle decisioni operative e l'apprendimento, in particolare nelle organizzazioni a commessa.

A tal fine si sono svolti:

- un'analisi approfondita della letteratura e degli studi empirici sulle variabili di complessità nei progetti;
- casi studio multipli su progetti di navi da crociera di aziende leader del settore delle costruzioni navali.

SETTORI DI APPLICAZIONE

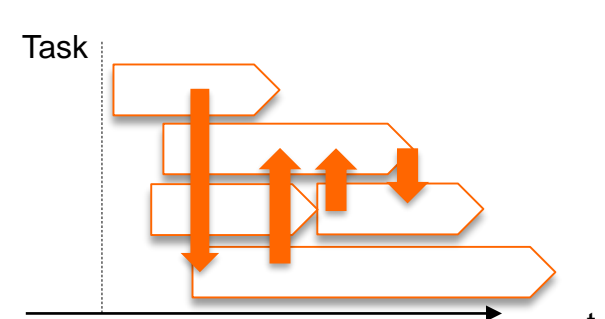
- Imprese a gestione multi-progetto:

- costruzioni navali
- infrastrutture
- sistemi informativi



- Progetti complessi:

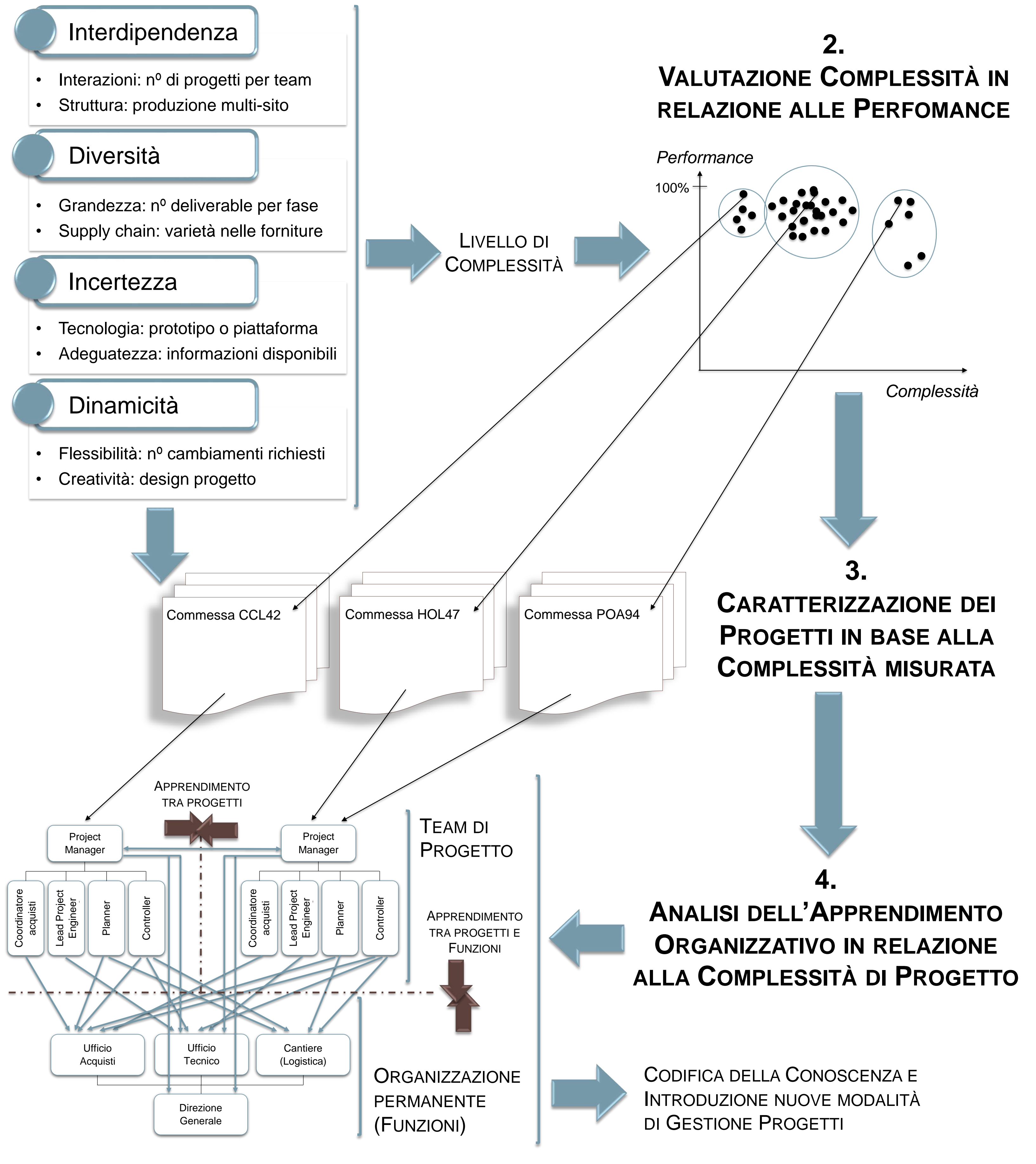
- innovazione strategica
- cambiamento organizzativo
- sviluppo nuovo prodotto/processo



FRAMEWORK DI ANALISI

1. DIMENSIONI DI COMPLESSITÀ ED ESEMPI DI INDICATORI

- Interdipendenza**
 - Interazioni: n° di progetti per team
 - Struttura: produzione multi-sito
- Diversità**
 - Grandezza: n° deliverable per fase
 - Supply chain: varietà nelle forniture
- Incertezza**
 - Tecnologia: prototipo o piattaforma
 - Adeguatezza: informazioni disponibili
- Dinamicità**
 - Flessibilità: n° cambiamenti richiesti
 - Creatività: design progetto



ASPETTI INNOVATIVI PER LE IMPRESE

- Framework di riferimento per la valutazione dei fattori e del livello di complessità dei propri progetti, in particolare in ottica multi-progetto
- Evidenza dell'influenza della complessità di progetto sull'apprendimento organizzativo, al fine di individuare nuove modalità di gestione progetti

Ing. Elena Pessot
Prof. Alberto F. De Toni

Info:
Tel. +39 0432 558043
elena.pessot@uniud.it

Riferimenti bibliografici

De Toni, A.F. and Pessot, E. (2015). Measurement of complexity in manufacturing systems: a systematic literature review and a conceptual framework. Paper presented to the 6th Annual Conference of the European Decision Sciences Institute (EDSI 2015), May 31 - June 3, 2015, Taormina, Italy.

De Toni, A.F. and Pessot, E. (2017). How does complexity influence learning in projects? A multiple case study. Paper to be presented to the 8th Annual Conference of the European Decision Sciences Institute (EDSI 2017), May 29 - June 1, 2017, Granada, Spain.

De Toni, A.F. and Pessot, E. (2017). Complexity in projects and project management: a systematic literature review and a research agenda. Paper under review in *International Journal of Project Management*

NOISE AND VIBRATION CONTROL OF CYLINDRICAL STRUCTURES WITH TUNEABLE VIBRATION ABSORBERS

VIBRO-ACOUSTIC CONTROL

Critical issues of vibro-acoustic control:

- ✓ High excitations levels
- ✓ Complexity of the disturbance (stochastic distribution in space and time)
- ✓ Severe mass and volume constrains

Classical remedies:

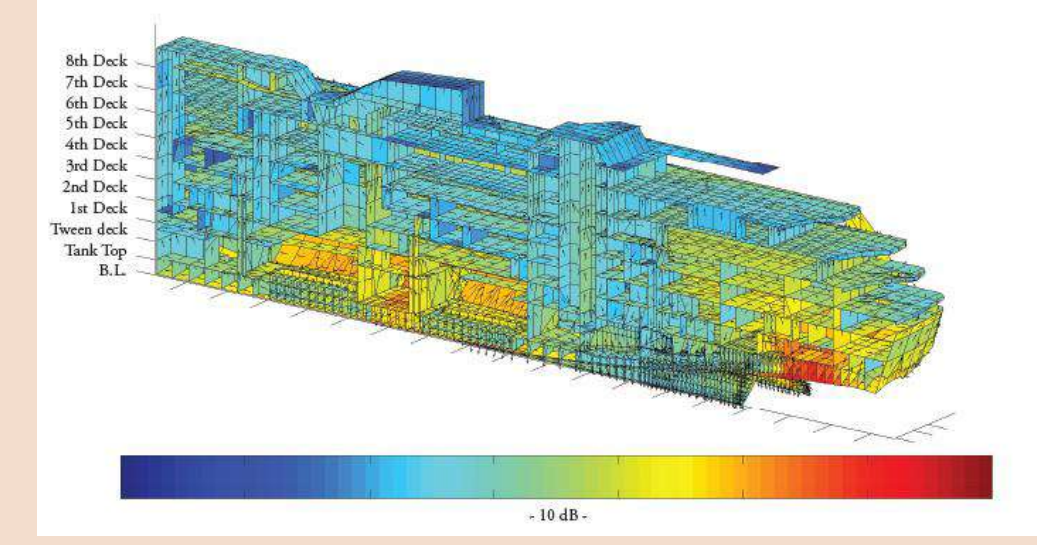
- ✓ Mass-stiffness-damping treatments
- ✓ Sound absorption materials
- ✓ **Tuned Vibration Absorbers**
- ✓ Active structural-acoustic control systems

APPLICATIONS

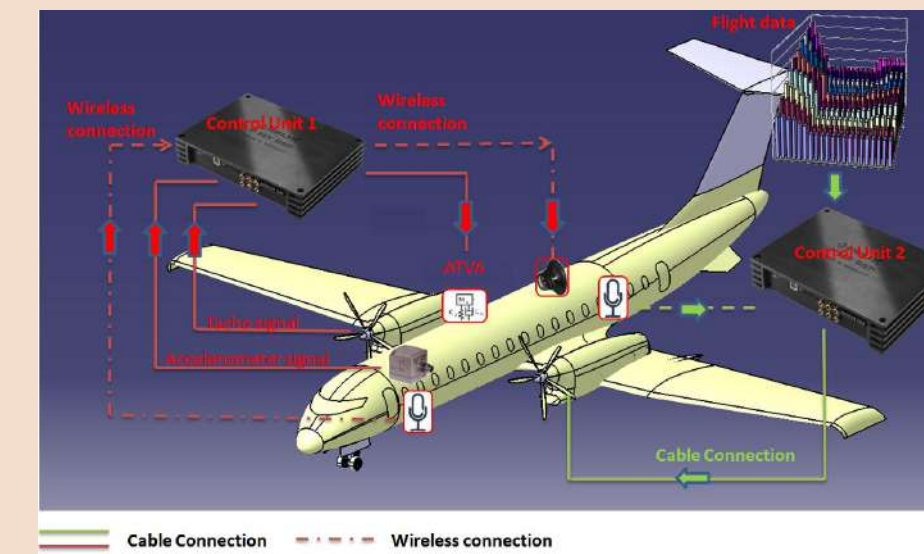
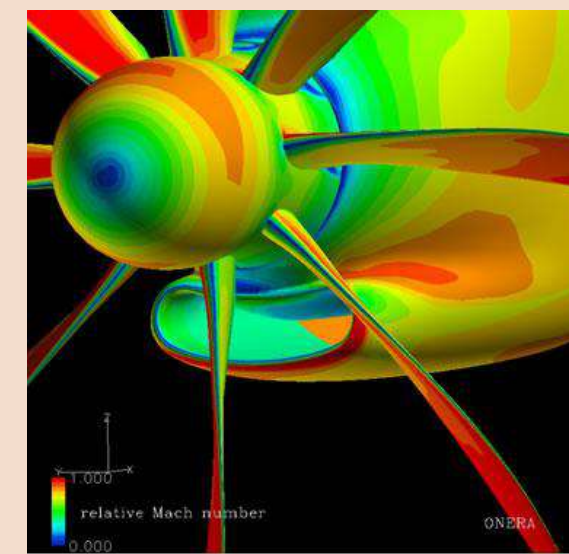
Automotive



Naval



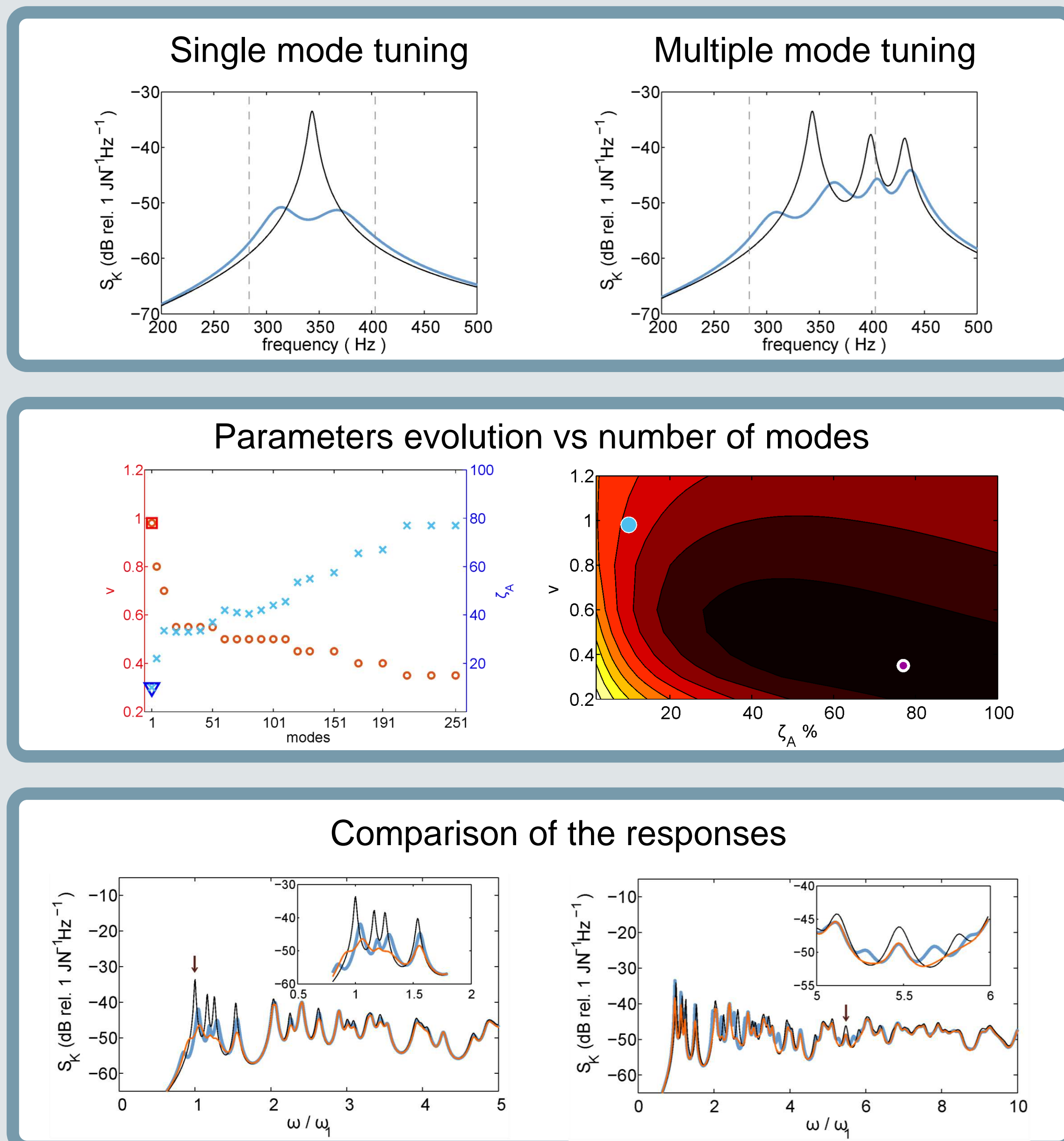
Aeronautics



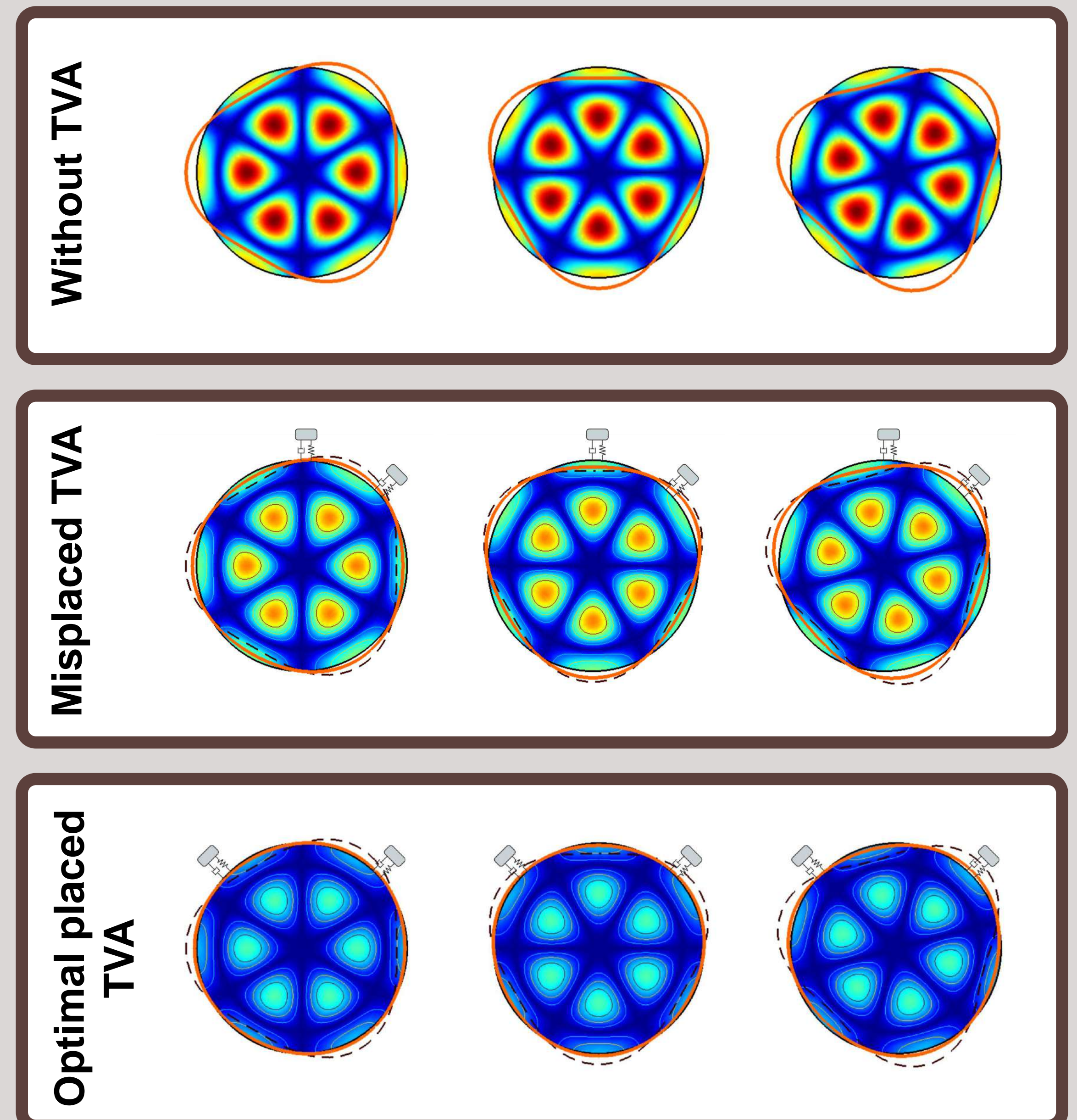
Loudspeakers



TUNING CONSIDERATIONS



POSITIONING CRITERIA

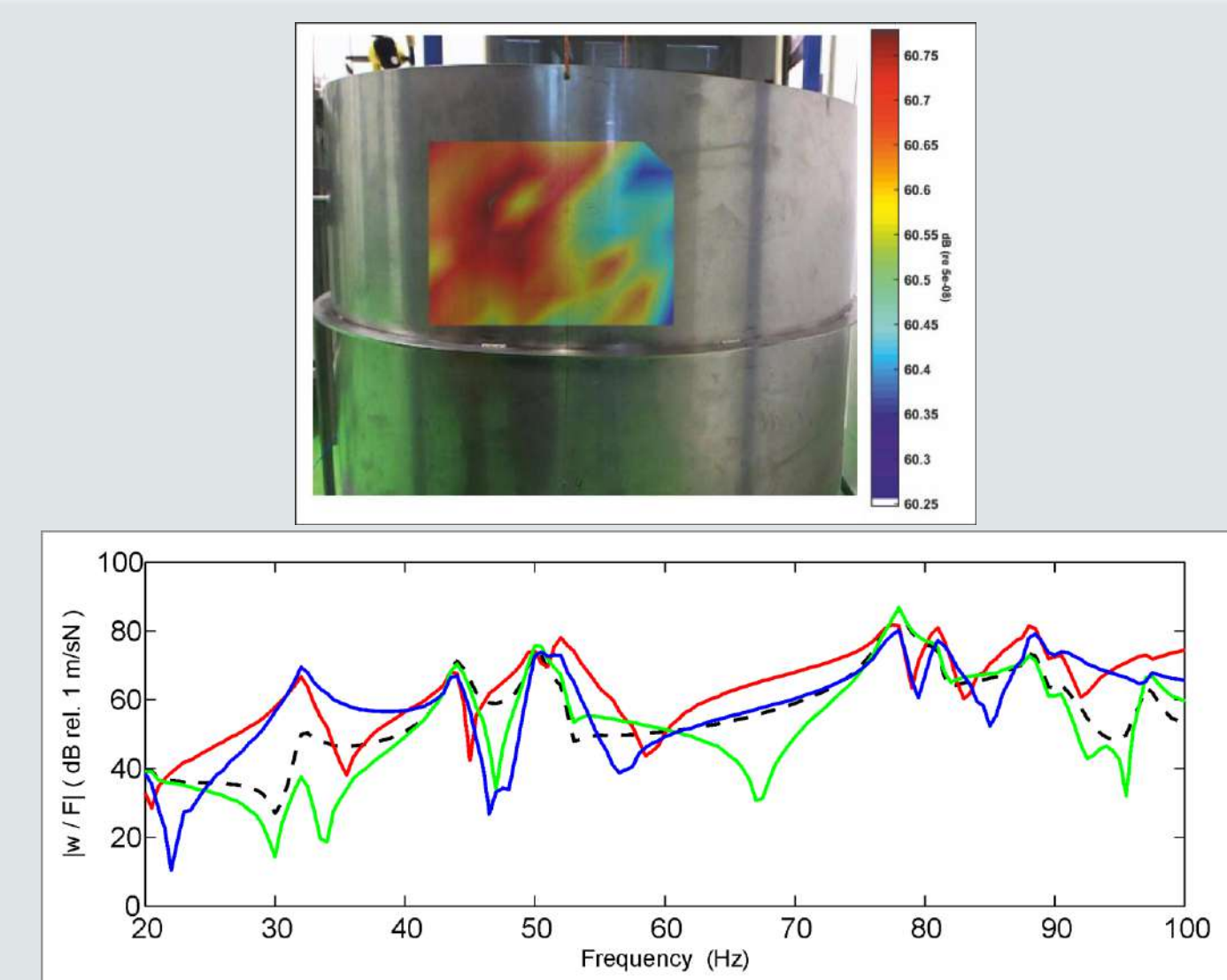


CONCLUSIONS

The presented study shows that:

- The classical single mode optimization procedure is not suitable for high modal overlap factor structures;
- An optimal positioning criteria for the TVAs is required to obtain greater reduction in both the structural and acoustic response.

EXPERIMENTAL SETUP



References

- E. Turco and P. Gardonio *On the use of tuneable mass dampers for broad-band noise control in a cylindrical enclosure. ICSV22, Florence, Italy 2015*
- E. Turco, P. Gardonio and L. Dal Bo *Time-varying shunted electro-magnetic tuneable vibration absorber. MoViC RASD 2016, Southampton, UK 2016*
- E. Turco and P. Gardonio *Sweeping shunted electro-magnetic tuneable vibration absorbers: design and implementation. Journal of Sound and Vibration (under review)*
- P. Gardonio and E. Turco *Tuning and poitioning of Tuned Vibration Absorbers and Helmholtz Resonators for broad-band control. Journal of Sound and Vibration (under review)*

Dott. Emanuele Turco
Prof. Paolo Gardonio

Info:
turco.emanuele.1@spes.uniud.it
paolo.gardonio@uniud.it



**UNIVERSITÀ
DEGLI STUDI
DI UDINE**
hic sunt futura

PHYSICAL SCIENCES AND ENGINEERING

30° ciclo

Corso di dottorato in Ingegneria Industriale e dell'Informazione

Context-Based Goal-Driven Reasoning for Improved Target Tracking

What is tracking?

Target tracking is a dynamic estimation problem where generally:

- States of interest change in the time with unknown dynamics
- Measurements' origins are uncertain
- There are false measurements
- Some measurement might be missing
- Initial (t_0) guesses of estimates might not be available

Challenges in target tracking

Ground target tracking can suffer from:

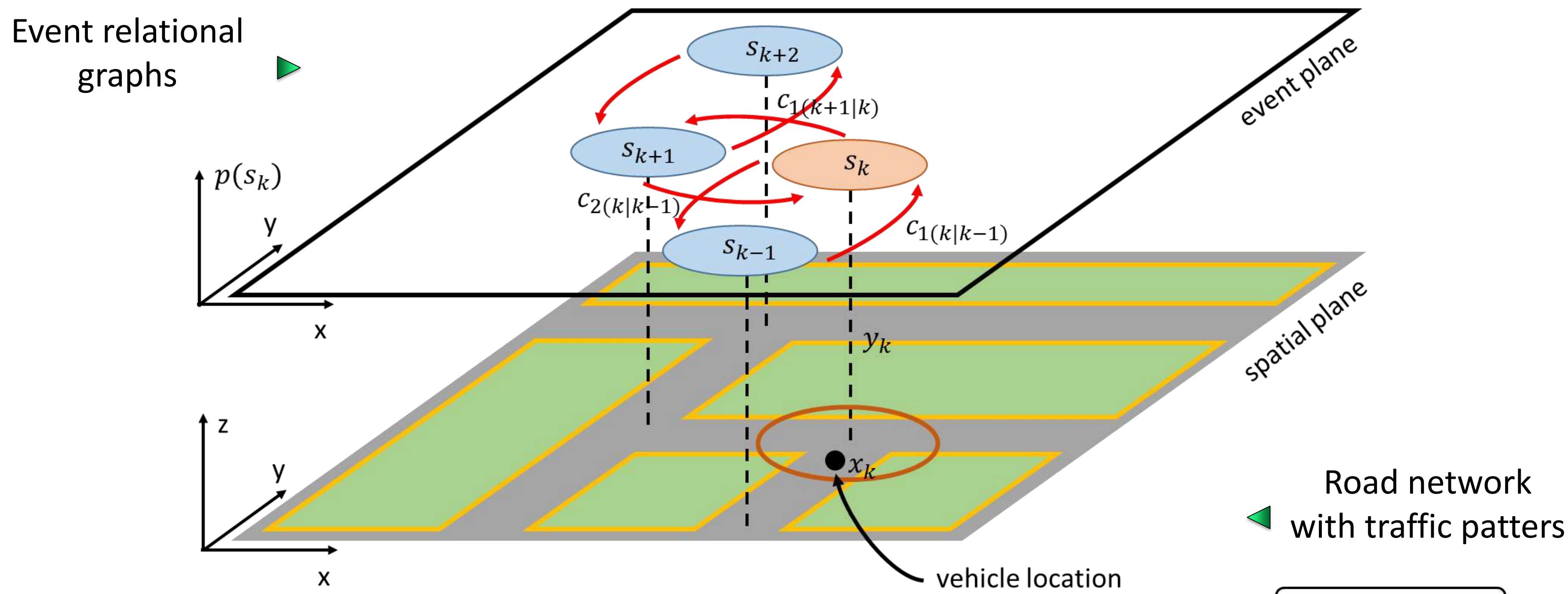
- low visibility
- high clutter
- high target density
- complex target dynamics, e.g. stop and go maneuvers
- masking in Doppler blindness.

The exploitation of contextual information (CI) is highly desirable to improve tracking performance.

How could be context exploited?

- At the **object assessment** level, CI constrains either the system or measurement model/parameters with context
- At the **situation assessment** level, solve CI reasoning as a **problem of activities and intent (goal) recognition**
- Infer** an entity's **plan** based on the **observed** entity's **actions** and their effects
- Use **context** for establishing **links** between **events** and **entities**
- Use **context** for **adjusting** the **confidence** that an entity is following a certain **plan**

Context as events in an urban environment



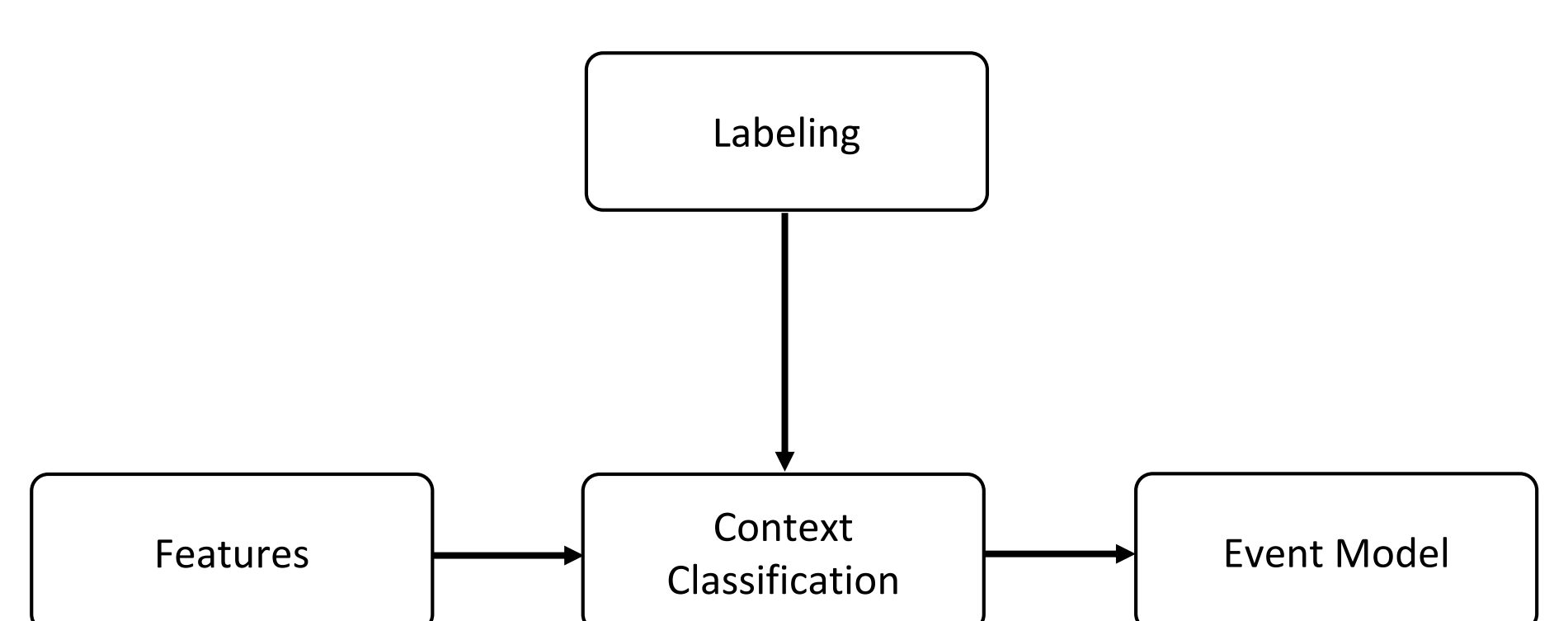
CI exploitation at situation assessment level

Context influences the choice of system model

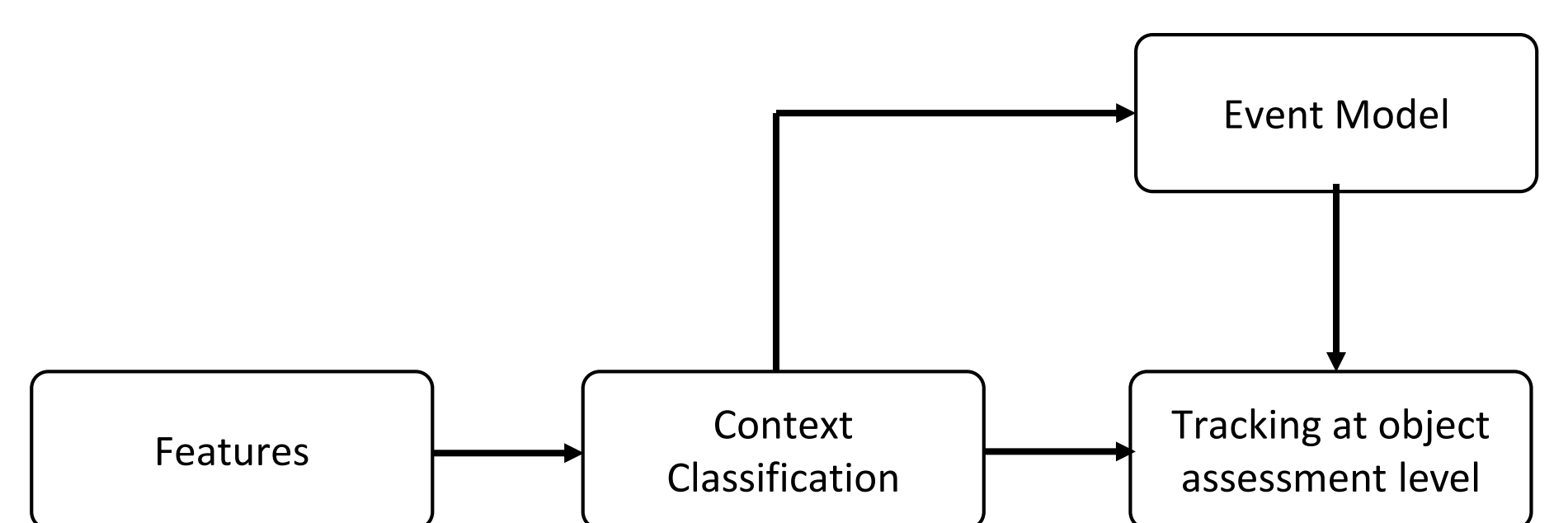
$$x_k = F(m_k)x_{k-1} + G(m_k)v_k$$

$$y_k = H(m_k)x_k + w_k$$

Learning phase



Evaluation phase



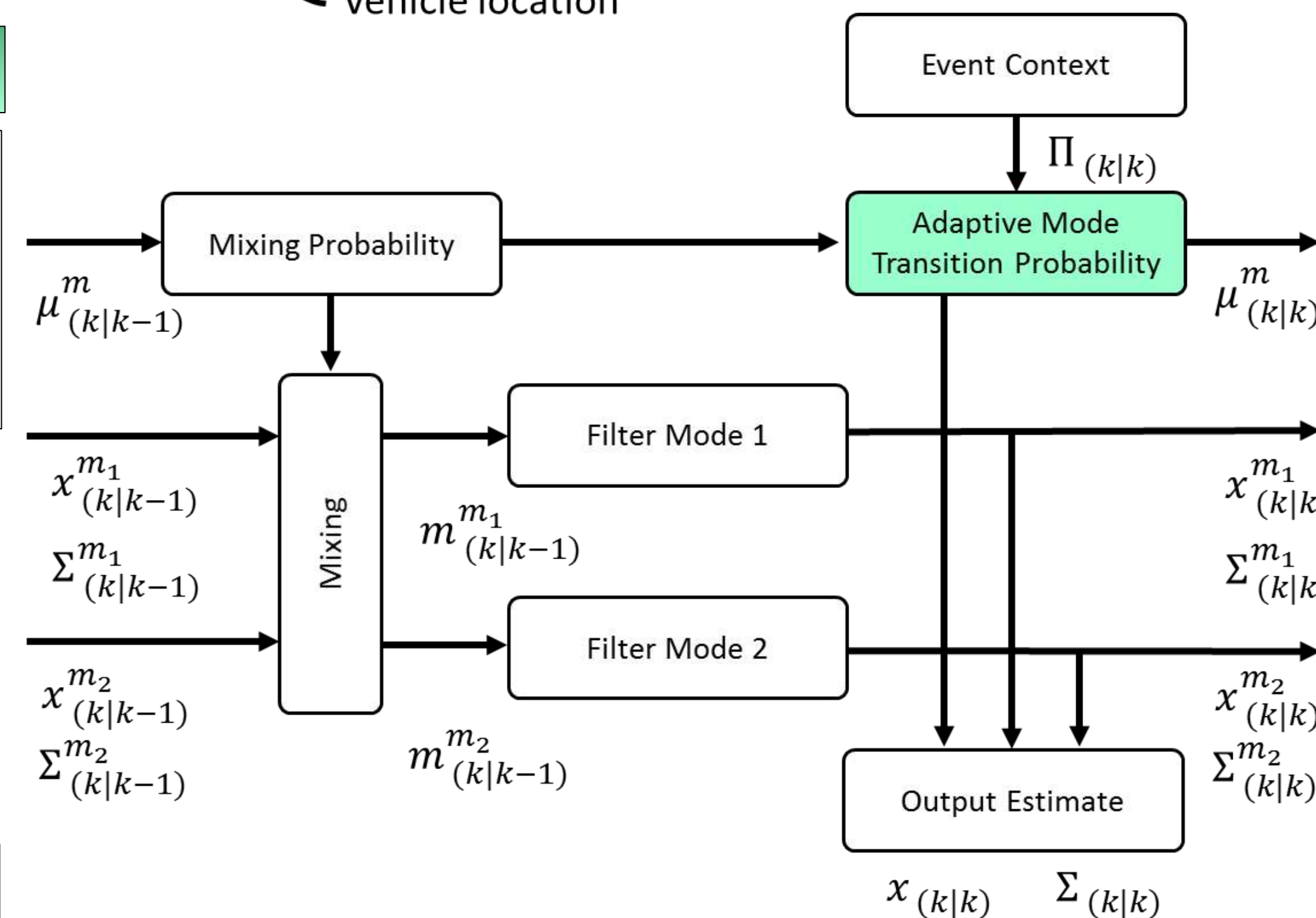
Context-Aware Data Fusion

System under consideration
 $x_{k+1} = f_k(x_k) + v_k$ or $p(x_{k+1}|x_k)$,
 $y_k = h_{y_k}(x_k) + w_k$ or $p(y_k|x_k)$,
 $c_k = h_{c_k}(x_k)$ or $p(c_k|x_k)$,

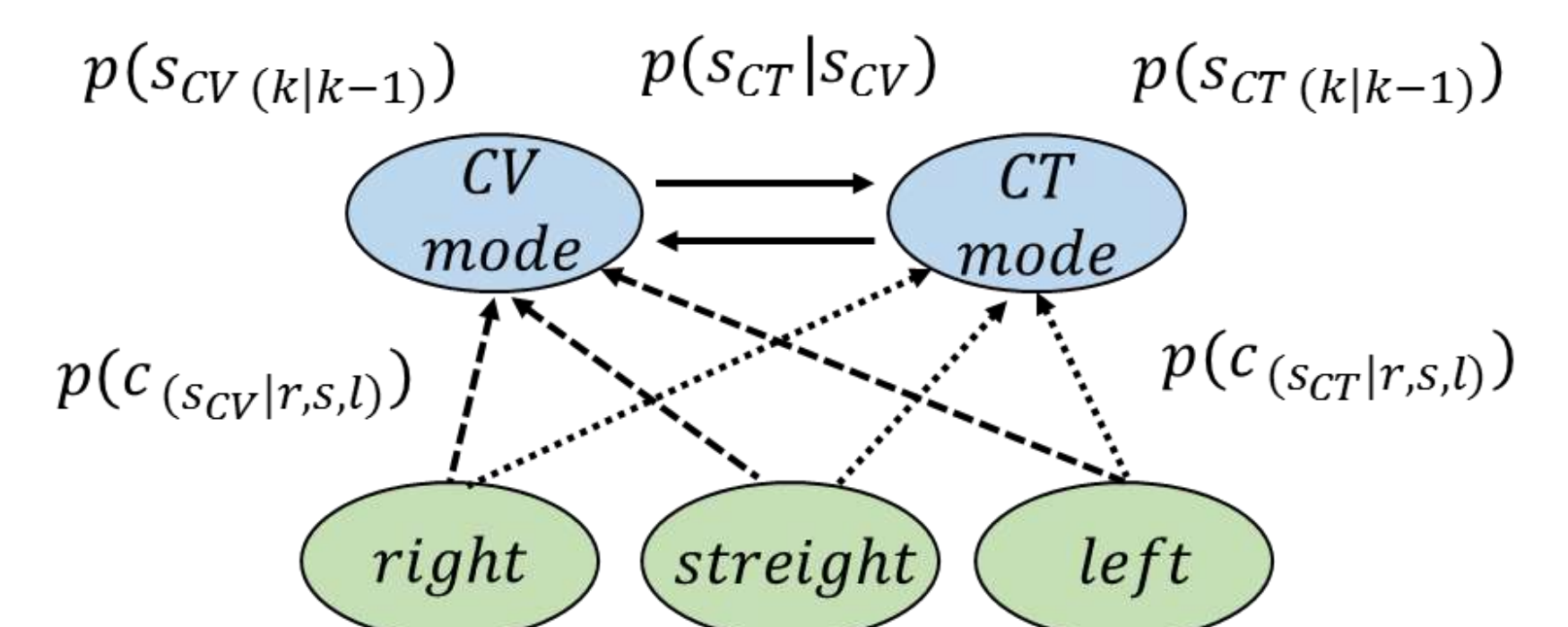
Bayesian inference conditioned on CI

$$p(\mathbf{X}_{k-1}|y_{1:k-1}, c_{1:k-1}) \xrightarrow{\text{Prediction}} p(\mathbf{X}_k|y_{1:k-1}, c_{1:k-1})$$

$$p(\mathbf{X}_k|y_{1:k-1}, c_{1:k-1}) \xrightarrow{\text{Measurement Update}} p(\mathbf{X}_k|y_{1:k}, c_{1:k})$$



Context learning and inference

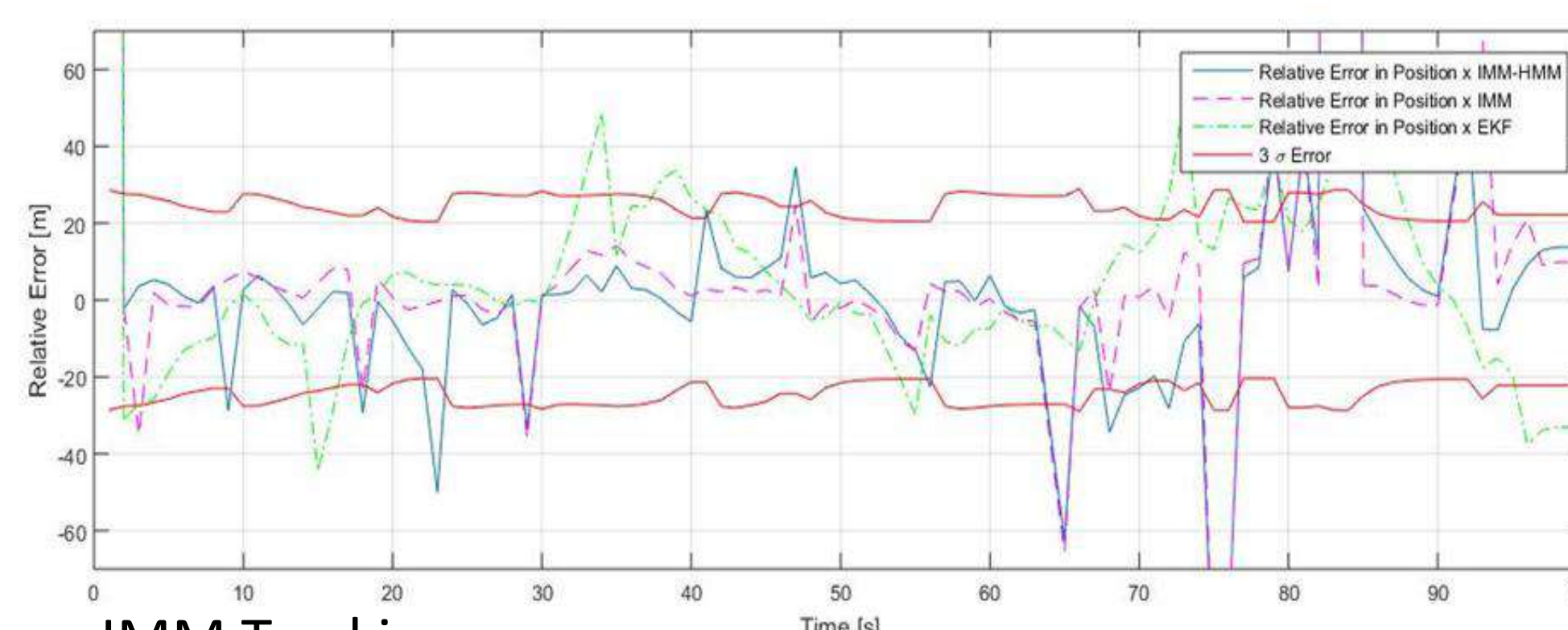
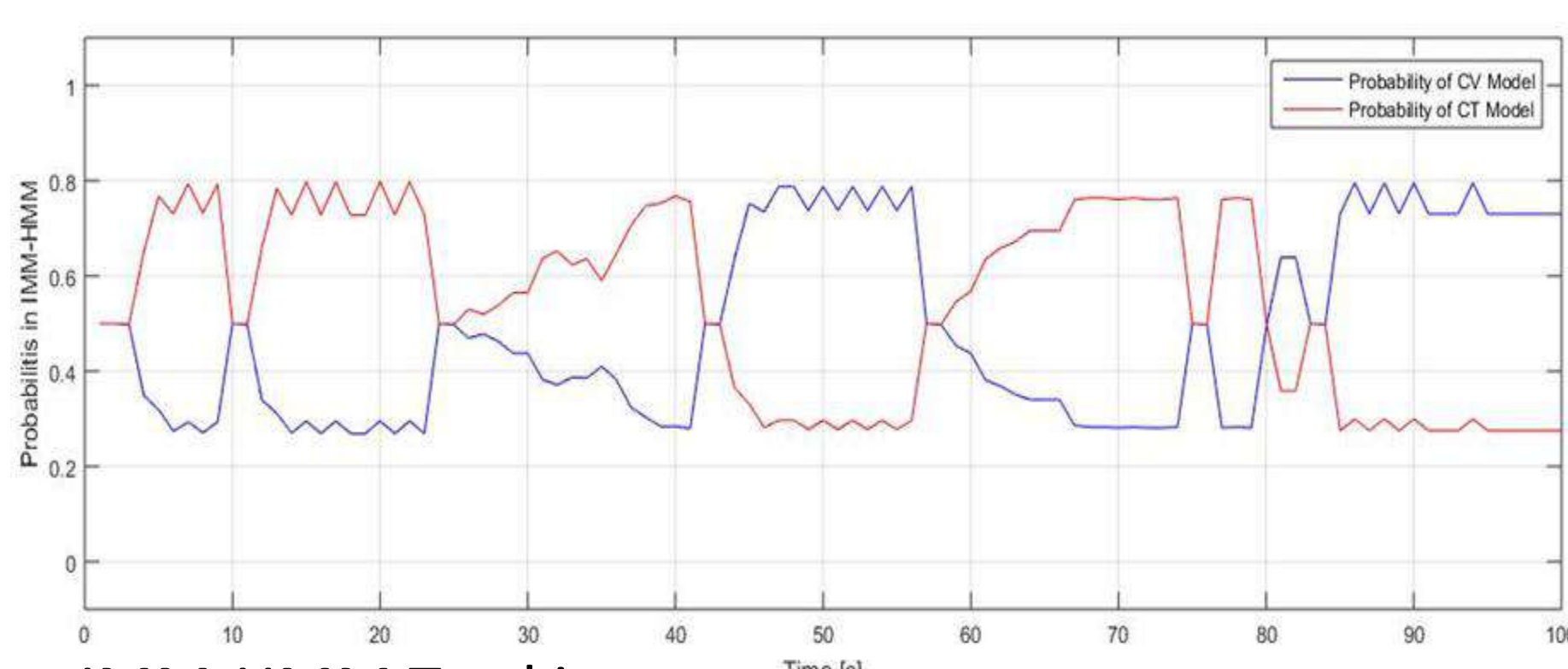
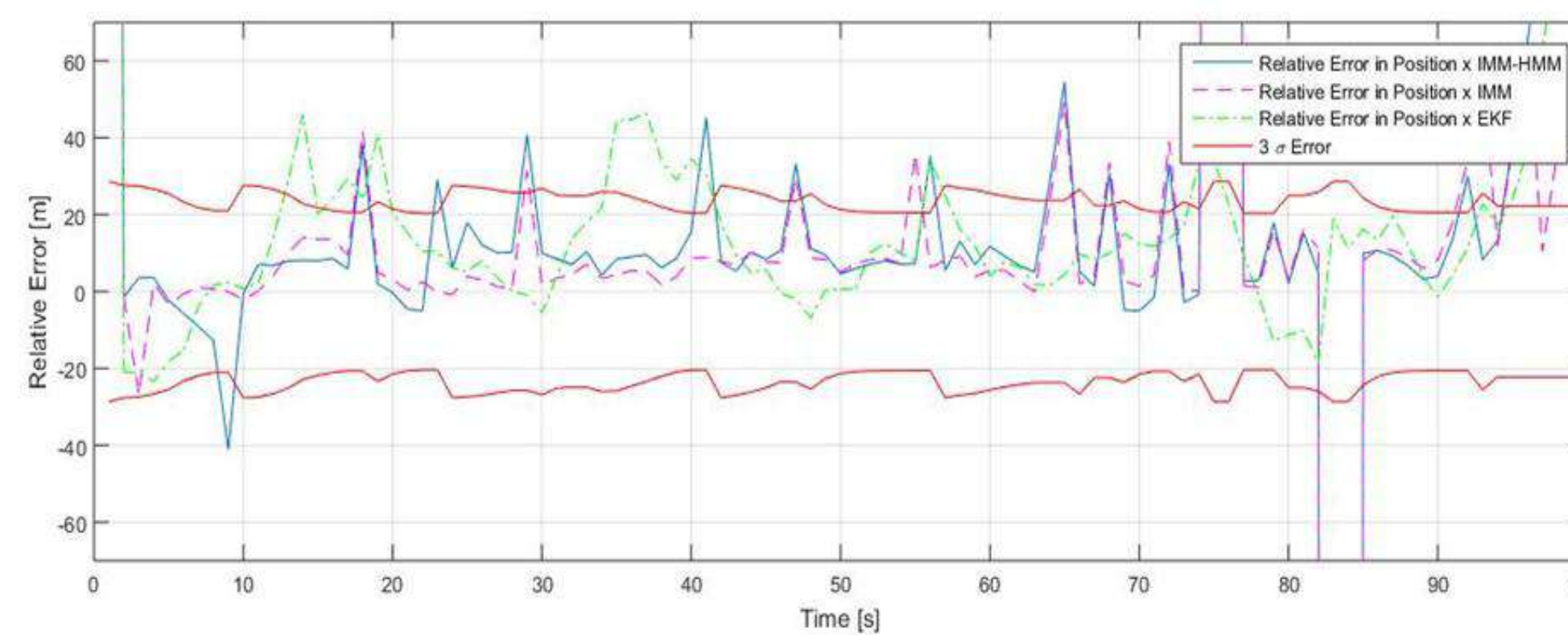
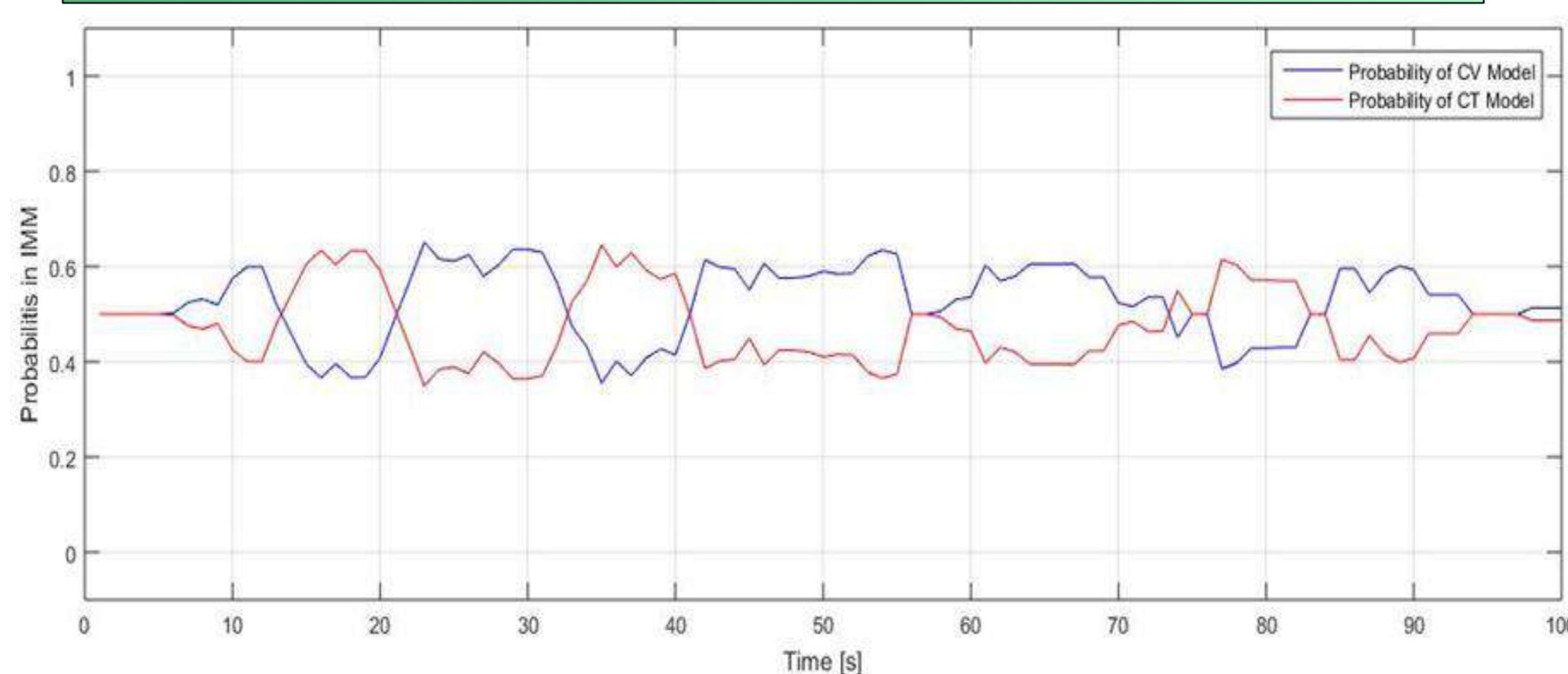


- As the target progresses through the road network and forming a chain of events, the DBN could infer on target's future actions based on its past.
- This knowledge could be used for switching the tracking model to better track the target
- Similarly, relevant context could be discovered or selected based on target's future or past actions, respectively.

Bayesian network inference

$$P(Y_{1:t}, X_{1:t}) = \prod_{t=1}^T P(X_{i|t}|X_{i|t-1})$$

Example of CI exploitation



IMM-HMM Tracking

Mean error in position X = -26.27 m
 Mean error in position Y = 28,60 m

- Mertens, M.; Ulmke, M.; *Ground Moving Target Tracking with context information and a refined sensor model*, 11th International Conference on Information Fusion, Cologne, 2008, 1-8.
- Zhu, Y.; Nayak M. N.; Roy-Chowdhury K. A.; *Context-aware activity modeling using hierarchical conditional random fields*; Transactions on Pattern Analysis and Machine Intelligence, vol 37 no. 7, pp. 1360-1372, 2015
- Vaci L.; Snidaro, L.; Foresti, L. G.; *Encoding context likelihoods functions as classifiers in particle filters for target tracking*, Proceedings on Multisensor Fusion and Integration, Baden-Bade, Germany, IEEE, 2016. pp. 310-315
- Snidaro, L.; Garcia, J.; Llinas, J.; *Context-based information fusion: a survey and discussion*, Information Fusion, vol. 25, 16-31, 2015.
- Snidaro, L.; Vaci, L.; Garcia, J.; et al.; *A framework for dynamic context exploitation*, 18th International Conference on Information Fusion, 2015.

IMM Tracking

Mean error in position X = -30,74m
 Mean error in position Y = 31,22 m

Dr. Lubos Vaci
 Dr. Lauro Snidaro

lubos.vaci@uniud.it
 lauro.snidaro@uniud.it



UNIVERSITÀ
 DEGLI STUDI
 DI UDINE
 hic sunt futura

PHYSICAL SCIENCES AND ENGINEERING

30° ciclo

Corso di dottorato in Ingegneria Industriale e dell'Informazione

An ADAS Design Based on IoT V2X Communications

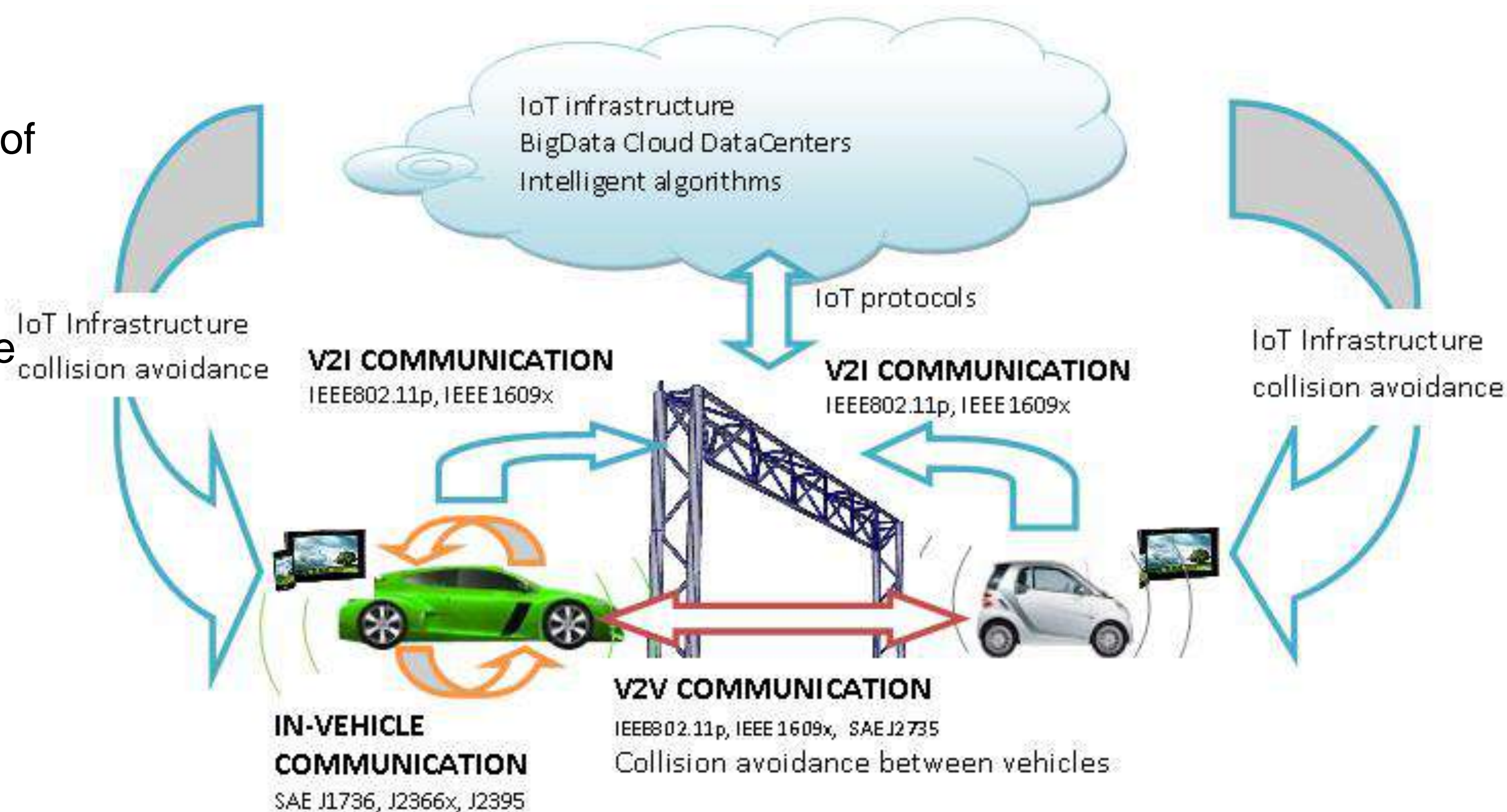
Proposed approach

The proposed system design approach includes:

1. Integration Definition (IDEF) modeling methodology for the development high complex systems;
2. Data Flow analysis;
3. Using IoT reference model and standards IEEE, ETSI for vehicle networks to provide comparability with other systems in the future;

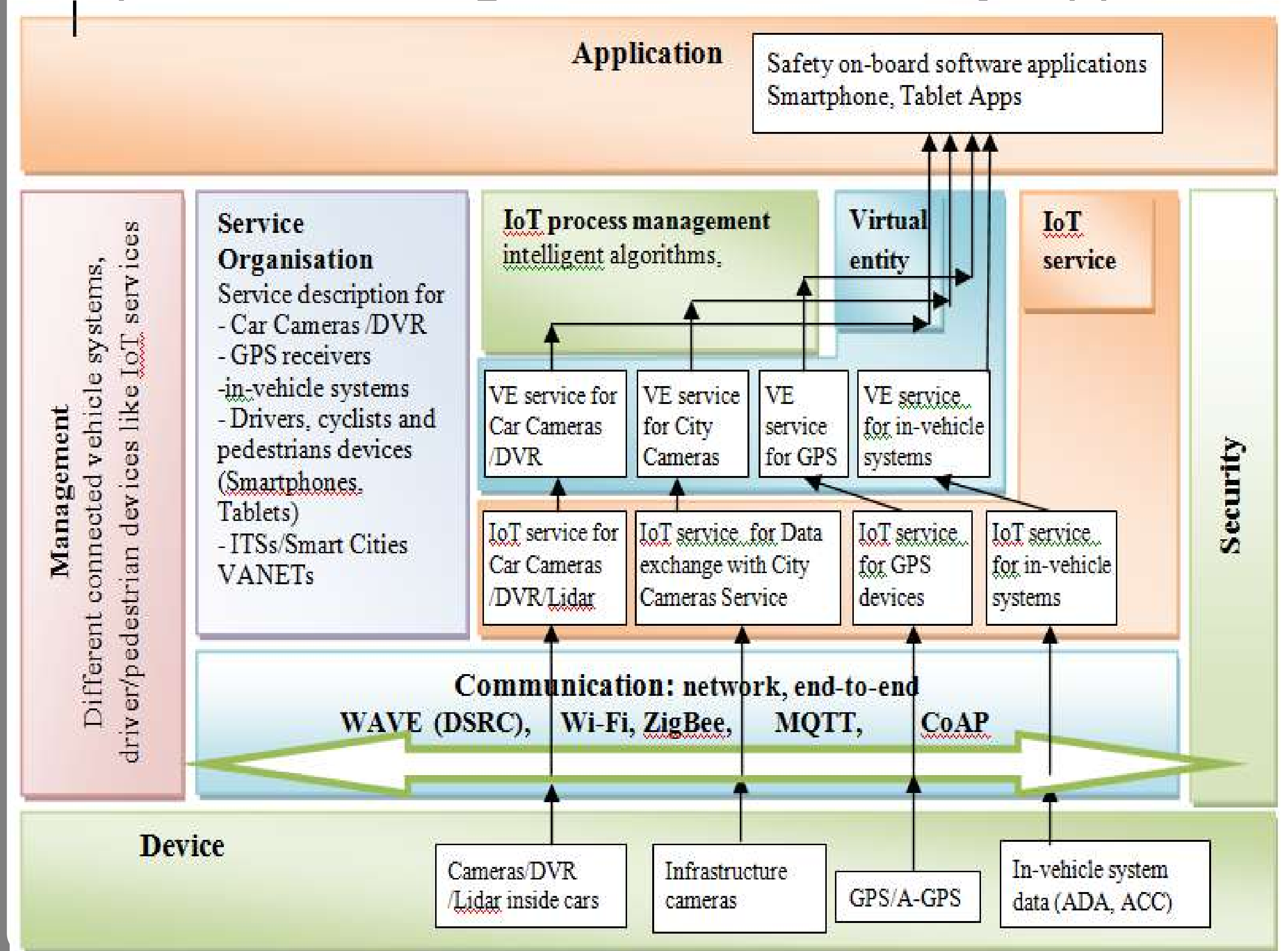
Innovations:

1. An ADAS design approach which provides the development of the system architecture and its update with the Standards and technologies;
2. Cooperative ADAS architecture is developed using a Design Approach 1 that ensures the comparability with different kind of existing in-vehicles and V2I systems, ITSs and VANETs.
3. The proposed approach Allows to move from "Intranet of Things" to the "Internet of Things"

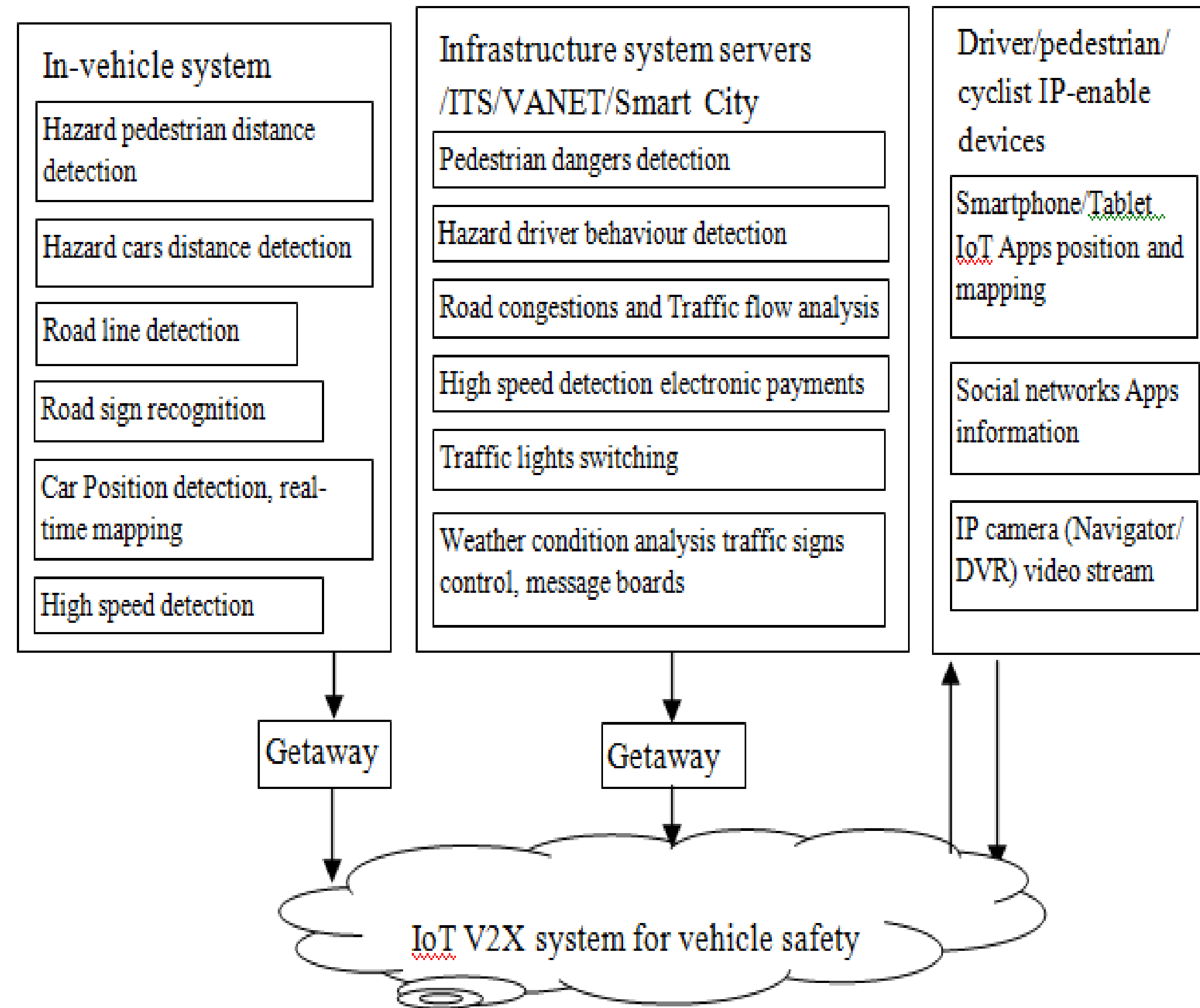


IoT ARM

IoT levels: Device, Communication, IoT service, IoT process management, Virtual entity, App



Application level



Dott. Nadezda Yakusheva E-mail: yakusheva.nadezda@spes.uniud.it
 Prof. Gian Luca Foresti E-mail: gianluca.foresti@uniud.it
 Prof. Christian Micheloni E-mail: christian.micheloni@uniud.it

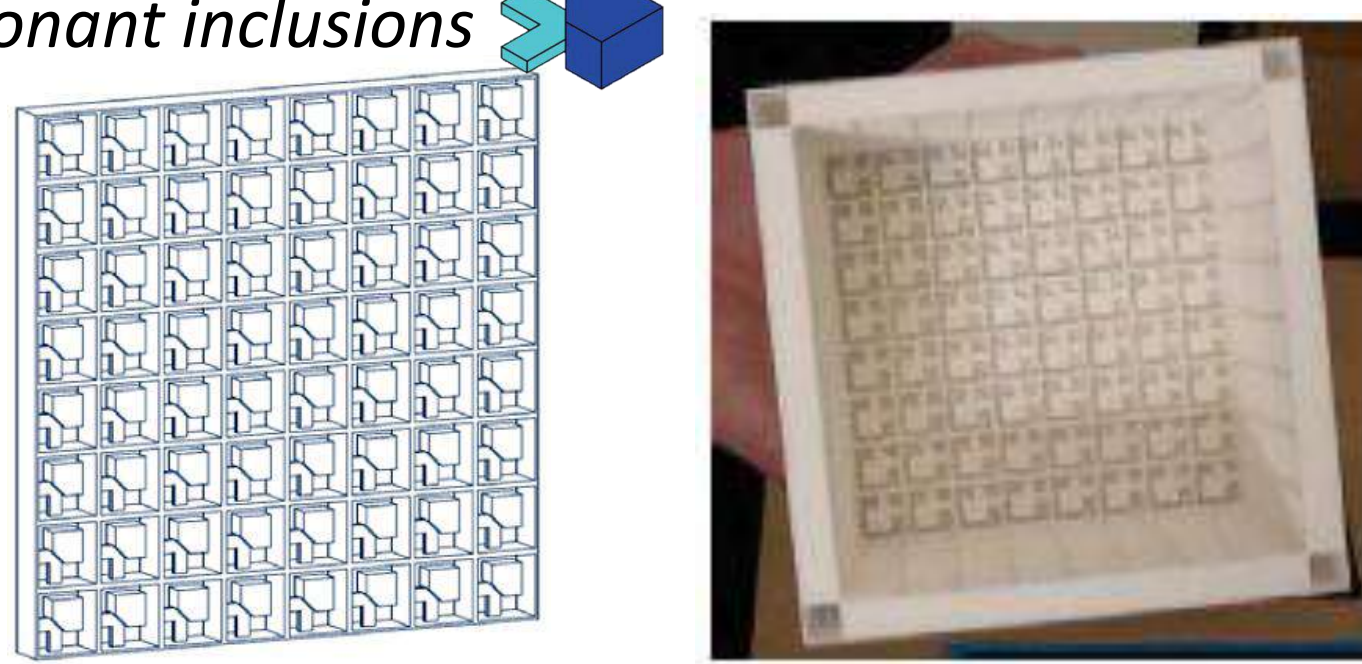
Metamaterial panel with piezoelectric patches connected to multi-resonant electrical shunts

1 Introduction

Metamaterials are material systems whose overall vibro-acoustic properties originate from engineered sub-wavelength periodic structures rather than inherent material properties.

Metamaterials possess unique wave filtering capabilities due to the existence of frequency ranges over which a free wave propagation is stopped (**STOP BANDS, BAND GAPS**).

* Resonant inclusions



2 Modeling

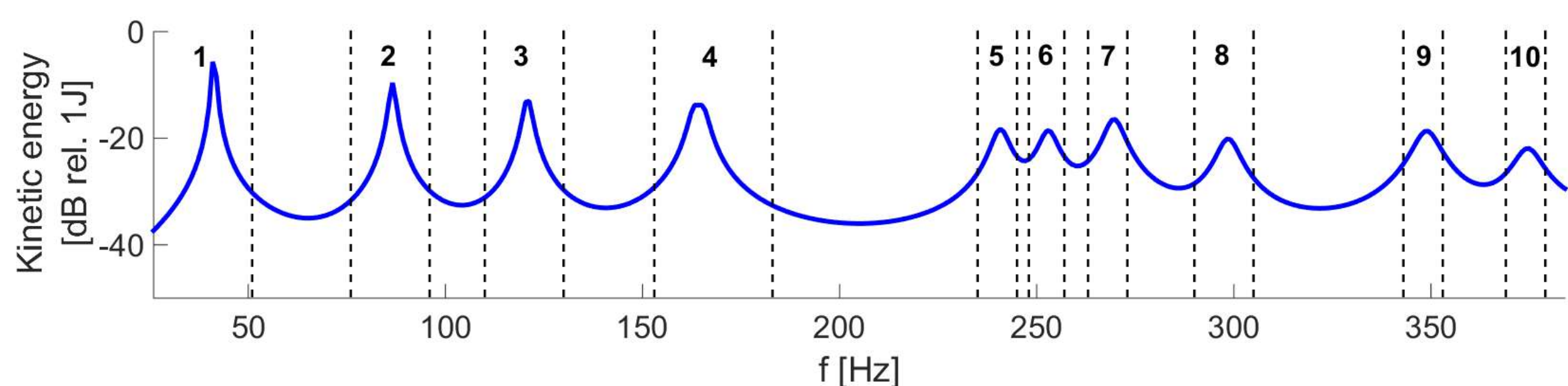
The flexural response of the plate with the array of shunted piezoelectric patch transducers is derived from a state-space formulation which is based on the three canonical matrix equations of the electro-mechanical response of the system and the electrical response of the shunt circuits:

$$\begin{aligned} \mathbf{M}_t \ddot{\mathbf{q}}(t) + \mathbf{C}_p \dot{\mathbf{q}}(t) + \mathbf{K}_t \mathbf{q}(t) + \boldsymbol{\theta}_{pe} \mathbf{v}_s(t) &= \boldsymbol{\Phi}_p \mathbf{f}_p(t), \\ -\boldsymbol{\theta}_{pe}^T \dot{\mathbf{q}}(t) + \mathbf{C}_{pe} \dot{\mathbf{v}}_s(t) &= \mathbf{i}_s(t), \\ \frac{v_{s,i}(\omega)}{i_{s,i}(\omega)} &= \frac{\lambda_{s,i}(\omega)}{i_{s,i}(\omega)} = -Z_{s,i}(\omega). \end{aligned}$$

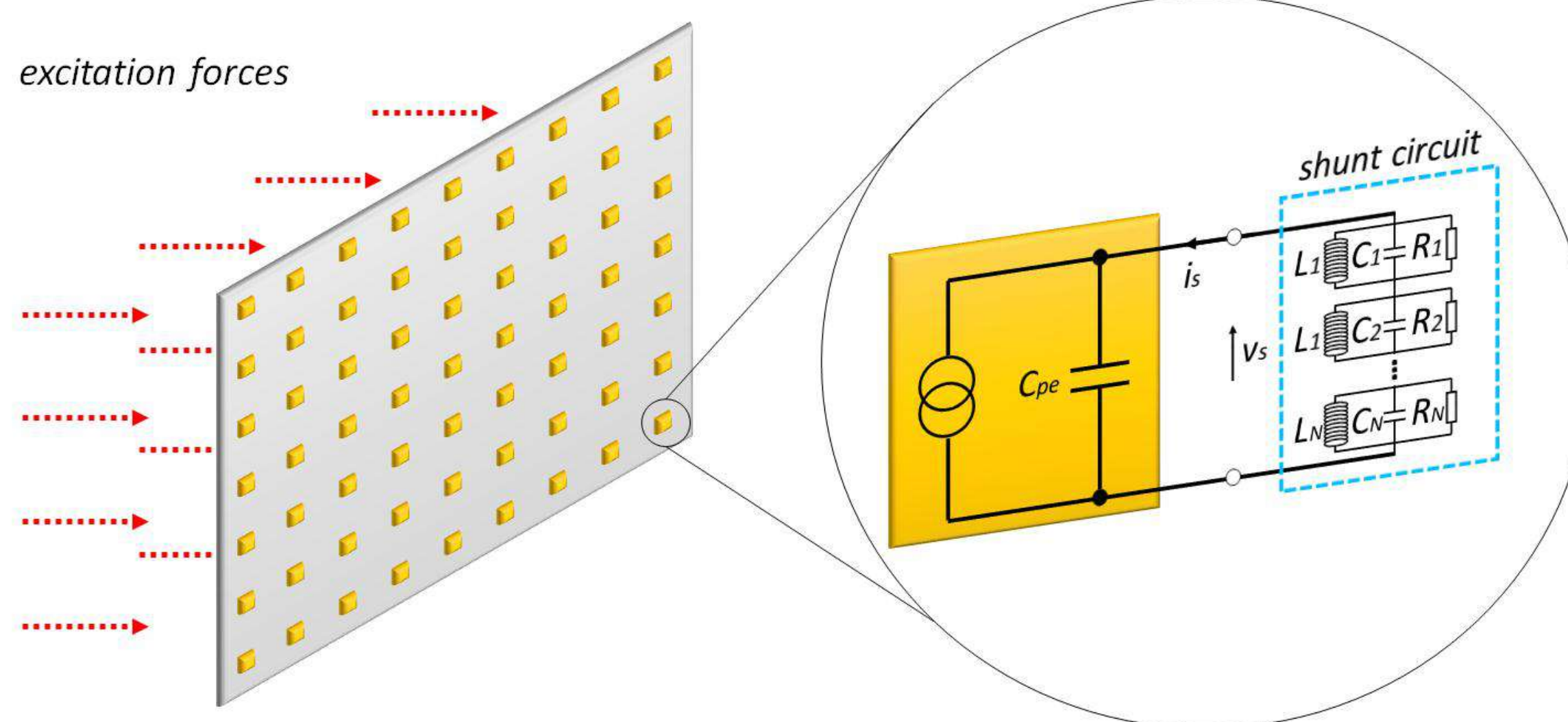
The overall system response is presented in terms of the time averaged total kinetic energy and time averaged total electrical power absorbed by the shunt circuits.

3 Tuning strategy

The optimal single mode shunt parameters: f_s and Q_s , that would reduce the low frequency narrow resonance peaks and mid frequencies wide band crests have been derived numerically considering the 10 bands highlighted below in the spectrum of the kinetic energy PSD.



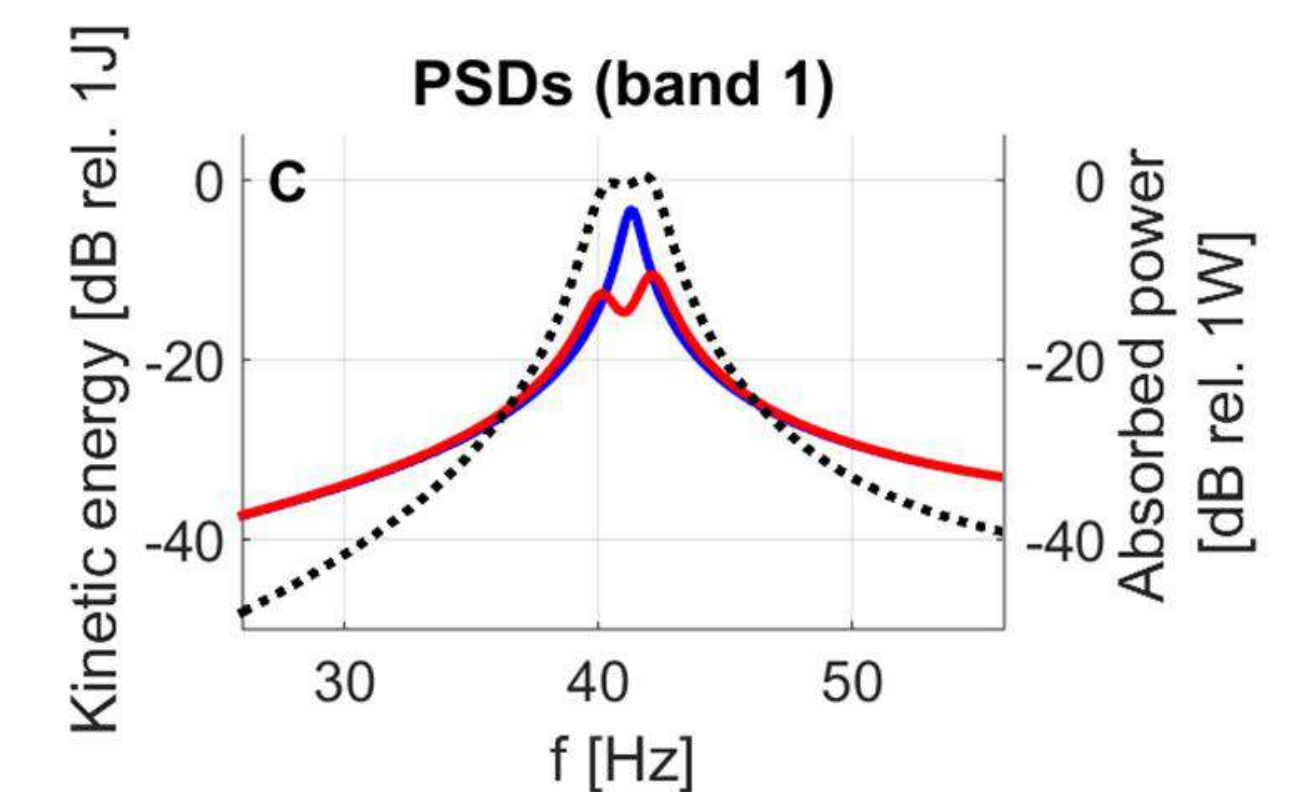
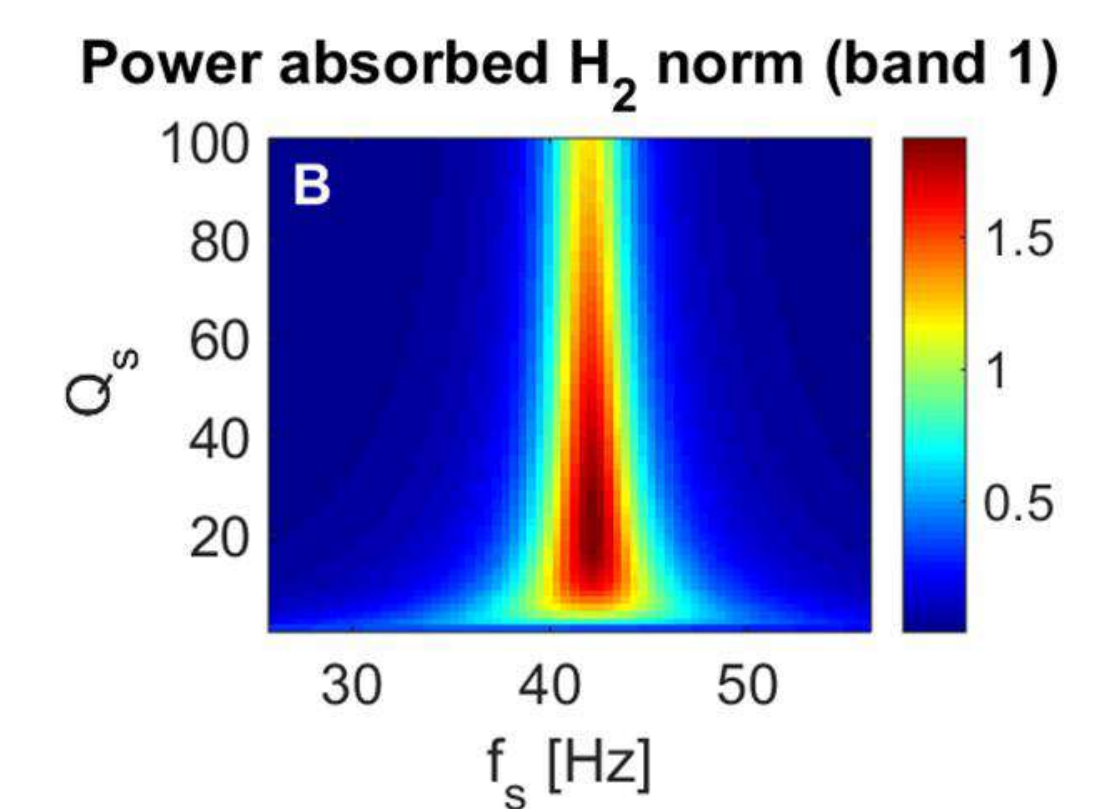
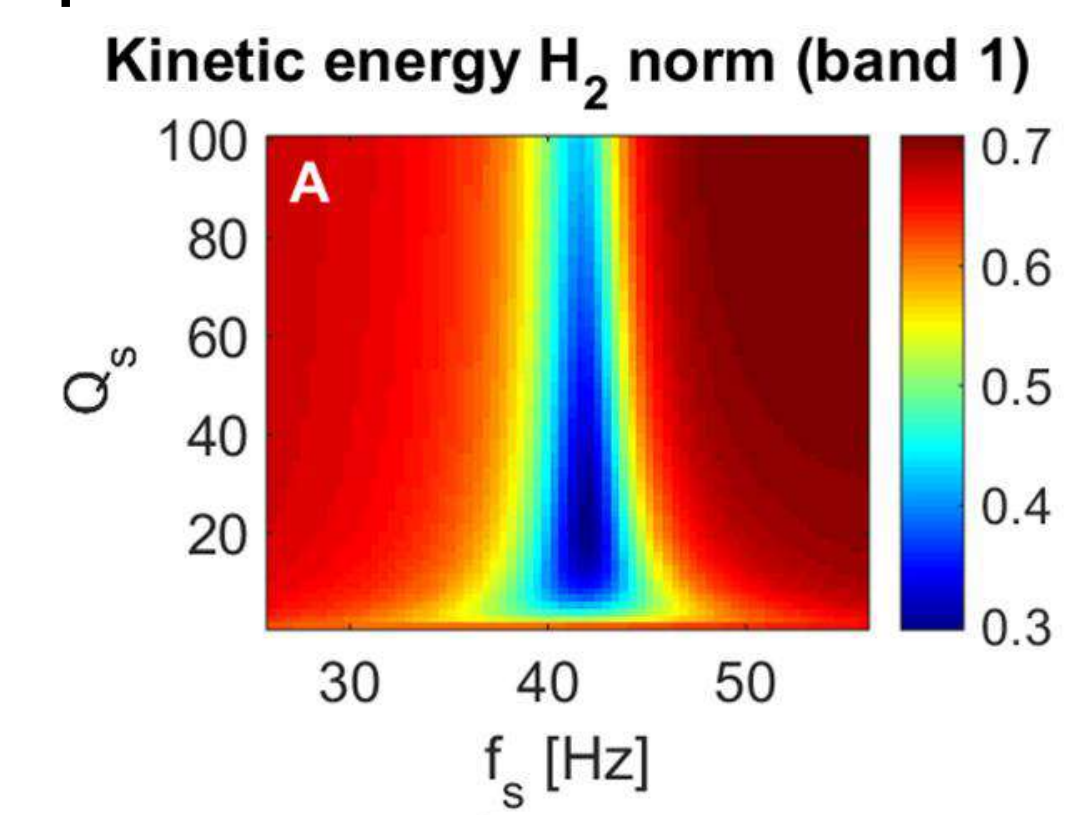
Objective



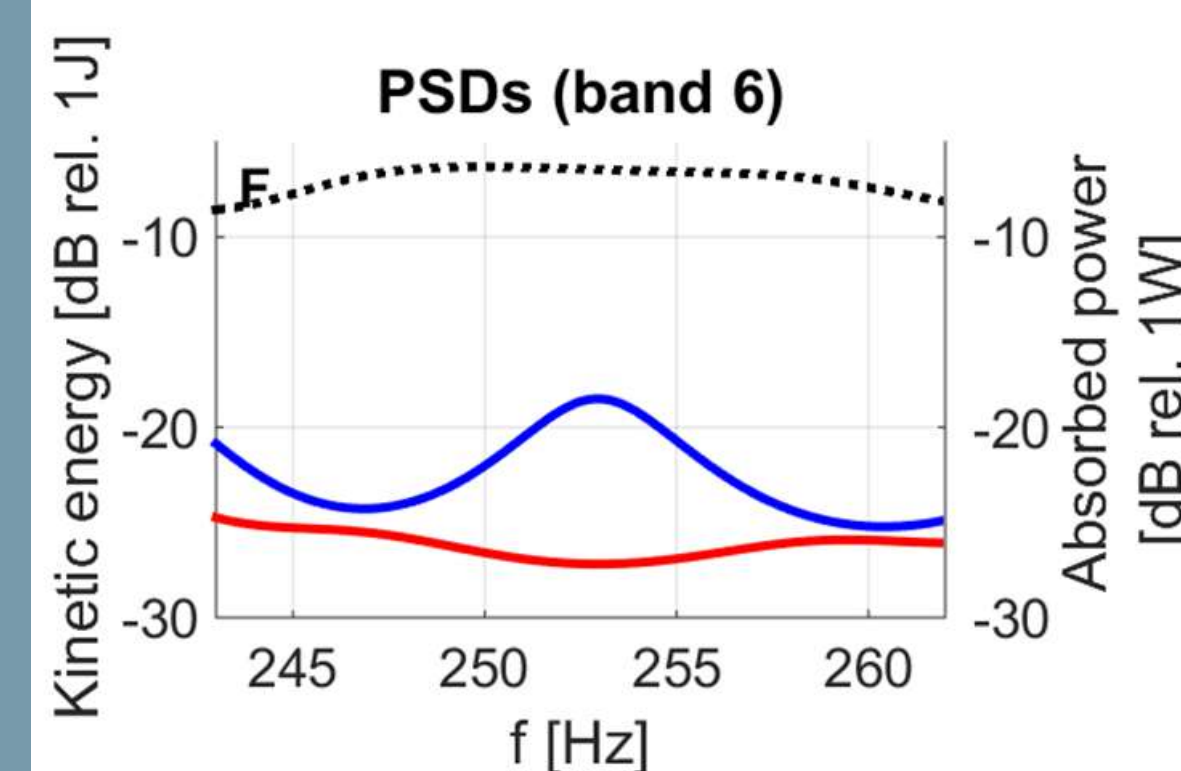
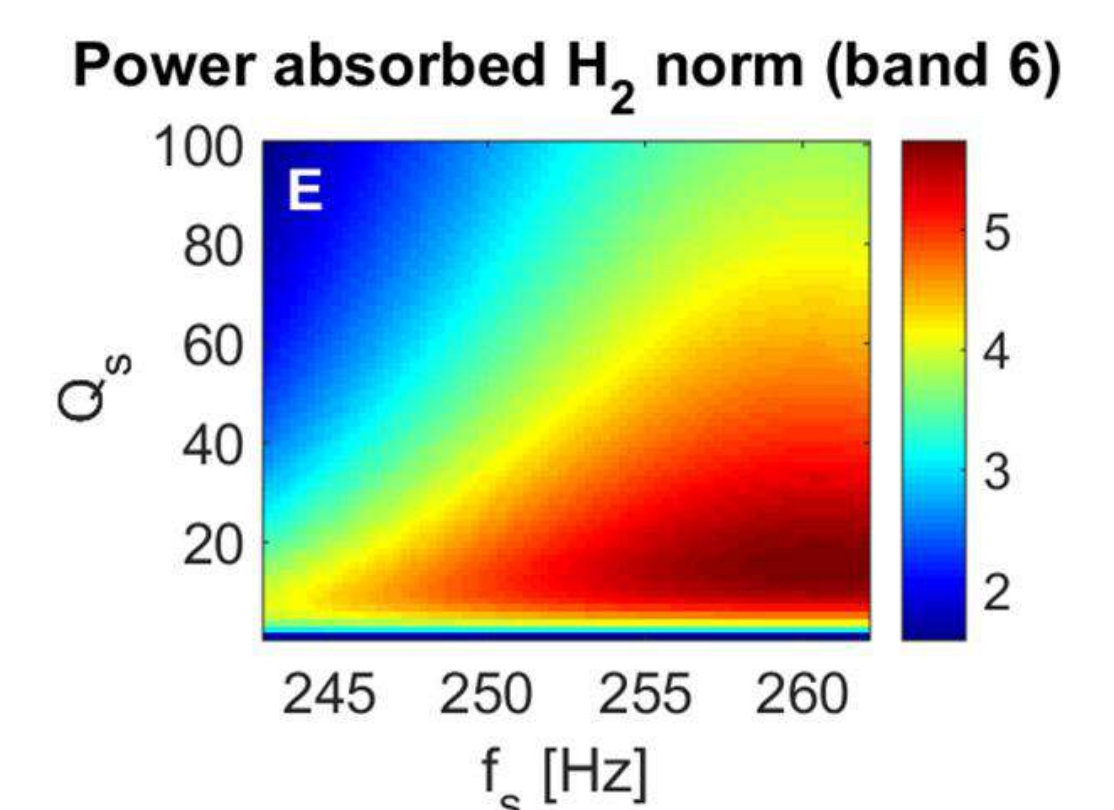
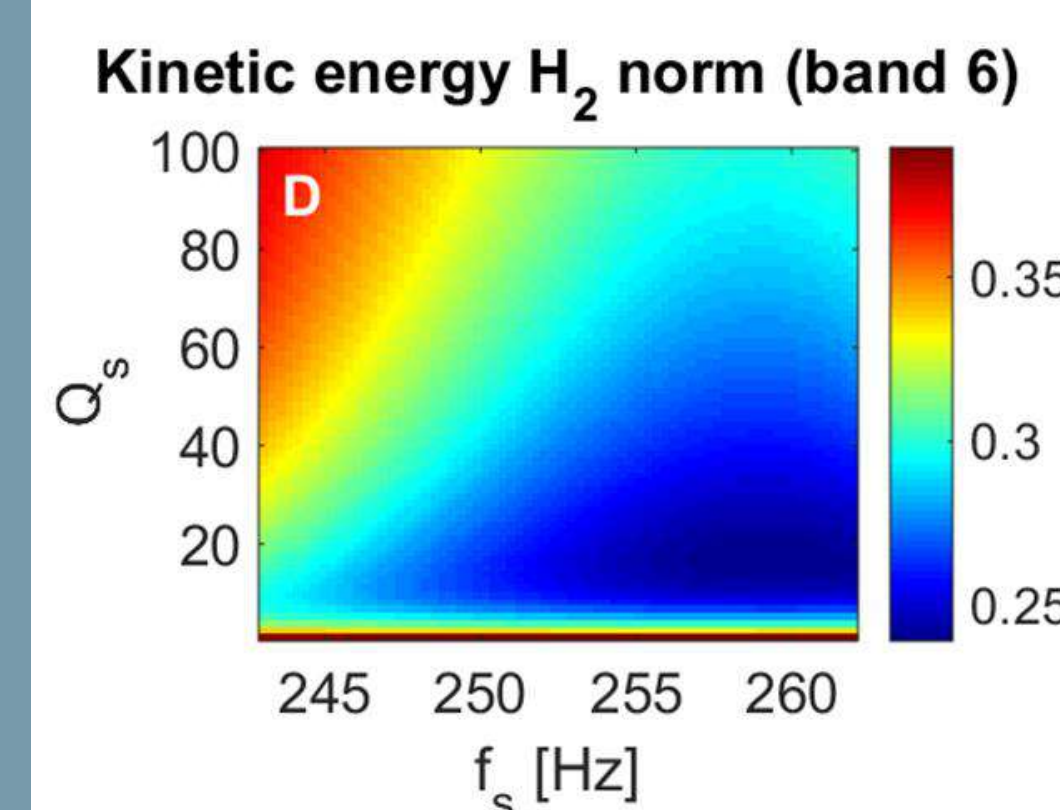
Feasibility studies on the metamaterial panel with arrays of piezoelectric patch transducers connected to multi-resonating electrical shunts for broad band vibration control.

Simulation results

Plots A, D and B, E present the panel flexural kinetic energy and the electric power absorbed by a RLC shunt averaged in the frequency bands 1 and 6 with respect to the resonance frequency f_s and quality factor Q_s of a simple RLC shunt.

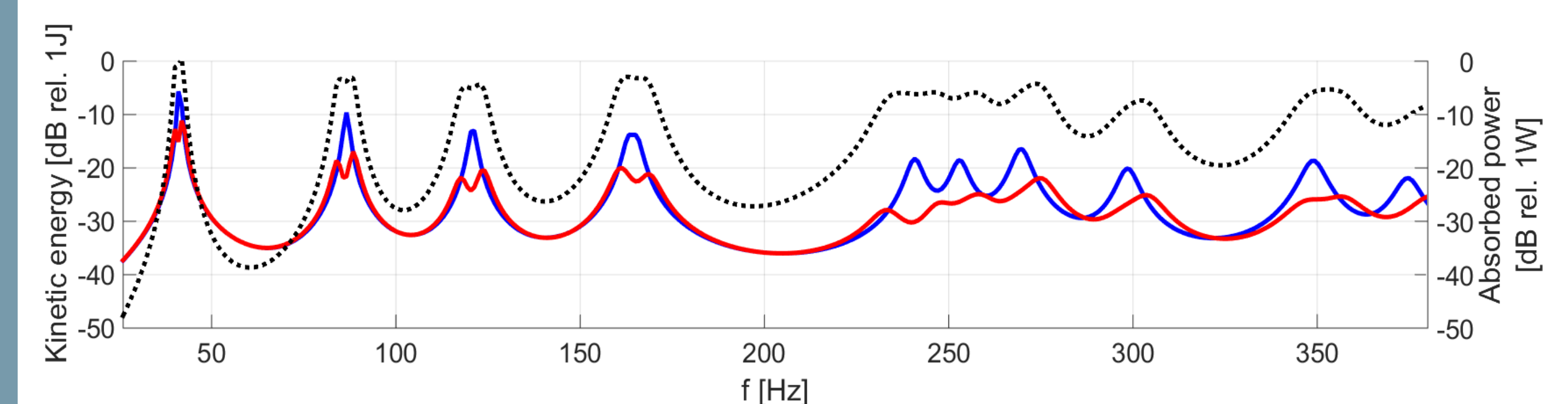


C Flexural kinetic energy PSD (open circuit blue line; optimal RLC shunts red line) and the absorbed power PSD (optimal RLC shunts dotted black) within band 1.



F Flexural kinetic energy PSD (open circuit blue line; optimal RLC shunts red line) and the absorbed power PSD (optimal RLC shunts dotted black) within band 6.

The optimal values of f_s and Q_s have been implemented into multi-resonant shunts formed by a sequence of the parallel RLC branches.



Dott. Michal Zientek
Prof. Paolo Gardonio

Info:
Tel. +39 0432 558035
Fax. +39 0432 558251
michal.zientek@uniud.it
paolo.gardonio@uniud.it

Reference

M. Zientek, P. Gardonio
Metamaterial panel with arrays of piezoelectric patches connected to multi-resonant electrical shunts.
ICSV 24th, London, UK

* Department of Mechanical Engineering,
Katholieke Universiteit Leuven, Belgium

Acknowledgement

The authors gratefully acknowledge the European Commission for its support of the Marie Curie program through the ITN ANTARES project (GA 606817)



ANTARES



Wall transform mechanism in a viscosity stratified turbulent flow

Abstract

Turbulent Poiseuille flow of two immiscible liquid layers inside a rectangular channel has been performed adopting a Direct Numerical Simulation of wall bounded flow, coupled with the Phase Field Model (PFM). A thin liquid layer (h_1) flows on top of a thick liquid layer (h_2), such that $h_1/h_2 = 1/9$, they have same density but different viscosity, which are: $\lambda = \nu_1/\nu_2 : \lambda = 1, \lambda = 0.875$ and $\lambda = 0.75$, aim is only to investigate the situation where water is used to transport of oil in pipelines industries. Liquid-liquid interface produces remarkable turbulence modulation inside the channel compared to Single Phase (SP).

Methodology

Eqs. 1-2 describe the conservation of mass (continuity) and momentum (Navier-Stokes) of the system, with $\mathbf{u} = (u_x, u_y, u_z)$ being the velocity field and p the corrected pressure field. Eq. 3 is the Cahn-Hilliard equation that describes the transport of the order parameter ϕ used to model the binary mixture: ϕ is constant in the bulk fluid regions (where $\phi = \pm 1$) and changes smoothly across the fluid-fluid interface. The free energy functional $F(\phi)$ of the system (Eq. 4), is the sum of two different contributions: a double well potential $f(\phi)$ that accounts for the phobic behavior of the phases and the variation of the free energy functional is called chemical potential μ and controls the behavior of the interfacial layer (Eq. 5).

$$\nabla \cdot \mathbf{u} = 0 \quad (1)$$

$$\frac{\partial \mathbf{u}}{\partial t} = -\mathbf{u} \cdot \nabla \mathbf{u} - \nabla p + \frac{1}{\text{Re}_\tau} \nabla^2 \mathbf{u} + \nabla \cdot [k(\phi, \lambda)(\nabla \mathbf{u} + \nabla \mathbf{u}^T)] + \frac{3}{\sqrt{8} \text{We} \text{Ch}} \mu \nabla \phi \quad (2)$$

$$\frac{\partial \phi}{\partial t} = -\mathbf{u} \cdot \nabla \phi + \frac{1}{\text{Pe}} \nabla^2 \mu \quad (3)$$

$$F(\phi) = f(\phi) + \frac{1}{2} \text{Ch}^2 |\nabla \phi|^2 = \frac{1}{4} (\phi - 1)^2 (\phi + 1)^2 + \frac{1}{2} \text{Ch}^2 |\nabla \phi|^2 \quad (4)$$

$$\mu = \frac{\delta F}{\delta \phi} = \phi^3 - \phi - \text{Ch}^2 \nabla^2 \phi \quad (5)$$

Results and Discussion

Our results indicate that the wall normal transport of momentum is reduced, with a significant proportion of the mean flow energy being lost into interface deformation for reducing λ , the volume flowrate further increases (up to 10% for $\lambda = 0.75$). This is a direct consequence of the presence of a thin liquid layer with lower viscosity that reduces the mean shear stress at the upper wall. Since our simulations are run with an imposed pressure gradient, reducing the wall stress produces an increase of the mean volume flowrate.

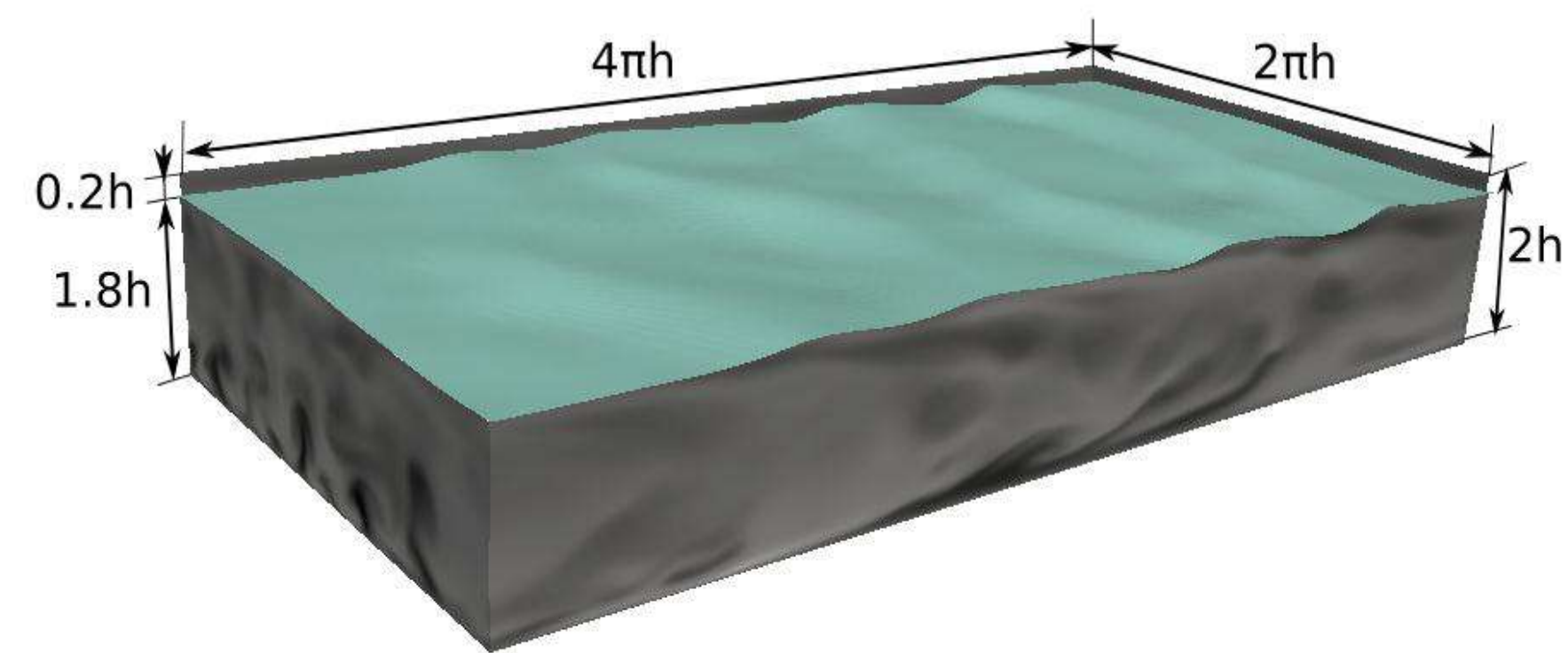


Figure 1: Sketch of the computational domain, while a thin water layer on top of oil layer, Initial thickness ratio between the two liquid layers is $h_1/h_2 = 1/9$. The distribution of Stream wise fluctuation with deformed liquid-liquid interface are also shown.

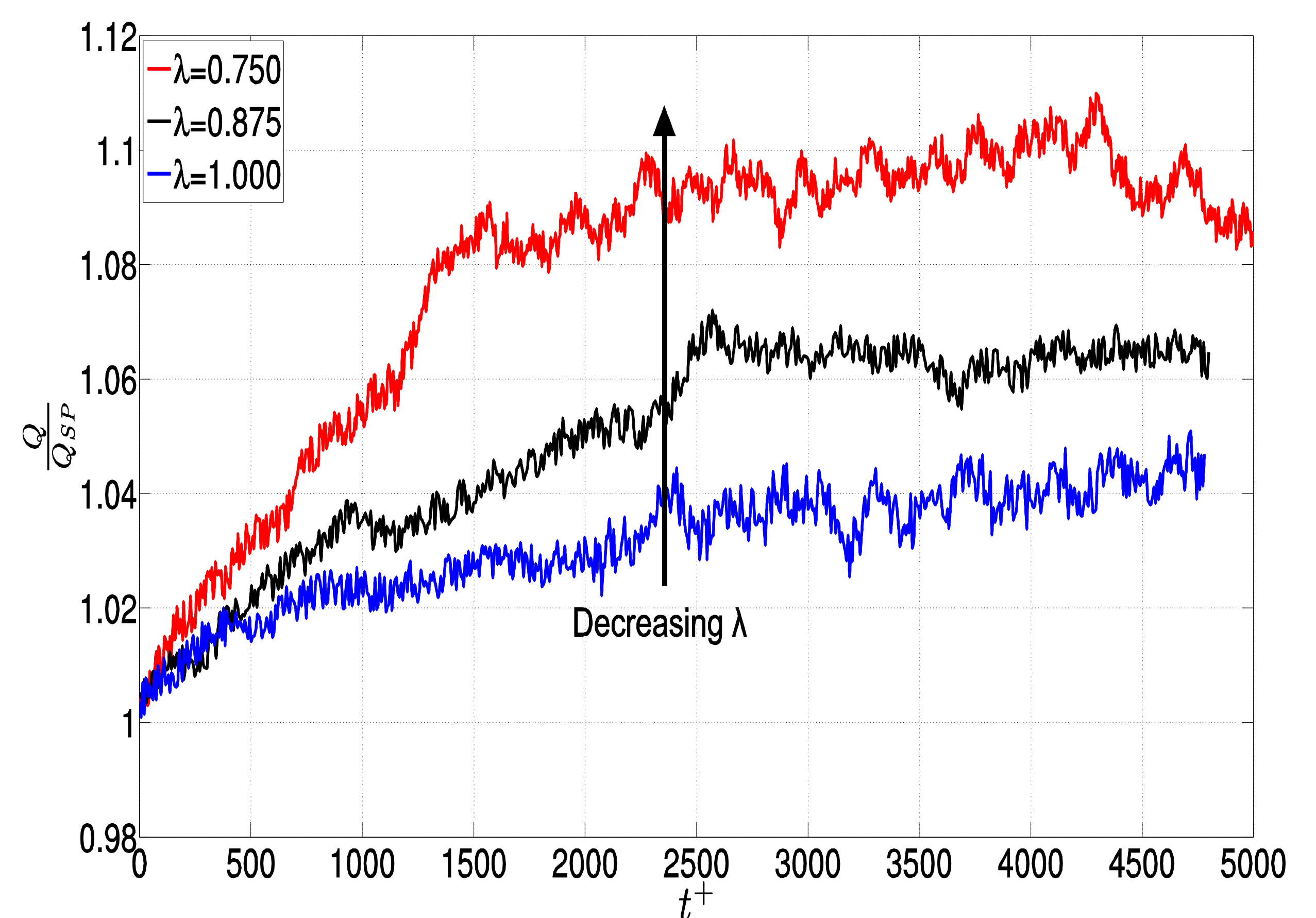


Figure 2: Time evolution of the volume flowrate Q , normalized by the reference volume flowrate for the single phase flow Q_{SP} , for the viscosity stratified liquid-liquid flow at $\text{Re}_\tau = 100$

Dott. Somayeh Ahmadi
Prof. Alfredo Soldati

Info:

Ahmadi.somayeh@spes.uniud.it

Bibliography:

Ahmadi, S., Roccon, A., Zonta, F., & Soldati, A. (2016). Turbulent drag reduction in channel flow with viscosity stratified fluids. *Computers & Fluids*.



UNIVERSITÀ
DEGLI STUDI
DI UDINE
hic sunt futura

PHYSICAL SCIENCES AND ENGINEERING

30° ciclo

Corso di dottorato in Scienze dell'ingegneria
energetica e ambientale

Introduction

The aim of the project is the development of a methodology to perform failure analysis that can be applied in Electrolux Professional. This methodology includes a preliminary of the chemical compatibility of materials and evaluation of their durability.

Methodology used in the research

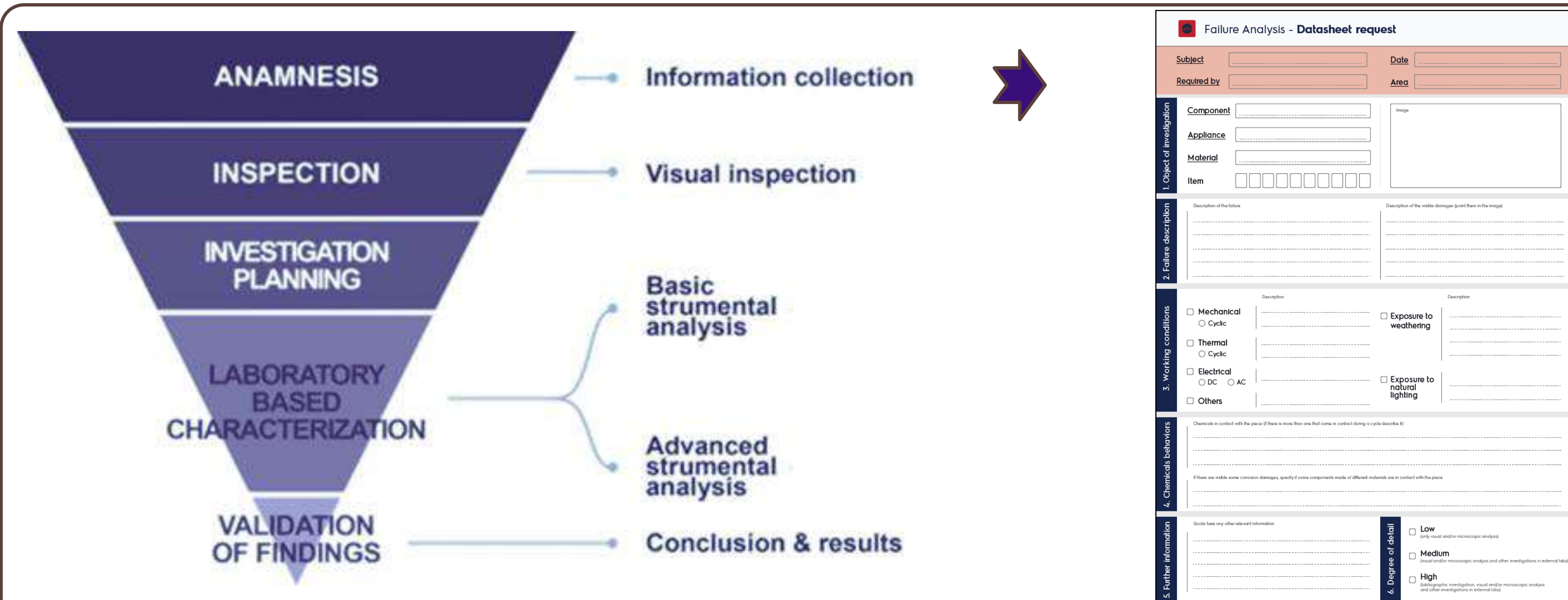


Fig. 1 Schematic view of the failure analysis procedure and failure analysis form used in Electrolux Professional. Based on the failure analysis procedure developed in this work (Fig. 1), a failure analysis form was implemented in order to make available all the information needed during this type of investigation. This procedure is currently in use in Electrolux Professional.

Examples of failure analysis

Failure of a condenser in a blast-chiller



Fig. 3 Failed plates heat exchanger

The heat exchanger (Fig. 3) was used to cool the refrigerating fluid (R404a) with tap water. The condenser operated for 8-9 months in a marine environment. After this time mixing of the fluids was reported with perforation of the plate. The plate presenting perforation was investigated by morphological, chemical and electro-chemical analysis. It was found that the failure was due to a crevice corrosion process due to high concentration of chlorides (Fig. 4).

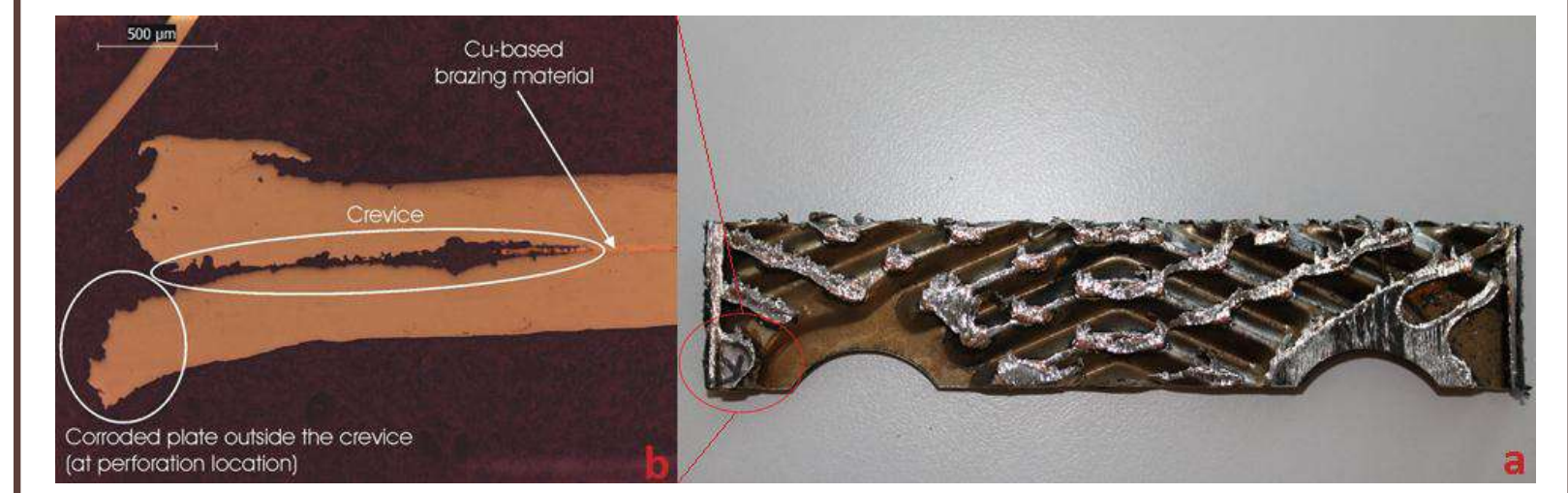


Fig. 4 a) perforated plate b) enlargement of the zone near the hole

Degradation of Teflon coated plates



Fig. 5 Example of plate before (left) and after (right) a month of work in field

The degradation of a ribbed Teflon coated aluminium plate was investigated. This plate was used as cooking surface in a food warmer showing, in field test, a decrease of its anti-sticky property. In the Fig. 5 can be see the difference between a new plate (left) and a plate used for a

month (right). The degradation of a composite PTFE coating, subjected to thermal aging, has been investigated to simulate the operating conditions. Stylus profilometry and SEM analysis evidenced that thermal aging causes crazing of the polymeric matrix (Fig. 6) due to thermal stresses.

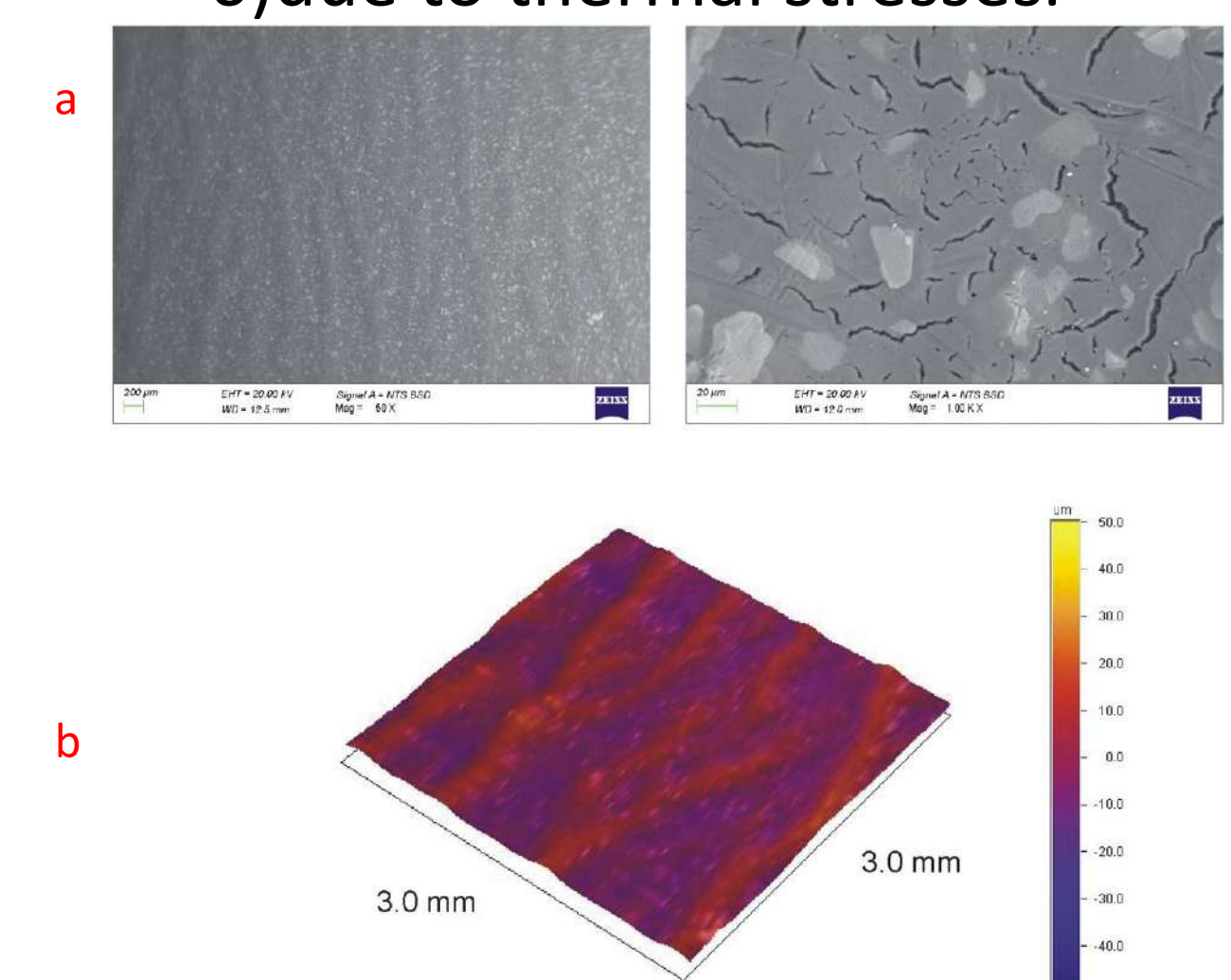


Fig. 6 (a) SEM back-scattered image and (b) topographic map acquired by means of a stylus profilometer of a plate aged for 2 weeks at 300 °C

Conclusions and future work

- The developed protocol was applied to different internal cases, proving to be effective for organization of failure analysis activities at Electrolux Professional.
- The database for the chemical compatibility was populated (18 corporates sources and 1 handbook) and was successfully used during anamnesis to evaluate if the environment can take part in the failure process.
- Based on the failure analyses performed in the framework of this PhD research, future work will focus on to different topics:
 - Assessment of the corrosion resistance of a different types of austenitic steel alloy for application in the condenser of blast-chillers and other applications in the field of food service industry.
 - Investigation of the effect of thermal and chemical degradation processes of Teflon coated plates.

Acknowledgement:

The author would like to thank The Research Hub by Electrolux Professional for technical and economic support (A.G. PhD scholarship).

Publications:

Lanzutti, A.Gagliardi, A. Raffaelli, M. Simonato, R. Furlanetto, M. Magnan, F. Andreatta, L. Fedrizzi, "Failure Analysis of Gears, Shafts and Keys of Centrifugal Washers Failed During Life Test" Engineering Failure Analysis, submitted.
F. Andreatta, A. Lanzutti, M. Simonato, A. Gagliardi, M. Magnan, L. Fedrizzi, "Degradation of Coatings Employed in the Food Service Industry", proceedings of SMT31 Conference, Submitted.

Dott. Andrea Gagliardi

Info:
Tel. +39
gagliardi.andrea@spes.uniud.it
andrea.gagliardi@electrolux.it

Prof. Francesco Andreatta
Prof. Lorenzo Fedrizzi
dott. Michele Simonato
dott. Riccardo Furlanetto

Methodological proposal for the preliminary dynamic assessment of soil-structure interaction on energy production and distribution facilities through ambient vibration tests

Objectives

The objective of this study is to provide an **operational tool** to be used in **decision making** process in case of seismic emergency management. In particular it can be useful for the preliminary assessment of damage in strategic structures as the ones related to energy production. Moreover, it may provide useful index on the dynamic behavior of structures in order to address further investigations.

Methods

The methods used in this work are the ones of the Operational Modal Analysis, in ambient vibration condition. There are two reasons why forced vibrations are not suitable to be used on energy production and distribution facilities: that they are quite expensive and that they require the activities to be paused during the tests. As a matter of fact, the second factor can lead to a significant economic loss. Ambient vibration tests are, instead, cheap, quick and can be performed on the facility during its regular activity.

Data acquisition was performed using different instruments: tri-axial portable tromograph Tromino (Moho); Trillium – Centaur seismic station (Nanometrics); geophones linear and spatial arrays.

Data were analyzed through SSR (Standard Spectral Ratio) technique, HVSR (Horizontal to Vertical Spectral Ratio) or techniques based on signal deconvolution. In some cases a comparison with FEM (Finite Element Model) has been possible.

Case studies

Buildings

The method was tested on 6 strategic buildings in Matera and 2 in Ferrara in the framework of the CLARA Smartcities project. The frequency of the firsts modes has been deduced and compared to the one of the soil, in order to assess the double resonance possibility.

Dams

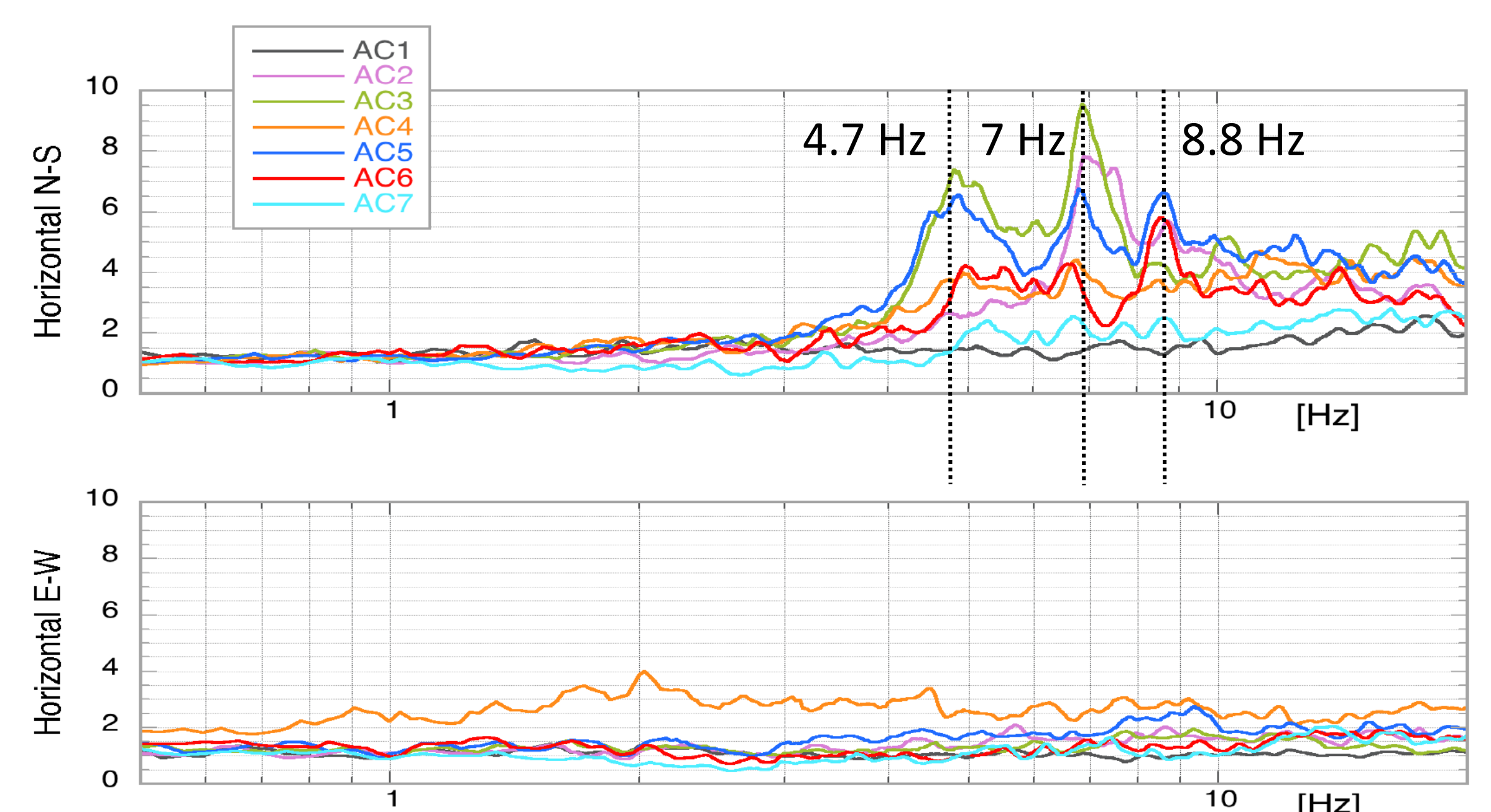
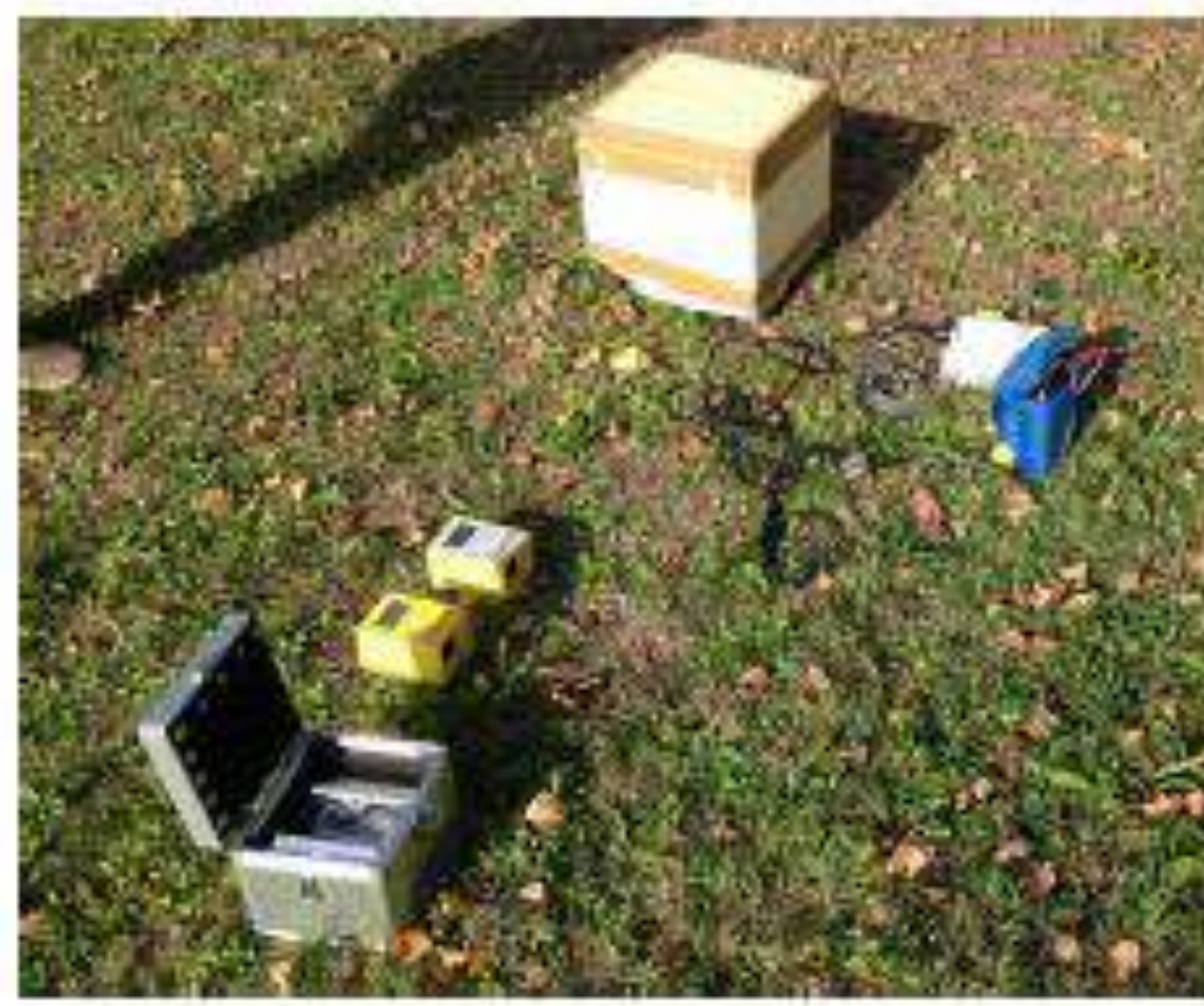
A survey was performed with Tromino instruments at the top of two arch dams in Central Italy. The results were confirmed by FEM and vibrodyne tests previously obtained by the owners of the dams. On arch dams there's an important rocking component. Therefore, the program XNSR (Mucciarelli et al., 2013) was used to identify the real vibrational plane through its azimuth and dip angle.

Windmills

A test on a windmill field has been performed in April 2017, in order to assess the soil-structure and structure-structure interaction. Three spatial arrays and four linear arrays were performed. Moreover, the geophones were installed at the top and bottom of the wind turbine. The results will be available soon.

Conclusions

The thesis suggests a set of instruments to be used on energy related facilities, with different instruments and for different purposes. Real case studies will be useful to explain all the possibilities.



Dott.ssa Giulia Massolino
Prof. Antonino Morassi

Info:

Tel: +39 040 2140 432

Mail: massolino.giulia@spes.uniud.it

References

- Bukenya P., Moyo P. and Oosthuizen C.; 2012. *Comparative study of operational modal analysis techniques using ambient vibration measurements of a concrete dam*. Proceedings of ISMA2012-USD2012.
- Ivanović S.S., Trifunac M.D. and Todorovska M.I.; 2000. *Ambient vibration tests of structures – a review*. ISET Journal of Earthquake Technology, Paper NO. 407, Vol. 37, No. 4, December 2000, pp. 165-197.
- M. Mucciarelli, T.A. Stabile, M.R. Gallipoli, D. Zuliani, G. Massolino; 2016. *XNSR – a software for a different approach to single-station spectral ratio*. 35th General Assembly of the European Seismological Commission, ESC2016-593.



**UNIVERSITÀ
DEGLI STUDI
DI UDINE**
hic sunt futura

PHYSICAL SCIENCES AND ENGINEERING

30° ciclo

**Corso di dottorato in Scienze dell'ingegneria
energetica e ambientale**

Analisi delle prestazioni termiche in sistemi di raffreddamento avanzati di palette di turbine a gas

Ambito della ricerca

L'aumento delle prestazioni e la riduzione dei consumi sono i due punti cardine su cui viene basata la progettazione delle turbine a gas di nuova generazione. Questi dispositivi vengono oggi utilizzati sia in ambito aeronautico, come propulsori della maggioranza dei velivoli (Fig. 1), sia in ambito energetico accoppiandoli a generatori di energia elettrica.

Le prestazioni dei turbo-gas possono essere incrementate aumentando la temperatura dei gas in camera di combustione (4 in Fig. 1), aumentandone di fatto l'energia con cui questi ultimi impattano sulle palette dei vari stadi della turbina permettendone la rotazione (5, 6 in Fig. 1).

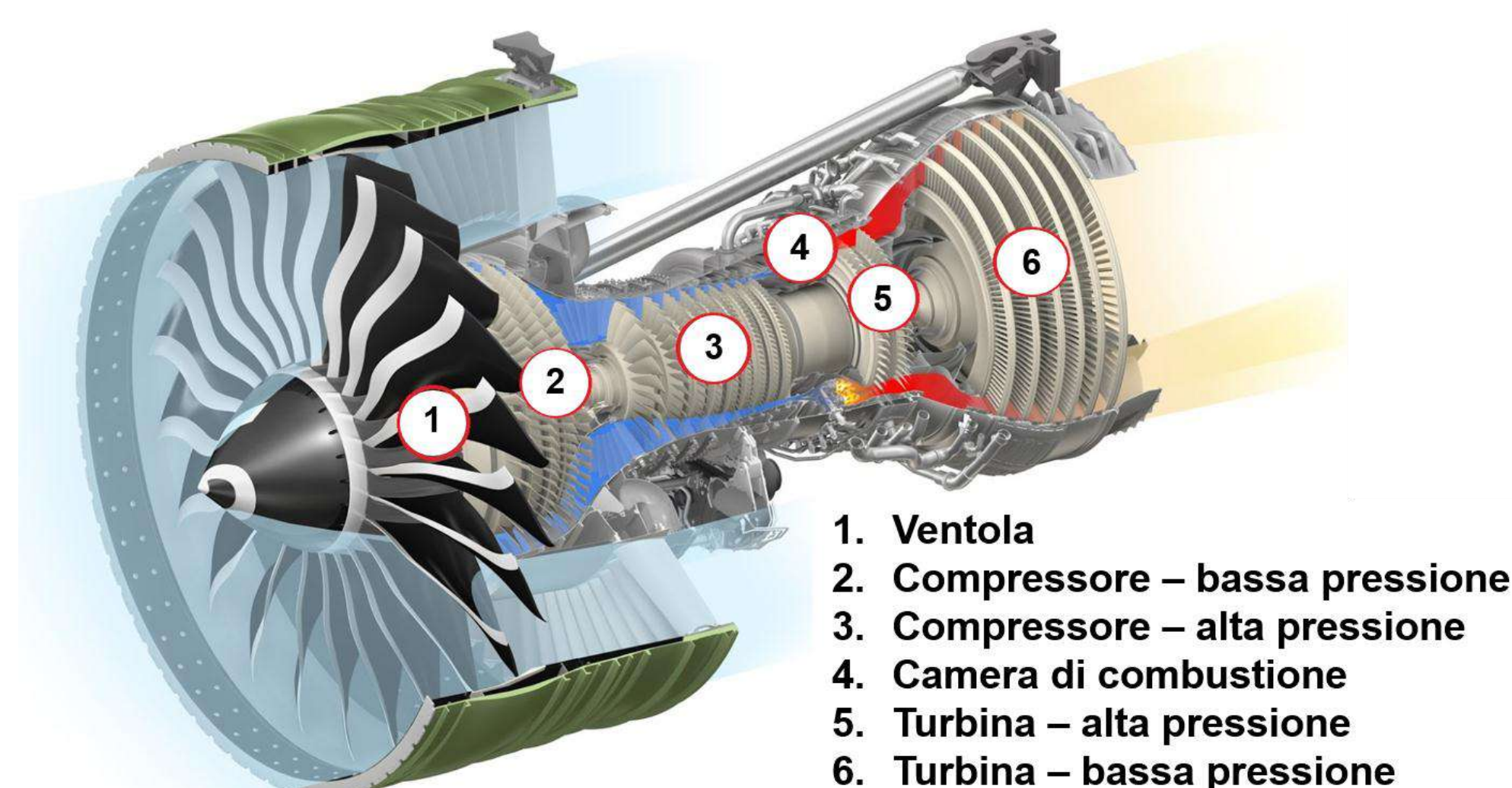


Figura 1: Esempio di turbo-gas aeronautico

All'aumento della temperatura dei gas corrisponde un aumento degli stress termici e meccanici sulle palette della turbina, soprattutto nei primi stadi a ridosso della camera di combustione.

Al fine di allungare la vita utile di questi componenti senza penalizzarne le prestazioni, le aziende produttrici di questi dispositivi hanno investito ingenti capitali principalmente su due filoni di ricerca: lo sviluppo di materiali più resistenti alle alte temperature e la progettazione di sistemi di raffreddamento delle zone termicamente più sollecitate.

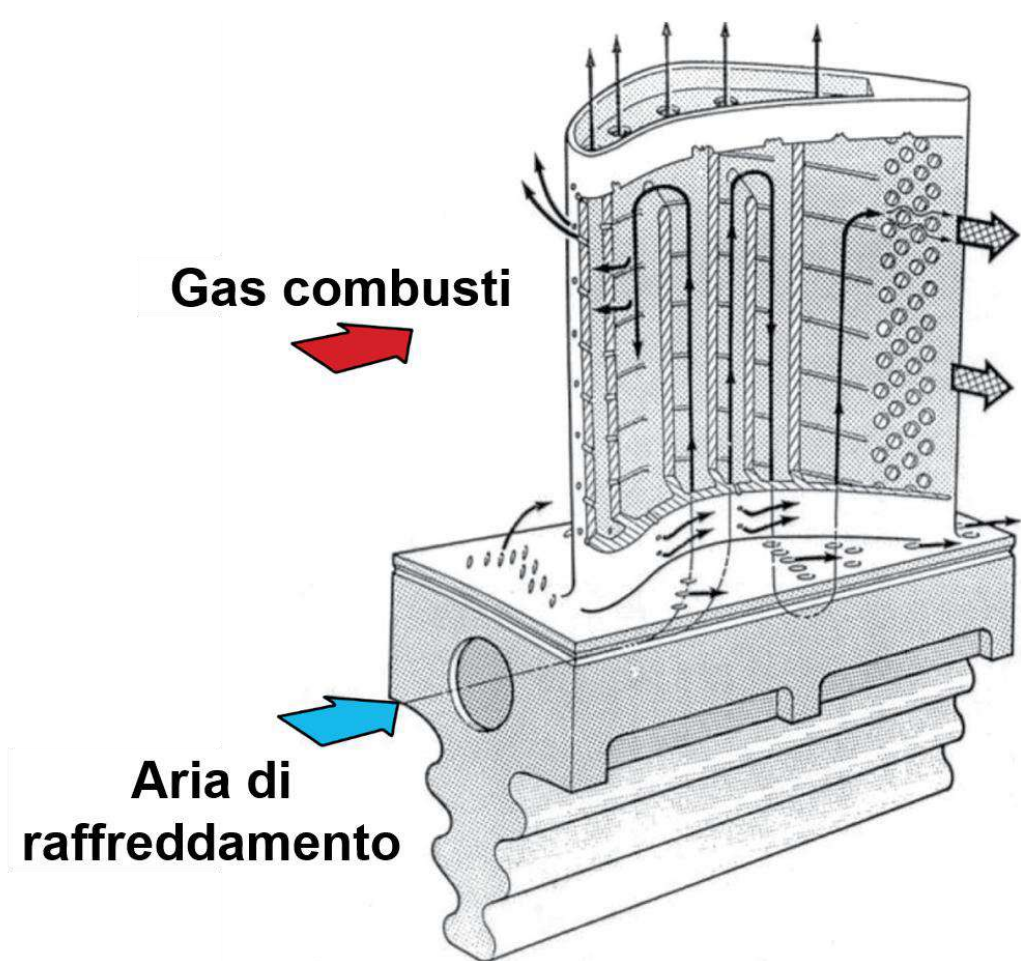
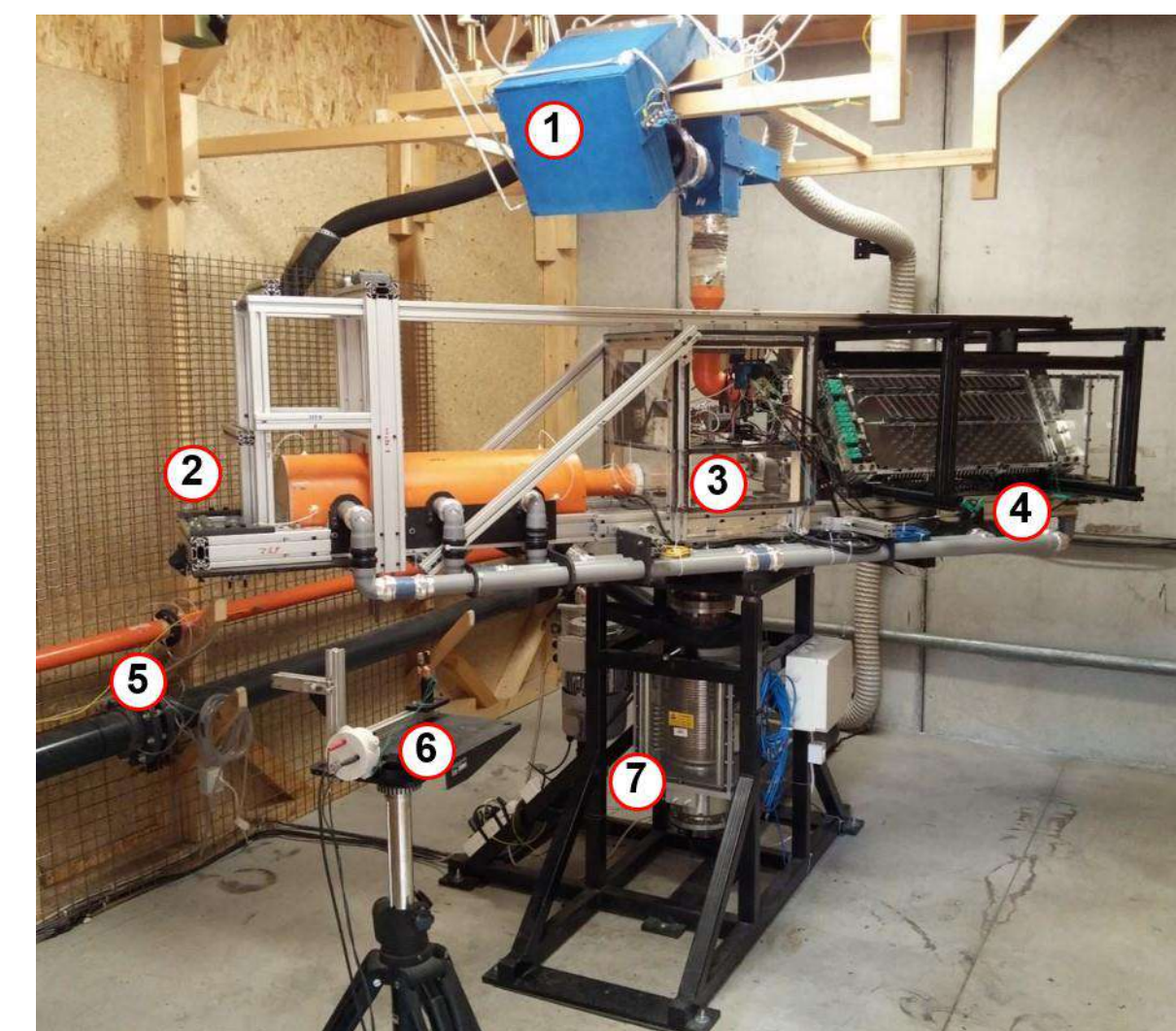


Figura 2: Schema di raffreddamento interno di palettatura rotorica

Il secondo filone è proprio quello sul quale è incentrato questo progetto di dottorato, ovvero lo sviluppo di una metodologia sperimentale di valutazione dello scambio termico in sistemi di raffreddamento avanzati per palette di turbine a gas (Fig. 2).



1. Sistema raffreddamento aria-N₂
2. Contrappesi
3. Strumentazioni a bordo
4. Sezione di misura
5. Diaframma per misura della portata d'aria di raffreddamento
6. Fotodiodo per rilevazione della velocità di rotazione
7. Giunto rotante

Figura 3: Impianto di prova sperimentale

Tecnica sperimentale

Nel Laboratorio di Macchine a Fluido è stato realizzato un impianto di prova che permette di testare geometrie di raffreddamento palare realistiche, sia in condizioni statiche, che in rotazione al fine di simulare il comportamento di entrambe le tipologie di palettatura (statoriche e rotoriche). Al fine di valutare lo scambio termico di questi componenti è stata sviluppata la tecnica che prende il nome di Termografia ai Cristalli Liquidi in Transitorio (TCLT).

Note le evoluzioni temporali della temperatura del flusso d'aria di raffreddamento e della temperatura della superficie di misura, ottenuta analizzando l'intensità di colore di particolari cristalli liquidi spruzzati direttamente su di essa, è possibile calcolare un indicatore dello scambio termico.

Questa tecnica permette di ottenere mappe dettagliate di scambio termico (Fig. 4) in tempi relativamente brevi rispetto ad altre tecniche utilizzate in questo ambito, permettendo così un più facile e immediato confronto tra differenti geometrie di raffreddamento palare.

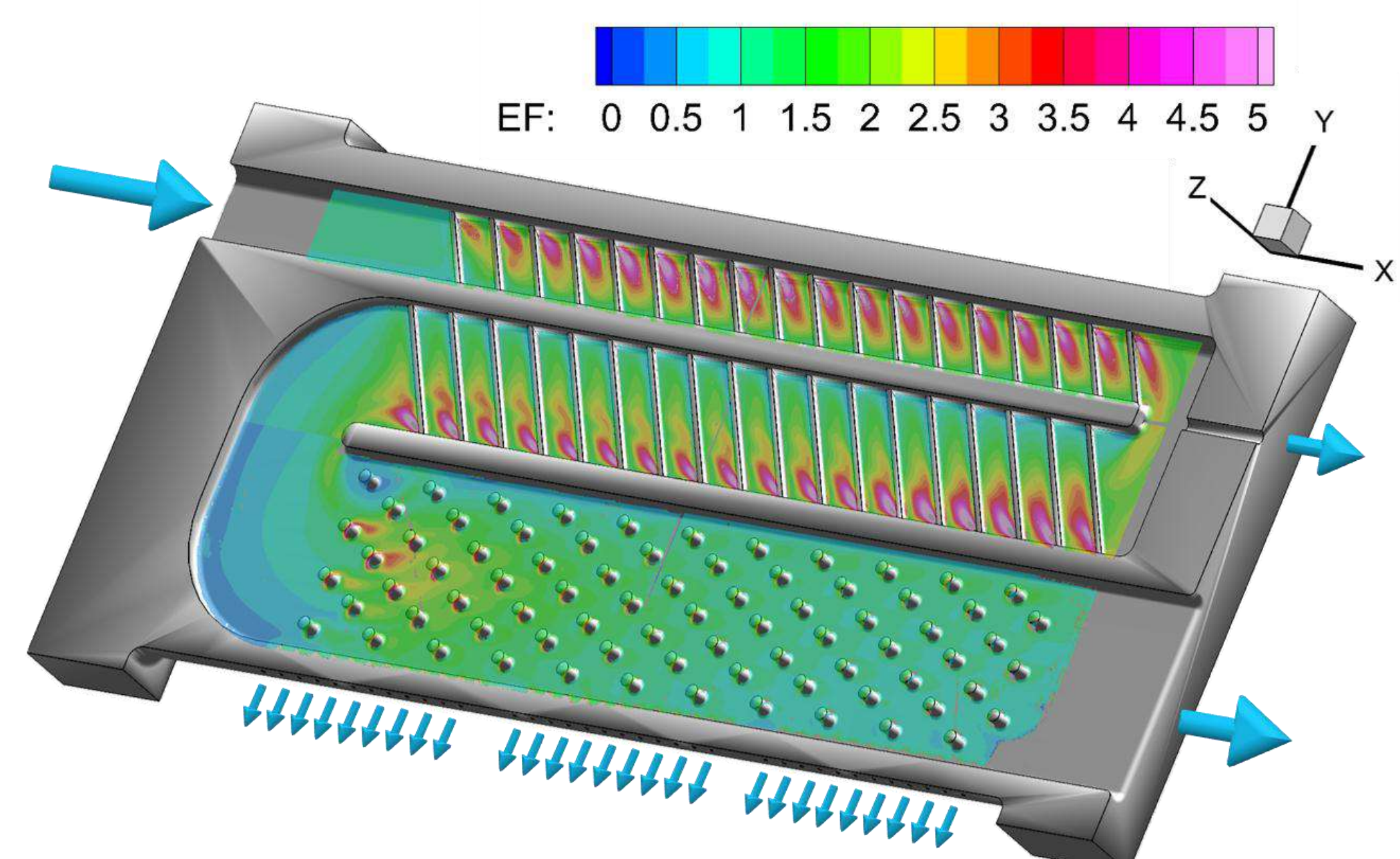
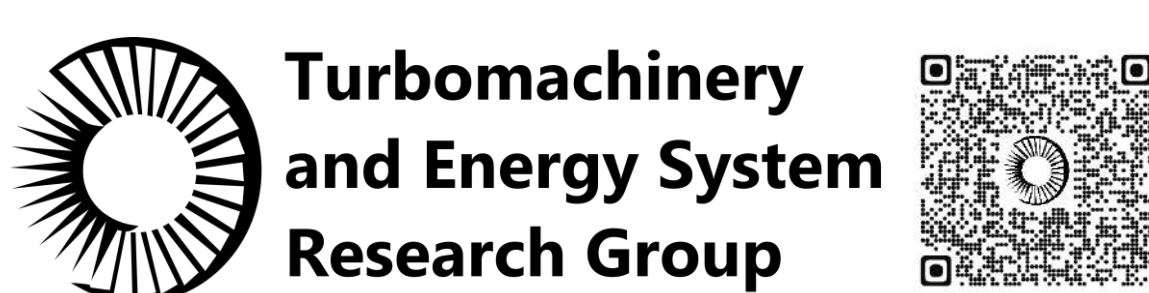


Figura 4: Mappa di scambio termico



Dott. Ing. Fabio Pagnacco
Prof. Luca Casarsa

Info:

Tel. +39 0432 558049

pagnacco.fabio@spes.uniud.it

Riferimenti bibliografici

- "Rotating heat transfer measurements on a multi-pass internal cooling channel - I: Rig development", Proceedings of ASME Turbo Expo 2016, Volume 5B-2016
- "Rotating heat transfer measurements on a multi-pass internal cooling channel - II: Experimental tests", Proceedings of ASME Turbo Expo 2016, Volume 5B-2016
- "Rotating heat transfer measurements on realistic multi-pass geometry", ATI 2016, Energy Procedia, Vol. 101 – pp. 758-765
- "Gas turbine blades internal cooling: design, development and validation of a new rig for heat transfer measurement under rotation", ETC 2017

Riconoscimenti

L'attività di ricerca è stata eseguita in collaborazione con Siemens Industrial Turbomachinery Limited.

COALESCENCE & BREAKAGE OF DROPS IN TURBULENCE

INTRODUCTION:

Prediction of breakup and coalescence rates of a swarm of liquid drops immersed in a turbulent liquid flow (liquid/liquid emulsion) is crucially dependent on a number of hard-to-tackle factors. Among many others these include turbulence, turbulence/interface interactions, surface tension effects and viscosity gradients.

Each single of these effects has a specific action on breakup and coalescence, and we can envision drops dynamics as the ultimate result of a complex competition between destabilizing and stabilizing effects.

Destabilizing effects are primarily due to the combined effects of fluctuating inertial and shear terms acting at the drops interface. Stabilizing effects are due to surface tension, which is a restoring force acting to preserve drops sphericity. The outcome of this competition determines drops deformation, breakage and coalescence.

In this picture, viscosity gradients across the interface of the drops can act as modulators of the localized shear stresses and can amplify or damp the initial turbulence perturbations to the point of changing profoundly the final result.

METHODOLOGY:

We consider a swarm of 256 large and deformable drops (density ρ_D , viscosity η_D) dispersed in a turbulent carrier flow (density ρ_c and viscosity η_c).

The evolution of this complex turbulent multiphase flow is described here employing a Phase Field Method (PFM), constituted by the Navier-Stokes (2) and Cahn-Hilliard (3) equations. The two phases are assumed to have the same density ($\rho_c = \rho_D$) but different viscosity ($\eta_D \neq \eta_c$).

$$\nabla \cdot \mathbf{u} = 0 \quad (1)$$

$$\frac{D\mathbf{u}}{Dt} = -\nabla p + \frac{1}{Re_\tau} \nabla \cdot (\bar{\eta}(\nabla \mathbf{u} + \nabla \mathbf{u}^T)) + \frac{\alpha}{We} \nabla \cdot \boldsymbol{\tau}_c \quad (2)$$

$$\frac{D\phi}{Dt} = \frac{1}{Pe} \nabla^2 (\phi^3 - \phi - Ch^2 \nabla^2 \phi) \quad (3)$$

The equations have been solved using a pseudo-spectral approach in a closed channel geometry. A Fourier series is adopted for the streamwise (x) and spanwise (y) direction while an expansion based on the Chebyshev-Tau polynomials is used for the wall-normal direction (z).

RESULTS:

During the motion, each droplet can interact with the turbulent structures and with the surrounding droplets, the possible interactions can be classified as follows:



The balance between these two phenomena is controlled by the **Weber number We**, ratio between inertia and surface tension forces, and by the **viscosity ratio λ** , ratio between drop and external fluid viscosity.

The relative importance of these two phenomena can be evaluated considering the number of drops in the channel over time. In Fig.1, panels (A)-(I), snapshots of the system when a steady-state is reached are reported.

In particular can be noticed that We and λ have a strong effect, decrease of We or increase of λ promote the coalescence. In Fig.1 panels (J)-(L) the dimensionless number of drops (N/N_0) is reported over time for all the 15 simulations performed.

We=0.75

We=1.50

We=3.00

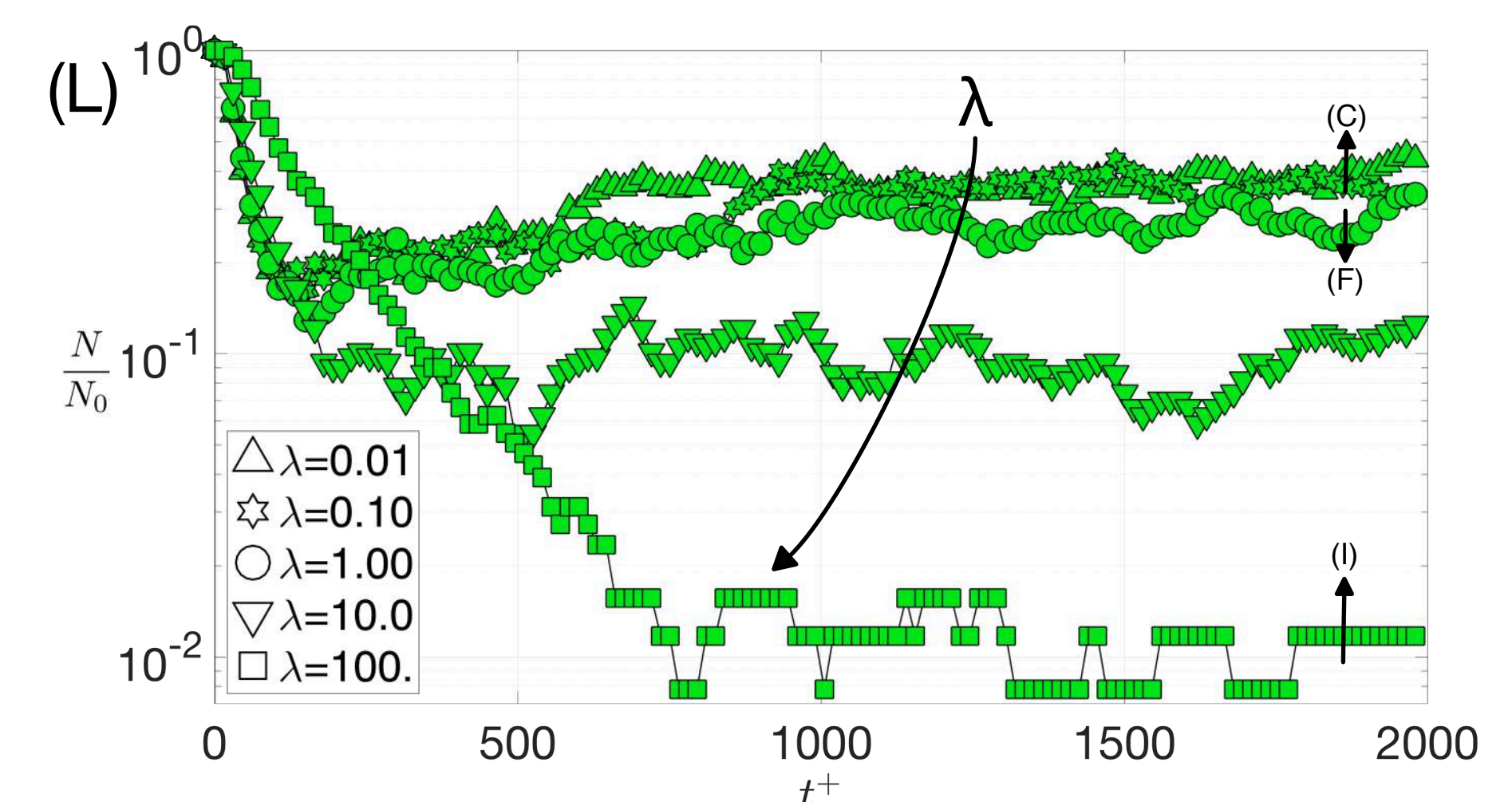
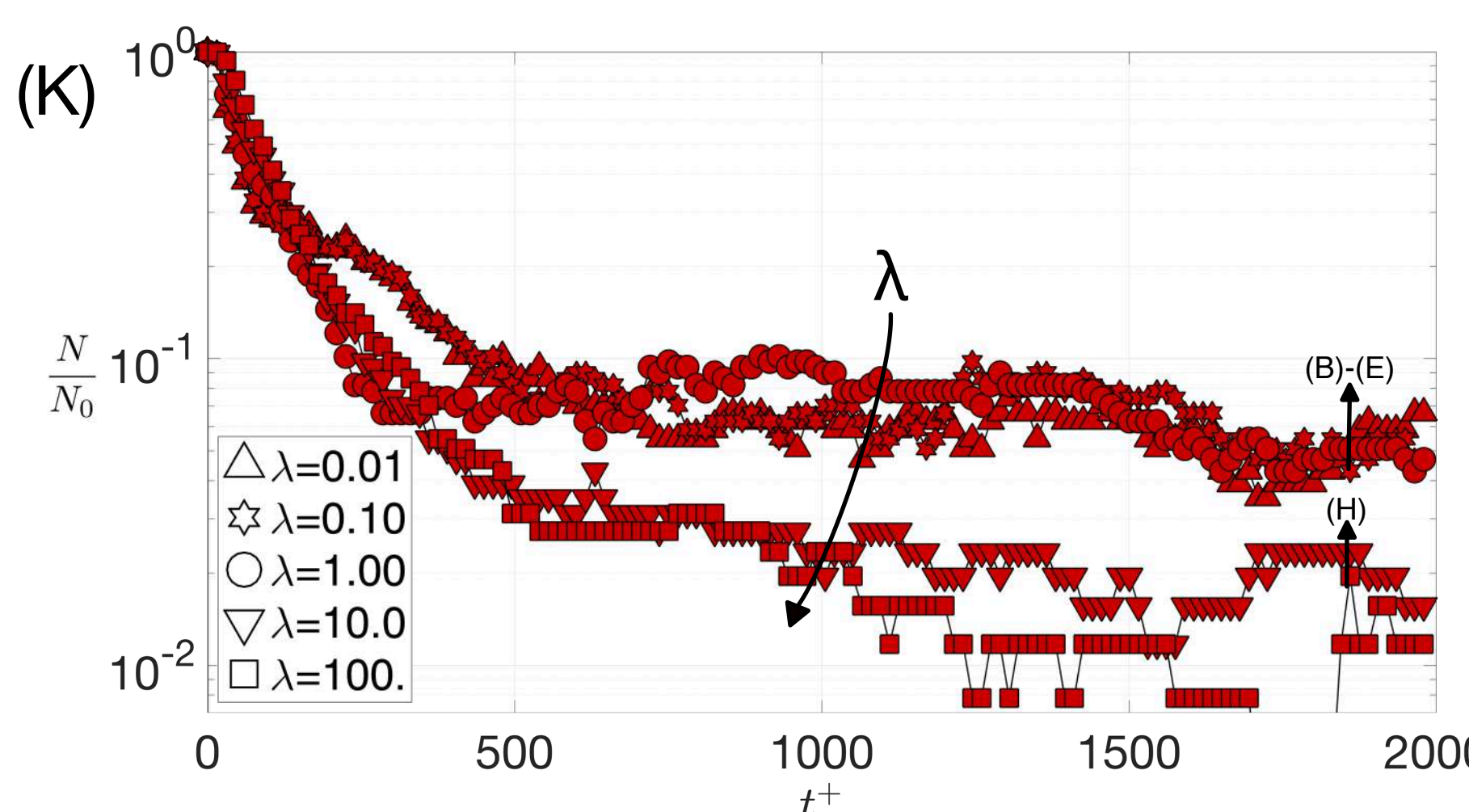
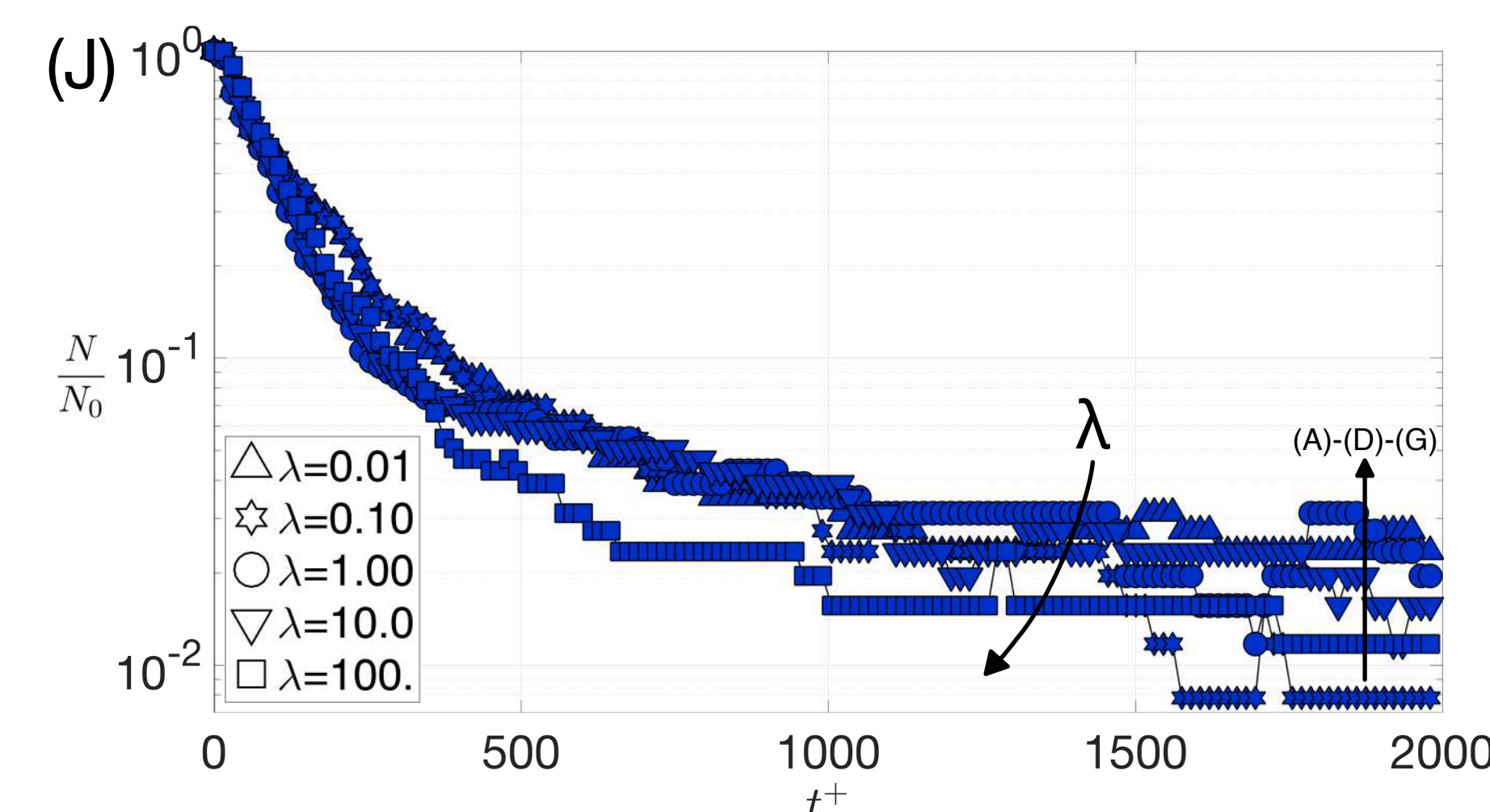
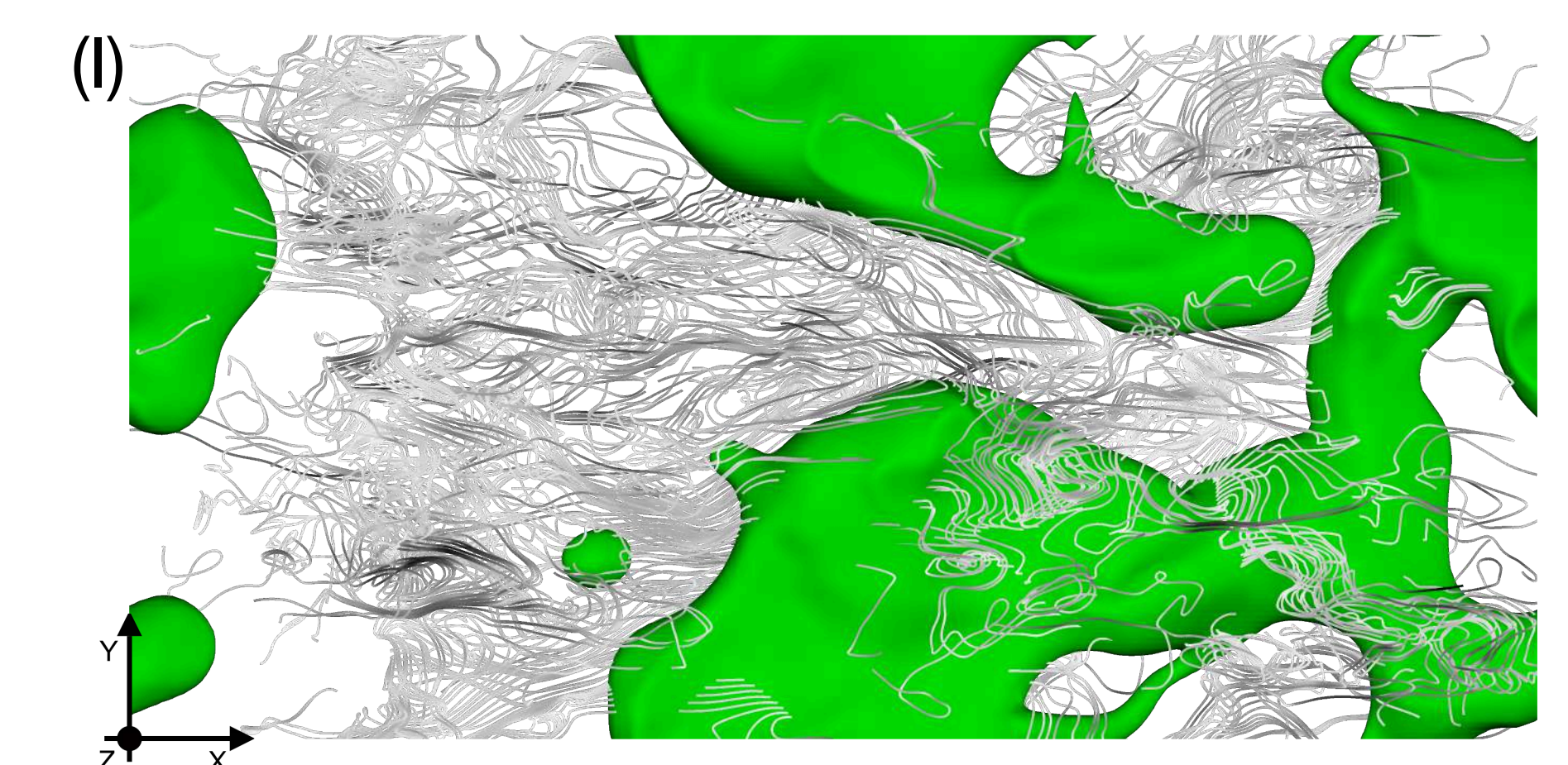
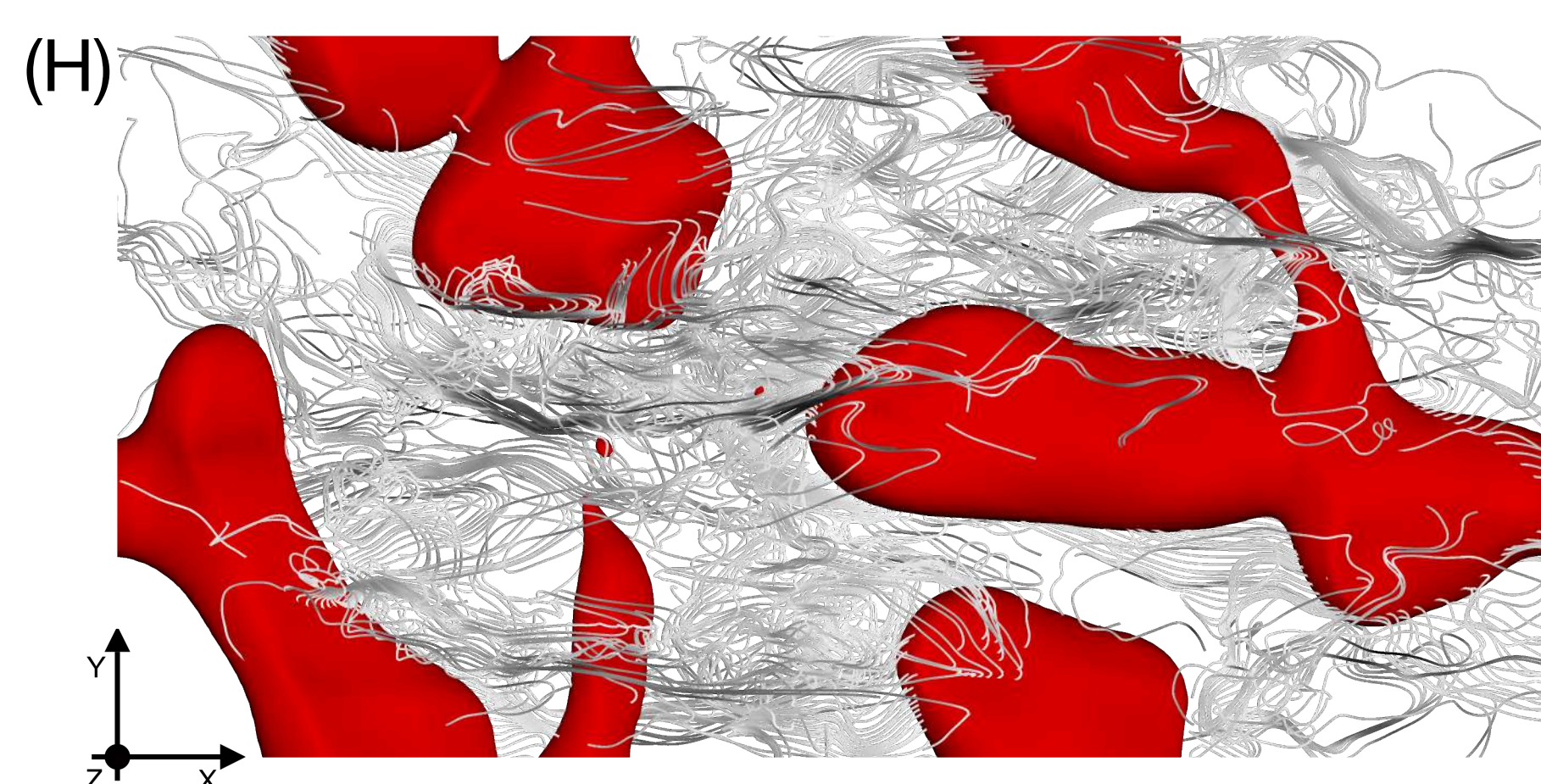
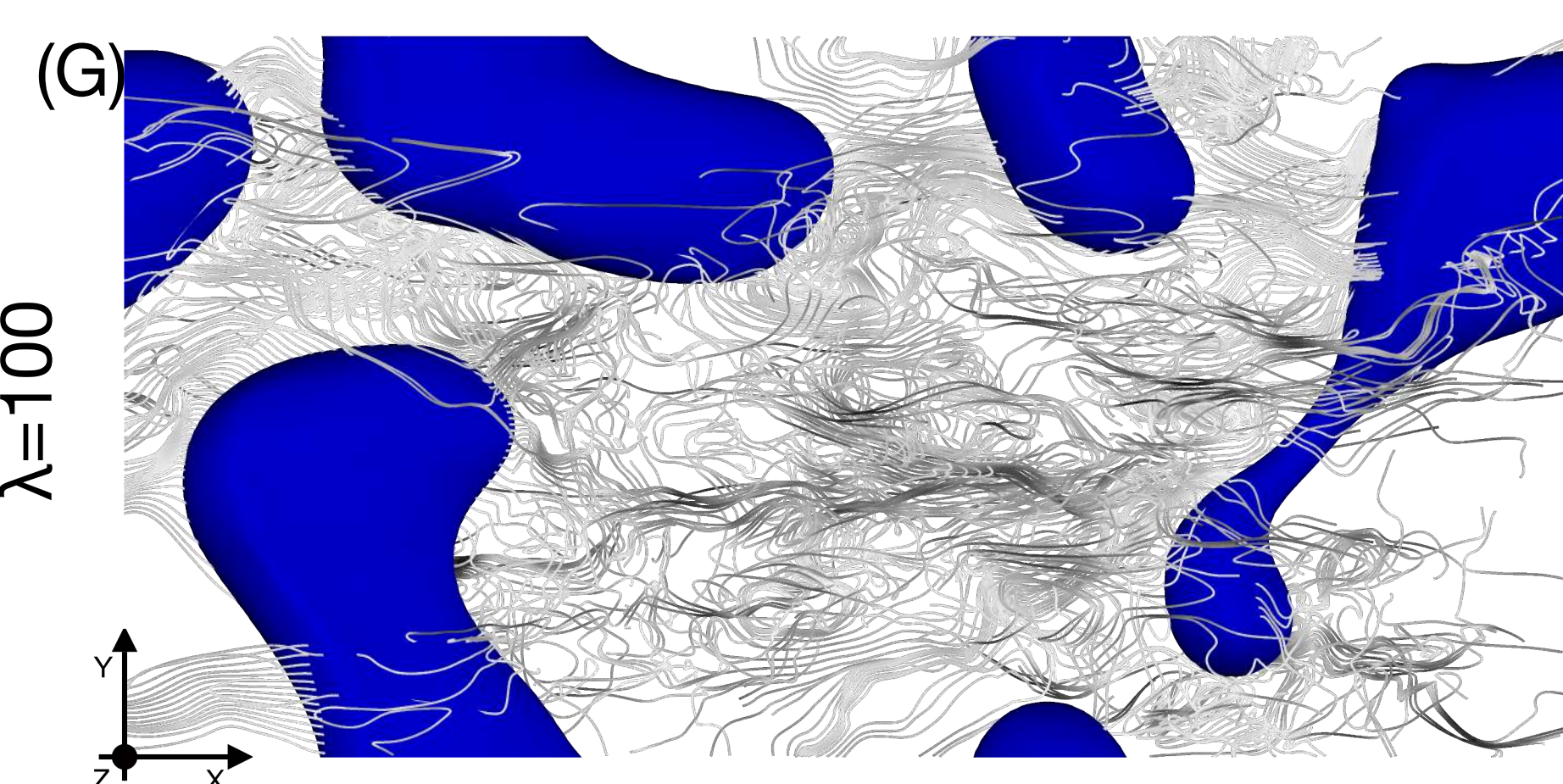
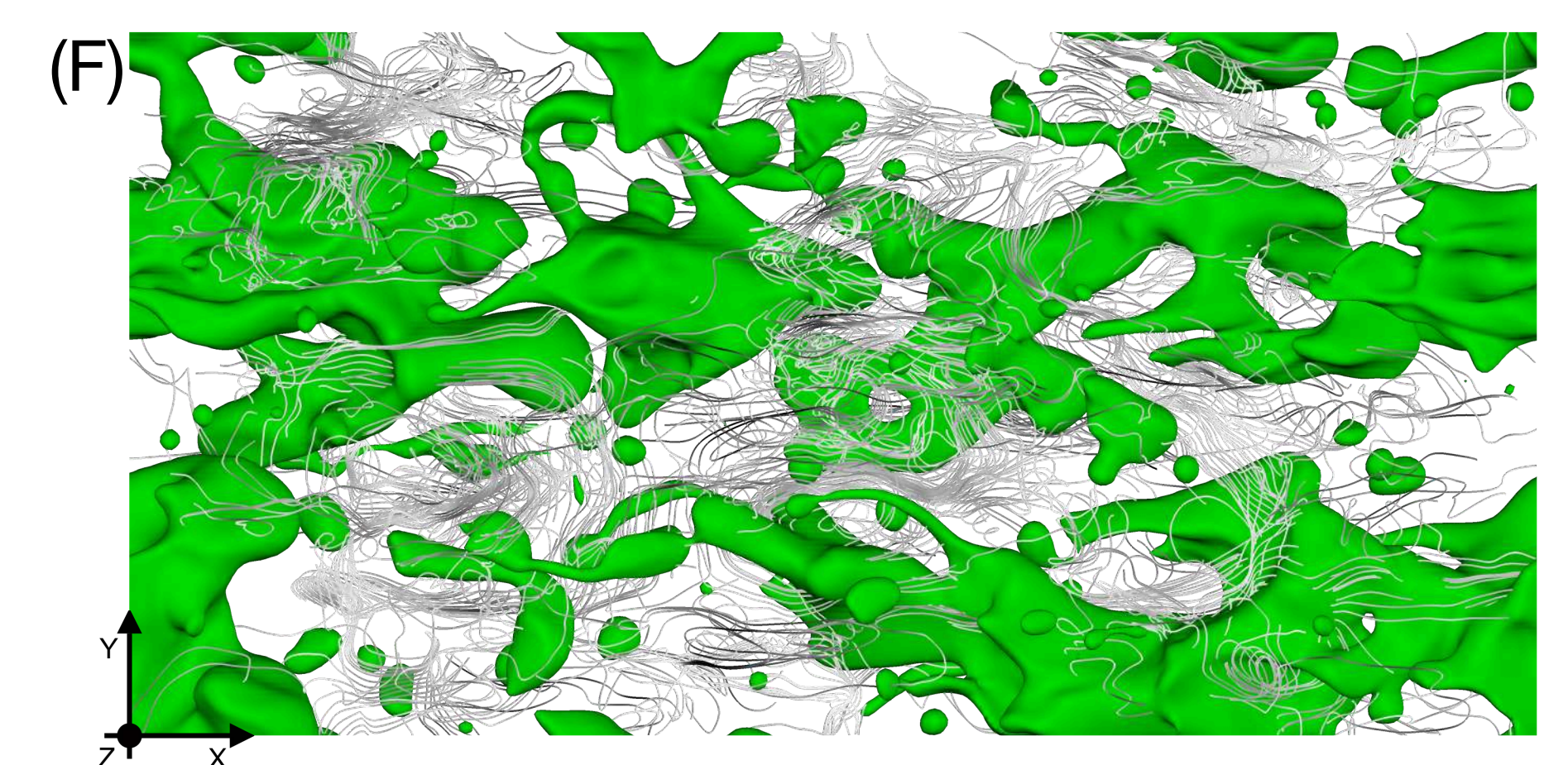
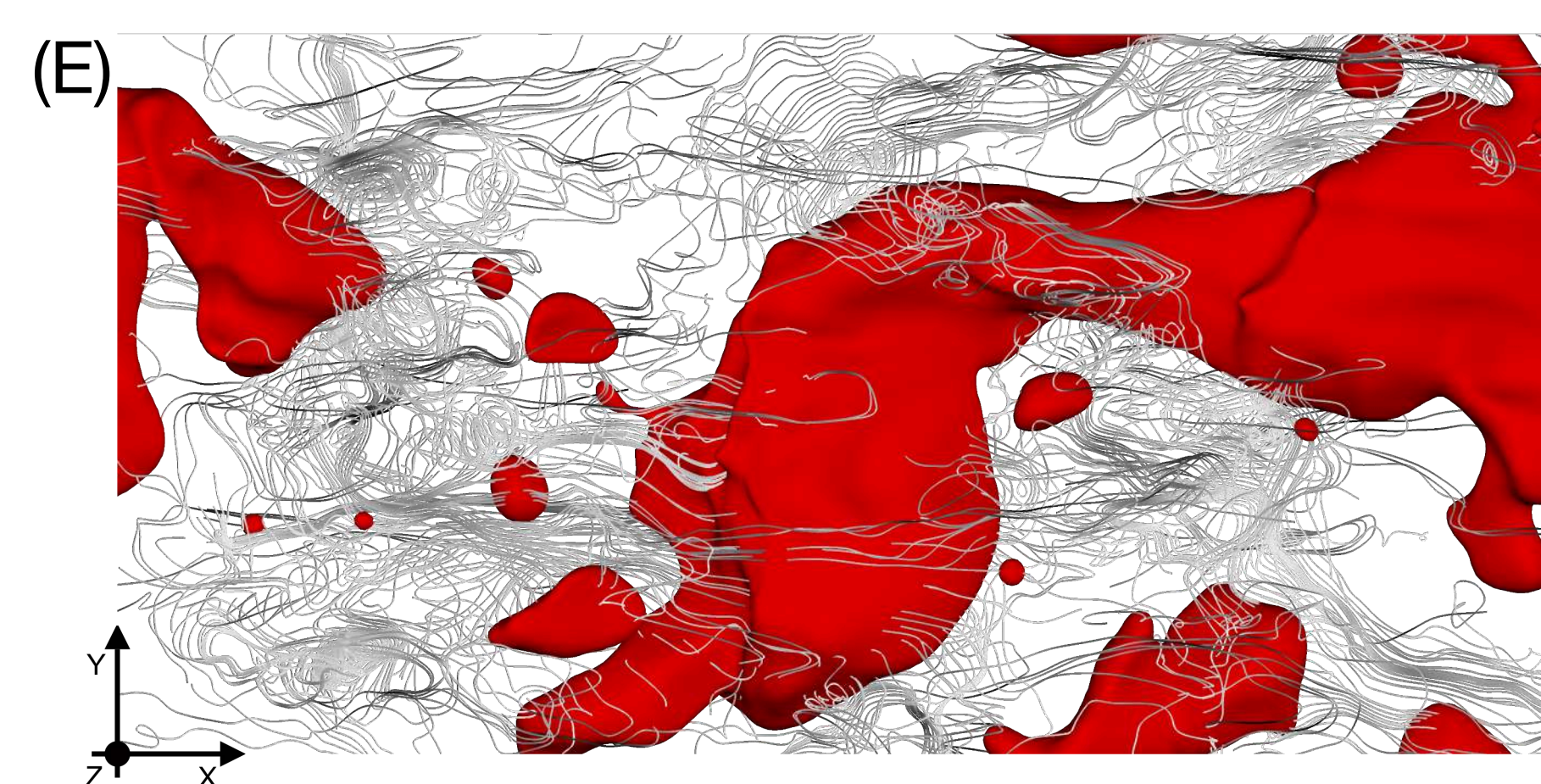
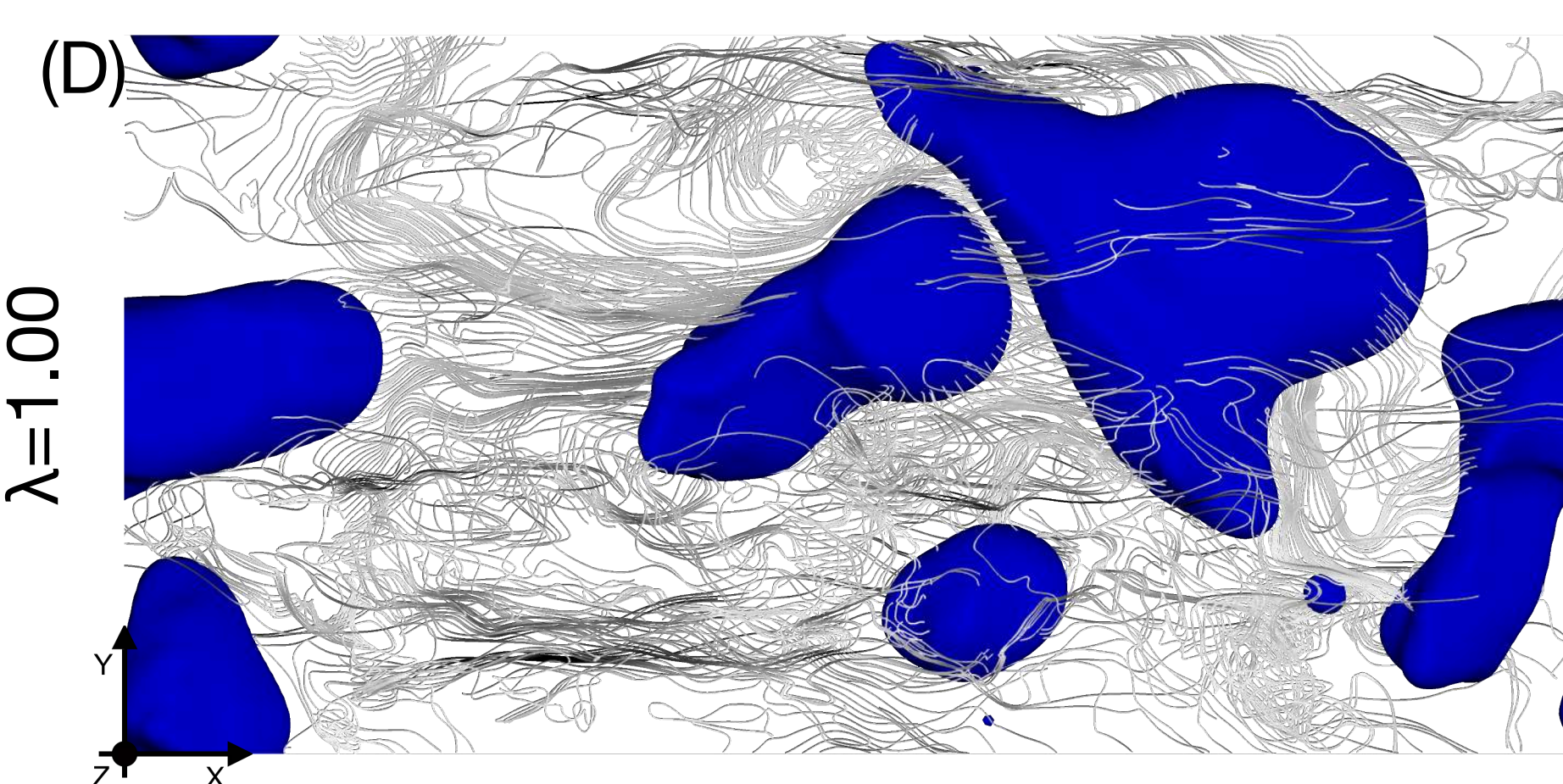
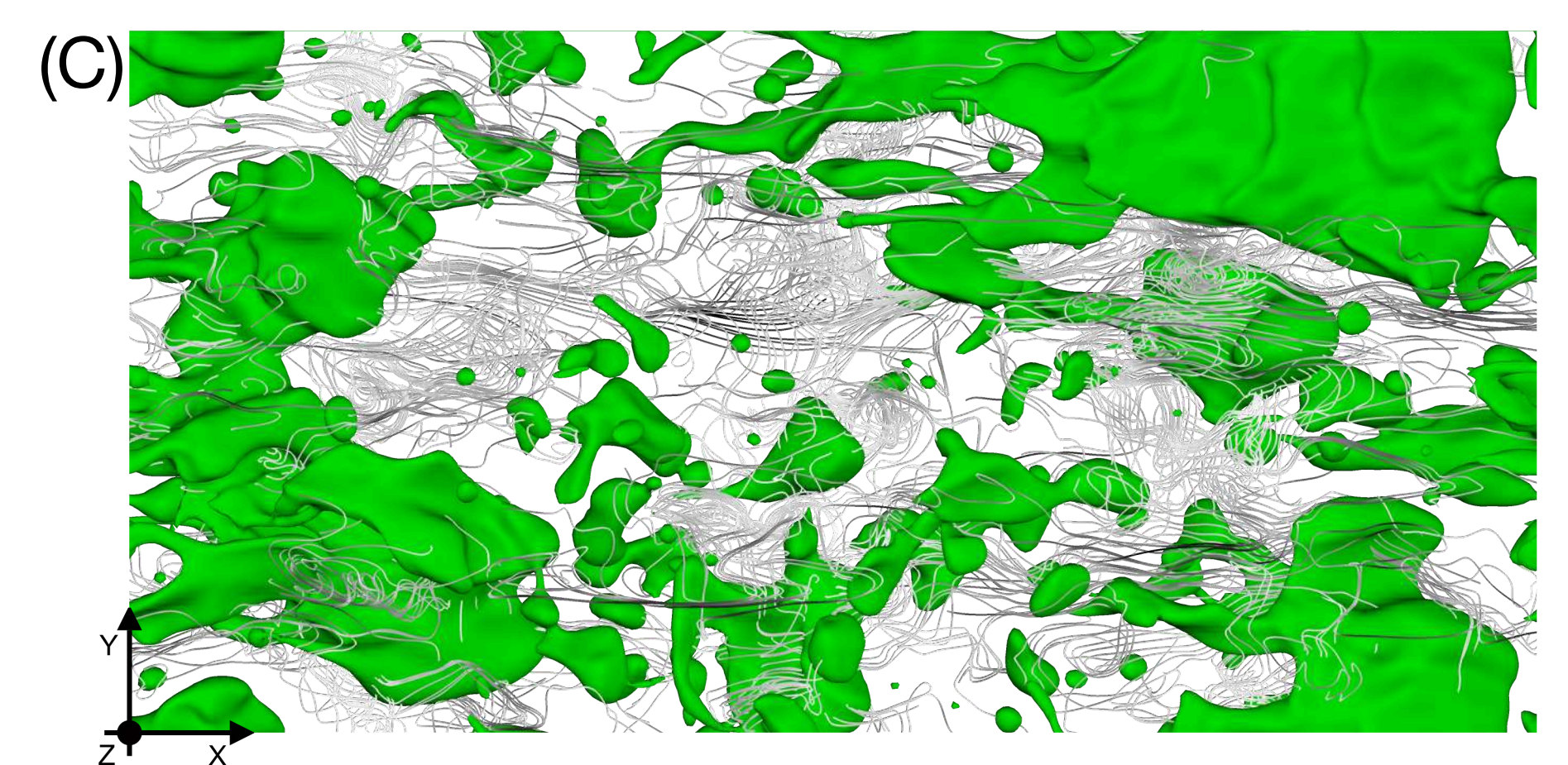
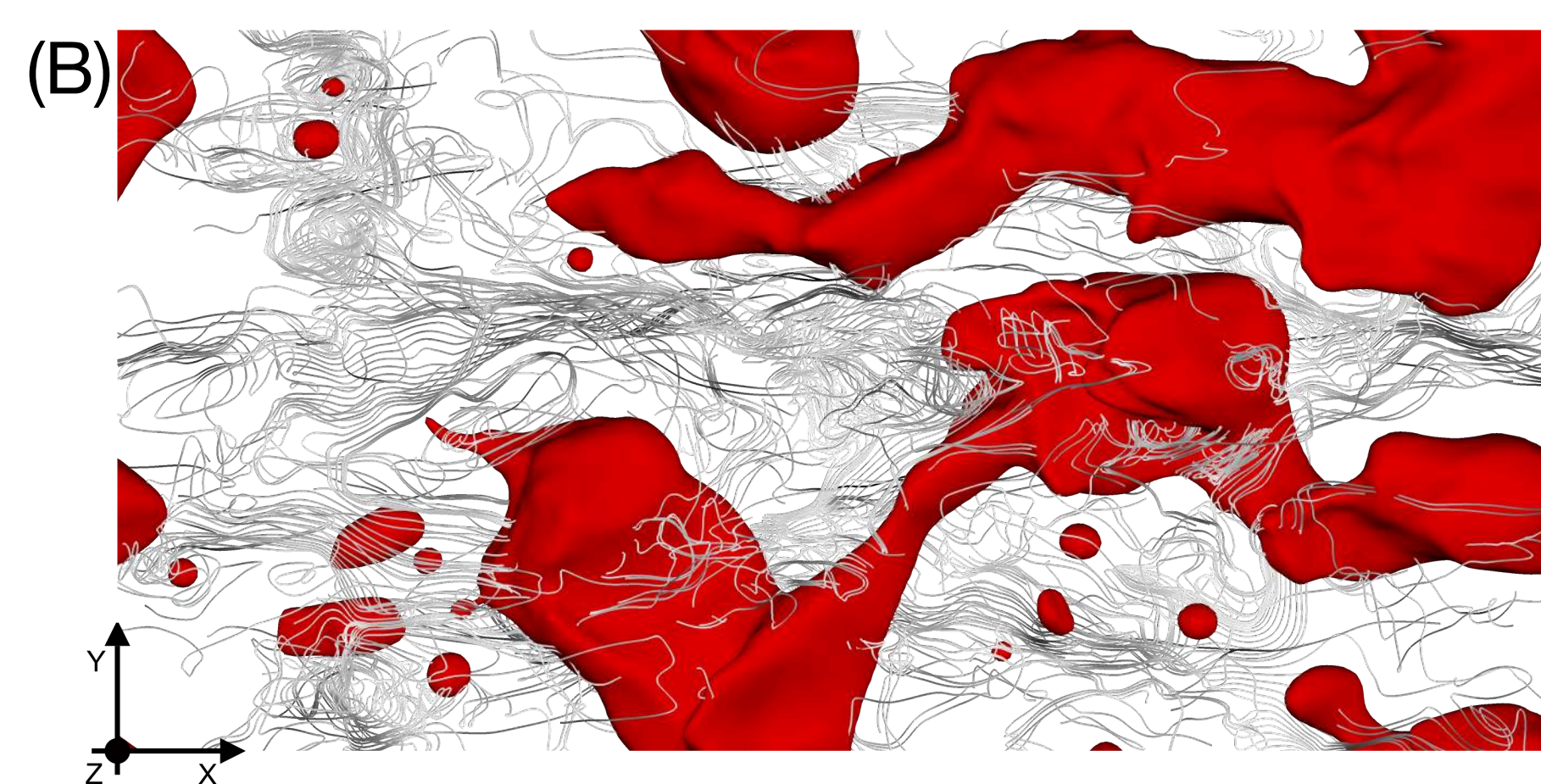
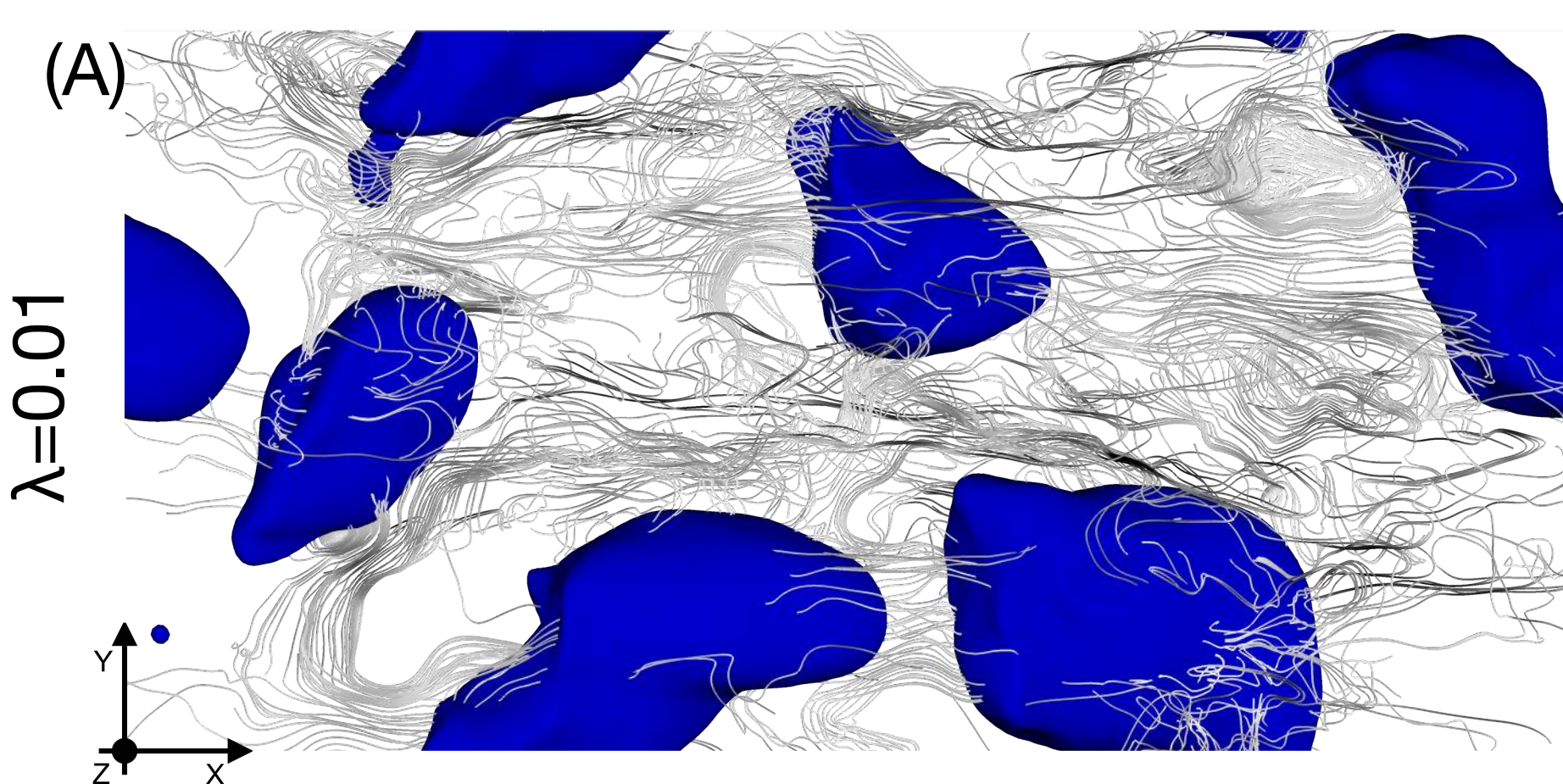


FIG. 1: In the panels (A)-(I), top views of the drops' shape for different values of the We and λ are reported. All the panels show the configuration at a time $t^+=1850$, at this stage a statistical steady-state for the number of drops is reached. Moving from top to bottom the drop viscosity increase and moving from the left to the right the We increase (surface tension decrease). In the panels (J)-(L) the dimensionless number of drops N/N_0 are reported over time for the three We numbers and five viscosity ratios λ . Either from the qualitative (A)-(I) that from the quantitative (J)-(L) panels the role played by the drop viscosity is clear, shape and topology of the dispersed phase are altered, more precisely an increase of the drop viscosity (increase of λ) promote the coalescence phenomena and inhibit the breakage events.

roccon.alessio@spes.uniud.it



Dott. Alessio Roccon
Prof. Alfredo Soldati



UNIVERSITÀ
DEGLI STUDI
DI UDINE
hic sunt futura

PHYSICAL SCIENCES AND ENGINEERING

30° ciclo

Corso di dottorato in Scienze dell'Ingegneria
Ambientale ed Energetica

Numerical Simulation of Thin Film Breakup on Non-wettable Surfaces

1. Introduction

- Phenomena involving thin layer of liquid (still/moving droplets, ensemble of rivulets or continuous film) are affected by discontinuities due to dry-patch and contact line occurrence.
- Liquid layer evolution is involved in several engineering applications. For example, in **CO₂ chemical absorption through structured packing columns** post-combustion CO₂ flows up while liquid solvent falls down through a collection of corrugated sheets.

2. Mathematical model

- Lubrication approximation: 3D physical problem is reduced to a 2D mathematical problem.
- Film flowing down an inclined plate: α and τ_a are the plate inclination and the shear applied by an external gas flow; h_∞ and u_∞ are the undisturbed film height and velocity according to Nusselt theory.
- Assuming $Re = \rho u_\infty h_\infty / \mu \leq 1$, continuity and momentum equations give:

$$\frac{\partial h}{\partial t} = -\nabla \cdot \mathbf{Q} = -\nabla \cdot \left(-\frac{\nabla p}{3\mu} h^3 + \frac{\tau_a}{2\mu} h^2 \right) \quad (1)$$

- Pressure field is given by hydrostatic, capillary and disjoining contributions:

$$p = \rho g (h \cos \alpha - x \sin \alpha) - \sigma \kappa - \Pi \quad (2)$$

$$\kappa = \frac{\partial^2 h}{\partial x^2} \left[1 + \left(\frac{\partial h}{\partial x} \right)^2 \right]^{-3/2} + \frac{\partial^2 h}{\partial y^2} \left[1 + \left(\frac{\partial h}{\partial y} \right)^2 \right]^{-3/2} \quad (3)$$

$$\Pi = \left[\left(\frac{\delta}{h} \right)^n - \left(\frac{\delta}{h} \right)^m \right] \frac{(n-1)(m-1)\sigma}{n-m} \frac{1}{\delta} (1 - \cos \theta_e) \quad (4)$$

θ_e and δ being equilibrium contact angle and precursor film height, $n > m > 1$.

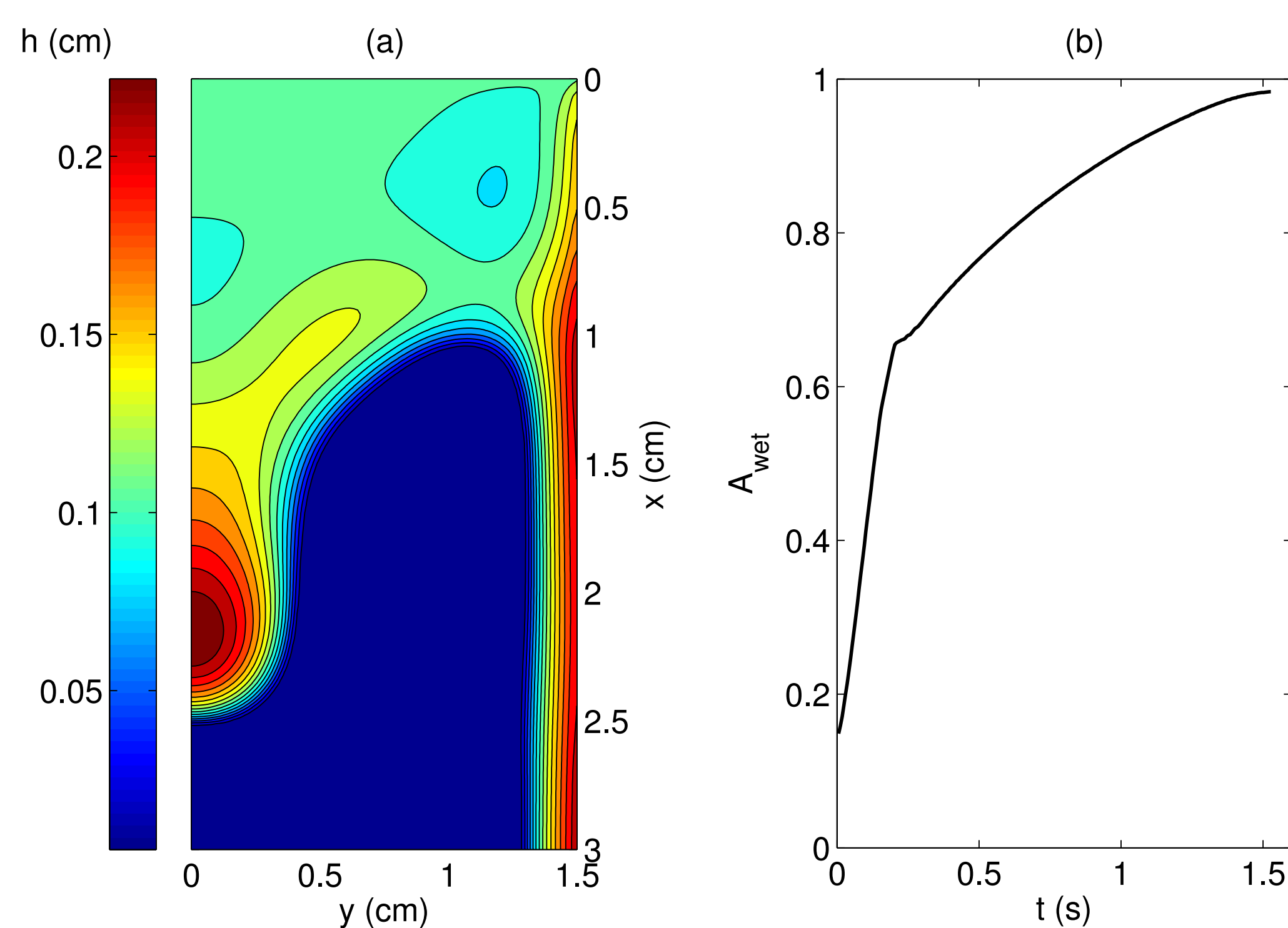


Figure. Liquid layer over the inclined plate at $t = 0.18$ s (a); normalized wetted area as a function of time (b); $\theta_e = 60^\circ$, $Ka = 14.8$, $We = 0.234$.

3. Numerical method

- Eqs. (1), (2) and (4) are solved numerically by means of the Finite-Volume-Method on a 2D structured grid.
- Convective term $\nabla \cdot \mathbf{Q}$ of eq. (1) is discretized via a first-order upwind scheme by decomposing the film flux in $Q^+ = u^+ h$ and $Q^- = u^- h$.
- Pressure gradient on each element face is computed with a centered difference; capillary pressure contribution is discretized via a second order centered scheme.
- Time marching by means of ADI approximate factorization allows to reach time step Δt up to 10^6 times as high as the explicit one.

4. Application to CO₂ absorption

- Gravity driven flow down an inclined plate is the simplest configuration for describing the hydrodynamics through structured packing.
- Disjoining pressure, eq. (4), allows modeling surface wettability (defined by equilibrium contact angle) and capturing contact line.
- Lateral boundary $y = L_y$ is treated as a wall.
- Liquid layer configuration (i.e. wetted area) depends on Kapitza and Weber numbers:

$$Ka = \sigma \left(\frac{\rho}{\mu g} \right)^{1/3}; \quad We = \frac{\rho u_\infty^2 h_\infty}{\sigma} \quad (5)$$

5. Conclusion and future work

- 2D model based on lubrication theory is able to compute film height and capture contact line, allowing for a significant reduction in computational cost in comparison to fully 3D V.O.F. method.
- Lubrication theory is still valid for high values of contact angle modeling capillary pressure through eq. (3).
- Simulation of shear driven film and complex geometries still pending.

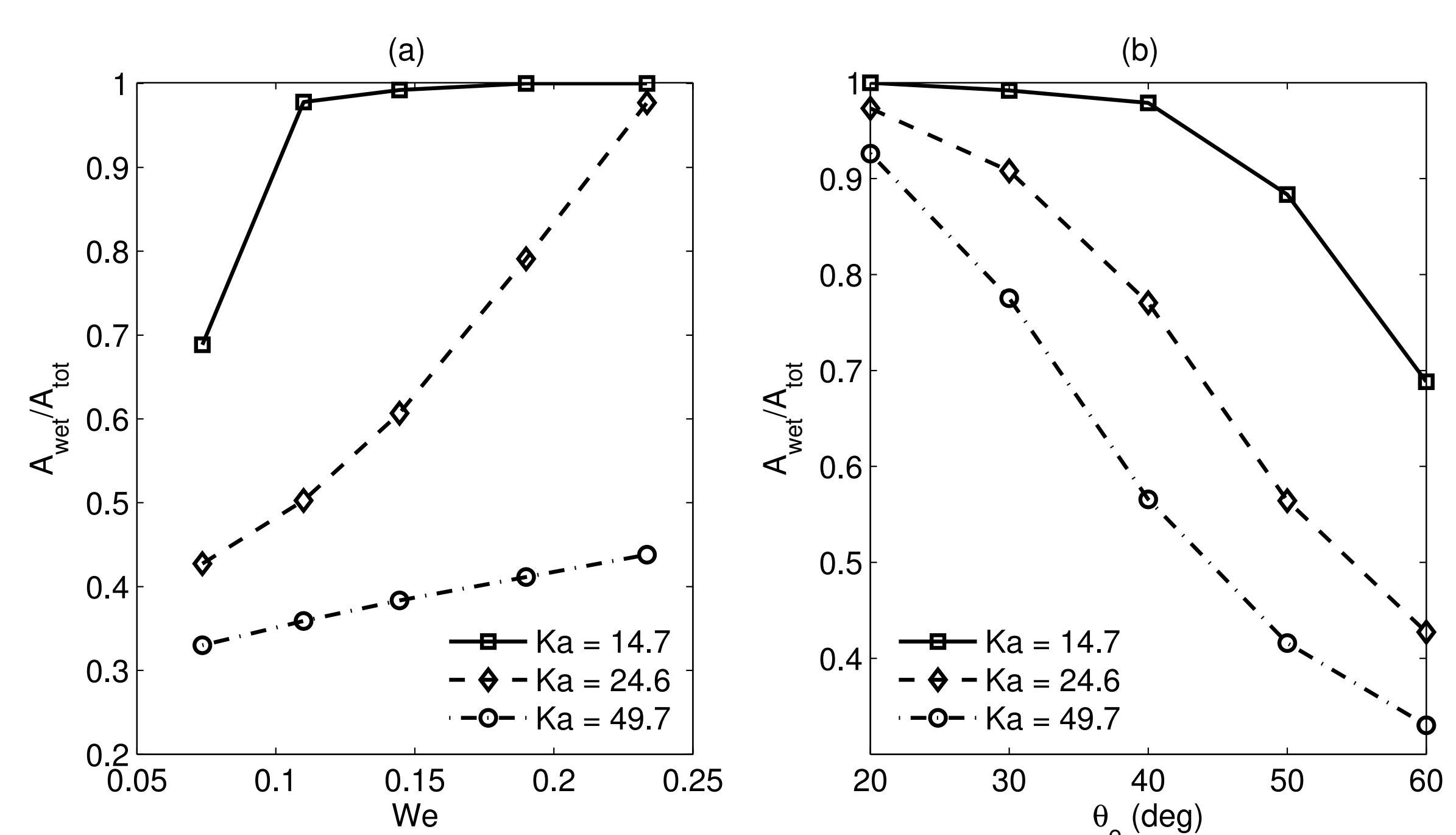


Figure. Influence of Ka , We and θ_e on normalized wetted area, 3×1.5 cm² plate simulated.

Dott. Nicola Suzzi
Prof. Giulio Croce

Info:
suzzi.nicola@spes.uniud.it
nicola.suzzi@cern.ch

Bibliography:

- N. Suzzi, G. Croce, P. D'Agaro *J. of Physics: Conference Series* **655** (2015) 012041
- N. Suzzi, G. Croce *J. of Physics: Conference Series* **796** (2017) 012038



**UNIVERSITÀ
DEGLI STUDI
DI UDINE**
hic sunt futura

PHYSICAL SCIENCES AND ENGINEERING

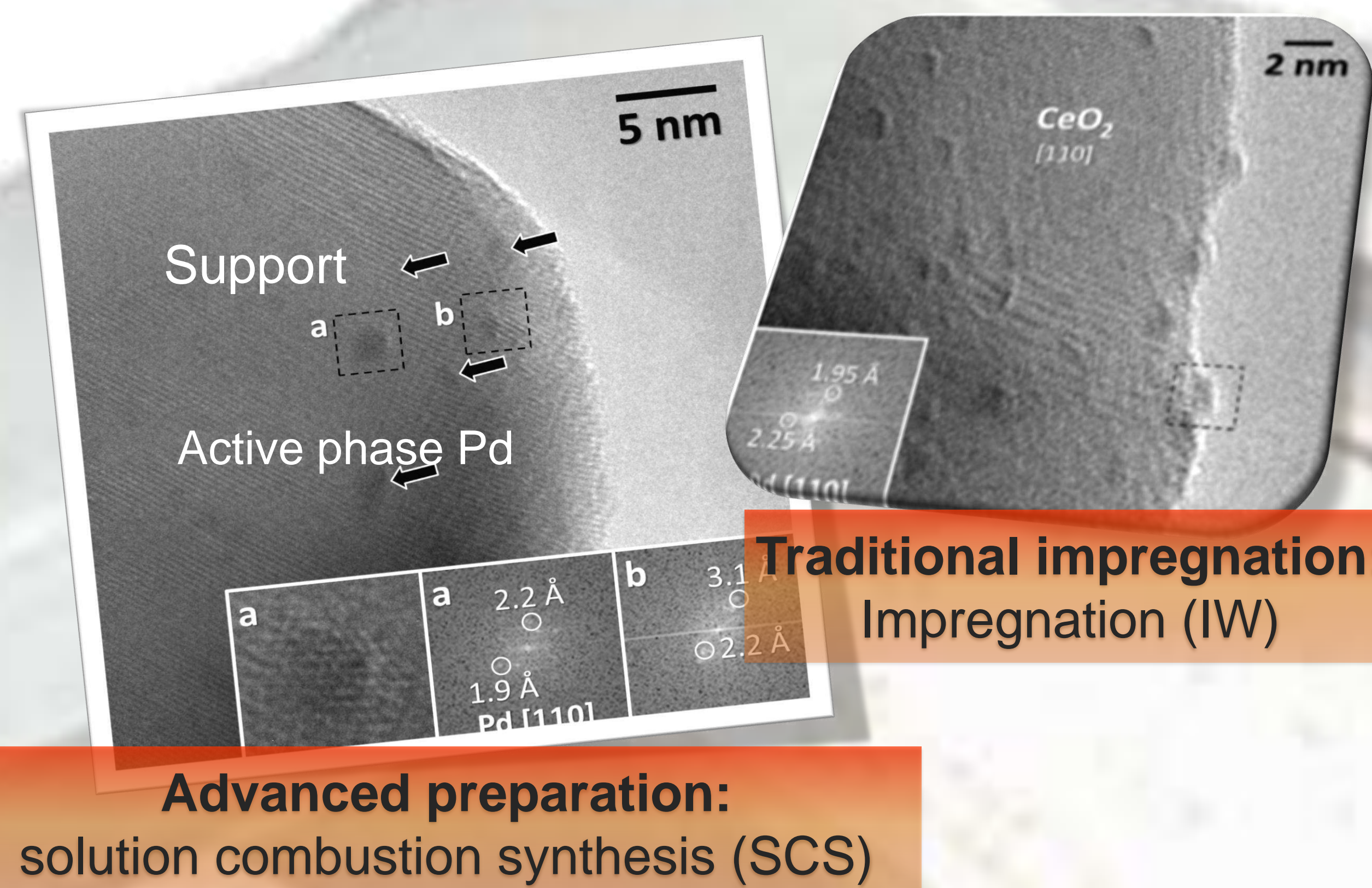
30° ciclo

Corso di Dottorato in Scienze dell'Ingegneria Energetica e Ambientale

The main goal of this PhD work is the study of new palladium based catalysts for the abatement of unburned methane from natural gas fuelled vehicles (NGVs). In particular our proposal is to investigate simple and fast *one-step* synthesis methods to obtain catalytic materials with high activity at low temperatures and good resistance to water poisoning.

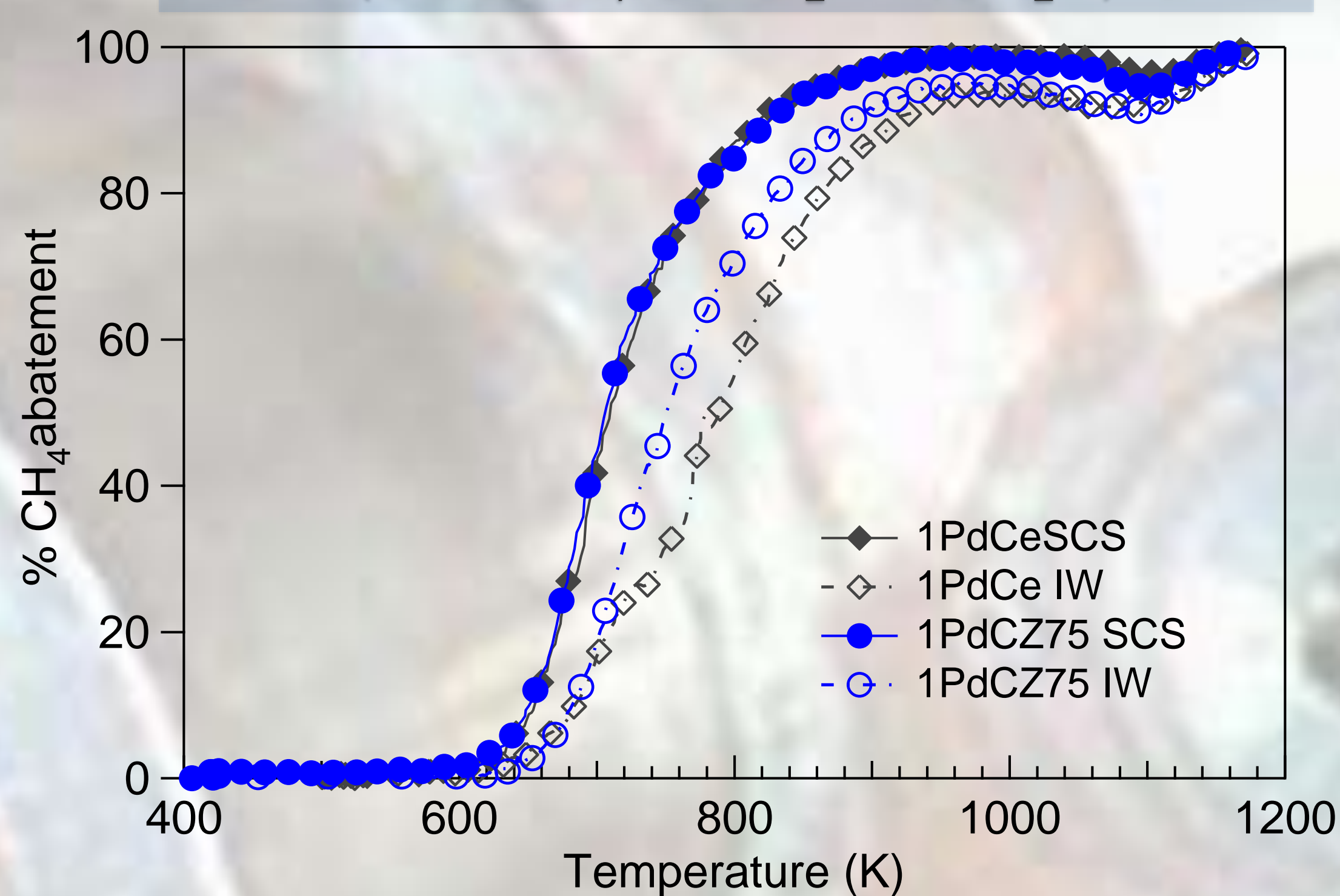
BACKGROUND

Natural gas, where methane (CH_4) is the main compound, represents a green choice against traditional spark ignited engines with a reduction of CO_2 up to 25% and lower polycyclic aromatic hydrocarbon (PAH) and PM_{10} emissions. However unburned CH_4 is a greenhouse gas with high environmental impact, its *Global Warming Potential* (GWP) being 20 times than that of CO_2 . Exhaust gas emissions from NGVs contain 500-1000 ppm CH_4 and large amount of water vapor (10-15%). To reduce methane emissions, catalytic oxidation is applied at tailpipe. Palladium catalysts are recognized to be the most active materials for methane combustion and in particular Pd/ CeO_2 based catalysts show interesting catalytic properties. Tailoring of catalytic properties through suitable supports and synthesis methods is one of the goal of this reaserch project. Solution combustion synthesis is an advanced technique to prepare nanocatalysts in one-step and with short reaction time and it has been showed to be an effective method to prepare catalysts with higher activity compared to their correspondent impregnated ones [1][2][3].



Pd/ CeO_2 BASED CATALYSTS: RESISTANT MATERIALS FOR METHANE EMISSIONS ABATEMENT FROM NGVs

Catalytic activity
(0.5% CH_4 , 2% O_2 ; 10% H_2O)



SCS catalyst		IW catalyst	
One-step synthesis		Multi-step synthesis	
More active		Less active	
Resistant to water		Sensitive to water	

CONCLUSIONS

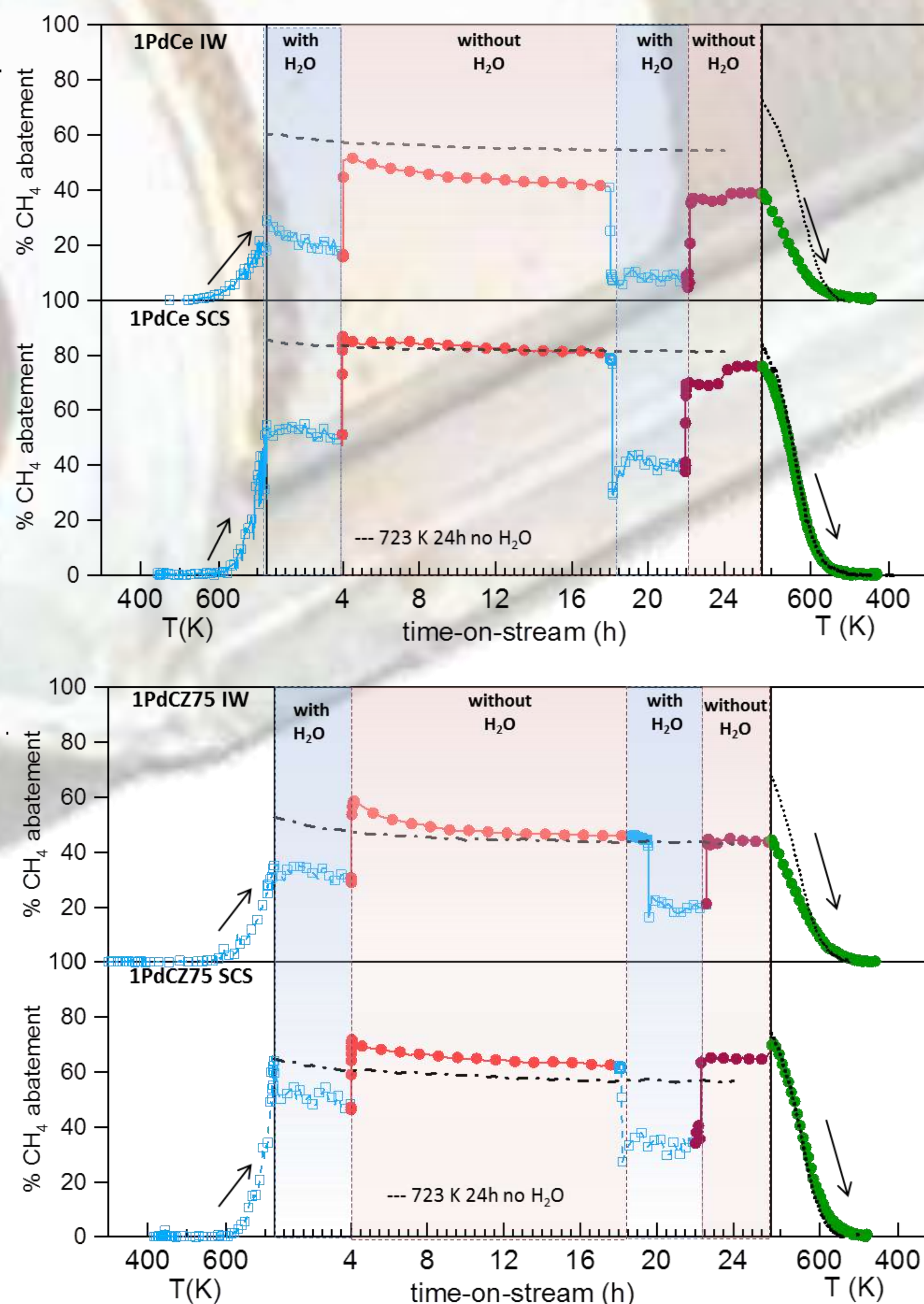
Solution combustion synthesis is an effective method to obtain efficient Pd catalysts with very good catalytic performance. In addition, the catalysts prepared by SCS are less susceptible to water deactivation with better long-term stability compared to IW catalysts which suffer much more the presence of water with a strong reduction in catalytic activity.

Ing. **Alessandra Toso**
Prof. **Alessandro Trovarelli**
Dott.ssa **Sara Colussi**

Info:
Tel. +39 0432 558763
toso.alessandra@spes.uniud.it

References
[1] S. Colussi *et al.* *Angew. Chem. Int. Ed.* 2009, 48, 8481–8484
[2] S. Colussi *et al.* *Ind. Eng. Chem. Res.* 2012, 51, 7510–7517
[3] S. Colussi *et al.* *ChemCatChem* 2015, 7, 2222–2229

Regeneration of H_2O -poisoned catalysts at $T = 723 \text{ K}$ (0.5% CH_4 , 2% O_2 ; 10% H_2O)



Acknowledgments

This research project is developed in collaboration with Ford Motor Company



**UNIVERSITÀ
DEGLI STUDI
DI UDINE**
hic sunt futura

PHYSICAL SCIENCES AND ENGINEERING

30° ciclo

**Corso di dottorato in Scienze dell'ingegneria
energetica e ambientale**

Nano Strutture per Macro Problemi: Nano-Tubi di Carbonio per la Rimozione di Antibiotici

Introduzione

I fluorochinoloni (FQs) sono una classe di antibiotici sintetici utilizzati nel trattamento di malattie infettive sia negli esseri umani che negli animali. Il loro uso irrazionale ha portato ad un grave problema di inquinamento ambientale ed alla nascita del fenomeno di farmaco resistenza verso questa classe di composti. Per queste ragioni, l'efficace rimozione di queste specie dall'ambiente è argomento di primario interesse. Tra le tecniche di rimozione, particolarmente interessante è la tecnica basata sull'adsorbimento, per la sua semplicità e i bassi costi. La comprensione dei meccanismi di adsorbimento a livello molecolare (Figura 1a) può contribuire a migliorare l'efficienza dei sistemi adsorbenti nel trattamento delle acque reflue. I nano-tubi di carbonio (CNTs) sono qui proposti come sistemi adsorbenti per la rimozione di FQs grazie alla loro elevata capacità di adsorbimento e di rigenerazione. Attraverso simulazioni di dinamica molecolare (MD), è stato studiato l'adsorbimento su CNT di ciprofloxacina (CFX), il FQ più prescritto al mondo.

Scopo

Lo scopo di questo lavoro è studiare il meccanismo di adsorbimento della forma neutra (nCFX) e zwitterionica (zwCFX) della ciprofloxacina (Figura 1b) sulla superficie interna ed esterna di un nano-tubo di carbonio attraverso simulazioni di dinamica molecolare.

Risultati

Simulazioni nel vuoto sono state condotte per studiare l'interazione tra CFX e CNT, espressa attraverso il calcolo delle energie di interazione (E_{int}) riportate in Tabella 1.

Tabella 1 Energie di interazione in vuoto per 1, 2, 4 ed 8 molecole di CFX calcolate secondo l'equazione: $E_{int} = E_{CNT+CFX} - (E_{CNT} + E_{CFX})$

	E_{int} kcal mol ⁻¹	X2 E_{int} kcal mol ⁻¹	X4 E_{int} kcal mol ⁻¹	X8 E_{int} kcal mol ⁻¹
zwCFX out surf	-26.8	-17.9	-22.3	-21.7
nCFX out surf	-24.9	-26.2	-26.0	-25.1
zwCFX ins surf	-34.9	-39.5	-29.4	-31.9
nCFX ins surf	-43.2	-42.3	-40.15	-34.3

Si può osservare che le E_{int} sono tutte negative, indice che nCFX e zwCFX rimangono adsorbiti sulla superficie del CNT grazie ad interazioni di tipo π (Figura 2).

Lo studio è proseguito con la stima dell'energia libera di adsorbimento (ΔG_{ads}) in acqua attraverso il calcolo del potential of mean force (PMF) (Figura 3) estratto da una serie di simulazioni di tipo Umbrella Sampling (US). In Tabella 2 vengono riportati i valori di ΔG_{ads} calcolati.

Tabella 2 ΔG_{ads} calcolati per nCFX e zCFX sulla superficie interna ed esterna del CNT.

	ΔG_{ads} kcal mol ⁻¹
zwCFX out surf	-9.5
nCFX out surf	-3.6
zwCFX ins surf	-12.5
nCFX ins surf	-21.1

Tutti i ΔG_{ads} sono negativi, indice che le specie si adsorbono spontaneamente.

Adsorbimento spontaneo di CFX su CNT : rimozione ambientale di fluorochinoloni da acque reflue.

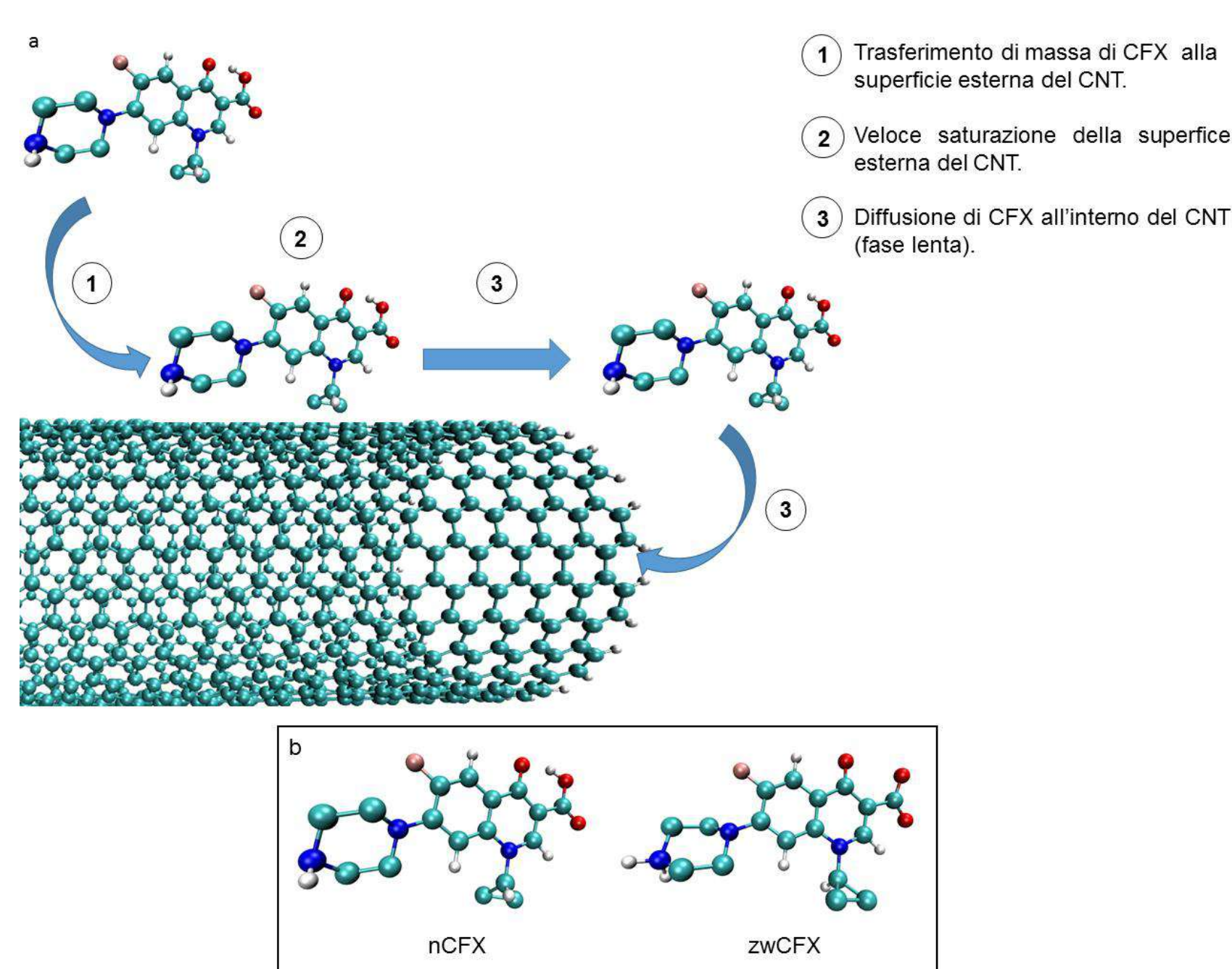


Figure 1 (a) meccanismo di adsorbimento riportato in letteratura, (b) strutture di nCFX e zwCFX.

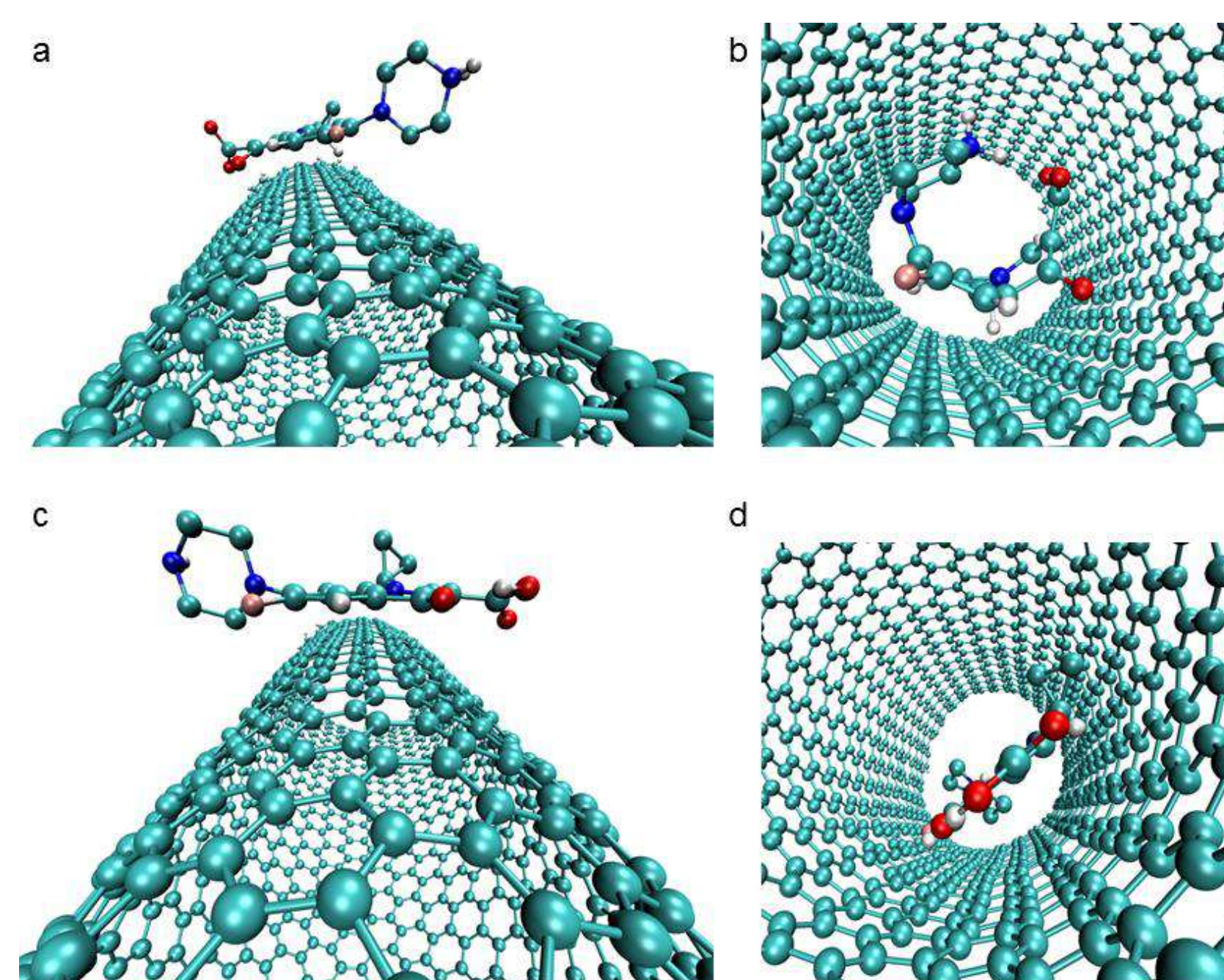


Figure 2 strutture di zwCFX alla superficie esterna (a) e interna (b); strutture di nCFX alla superficie esterna (c) e interna (d).

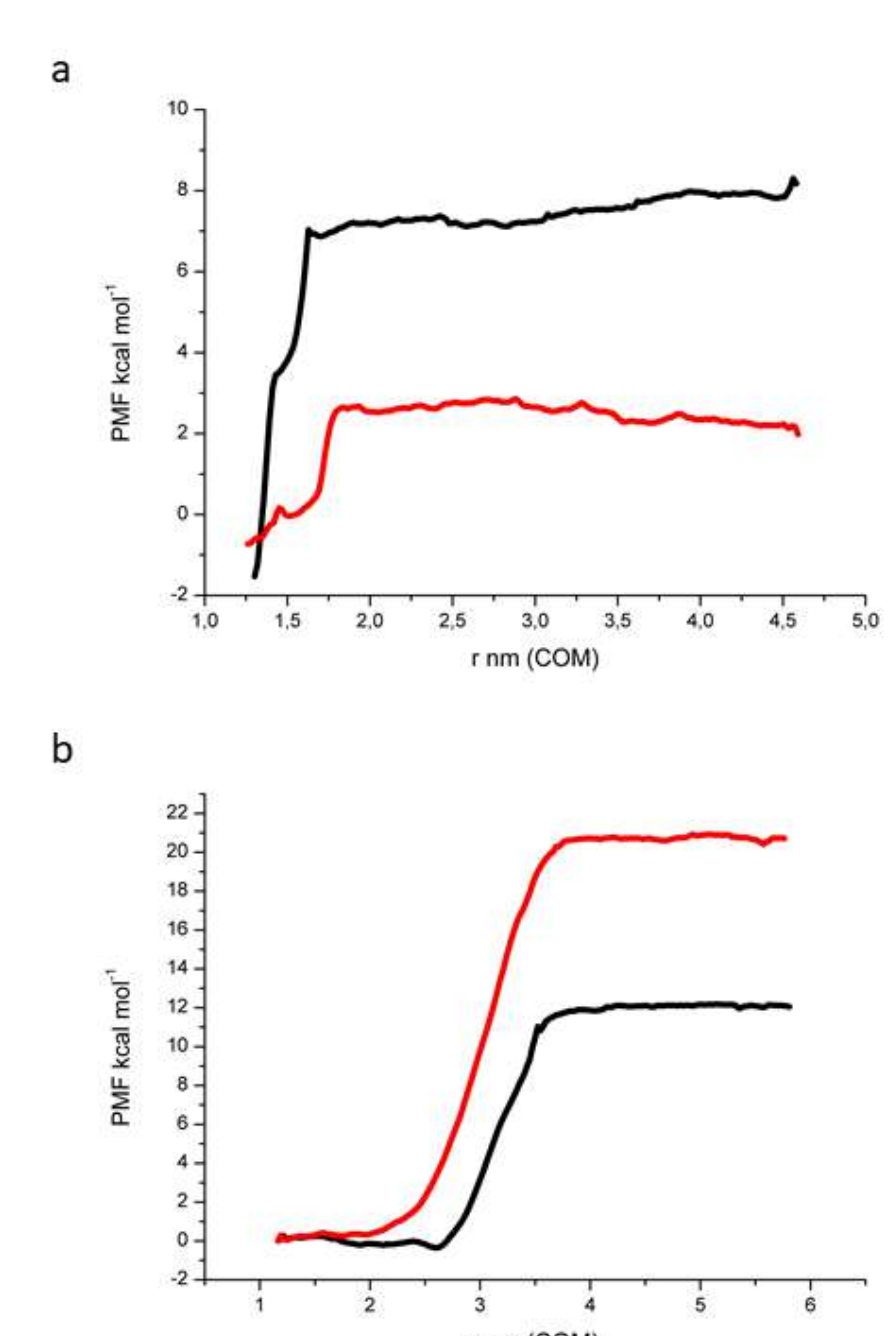


Figure 3 PMF vs. distanza tra i due centri di massa (COM) di zwCFX (curva nera) o nCFX (curva rossa) e CNT per a) adsorbimento alla superficie esterna, b) adsorbimento alla superficie interna.



Dott. Daniele Veclani
Prof. Andrea Melchior
Info:
Tel. +39 0432 558859
veclani.daniele@spes.uniud.it

Riferimenti bibliografici

V. M. Nurchi, G. Crisponi, J. I. Lachowicz, M. A. Zoroddu, M. Peana, S. Medici, D. Veclani, M. Tolazzi, A. Melchior, *J. Pharm. Sci.* 93 (2016) 380-391

M. M. Dell'Anna, V. Censi, B. Carrozzini, R. Caliendo, N. Denora, M. Franco, D. Veclani, A. Melchior, M. Tolazzi, P. Mastorilli, *J. Inorg. Biochem.* 163 (2016) 346-361